

Deposit & Copying of Dissertation Declaration



UNIVERSITY OF
CAMBRIDGE

Board of Graduate Studies

Please note that you will also need to bind a copy of this Declaration into your final, hardbound copy of thesis - this has to be the very first page of the hardbound thesis.

1	Surname (Family Name)	Forenames(s)	Title
	TAN	SIN LIH	MISS
2	Title of Dissertation as approved by the Degree Committee		
	The physiological role of P2X4 receptors in lysosome function		

In accordance with the University Regulations in *Statutes and Ordinances* for the PhD, MSc and MLitt Degrees, I agree to deposit one print copy of my dissertation entitled above and one print copy of the summary with the Secretary of the Board of Graduate Studies who shall deposit the dissertation and summary in the University Library under the following terms and conditions:

1. Dissertation Author Declaration

I am the author of this dissertation and hereby give the University the right to make my dissertation available in print form as described in 2. below.

My dissertation is my original work and a product of my own research endeavours and includes nothing which is the outcome of work done in collaboration with others except as declared in the Preface and specified in the text. I hereby assert my moral right to be identified as the author of the dissertation.

The deposit and dissemination of my dissertation by the University does not constitute a breach of any other agreement, publishing or otherwise, including any confidentiality or publication restriction provisions in sponsorship or collaboration agreements governing my research or work at the University or elsewhere.

2. Access to Dissertation

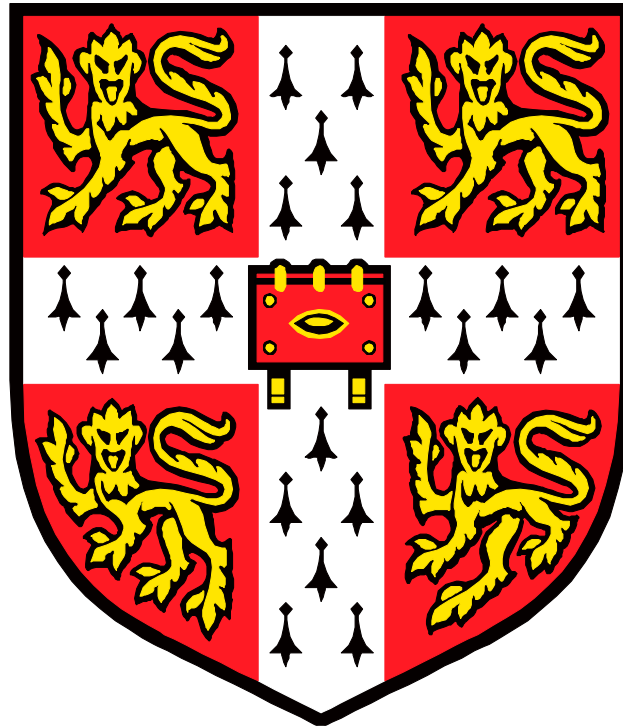
I understand that one print copy of my dissertation will be deposited in the University Library for archival and preservation purposes, and that, unless upon my application restricted access to my dissertation for a specified period of time has been granted by the Board of Graduate Studies prior to this deposit, the dissertation will be made available by the University Library for consultation by readers in accordance with University Library Regulations and copies of my dissertation may be provided to readers in accordance with applicable legislation.

3	Signature	Date
		10/10/2017

Corresponding Regulation

Before being admitted to a degree, a student shall deposit with the Secretary of the Board one copy of his or her hardbound dissertation and one copy of the summary (bearing student's name and thesis title), both the dissertation and the summary in a form approved by the Board. The Secretary shall deposit the copy of the dissertation together with the copy of the summary in the University Library where, subject to restricted access to the dissertation for a specified period of time having been granted by the Board of Graduate Studies, they shall be made available for consultation by readers in accordance with University Library Regulations and copies of the dissertation provided to readers in accordance with applicable legislation.

The physiological role of P2X4 receptors in lysosome function



Sin Lih Tan

University of Cambridge

Robinson College

This dissertation is submitted for the degree of Doctor of Philosophy

April 2017

Preface

Declaration

This dissertation is the result of my own work and includes nothing which is the outcome of work done in collaboration except as declared in the Preface and specified in the text. This work was conducted in the Department of Pharmacology, University of Cambridge, between October 2013 and December 2016. No part of this thesis has been submitted for any other qualification.

Statement of length

This thesis does not exceed the prescribed word limit of 60,000 words.

Acknowledgements

Firstly, I would like to express my sincere gratitude to my first supervisor, Dr Ruth Murrell-Lagnado, for her continuous support and guidance throughout my PhD studies. Her systematic supervision, motivation and immense patience have helped me in various situations in my PhD research and writing this thesis. During my doctorate training, Ruth has always encouraged me to challenge scientific hypotheses, critically analyse data and effectively delivery presentations with confidence. I could not have imagined having a better supervisor for my PhD studies and am grateful for the opportunity of being part of her research group.

I would also like to express my deepest gratitude to my second supervisor, Dr Ewan St. John Smith. During my transition from Ruth's lab to his lab at the end of my second year he was very kind and supportive in providing valuable lab resources and guidance in successfully completing my PhD.

I thank my fellow members of the two labs, Dr Lucy Robinson, Dr Marie Brunet, Dr Shyam Srivats, Dr Laura-Nadine Schuhmacher and Dr Zoe Husson for the stimulating discussion and support during my PhD training and transition of labs.

A special gratitude goes out to Yousef Jameel Scholarship and Cambridge Trust for their invaluable funding support towards research expenses and living expenses.

I thank all of my friends for the times that we have had together in Cambridge. Furthermore, I would like to thank Nathan Procter for the unfailing support and assistance during my difficult times. Finally, I extend my sincere gratitude to my parents and siblings who have provided emotional support and encouragement in life.

Abstract

P2X4 receptors (P2X4R) are ligand-gated ion channels activated by ATP and with a high permeability to Ca^{2+} . They are predominantly localised to lysosomes and from there can traffic to the cell surface. ATP levels within the lysosome are high but P2X4Rs are inhibited by the acidic pH. Previously, it was shown that the alkalinisation of lysosomes using pharmacological reagents was sufficient to activate P2X4Rs, which promoted homotypic lysosome fusion. The main aim of this study was to identify physiological regulators of lysosomal P2X4Rs and to examine their role in lysosome Ca^{2+} signalling and fusion.

The first candidate I investigated was P2X7R, which is typically co-expressed with P2X4R in immune and epithelial cells, and which has already been shown to induce changes in lysosome properties upon activation. I co-expressed these two receptors in normal rat kidney (NRK) cells and in HeLa cells and looked for a synergistic interaction between them in promoting lysosome fusion, as assessed by measuring the size of lysosomes. My results showed a significant increase in lysosome size following activation of P2X7R but only in the presence of P2X4R. Neither receptor alone was sufficient to promote lysosome fusion in response to the agonist BzATP. LAMP-GECO was used to measure changes in cytosolic $[\text{Ca}^{2+}]$ within the vicinity of the lysosome. Fusion of the Ca^{2+} reporter (GECO) to the C-terminus of LAMP-1 targets GECO to the cytosolic surface of the lysosome. Co-expression of P2X4R with P2X7R augmented the P2X7R-induced Ca^{2+} signal suggesting that P2X4Rs mediate lysosomal Ca^{2+} efflux downstream of P2X7R stimulation. Next, I showed that the expression of P2X4R was sufficient to potentiate the cytosolic Ca^{2+} response to the activation of endogenous histamine H1 receptors and to promote lysosome fusion. Similar results were obtained with P2Y2R stimulation, which also couples to the phospholipase C pathway. Therefore, lysosomal P2X4Rs can be recruited downstream of P2X7R and G_q -coupled GPCRs activation to modulate lysosome function.

Further experiments were conducted to look at differences in the trafficking behaviour of human and rat P2X4Rs. A series of mutants were made to understand the amino acid sequence differences that may account for difference in the localisation of human and rat P2X4Rs. A further examination was conducted to examine a role for P2X4Rs in autophagic flux. My results suggest a synergistic interaction between P2X4R and P2X7R which inhibits autophagic flux, similar to the effect of bafilomycin treatment. Therefore, the effect of P2X4/7R in autophagy may be mediated by the alkalinisation of lysosomes.

Altogether the results of my project improve our understanding of how the P2X4R Ca^{2+} channel regulates lysosome function.

Contents

1. Introduction	1
1.1.1. The discovery of ATP as a signaling molecule	1
1.1.2. Mechanism of ATP release	3
1.1.3. Mechanism of ATP degradation	3
1.2. Purinergic receptors	3
1.2.1. P1 receptors	4
1.2.2. P2Y receptors	4
1.2.3. P2X receptors	5
1.3. Heteromerisation of P2X receptors	6
1.4. Crystal structure of P2XR	7
1.5. The functional properties and tissue distribution of P2XRs	11
1.5.1. P2X1R	11
1.5.2. P2X2R	12
1.5.3. P2X3R	12
1.5.4. P2X4R	13
1.5.5. P2X5R	14
1.5.6. P2X6R	14
1.5.7. P2X7R	15
1.6. P2X-like receptor in <i>Dictostylium</i>	17
1.7. P2XR pharmacological properties	18
1.8. P2XR modulators	21
1.9. Structure function analysis of P2X4 receptors	23
1.10. Trafficking and targeting of P2X4R	23
1.11. Physiological and pathological roles of P2X4R	24

1.12. A role for lysosomal P2X4R in lung alveolar type II cells	26
1.13. Lysosome structure	27
1.14. The function of lysosomes	28
1.14.1. Autophagy	29
1.14.2. The molecular mechanisms of autophagy	29
1.14.3. Autophagy in disease	32
1.15. Lysosome dysfunction and disease	33
1.16. Regulation of lysosome acidification	34
1.17. The mechanisms of lysosome fusion	35
1.18. Lysosomes contain ATP	38
1.19. Lysosomes as intracellular Ca²⁺ stores	38
1.20. P2X4Rs function as a Ca²⁺ release channel	42
1.21. Cytosolic Ca²⁺ signalling and the ER	44
1.21.1. Ion channels in the ER	44
1.21.2. Ca²⁺ signalling between the ER and lysosomes	44
2. Thesis Aim	50
3. Material & Methods	51
3.1. Cell culture	51
3.1.1. Cell lines	51
3.1.2. Cell maintenance	51
3.1.3. Isolation and culture of bone derived macrophages (BMDM)	52
3.1.4. Transfection	52
3.2. Cell based assays	53
3.2.1. Single cell Ca²⁺ imaging	53
3.2.2. Analysis of Ca²⁺ signals in cell population	55

3.2.3. Pulse chase analysis	55
3.2.4. Lysosome position analysis	56
3.2.5. Lysosome size analysis	56
3.3. Biochemistry	56
3.3.1. Analysis of protein expression	56
3.3.2. Western blot	57
3.3.3. Surface biotinylation proteins	58
3.3.4. Immunocytochemistry	59
3.4. Molecular biology	60
3.4.1. Point mutation of P2X4	61
3.4.2. Bacteria transformation	62
3.4.3. Miniprep of DNA	63
3.4.4. Sequencing of P2X4 mutants	63
3.4.5. Gibson assembly of ligation of human P2X4	63
3.5. Confocal Microscopy	63
3.6. Data analysis	65
4. Investigating the role of P2X4R in lysosome function	66
4.1. Introduction	66
4.2. Results	67
4.2.1. Characterisation of the subcellular distribution of wild type and mutant P2X4R in NRK and HeLa cells	67
4.2.2. Role of P2X4R in the endocytosis pathway	74
4.2.3. Pharmacological alkalinisation of lysosomes induces lysosome fusion	76
4.2.4. A comparison of homotypic lysosome fusion in	79

macrophages from WT and P2X4 ^{-/-} mice	
4.2.5. The role of the P2X7R in promoting P2X4R-dependent lysosome fusion	81
4.2.6. The effect of P2X4R and P2X7R on the subcellular distribution of lysosomes	90
4.2.7. The synergistic role of P2X4R and P2X7R in lysosome fusion is Ca ²⁺ dependent	93
4.2.8. P2X7R stimulation induces lysosomal alkalinisation that is dependent on extracellular Ca ²⁺	95
4.2.9. Cytoplasmic Ca ²⁺ signals generated by P2X4R and P2X7R	98
4.3. Investigating role of H1R in P2X4R regulation	103
4.3.1. Effect of H1R activation in lysosome fusion	103
4.3.2. H1R activation alkalinises lysosome pH	105
4.3.3. A synergistic interaction between H1R and P2X4R contributes to cytoplasmic Ca ²⁺ signaling	107
4.3.4. Effects of enhanced expression of P2X4R on ER Ca ²⁺ content	112
4.3.5. Investigating effect of P2YR and P2X4R in Ca ²⁺ regulation	114
4.3.6. Effect of lysosome Ca ²⁺ content depletion in P2X4R expressing cells	121
4.4. Discussion	123
5. Investigating a role for P2X4R in autophagy	133
5.1. Introduction	133
5.1.1. P2X7R and autophagic flux	133
5.1.2. Assays and interpretations of autophagy	134

5.2. Material & Methods	136
5.2.1. Cell lines	136
5.2.2. Cell maintenance	136
5.2.3. Cells sorting	136
5.2.4. Autophagy assay	137
5.3. Results	138
5.4. Discussion	147
6. Characterisation of the subcellular distribution of human and rat P2X4R	153
6.1. Introduction	153
6.2. Results	154
6.3. Discussion	166
7. Conclusion	169
7.1. Potential effects of P2X4R in health and diseases	172
8. Future Directions	177
8.1. The effect of lysosomal P2X4Rs in exocytosis	177
8.2. The effect of P2X4/7Rs in autophagy	177
8.2.1. The effect of P2X4/7Rs in autophagolysosome degradation	177
8.2.2. Determining the Ca²⁺ dependence of LC3-II accumulation	179
8.3. The sub-cellular distribution of human and rat P2X4R	179
9. Bibliography	181

Lists of abbreviations

2-MeSATP	2-Methylthioadenosine-5'-triphosphate
AD	Alzheimer's disease
ADP	adenosine diphosphate
AMP	adenosine monophosphate
ATG	autophagy related protein
AT-II cells	alveolar type-II epithelial cells
ATP	adenosine 5'-triphosphate
Baf-A1	bafilomycin-A1
BAPTA	1,2-bis-(o-aminophenoxy)ethane-N,N,N',N'-tetra-acetic acid
BDNF	brain-derived neurotrophic factor
BMDMs	bone marrow derived macrophages
BSA	bovine serum albumin
BzATP	2',3'-O-(4-benzoyl-benzoyl)-ATP
cADPR	cyclic ADP-ribose
CaM	calmodulin
cAMP	cyclic adenosine monophosphate
CAX	Ca ²⁺ /H ⁺ exchangers
CV	contractile vacuole
DMEM	Dulbecco's modified Eagle's medium
DR	Texas Red 10-kDa Dextran
EBSS	Earle Balance Salt Solution
EDTA	ethylene di-amine tetra-acetic acid
EGFP	enhanced green fluorescence protein

ER	endoplasmic reticulum
FACE	fusion-activated Ca ²⁺ entry
FBS	fetal bovine serum
FITC	fluorescein isothiocyanate
GPCR	G protein coupled receptor
GPN	glycyl-L-phenylalanine-betanaphthylamide
H1R	histamine-1 receptor
HEK	human embryonic kidney
HEK293	human embryonic kidney
HeLa	Human cervical cell line
HOPs	homotypic fusion and vacuole fusion protein sorting
HRP	horse radish peroxidase
IL	interleukin
IP ₃ R	inositol 1,4,5 triphosphate receptor
IPC	ischemic preconditioning
LAMP	lysosomal associated membrane protein
LBs	lamellar bodies
LC3	microtubule-associated protein light chain 3
LDL	low-density lipoprotein
LE	late endosome
LMP	lysosomal membrane permeabilisation
LPS	lipopolysaccharide
LSD	lysosomal storage disease
MA	methylamine

MLIV disease	mucopolipidosis type IV disease
mRFP	monomeric red fluorescence protein
mTORC1	mammalian target of rapamycin complex 1
NAADP	nicotinic acid adenine dinucleotide phosphate
NES	normal extracellular solution
NPC	Niemann-Pick type C
NRK	normal rat kidney
OG	Oregon Green 488 10-kDa Dextran
P2XR	P2X receptor
P2YR	P2Y receptor
PAGE	polyacrylamide gel electrophoresis
PAMP	pathogen-associated molecular pattern
PBS	phosphate buffered saline
PE	phosphatidylethanolamine
PEI	Poly-ethyl enimine
PFA	paraformaldehyde
PGE2	prostaglandin E2
PI(3,5)P ₂	phosphatidylinositol 3,5-bisphosphate
PI(4,5)P ₂	phosphatidylinositol 4,5-biphosphate
PI ₃	phosphatidyinositol-3
PLC	phospholipase C
PMSF	phenylmethylsulfonyl fluoride
PNI	peripheral nerve injury

PPADs	pyridoxalphosphate-6-azophenyl-2,4-disulphonic acid
PS1	presenilin1
RPE	retinal-pigmented epithelium
RyR	ryanodine receptor
SDS	sodium dodecyl sulphate
SERCA	sarco/endoplasmic reticulum Ca ²⁺ -ATPase
SNARE	soluble <i>N</i> -ethylmaleimide-sensitive fusion protein attachment protein receptors
SOC	store-operated Ca ²⁺
TIRF	total internal reflection fluorescence
TLR	toll-like receptor
TM	transmembrane
TNP-ATP	2,3'-O-(2,4,6-trinitrophenyl)-ATP
TPC	two pore channel
TRPML	transient receptor potential Mucolipin
UDP	uridine diphosphate
UTP	uridine-5'-triphosphate
VAMP	vesicle associated membrane protein
V-ATPase	vacuolar-type H ⁺ -ATPase
Vps	vacuolar protein sorting
WT	wild type
zfP2X4R	zebra fish P2X4 receptor
β-Hex	beta hexosaminidase

1. Introduction

1.1. The discovery of ATP as a signaling molecule

Adenosine 5'-triphosphate (ATP) is a universal energy carrier within cells (**Fig. 1**). ATP was first discovered in 1929 and isolated from liver and muscle tissues by Karl Lohmann (Lohmann, 1929). In 1937, Hans Krebs described a key cellular process, the citric acid cycle that generates ATP during aerobic respiration (Krebs, 1937). Subsequently, ATP was shown to function as the main energy source within cells by Fritz Lipmann (1936-1941) (Sacktor, 1955; Singleterry et al., 2014). The ability of ATP to store and release energy is mainly due to the presence of energy-rich phosphate bonds, such that hydrolysis of ATP to adenosine diphosphate (ADP) and adenosine monophosphate (AMP) generates energy for cellular functions such as muscle contraction (Jarvis and Khakh, 2009; Sacktor, 1955). These ideas were quickly accepted and later in 1953 both scientists, Hans Krebs and Fritz Lipmann, shared the Nobel Prize in Physiology or Medicine.

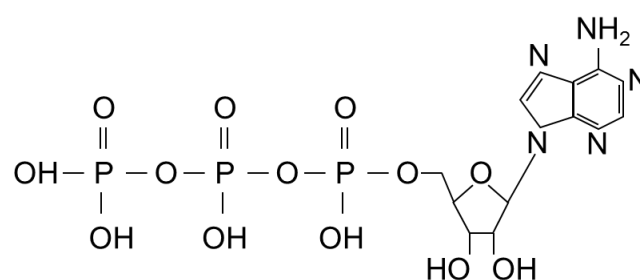


Figure 1 The chemical structure of ATP (adenosine 5'-triphosphate).

The idea proposed by Geoffrey Burnstock that ATP also functions as a signalling molecule was not so readily accepted. The first evidence indicating extracellular

adenine as a signalling molecule was shown in the cardiovascular system. Drury and Szent-Gyorgyi showed that the intravenous injection of adenine compounds induced bradycardia, disruptions in the conduction of cardiac excitation waves and the dilation of coronary arteries (Drury and Szent-Györgyi, 1929). Following this study, ATP was recognised to play a role at the neuromuscular junction where it was shown to potentiate the effects of acetylcholine (ACh) in producing skeletal muscle contraction (Buchthal and Folkow, 1948). Emmelin and Feldberg (1948) also demonstrated complex effects in response to the intravenous injection of ATP into cats, including circulatory, respiratory and muscle reflex responses. Furthermore, ATP was shown to be released from sensory nerves to produce vasodilation of rabbit ear arteries (Holton, 1959).

In 1962, Geoffrey Burnstock and colleagues showed effects of ATP in neurotransmission within the gastrointestinal tract and went on to describe its actions in mediating relaxation of the smooth muscle of the ileum (Burnstock et al., 1970). ATP was thus described as a neurotransmitter to mediate non-adrenergic and non-cholinergic transmission within the autonomic nervous system. Burnstock suggested that ATP satisfied all the criteria for it to be classified as a neurotransmitter, as originally proposed by Henry Dale: It can be synthesised and stored in nerves, exogenous application binds and activates the post-synaptic receptors, and enzymatic inactivation or uptake of neurotransmitter takes place. Two year later, Geoffrey Burnstock proposed the Purinergic Hypothesis describing ATP as a neurotransmitter that binds to purinergic receptors (Burnstock, 1972).

1.1.1. Mechanism of ATP release

In neuronal cells, ATP is stored in synaptic vesicles and released via exocytosis in response to depolarisation of the nerve terminal (Reichardt and Kelly, 1983). Exocytic release of ATP also occurs in many other cells including pancreatic acinar cells, hepatocytes and glial cells (Fitz, 2007; Krause et al., 1996). Additionally, ATP can be released via channels in the membrane such as the pannexin-1 hemichannel (Bao et al., 2004). Mechanical stress has been shown to activate the plasma membrane pannexin-1 receptor to enable ATP release to the extracellular environment (Bao et al., 2004). Under pathological conditions such as hypoxia, inflammation, and following mechanical injury it is also likely that uncontrolled ATP release occurs because of cell lysis. This is thought to contribute to a massive upregulation of purinergic signalling.

1.1.2. Mechanism of ATP degradation

Ecto-nucleotidases are enzymes that hydrolyse nucleotides in the extracellular environment (Robson et al., 2006). They are sub-classified into four classes including the ecto-nucleoside triphosphate diphosphohydrolases (ENTPDase), ecto-5'-nucleotidase (eN), ecto-nucleotide pyrophosphatase/phosphodiesterases (E-NPPs), and alkaline phosphatases (APs) (Zimmermann et al., 2012). Rapid ATP breakdown by ecto-nucleotidases ensures the localised action of purinergic signalling and the availability of ADP and adenosine for cell signalling (Zimmermann et al., 2012).

1.2. Purinergic receptors

Purinergic receptors are classes as either P1, which are activated by adenosine, or P2, which are activated by ATP and ADP. P2 receptors are sub-categorised into two distinct families; ionotropic P2X receptors (P2XRs) and metabotropic P2Y receptors

(P2YRs). Early on, receptor classification was based upon differences in pharmacological and kinetic properties (Burnstock and Kennedy, 1985). P2T receptors were described which were selective for ADP and expressed in platelets, but these were later shown to be a subtype of P2Y receptors. Similarly, P2U, were described as activated by pyrimidines like UTP, but these were also shown later to be a subtype of P2Y receptor (Burnstock, 2006; Gordon, 1986). We now know that within the family of P2Y receptors are GPCRs gated by ATP, ADP, UTP, UDP and UDP-glucose. It was not until the early 1990s, that the first P2Y purinergic receptor was cloned by Eric Bernard's group, and later Alan North and Ann-Marie Surprenant's group cloned the first P2X receptor (Valera et al., 1994; Webb et al., 1993).

1.2.1. P1 receptors

P1 receptors are also known as adenosine receptors (A receptors). Four subtypes have been identified: A₁, A_{2A}, A_{2B}, and A₃ receptors. Both A_{2A} and A_{2B} receptors are G_{αs}-coupled GPCRs and stimulate adenylyl cyclase activity, whereas A₁ and A₃ receptors couple to G_{αi} and inhibit adenylyl cyclase activity. Adenosine receptors are mainly found in the respiratory, nervous, and cardiovascular systems (Burnstock, 2006). They exert a cytoprotective role, including protection from ischemia, maintaining oxygen demands and triggering anti-inflammatory responses. Therefore, adenosine receptors are potential therapeutic targets for cardiovascular and inflammatory diseases (Jacobson and Gao, 2006).

1.2.2. P2Y receptors

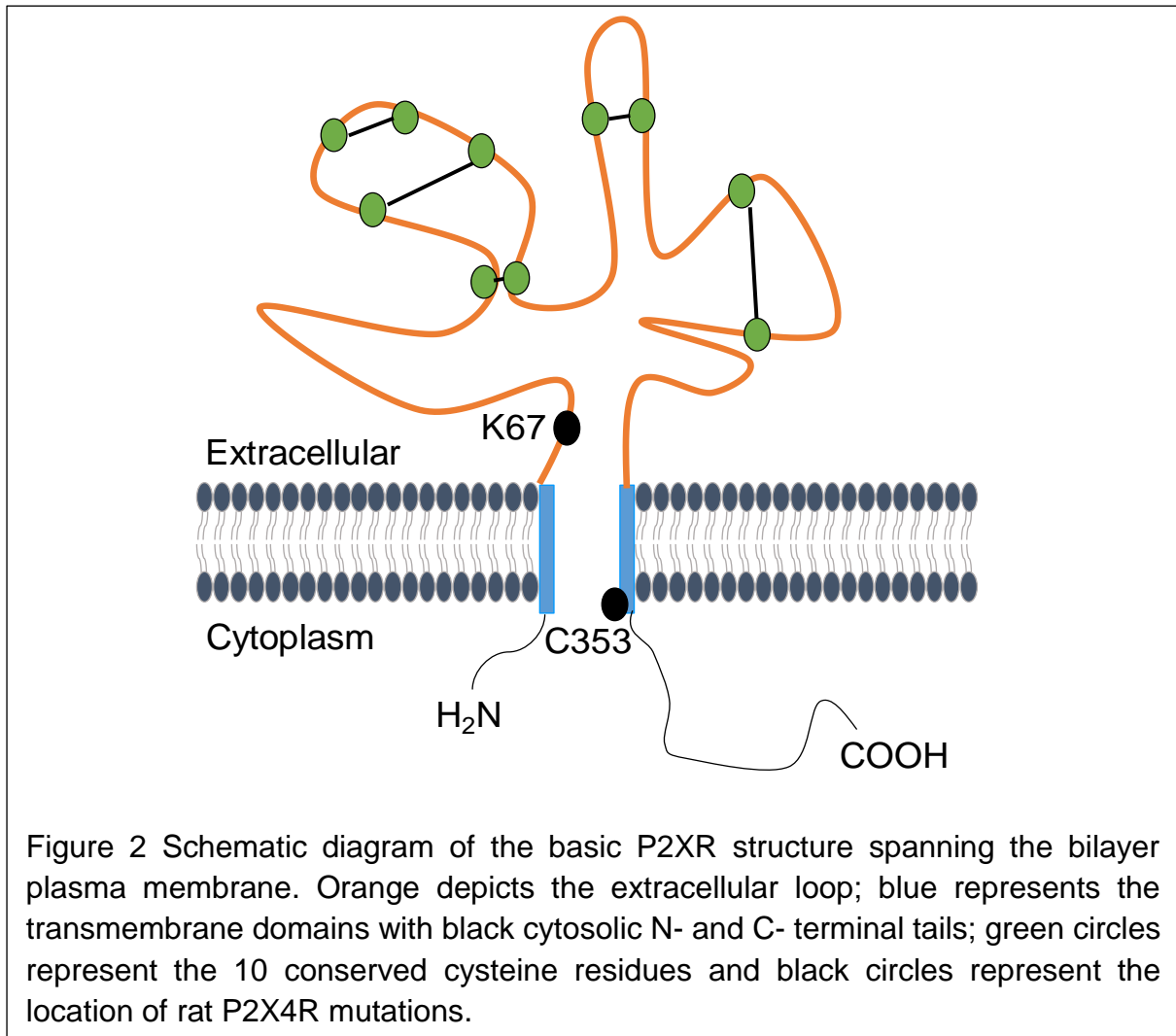
There are 8 subtypes of P2YR which share the same general structure of seven transmembrane domains, an extracellular N-terminus and intracellular C-terminus.

P2Y₁R, P2Y₂R, P2Y₄R, P2Y₆R and P2Y₁₁R are G_{αq}-coupled GPCRs that activate PLC, whereas P2Y₁₂R, P2Y₁₃R and P2Y₁₄R are G_{αi}-coupled GPCRs that inhibit adenylyl cyclase. With regards to their activation, P2Y₁R, P2Y₁₂R and P2Y₁₃R are activated by ADP with an EC₅₀ of 100 nM, P2Y₁₁R is activated by ATP, and P2Y₂R and P2Y₄R are nearly equipotently activated by UTP and ATP. However, P2Y₄R is preferentially activated by uracil nucleotides (Abbracchio et al., 2006), P2Y₆R and P2Y₁₄R are activated by UDP, and lastly P2Y₁₄R is activated by UDP-glucose (Jacobson et al., 2015). P2YRs are widely distributed in many different cell types, including, platelets, osteoclasts, endothelial and immune cells to mediate a wide array of physiological functions.

1.2.3. P2X receptors

P2XRs have a trimeric structure with a central pore that allows sodium (Na⁺), potassium (K⁺) and calcium (Ca²⁺) ions to permeate following agonist activation (Saul et al., 2013). The subtypes share less than 50 % similarity in their amino acid sequences and their length varies from 379 to 595 amino acids, with P2X₇R being the longest (Gever et al., 2006) and P2X₄R fairly short at 384 amino acids (North, 2002). All receptors share a similar overall structure, with each subunit having a large extracellular domain, two transmembrane domains and cytoplasmic N- and C-termini (**Fig. 2**). The extracellular loop is the largest component of the receptor and contains 10 cysteine residues, which form disulphide bonds and are conserved in all P2XR subtypes (North, 2002). The extracellular domain is the key component for the binding of agonists, antagonist, and allosteric ligands that modulate the activity of P2XRs. The N-terminal tail of P2XRs is relatively short, ranging between 20 to 30 amino acid residues. In contrast, the length of C-termini of P2XRs differs from approximately 30

amino acid residues in P2X6R to 236 residues in P2X7R (Kaczmarek-Hájek et al., 2012).



1.3 Heteromerisation of P2X receptors

P2XRs are either homotrimers or heterotrimers, and subunit composition dictates receptor function. Only P2X6R is unable to form functional homotrimers (Torres et al., 1999). Thus far, heterotrimers that have been characterised include P2X1/2R, P2X1/4R, P2X1/5R, P2X2/3R, P2X2/6R, and P2X2/6R (Coddou et al., 2011). Even though P2X7R does not appear to form heterotrimers (Torres et al., 1999), there is

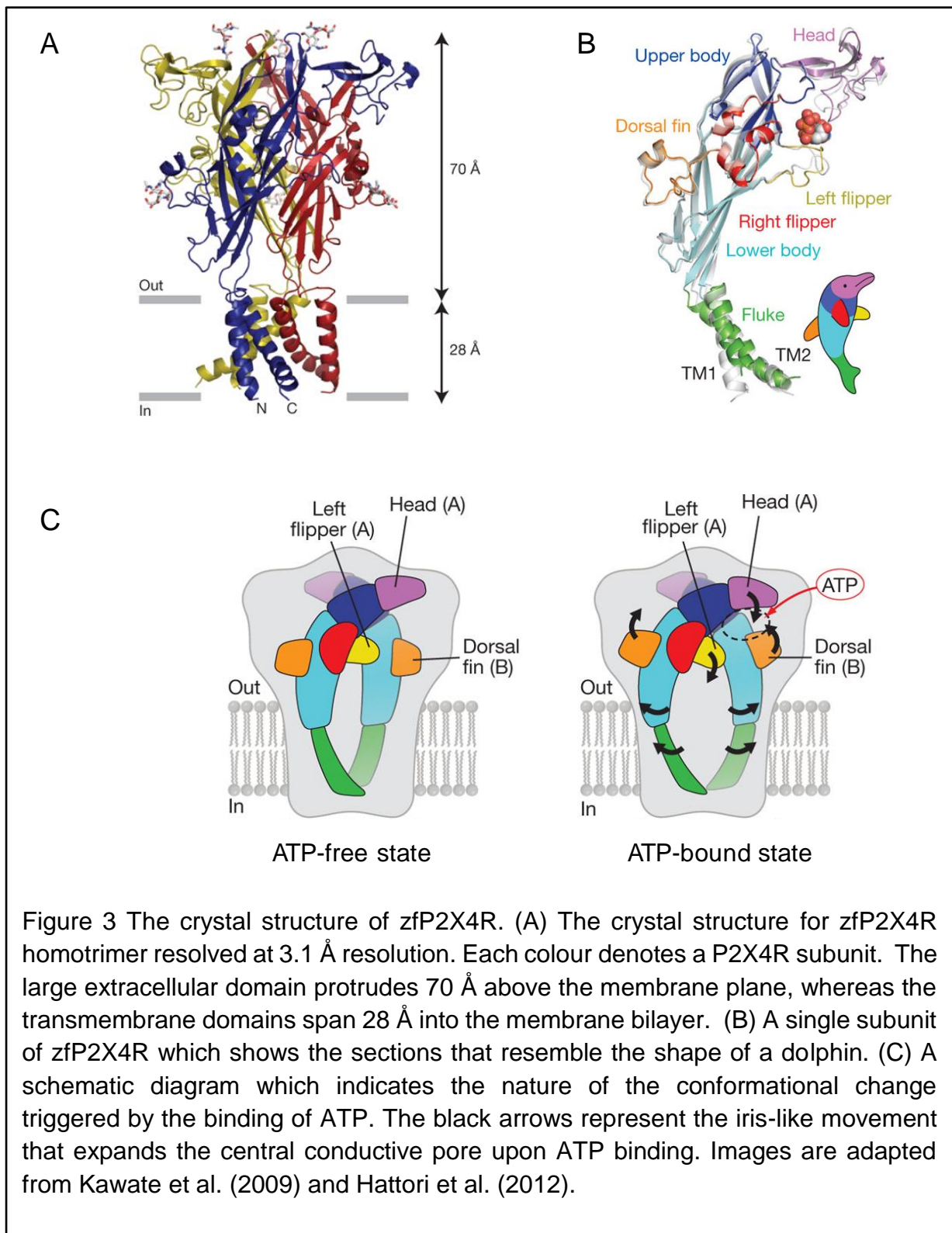
evidence showing that P2X7R homotrimers interact with P2X4R homotrimers (Antonio et al., 2011; Boumechache et al., 2009; Guo et al., 2007). In addition to heterotrimerisation, there is evidence that P2XR can form higher order complexes including dimers of trimers and trimers of trimers (Nicke et al., 1998; Torres et al., 1999). Receptor density has been shown to affect receptor gating properties, perhaps because of the formation of these stable higher order complexes (Fujiwara and Kubo, 2004).

1.4 Crystal structure of P2XR

The crystal structure of zebra fish P2X4R (zfP2X4R) was the first to be described by Kawate et al. (2009) at 3.1 Å resolution (**Fig. 3A**). zfP2X4R was crystallised in an ATP-free state with N- and C- termini truncated to aid crystallisation. The overall architecture of the zfP2X4R subunit was described as resembling the shape of a dolphin, with the large extracellular domain as the head region with both upper and lower bodies and transmembrane domain akin to the fluke (**Fig. 3B**). The large extracellular domain protrudes ~70 Å above the membrane plane and is enriched with disulphide bonds. The transmembrane α -helices span ~28 Å and are oriented in an anti-parallel manner which angles ~45° away from the membrane plane. The study proposed two ion access pathways, the first mediated through fenestrations located within the extracellular domain close to the transmembrane domains. The second was suggested as the central pore of the homotrimer, with activation of the receptor resulting in an enlargement of this opening to allow ion flux (Kawate et al., 2009). Kawate et al. (2009) speculated that the ATP binding site is located in a deep groove at the interface between each subunit and this was supported by evidence from mutagenesis studies which indicated an important role for eight amino acids that are

highly conserved throughout the P2XR family. Of these, Lys 70 (rat P2X4R is K67), Lys 72, Thr 189, Asn 296, Arg 298 and Lys 316 were shown to extend towards the proposed ATP binding groove, suggesting they could have a crucial role in ATP binding (Jiang et al., 2000; Kawate et al., 2009; Roberts et al., 2008).

Later, the same group published the crystal structure of zfP2X4R in an open, ATP-bound state (Hattori and Gouaux, 2012). This provided substantial information about the structural changes that occur upon agonist binding and the residues that line the open pore. This direct comparison of ATP-free and ATP-bound states demonstrated that the ATP-binding pocket is indeed located ~ 40 Å from the transmembrane domains. The adenine base of ATP is recognised by Thr 189, which forms hydrogen bonds located deep within the ATP binding pocket. Furthermore, the study showed that Lys 70 forms a crucial interaction with the triphosphate group which resides at the centre of the ATP structure (Hattori and Gouaux, 2012). The upper body of the extracellular domain is comprised of β sheets that are expected to be rigid and resistant to conformational change (Kawate et al., 2009). A substantial difference observed in the ATP-bound state was that the lower body domain flexed outwards. This in turn expanded the transmembrane helices away from the central axis, thereby increasing the opening between the ion-conducting second transmembrane domains (TM2) (Hattori and Gouaux, 2012). Specifically, TM1 and TM2 rotate anti-clockwise away from the central axis of P2X4R, an iris-like movement, thereby expanding the conductive pore. The central conduction pore is highly acidic, which attracts cations and repels anions thus explaining the cation selective permeability of P2X4Rs (Hattori and Gouaux, 2012).



Recently, the crystal structures of P2X3R and P2X7R were also published. The human P2X3R (hP2X3R) was crystallised in several states, including apo/resting, an agonist-bound/open-pore, an agonist-bound/closed-pore/desensitised, and two antagonist-bound/closed states (Mansoor et al., 2016). This study provides a detailed insight into several aspects of the structure. Importantly the construct used for crystallisation included more of the cytoplasmic domain than the previously solved zfP2X4 structure. It is evident that the proximal cytoplasmic domains form a structure that plays a key role in the gating of the receptor. The open state of hP2X3R shows a feature whereby the cytoplasmic residues form into a domain called the 'cytoplasmic cap'. This cap includes β -strands from both termini, which associate to form a structure at the cytoplasmic surface of the central pore. This cap is only visible in the ATP-bound open state and not in the apo or desensitised states of hP2X3R indicating a role in regulating the stability of the open state. They generated a chimeric construct that included N-terminus of P2X2R substituted for the equivalent region of P2X3R, and, unlike wild type P2X3R, this chimera desensitised slowly. This mutant exhibited a rigid cap with several hydrophobic bonds that stabilised its cytoplasmic cap structure, indicating an association between the stability of this domain and the rate of desensitisation.

In the same year, Karasawa and Kawate (2016) crystallised P2X7R from panda (*Ailuropoda melanoleuca*) (pdP2X7R). pdP2X7R was solved at ~ 3.5 Å and obtained in the apo state, co-crystals of ATP with the antagonist state, and the antagonist-only state. Overall, pdP2X7R shares the similar dolphin-like architecture of zfP2X4R and at the amino acid level it has 45 % similarity with zfP2X4R and 38 % similarity with hP2X3R. In analysing pdP2X7R, they identified an allosteric site where several known antagonists bind, which is proximal to the ATP binding pocket. There are 13 residues surrounding this allosteric site which protrudes from β -sheets ($\beta 4$, $\beta 13$ and $\beta 14$) in the

upper body domain of the neighbouring subunits and is referred to as a 'turret-like' structure. The turret-like structure and inter-subunit cavity are much narrower in zfP2X4R and hP2X3R than in pdP2X7R. A series of cysteine mutations were introduced in the drug-binding cleft and at least four residues (F103C, K110C, T308C, and I310C) were identified where modification by a large cysteine-reactive agent was sufficient to hinder the ATP-mediated conformation change required for channel activation (Karasawa and Kawate, 2016). Narrowing of the turret-like structure upon ATP binding appears to be required for P2X7R activation. However, the presence of an antagonist locks the inter-subunit cavity and turret-like structure diameter, thus hindering the movement of the pore-lining helices for channel opening. Similarly, in the ATP-bound open state, this allosteric site becomes relatively inaccessible to antagonists suggesting that they might not be effective inhibitors at high ATP concentrations.

1.5 The functional properties and tissue distribution of P2XRs

1.5.1 P2X1R

P2X1R has the highest affinity for ATP of all P2XRs, with an EC₅₀ of ~1 μM (Coddou et al., 2011). After activation, P2X1R exhibits fast desensitisation with a slow recovery period. Following agonist stimulation, P2X1R permeates cations with relatively high Ca²⁺ permeability over Na⁺ ($P_{Ca}/P_{Na} = \sim 4.5$). P2X1R is predominantly expressed in smooth muscle cells and platelets, such that P2X1R knockout mice demonstrate a reduction in thrombus formation and platelet aggregation, suggesting a key role for P2X1R in thrombosis (Hechler et al., 2003). In addition to platelet function, P2X1R also plays a crucial role in the contraction of the vas deferens, as demonstrated by male P2X1R knockout mice being infertile not due to lack of sperm production, but

rather an inability to get them to ejaculate (Mulryan et al., 2000). A role for P2X1R has also been demonstrated in the autoregulation of renal blood flow and the vasoconstriction of preglomerular arteries and afferent arterioles. Administration of the P2X1R antagonist, NF279 inhibited the effect of pressure-regulated afferent constriction in afferent arterioles (Guan et al., 2007). In addition, inhibition of P2X1R, using either the non-selective antagonist PPADS or the P2X1R specific antagonist IP5I, reduced the glomerular filtration rate, thus further implicating P2X1R in renal autoregulation (Osmond and Inscho, 2010; 2009).

1.5.2 P2X2R

P2X2R is activated by ATP with an $EC_{50} < 10 \mu\text{m}$ and exhibits slow desensitising kinetics. Following activation, P2X2R permeates cations, but with a lower Ca^{2+} permeability than P2X1R, $P_{\text{Ca}}/P_{\text{Na}} = \sim 2.5$. P2X2R is abundantly expressed in the central and peripheral nervous systems, but is also widely distributed in non-neuronal tissues, including smooth muscle, urothelium, the carotid bodies and the adrenal medulla. P2X2R is involved in various sensory functions including taste (Eddy et al., 2009; Finger et al., 2005), hearing (Housley et al., 2002) and chemosensing (Rong et al., 2003). A key role for P2X2R in chemosensation is shown by P2X2R-deficient mice failing to increase their ventilatory response to hypoxia. P2X2R-null mice also exhibited impaired intestinal peristalsis (Ren et al., 2003), demonstrating a role of P2X2R in enteric neurotransmission.

1.5.3 P2X3R

P2X3R is activated by ATP with an EC_{50} of $< 10 \mu\text{m}$, and following agonist stimulation, P2X3R generates a fast inward current that rapidly desensitises. The activation of

P2X3R results in a cation influx with similar permeability towards both Ca^{2+} and Na^{+} ($P_{\text{Ca}}/P_{\text{Na}} = \sim 1.2$). P2X3R is expressed in heart, spinal cord, dorsal root ganglia, intestine and urinary bladder (Elneil et al., 2001; Garcia-Guzman et al., 1997; Liu et al., 2009). Two independent knockout studies have demonstrated a role of P2X3R in nociception, both demonstrating that the lack of P2X3R attenuated the formalin-induced pain response (Cockayne et al., 2000; Souslova et al., 2000). Additionally, knockdown of P2X3R using short interfering RNAs (siRNAs) inhibited the development of hyperalgesia in neuropathic pain models (Barclay et al., 2002; Dorn et al., 2004). Given the expression of P2X3R in urothelium and suburothelium, P2X3R has been implicated in sensing urinary bladder distension. Mice lacking P2X3R exhibit decreased voiding frequency and an increased bladder capacity, thus indicating a role of P2X3R in physiological conditions (Cockayne et al., 2000, 2005). P2X3R has also been implicated in afferent cardiovascular signalling where it has been detected in aortic bodies in juvenile and adult rats (Ford et al., 2015). Lastly, P2X3R has also been shown to mediate a pivotal role in carotid body chemoreception where it forms heterotrimers with P2X2R (Ford et al., 2015).

1.5.4 P2X4R

P2X4R is activated by ATP with an EC_{50} ranging from 1-10 μM (Bernier et al., 2008; North, 2002; Surprenant et al., 1996). The binding of ATP opens the ion channel pore which has a very high Ca^{2+} permeability, $P_{\text{Ca}}/P_{\text{Na}} = 4.2$ (Jarvis and Khakh, 2009; Samways et al., 2014). Following agonist stimulation, P2X4R desensitises at a rate that is intermediate between the rapidly desensitising subtypes, P2X1R and P2X3R (within few milliseconds), and the very slowly desensitising subtypes that include P2X2 and P2X7R (> 20 seconds) (Khakh and North, 2012; Roberts et al., 2006). P2X4R is

very widely expressed, including the central and peripheral nervous systems, immune system, endothelial, epithelial, and skeletal, smooth and cardiac muscle (Bo et al., 1995, 2003; Buell et al., 1996; Naemsch et al., 1999; Soto et al., 1996; Xiang and Burnstock, 2005). It has been implicated in neuropathic and inflammatory pain and in vascular remodelling, further details are described in section 1.9 to section 1.12.

1.5.5 P2X5R

P2X5R is predominantly expressed in the immune system and central nervous system (Lê et al., 1997). The human isoform of P2X5R (hP2X5R) lacks both exon 3 and 10, thus encoding a truncated non-functional receptor that is retained in the endoplasmic reticulum (Bo et al., 2003; Kotnis et al., 2010). Despite the lack of plasma membrane hP2X5R, rat P2X5R (rP2X5R) has been shown to be activated by ATP with an $EC_{50} < 10 \mu\text{M}$ to generate rapidly activation with slow desensitisation rate (Coddou et al., 2011).

1.5.6 P2X6R

P2X6R is the only P2XR subtype that does not form a functional homotrimer. However, P2X6R does form functional heteromeric receptors with both P2X2R and P2X4R (Gever et al., 2006), and it is expressed with P2X2R and P2X4R in the central and peripheral nervous systems. However, due to the lack of P2X6R knockout mouse model, the function of the heteromeric receptors remains poorly understood. Although, one study has shown that P2X6R is expressed in myocardial tissues and is upregulated following chronic heart failure (Banfi et al., 2005).

1.5.7 P2X7R

P2X7R is significantly less sensitive to ATP than the other subtypes, with an $EC_{50} > 100 \mu\text{M}$ (Roberts et al., 2006). However, 2',3'-(benzoyl-4-benzoyl)-ATP (BzATP) is a more potent agonist at P2X7R than ATP ($EC_{50} \sim 10 \mu\text{M}$). Unlike other subtypes of P2XR, P2X7R-mediated currents do not desensitise after agonist application (Roger et al., 2008). Instead the prolonged application of a high concentration of agonist sensitises the receptor and facilitates the currents. There is also a change in the selectivity of the pore following sensitisation of the receptor which allows large organic cations (up to ~ 800 Da in size) to permeate. This change in permeability is associated with changes in the downstream signalling that contributes to cell blebbing, and ultimately can lead to cell death (Robinson et al., 2014).

There are species differences in the functional properties of P2X7R. Rat P2X7R (rP2X7R) sensitises faster than human P2X7R (hP2X7R). The rP2X7R has a calmodulin-binding motif within its C-terminal tail and this is known to contribute to receptor sensitisation: activation of rP2X7R increases calmodulin binding, which increases current facilitation, resulting in sensitised P2X7R potentiating the Ca^{2+} influx and a larger conductance (Roger et al., 2008, 2010). hP2X7R has a slower sensitisation than the rat isoforms due to a calmodulin-independent process, the detailed molecular process of which remains unclear (Roger et al., 2010). In addition, presence of cholesterol on the plasma membrane negatively regulate the sensitisation process of human and rodent P2X7R (Robinson et al., 2014). Cholesterol acts to suppress the channel pore opening, particularly large pores, limiting pore dilation and excess activation. There are also distinct species-dependent agonist

sensitivities, such that hP2X7R is comparably less sensitive to ATP and BzATP than the rodent P2X7Rs (Donnelly-Roberts et al., 2009; Rassendren et al., 1997).

Together with P2X4R, P2X7R is expressed in endothelium, microglial and epithelial cells, but P2X7R is also abundantly expressed in lymphocytes, monocytes, and macrophages (Surprenant and North, 2009). The role of P2X7R in the inflammatory response has been extensively studied and P2X7R is implicated in both chronic inflammatory and neuropathic pain. Mice in which P2X7R is knocked out show attenuated inflammatory and neuropathic pain phenotypes (Chessell et al., 2005; Honore et al., 2006, 2009). Furthermore, the activation of P2X7R induces the release of pro-inflammatory cytokines IL-1 β from microglial cells (Di Virgilio, 2007; Ferrari et al., 1997). One inducers of IL-1 β release is lipopolysaccharide (LPS), a pathogen-associated molecular pattern (PAMP) molecule. When LPS binds to toll-like receptors (TLRs) on macrophages, the inactive pro-IL-1 β accumulates in the cytoplasm, a process known as priming. Subsequently, ATP-dependent activation of P2X7R facilitates the conversion of pro-IL-1 β into mature IL-1 β and the release of the mature IL-1 β into the extracellular space (Ferrari et al., 1997). This process involves P2X7R mediated K⁺ efflux which triggers the assembly and activation of the NOD-like receptor (NLR)P3 inflammasome which in turn activates caspase-1 (formerly known as IL-1 β -converting enzyme) (Franceschini et al., 2015; Mariathasan et al., 2006). P2X7R knockout mice lack the ability to process pro-IL-1 β in response to ATP (Labasi et al., 2002; Solle et al., 2001). IL-1 β is thought to be packaged into either lysosomes or microvesicles, which are located at the vicinity of plasma membrane, and released via lysosomes exocytosis (Andrei et al., 2004; Dubyak, 2012) or microvesicle release (Bianco et al., 2005; MacKenzie et al., 2001).

1.6 P2X-like receptor in *Dictostylium*

A homologue of P2XR is found in the amoeba *Dictyostelium discoideum* and is called P2XAR. P2XAR localises within contractile vacuoles (CVs), which share some similarities with lysosomes (Fountain et al., 2007; Ludlow et al., 2009). Properties of P2XAR in *D. discoideum* suggest that mammalian P2XRs may have evolved as a receptor in intracellular compartments rather than at the plasma membrane. Functional studies have demonstrated that P2XAR is an ATP-gated cation channel ($EC_{50} \approx 100 \mu\text{M}$) that has a high Ca^{2+} permeability ($P_{\text{Ca}}/P_{\text{Na}} = \sim 2$) (Fountain et al., 2007; Ludlow et al., 2009). The CV is a lysosome-like organelle with an acidic luminal pH and high Ca^{2+} concentrations, which regulates osmoregulation of *D. discoideum* (Fountain et al., 2007). P2XAR is involved in osmoregulation by facilitating vacuole fusion followed by CV discharge under hypo-osmotic conditions (Parkinson et al., 2014). P2XAR facilitates the fusion between mature CVs and the plasma membrane of *D. discoideum* as demonstrated by P2XAR-null mutant causing an accumulation of tethered CVs to the plasma membrane without fusion (Parkinson et al., 2014). In response to ATP stimulation, P2XAR generates a localised Ca^{2+} signal in the immediate vicinity of the CV, which activates the Ca^{2+} sensitive Rab GAP to suppress the activity of Rab11a on the CV, thereby facilitating vacuole fusion with the plasma membrane. This is because the active Rab11a, Rab11s-GTP binds to drainin, thereby blocking drainin redistribution that is required for the fusion of vacuolar membrane to cellular surface (Parkinson et al., 2014). Interestingly, P2X4R is localised to lysosomes and thus, this model suggests that the lysosomal localisation of P2X4R in mammalian cells might represent a conserved mode of action to regulate the vesicle trafficking.

1.7 P2XR pharmacological properties

The pharmacological properties of different P2XRs reveal important differences, not least in sensitivity to ATP as mentioned previously. These differences are summarised in Table 1. P2X1R, P2X3R and P2X5R are activated by sub-micromolar concentrations of ATP whereas P2X2R and P2X4R are activated by low micromolar ATP concentrations. P2X7R however requires very high concentrations of ATP ($EC_{50} > 100 \mu\text{M}$; Roberts *et al.*, 2006). There are other agonists including BzATP, which is reasonably selective for P2X7R (EC_{50} of $\sim 10 \mu\text{M}$ for rP2X7R and EC_{50} of $\sim 100 \mu\text{M}$ for hP2X7R) (North, 2002; Rassendren *et al.*, 1997) but also acts as a partial agonist at P2X1R, P2X2R, P2X3R and P2X4R. With regards to the potency of BzATP against P2X4R, one study suggested a low EC_{50} for BzATP ($\sim 10 \mu\text{M}$) at rP2X4R (He *et al.*, 2003) but others have reported a much higher EC_{50} of $> 100 \mu\text{M}$ (Abdelrahman *et al.*, 2017; Guo *et al.*, 2007). However, others have used both a Ca^{2+} influx assay and patch clamp recordings, and found no response was observed following $100 \mu\text{M}$ BzATP administration to astrocytoma and HEK293 cells expressing rP2X4R, respectively (Abdelrahman *et al.*, 2017; Guo *et al.*, 2007). Unlike rP2X4R, mouse and human P2X4Rs are reported to have lower EC_{50} s of $\sim 3 \mu\text{M}$ and $< 1 \mu\text{M}$, respectively, for BzATP (Abdelrahman *et al.*, 2017). Another non-selective agonist is 2-methylthio-ATP (2-MeSATP) which is only a partial agonist at P2X4R and P2X7R, but it is a full agonist for the rest of the P2XR subtypes.

In terms of antagonists, suramin is a non-selective antagonist of all P2XRs and P2YRs (Jones *et al.*, 2000; Soto *et al.*, 1996), although, both P2X4R and P2X7R are relatively insensitive. PPADS is another commonly used P2XR antagonist that blocks P2X1R, P2X2R, P2X3R and P2X5R, but, it is a weak or ineffective antagonist of P2X4R and

P2X7R. PPADS antagonises P2X1, P2X2R, P2X3R and P2X5R with an IC₅₀ of 1-3 μM, whereas it antagonists P2X7R with an IC₅₀ of ~50 μM. As for P2X4R, PPADS exhibits species specific potency, whereby PPADS inhibits mouse and human P2X4R with an IC₅₀ of ~10 μM, rP2X4R is relatively insensitive (IC₅₀ > 100 μM) (Jones et al., 2000; Soto et al., 1996). Studies have proposed that a domain of approximately 100 amino acids between 81 to 183 located in the extracellular domain of rP2X4R may be the cause of species differences in PPADS sensitivity (Garcia-Guzman et al., 1997). TNP-ATP is a non-selective antagonist that inhibits P2X1R, P2X3R, P2X2/P2X3R at nanomolar concentrations, P2X7R with an IC₅₀ of > 30 μM, and also inhibits P2X4R at similar concentrations for human, rat, and mouse orthologues with an IC₅₀ of ~5-15 μM (Virginio et al., 1998).

Table 1. The pharmacological profile of rat P2XRs

Agonists (EC₅₀; μM)	P2X1R	P2X2R	P2X3R	P2X4R	P2X5R	P2X6R	P2X7R
ATP	<1	~1-10	~1-10	10	<10	-	100
BzATP	~0.7- 25	~6-30	0.08	>100	>500	-	~10
2-MeSATP	<1	1	<1	~10- 100 μM	<1	-	~200
Antagonists (IC₅₀; μM)							
Suramin	1-2	10	3	>300	~4	>100	>500
PPADS	1	~1-3	~1	>100	<3	>100	50
TNP-ATP	0.006	2	0.001	~5-15	-	-	>30

Notes: The table are adapted from Jarvis and Khakh, (2009), Coddou et al. (2011) and Khakh and North, (2012).

1.8 P2XR modulators

In term of modulators, the anti-parasitic drug ivermectin is a potent positive allosteric modulator of P2X4R (Khakh et al., 1999). Ivermectin potentiates the agonist potency profile of ATP-induced current mediated by P2X4R ($EC_{50} = \sim 0.25 \mu\text{M}$) (Khakh and North, 2012; Priel and Silberberg, 2004). Binding of ivermectin to the transmembrane domains of P2X4R has been suggested to stabilise the open state of P2X4R, resulting in an increased current (Hattori and Gouaux, 2012; Priel and Silberberg, 2004).

P2XRs can also be modulated by extracellular cations including protons and trace metals. For example, extracellular Mg^{2+} decreases the ATP-induced P2X7R activation (Miyoshi et al., 2010). The presence of extracellular Zn^{2+} acts as an allosteric modulator of all P2XRs, such that the P2X1R and P2X7R ATP-mediated currents are attenuated, but these currents are potentiated for the rest of P2XRs (Coddou et al., 2011). In addition, extracellular Cu^{2+} is a potent modulator of P2X7R, inhibiting currents with an IC_{50} of 0.5-4 μM (Virginio et al., 1998). For P2X2R, Cu^{2+} exhibits a biphasic effect such that it potentiates P2X2R-mediated currents at concentrations between 10 and 100 μM , but exhibits an inhibitory effect at millimolar concentrations (Coddou et al., 2011). ATP-induced currents in P2X4R expressing cells are inhibited by Cu^{2+} , but potentiated by Zn^{2+} , although, Zn^{2+} exhibits a biphasic effect such that low concentrations increase ATP potency, but it decreases ATP efficacy at higher concentrations (30 μM – 1 mM) (Coddou et al., 2011). Cu^{2+} inhibits channel activity of P2X4R by reducing the E_{max} of P2X4R-mediated current (Coddou et al., 2011). There is evidence to suggest that Cu^{2+} binds to histidines, aspartic acid, glutamic acids and cysteine (Aitken, 1999), and H140 in the extracellular domain of P2X4R is crucial for the inhibitory effect of Cu^{2+} (Coddou et al., 2003).

Protons also act as an allosteric modulator of P2XRs, affecting ATP-mediated currents. Extracellular protons enhance the potency of agonists at P2X2R without affecting the maximal agonist responses, such that acidification strongly increases the P2X2R-mediated current following ATP stimulation, but alkalinisation causes strong inhibition of the current (Clyne et al., 2002; Stoop et al., 1997). In contrast, an acidic extracellular environment reduces ATP potency for P2X1R, P2X3R and P2X4R without altering the maximum current amplitude. Despite the reduction in ATP potency, acidification only causes a modest reduction of ATP-mediated current for P2X1R and P2X3R and alkalinisation does not cause any effect in the current. This is different from P2X4R where acidification strongly attenuated ATP-mediated currents, whereas, alkalinisation increases the current, acidification shifted the ATP concentration-response relationship towards higher concentrations of ATP (Stoop et al., 1997). A mutagenesis study has identified the key residue involved in proton modulation of P2X4R, histidine 286. Mutation of this residue to alanine removes the inhibition of P2X4R currents by increasing pH (Clarke et al., 2000). H286 is located away from ATP-binding pocket, suggesting the allosteric modulation by protons may affect the gating of the receptor rather than ATP binding (Coddou et al., 2011). Similarly, acidification reduces both the potency and efficacy of ATP in P2X5R activity, whilst it only reduces the peak current of P2X7R without altering the potency of agonist binding (Gever et al., 2006; Virginio et al., 1998). These modulators provide additional regulators for receptor functioning.

1.9 Structure function analysis of P2X4 receptors

Several mutations within the TM2 domain have been identified of rP2X4R that play a dominant role in the gating of P2X4R. In particular, P2X4R-C353W renders the receptor non-functional and P2X4R-C353W acts in a dominant negative manner to inhibit wild type P2X4R activity suggesting that one subunit with this mutant within the trimeric assembly is sufficient to inhibit receptor function (Guo et al., 2007; Silberberg et al., 2005). P2X4R-K67A is non-functional and it has a mutation in the ATP binding pocket that prevents ATP binding (Silberberg et al., 2005; Stojilkovic et al., 2010). As shown in the crystal structure of ATP-bound zfP2X4R, the residue at Lys 70 of zfP2X4R, which is K67 in the rat isoform, is crucial in ATP binding due to ammonium residues at Lys 70 that are situated at the centre of the triphosphate of ATP where binding occurs in the ATP binding pocket (Hattori and Gouaux, 2012). Both of P2X4R-C353W and P2X4R-K67A are used as controls in this thesis.

1.10 Trafficking and targeting of P2X4R

Plasma membrane P2X4Rs are either rapidly retrieved and targeted to lysosomes, or shuttled between the plasma membrane and lysosomes for recycling of the receptor (Royle et al., 2005). Within the C-terminal domain is a non-canonical tyrosine-based motif (YXXGL, X denotes any amino acid), whilst the N-terminal domain contains a dileucine-like motif, and both of these motifs are important in the endocytosis and targeting of P2X4R to lysosomes (Qureshi et al., 2007; Royle et al., 2002, 2005). Endocytosis of P2X4R involves the AP2 clathrin adaptor protein complex which is responsible for recognising the tyrosine-based motif and the dileucine-like motifs of P2X4R (Royle et al., 2002, 2005).

The trafficking of P2X4R is cell specific. For example, in active microglial cells, P2X4Rs rapidly shuttle between the plasma membrane, late endosomes, and lysosomes (Boumechache et al., 2009), whereas in other cells such as bone marrow derived macrophages (BMDMs), the receptors stably reside in lysosomes (Toulme et al., 2010). Within lysosomes, P2X4R is able to resist degradation due to N-linked glycans that decorate the luminal/extracellular domain of P2X4R (Qureshi et al., 2007). Rapid constitutive endocytosis of P2X4R is mediated via dynamin and clathrin-dependent processes, and it is inhibited by dynasore, an inhibitor of dynamin that is required for clathrin-dependent coated vesicle formation during endocytosis (Royle et al., 2002; Boumechache et al., 2009).

1.11 Physiological and pathological roles of P2X4R

P2X4R is widely expressed in immune, epithelial and endothelial cells (North, 2002; Weinhold et al., 2010). It plays an important role in many different processes, including controlling blood pressure, neuropathic pain, and inflammation. Evidence for its role in neuropathic pain is growing. The first demonstration was the upregulation of plasma membrane P2X4R in microglial cells after peripheral nerve injury (PNI) (Tsuda et al., 2003). The upregulation of P2X4R was associated with tactile allodynia and pharmacological inhibition of P2X4R reversed tactile allodynia (Tsuda et al., 2003; Ulmann et al., 2008). Furthermore, knockout and knockdown studies showed that P2X4R deficiency was sufficient to attenuate the development of tactile allodynia. Moreover, intrathecal delivery of P2X4R-activated microglial cells to naïve mice was sufficient to induce tactile allodynia, supporting the evidence for a role of P2X4R in neuropathic pain (Tsuda et al., 2003). In addition, the upregulation of P2X4R in microglial cells regulates the release of brain-derived neurotrophic factor (BDNF),

which is suggested to modulate hypersensitive pain in PNI mice (Trang et al., 2009; Ulmann et al., 2008). Specifically, enhanced expression of P2X4R in microglial cells results in an increase in Ca^{2+} influx which triggers downstream signalling including p38-MAPK to induce soluble *N*-ethylmaleimide-sensitive fusion protein attachment protein receptors (SNARE)-dependent exocytosis of BDNF (Trang et al., 2009). With regards to inflammatory pain, P2X4R-deficient mice exhibit reduced inflammatory pain behaviour following complete Freund's adjuvant (CFA)-induced inflammation (Ulmann et al., 2010). The study showed that the lack of inflammatory pain behaviour is due to the reduction of P2X4R-dependent prostaglandin E2 (PGE2) production in P2X4R-deficient macrophages. In contrast, elevation of PGE2 production was observed following ATP-mediated P2X4R activation in wild type macrophages. These results suggest that the stimulation of P2X4R in macrophages is responsible for PGE2 release, a central mediator of inflammation that is directly related to hypersensitivity in inflammatory pain (Ulmann et al., 2010).

Apart from its role in pain, P2X4R in endothelial cells has been shown to mediate vascular remodelling such that shear stress in vascular endothelial cells stimulates P2X4R-mediated Ca^{2+} entry and production of the vasodilator nitric oxide (NO). Knockout of P2X4R in mice demonstrated raised blood pressure, a lack of vascular remodelling and decreased shear stress-induced release of NO, confirming the crucial role of P2X4R in the controlling vascular tone and vascular remodelling (Yamamoto et al., 1998). In addition to being a shear stress sensor, P2X4R in vascular endothelial cells has been suggested to exert a neuroprotective role via ischemic preconditioning (IPC). IPC is transient ischemia that recovers with subsequent reperfusion. There is evidence that shear stress stimulated P2X4R activation elevates the expression of the neuroprotective factor osteopontin (Ozaki et al., 2016). This P2X4R-dependent

osteopontin upregulation is required for IPC-mediated neuroprotection following middle artery occlusion in mice. However, inhibition of P2X4R, using 5-BDBD, blocked the upregulation of osteopontin, thereby inhibiting ischemic preconditioning-induced neuroprotection. Similarly, intracerebroventricular injection of osteopontin mimicked P2X4R-mediated neuroprotective effect of ischemic preconditioning in mice (Ozaki et al., 2016).

There is good evidence to suggest that P2X4R plays a role in inflammation given its wide co-expression with P2X7R, which plays a key role in immune responses. A study by Vaccari et al. (2012) suggested an early inflammatory role of P2X4R in inflammatory signalling, such that impaired inflammasome signalling was observed in P2X4R knockout mice after spinal cord injury with lower level of caspase-1 activation and interleukin-1 β (IL-1 β) cleavage. This P2X4R-mediated inflammatory response is suggested to be an initial inflammatory signal that is amplified by P2X7R. Consistently, another study demonstrated a synergistic interaction between P2X4R and P2X7R in releasing IL-1 β and IL-18 from bone-derived dendritic cells. The release of IL-1 β is attenuated in P2X4R-knockout dendritic cells suggesting a synergistic interaction between P2X4R and P2X7R in inflammatory response, but the detail mechanism is yet to be elucidated (Sakaki et al., 2013).

1.12 A role for lysosomal P2X4R in lung alveolar type II cells

P2X4Rs are widely expressed in lung tissues, including the intracellularly localised P2X4R in lamellar bodies (LBs) of the lung alveolar type-II (ATII) epithelial cells (Miklavc et al., 2010). LBs are lysosome related organelles that store surfactants, the release of which facilitates maintenance of surface tension in lungs. Exocytosis of LBs and the efficient release of surfactants requires a localised surge of Ca²⁺ at the

proximal fusion site between LBs and the plasma membrane, which is called fusion-activated Ca^{2+} entry (FACE) (Miklavc et al., 2010). The initial fusion between LBs and the plasma membrane opens a narrow fusion pore that allows influx of extracellular ATP and efflux of protons. The resultant activation of P2X4Rs mediates a localised Ca^{2+} signal, which triggers the widening of the fusion pore and surfactant release (Miklavc et al., 2010). In conjunction with the patch clamp technique, imaging studies confirmed that active P2X4Rs mediate the fusion of LBs and surfactant release, but fusion of LBs is attenuated upon removal of extracellular ATP (Miklavc et al., 2010). The over expression of the dominant negative mutant, P2X4R-C353W in ATII cells attenuated Ca^{2+} entry and caused a reduction in the number of LB fusions (Miklavc et al., 2010). The evidence suggests that P2X4R is essential in regulating the conventional fusion of LBs in ATII cells and shows a physiological role for P2X4Rs in lysosome-like compartments.

1.13 Lysosome structure

The lysosome is the primary degradative compartment of a cell that contains various acidic hydrolases as well as more than 25 different lysosomal transmembrane proteins (Xu and Ren, 2015; Zhong et al., 2016). The lysosome is a heterologous organelle that varies in size (0.1 μm - 1.0 μm in diameter in most mammalian cells), morphology, and distribution (Wartosch et al., 2015; Xu and Ren, 2015). The acidic nature of the lysosome is maintained by the vacuolar-type proton pump (V-ATPase), which maintains the pH at approximately pH 4.6 (section 1.16) (Mellman et al., 1986; Mindell, 2012).

1.14 The function of lysosomes

Lysosomes have been long regarded as a disposal organelle, but lysosomes are now recognised as organelles that modulate many cellular processes, including degradation of intro- and extracellular substrates and cell death.

Lysosomes receive substrates for degradation from different routes: extracellular components are delivered to lysosomes via the endocytic pathway and digestion of intracellular macromolecules or recycling of intracellular organelles occurs via the autophagy pathway, which will be discussed in the next section (Luzio et al., 2007). The endocytic pathway is tightly pH regulated, whereby pH gradually decreases from early endosomes (pH 6.0) to late endosomes (pH 5.5), and finally lysosomes (pH 4.6). The sequential drop in pH suggests that pH may be important in vesicular maturation, delivery of substrates, fusion of endosomes with lysosomes, and finally lysosome clearance. Tight regulation of lysosome pH is important to maintain lysosome biogenesis because most lysosome hydrolases have optimal activity under acidic conditions (Hu et al., 2015; Xu and Ren, 2015).

Due to the high content of hydrolytic enzymes, lysosomes can potentially be harmful and they have been shown to contribute to cell death. The release of lysosomal proteases is suggested to modulate apoptosis signalling. One example is via lysosomal membrane permeabilisation (LMP), a process where the membrane of lysosomes is permeabilised allowing the leakage of lysosome hydrolases, specifically cathepsins, into the cytoplasm to mediate apoptosis. Consistent with this, some cathepsins have been implicated to retain functional activity at neutral pH, such as cathepsin B, D and L (Boya and Kroemer, 2008). There is evidence showing that the microinjection of cathepsins into the cytoplasm is sufficient to trigger initiation and

progression of the apoptosis pathway (Appelqvist et al., 2013; Bivik et al., 2006; Schestkova et al., 2007). Furthermore, upregulation of cathepsin levels in the extracellular space is implicated in many human cancers (Gyrd-Hansen et al., 2004; Palermo and Joyce, 2008) and this enhanced level of cathepsins promotes cancer progression, such that it degrades the extracellular matrix (ECM) and its basement membrane to facilitate cancer invagination (Tardy et al., 2006). Evidence also shows that the knockout of specific cathepsins reduces tumour growth and cell proliferation (Vasiljeva and Turk, 2008). Despite the evidence of LMP in cancer and cell death, the exact molecular mechanisms and induction of LMP remain unknown.

1.14.1 Autophagy

Autophagy is a catabolic process, also known as self-digestion, that is essential for the recycling of intracellular organelles and macromolecules in response to nutrient and energy starvation. There are three main modes of autophagy: chaperone-mediated autophagy, microautophagy and macroautophagy (Zhang, 2013). Macroautophagy is suggested to be the main mode of autophagy, and hereafter will be referred as autophagy. It mainly degrades and recycles a large portion of cytoplasmic contents and organelles.

1.14.2 The molecular mechanisms of autophagy

Autophagy is stimulated by diverse stimuli, such as nutrient starvation, hypoxia and pathogen invasion and the central mediator of autophagy is mammalian target of rapamycin complex 1 (mTORC1). Activity of mTORC1 is regulated by anabolic input, for example, cellular nutrient status. Active mTORC1 constitutively inhibits the protein kinase ULK complex (the molecular complex for the autophagy induction), by

phosphorylation to reduce the activity of ULK complex (Gallagher et al., 2016). During nutrient starvation, the activity of mTORC1 is suppressed, thus relieving the ULK complex inhibition to recruit autophagy-related (ATG) proteins for autophagy initiation (Jung et al., 2009).

Following autophagy initiation, a double membrane bound vesicle, the autophagosome, is formed. The synthesis of autophagosomes is controlled by ATG proteins through vesicular nucleation, elongation, and maturation. Despite extensive study of autophagosome biosynthesis, the source of autophagosome membranes is only speculative, and although it may derive from the ER and/or mitochondria, it remains unclear (Tooze, 2010). Biosynthesis is followed by autophagosome elongation and maturation, before shaping and closure of the autophagosome, a process controlled by two ubiquitin-like conjugating systems (Wirawan et al., 2012; Zhou et al., 2013). Firstly, ATG7, the E1-like enzyme, activates ATG12. Then, the active ATG12 translocates to ATG10, an E2-like enzyme, to conjugate ATG12 with ATG5 into a complex (Van Limbergen et al., 2009). This ATG12-ATG5 complex is then formed into a multimeric structure with ATG16L1, which acts as an E3-ligase for the second ubiquitin-like mechanism to complete the autophagosome maturation (Ohsumi, 2014). The next steps involve the microtubule-associated protein light chain 3 (LC3). Under nutrient rich conditions, a low level of LC3 protein is cleaved into soluble LC3-I protein by ATG4, a cysteine protease (Hanada et al., 2007). In response to the initiation of autophagy, a combination activation of ATG7 (E1-like enzyme), which mediates formation of ATG12-ATG5-ATG16L1 complex (E3 ligase), is transferred to ATG3 (E2-like enzyme) to facilitate the conjugation of the soluble LC3-I protein and phosphatidylethanolamine (PE) to produce LC3-II protein. In conjunction with the activity of ATG3, the ATG12-ATG5-ATG16 multimeric complex facilitates the efficient

lipidation of LC3-I protein into LC3-II protein, which decorates both inner and outer membranes of autophagosomes (Hanada et al., 2007). In addition, the presence of LC3-II protein on autophagosomes has been suggested to facilitate the elongation and closure of autophagosomes (Nakatogawa et al., 2007; Shen and Mizushima, 2014). Taking advantage of the solubility of LC3 proteins from the soluble LC3-I protein into the lipidated form of LC3 protein (LC3-II), LC3 proteins act as a major marker in the investigation of autophagy process.

After the formation and maturation of autophagosomes, they are delivered to fuse with lysosomes. The fusion between autophagosomes and lysosomes forms autophagolysosomes (sometimes known as autolysosomes) where degradation occurs. The localised elevation of Ca^{2+} signals and the pH of lysosomes are important factors for the fusion between autophagosomes and lysosomes (Kawai et al., 2007). The fusion is suggested to be similar to the homotypic fusion of vacuoles in which the fusion is facilitated by the SNAREs Vam3 and Vti1 (syntaxin7 and VTI1B are the mammalian homologues). In addition, Rab7 has been shown to play an important role in this fusion; Rab7-depleted cells inhibit the fusion between autophagosomes and lysosomes, resulting an accumulation of LC3-II proteins (Ganley et al., 2011). Moreover, the knockdown of LAMP1 and LAMP2 proteins have also been shown to inhibit this fusion, suggesting a role for LAMP1 and LAMP2 in this fusion machinery, although the detailed mechanism underlying this fusion remains elusive (González-Polo et al., 2005; Luzio et al., 2007). Once both autophagosome and lysosome are fully integrated, content mixing enable the activation of hydrolases to undergo the lysosomal degradation and subsequently release resulting metabolites into cytoplasm.

1.14.3 Autophagy in disease

Autophagy is a cellular adaptation to starvation and acts as a sensor of cellular energy and nutrient status (Boya et al., 2013). Autophagy initiation in response to nutrient starvation allows degradation of intracellular organelles and metabolites to supply energy and/or nutrients to maintain cellular viability (Rubinsztein et al., 2012). One example of autophagy is during starvation which evokes the digestion of lipid droplets in the liver to generate free fatty acids from triglycerides as an energy supply (Singh et al., 2009). Studies suggest that autophagy acts as a double-edged sword; its tumour suppressor property inhibits the initial growth of cancerous cells but, conversely some studies have demonstrated a role of autophagy in the pro-survival pathway of cancer cells under unfavourable conditions. For example, autophagy sustains viability of cancerous cells by providing a consistent nutrient supply via aerobic glycolysis to sustain rapid proliferation and survival of cancer cells in a low nutrient microenvironment and hypoxic conditions (Choi et al., 2013). Additionally, autophagy has been suggested to prevent cancerous cells from programmed cell death upon metastasis (Wirawan et al., 2012).

It is tempting to associate autophagy with neurodegenerative diseases, for example Parkinson's disease, because of the pathological phenotype of mass aggregates observed in several neurodegenerative diseases that could be associated with impaired autophagic degradation. Despite the lack of direct evidence for impaired autophagy in neurodegenerative disease, studies have shown raised expression of α -synuclein in rat PC12 cells (a cell line derived from pheochromocytoma of adrenal medulla), which is a hallmark of Parkinson's disease, could disrupt the autophagosome biogenesis and lysosome acidification, thus resulting in the disruption

in autophagic clearance (McBrayer and Nixon, 2013; Winslow et al., 2010). Pathological manipulation to increase the autophagy process reduces α -synuclein in aggregates, indicating a potential therapeutic target in treating neurodegenerative disease via autophagy induction (Rubinsztein et al., 2012).

1.15 Lysosome dysfunction and disease

As lysosomes contribute to many different cellular processes, disruption of lysosomes has been implicated in several diseases. One example is Niemann-Pick type C (NPC) disease, an autosomal recessive disease. NPC disease arises from the loss of NPC1 and NPC2 proteins that are lysosomal-limiting membrane proteins and soluble lysosomal proteins, respectively (Garver et al., 2010). NPC2 transports cholesterol to lysosomes; however, the role of NPC1 remains elusive (Lloyd-Evans and Platt, 2010). NPC1 has been suggested to bind cholesterol in lysosomes given its sterol-sensing domain. This suggests both NPC1 and NPC2 proteins are important in regulating cholesterol level in cells (Lloyd-Evans and Platt, 2011). Given the importance of Ca^{2+} as an ubiquitous intracellular messenger and Ca^{2+} is concentrated in lysosomes, NPC1-mutant cells exhibit a reduction in lysosomal Ca^{2+} release, which may be one of the underlying factors contributing to the disruption in cholesterol trafficking and recycling (Lloyd-Evans et al., 2008). A study by Cao et al. (2015b) showed the increase of lysosome Ca^{2+} signals is sufficient to ablate the accumulation of cholesterol in lysosomes, a hallmark of NPC-mutant fibroblasts, and restored lysosomal membrane trafficking. This showed that the over expression of the lysosomal Ca^{2+} -activated big-conductance K^+ channel (BK) formed a macromolecular complex with lysosomal Ca^{2+} release channel, transient receptor potential mucuolipin (TRPML1). The complex enables BK channels to mediate counter cation influx that

facilitates the Ca^{2+} release from lysosomes via TRPML1, thereby reversing lysosomal storage defects in NPC cells.

In addition, mutations in the *Mcoln1* gene, encoding TRPML1, have been implicated in mucopolipidosis type IV (MLIV) disease (Bach, 2005). MLIV has the clinical features of disrupted endolysosomal membrane trafficking, reduced lysosomal Ca^{2+} release and excessive accumulation of undigested substrates (Cheng et al., 2010). The mutation in TRPML1 causes enlargement of late endosomes and lysosomes, probably due to disruption in lysosomal Ca^{2+} signalling, which in turn impacts the balance of lysosome fusion and/or fission (Cheng et al., 2010). Together, these pathological situations indicate the importance of lysosomal Ca^{2+} homeostasis in cellular function and suggest that the modulation of lysosomal Ca^{2+} channels such as TRPML1 and P2X4R could be potential therapeutic targets for treating lysosomal diseases.

1.16 Regulation of lysosome acidification

Lysosome pH is maintained at pH ~4.6 mainly by V-ATPase, a protein complex that utilises ATP to pump H^+ into the lumen of lysosomes (Colacurcio and Nixon, 2016; Forgac, 2007; Nishi and Forgac, 2002). The V-ATPase protein complex is comprised of at least 14 different protein subunits that hydrolyse ATP and drive H^+ uptake against the concentration gradient from the cytoplasm (Cotter et al., 2015). For each ATP molecule being hydrolysed by V-ATPase, two to four H^+ are transported across the lysosomal membrane (Colacurcio and Nixon, 2016; Cotter et al., 2015; Kettner et al., 2003). However, the accumulation of H^+ in the lumen of lysosomes generates a positive transmembrane potential that curbs V-ATPase activity, but a counter-ion flux, mediating cation efflux and/or anion influx, helps circumvent this, thereby sustaining active transport of H^+ into lysosomes (Steinberg et al., 2010). In cooperation with the

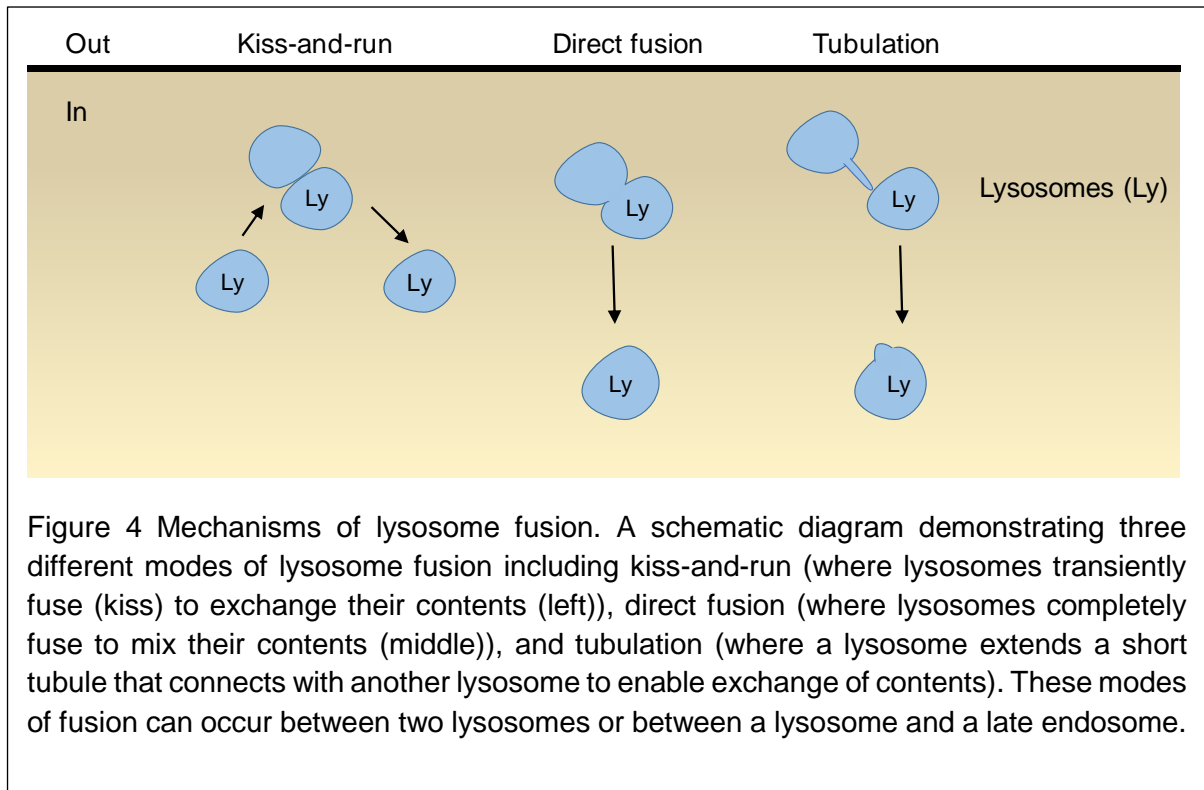
V-ATPase, the presence of the Cl^-/H^+ antiporter CIC-7 on the lysosome membrane has been shown to regulate the counterbalance of ion transportation such that the influx of two Cl^- influx and efflux of one H^+ into cytoplasm across the lysosome membrane also contributes to lysosome acidification. Knockdown of CIC-7 and disruption in the trafficking of CIC-7 to lysosomes result in reduced lysosome acidity (Di et al., 2006; Graves et al., 2008; Majumdar et al., 2011).

Disruption in lysosome pH has been implicated in pathological conditions. One example is the increase in lysosomes pH in fibroblasts with an Alzheimer-associated presenilin1 (PS1) mutation (Coffey et al., 2014). The study demonstrated that the PS1-mutation cells have an elevated lysosomal pH, reduced cathepsin D activity, and accumulation of autophagic substrates. An increase in intracellular cAMP restored the impaired lysosome function suggesting it has a pivotal role of lysosome pH. Inhibition of lysosome acidification may suggest that lysosome pH may be one of the contributing factors that causes a lysosome proteolysis defect, thereby exacerbates the progression of Alzheimer's disease.

1.17 The mechanisms of lysosome fusion

Lysosomes can fuse with several different cellular compartments, including late endosomes, phagosomes, autophagosomes, and the plasma membrane (Luzio et al., 2007, 2010). Fusion of lysosomes is essential for vesicular transport and for delivery of metabolites to cells. With regards to vesicular transport, several theories have been proposed as to the mechanisms of lysosome fusion including kiss-and-run, direct fusion, tubulation and fusion & fission (Bright et al., 2005; **Fig. 4**).

Lysosome fusion is composed of three consecutive steps, including tethering, formation of the trans-SNARE complex, and fusion. Tethering between late endosomes and lysosomes is facilitated by Rab7, which recruits vacuolar protein sorting (Vps) 18 and Vps 39, which are components of the homotypic fusion and vacuole fusion protein sorting (HOPs) complex. These proteins help the aggregation of late endosomes and lysosomes prior to fusion (Caplan et al., 2001; Poupon et al., 2003). Following tethering, both Q- and R- SNAREs that localise to late endosome and lysosome membranes, respectively are formed into a trans-SNARE complex between 2 organelles. In heterotypic fusion between late endosomes and lysosomes, the vesicle associated membrane protein-7 (VAMP7) forms a bundle with Q_a-, Q_b- and Q_c- SNAREs (syntaxin7, VTI1B and syntaxin8), to facilitate the fusion between late endosomes and lysosomes (Antonin et al., 2000; Luzio et al., 2007; Pryor et al., 2004). Complete formation of the trans-SNARE complex induces Ca²⁺ and calmodulin-dependent lysosome fusion (Luzio et al., 2007; Pryor et al., 2000).



Lysosome exocytosis is an important process for cellular mechanisms such as plasma membrane repair, secretion of hydrolytic enzymes, and upregulation of receptors (Samie et al., 2013). It is now known that both secretory and non-secretory lysosomes undergo exocytosis (Jaiswal et al., 2002; Xu and Ren, 2015). Similar to the secretory lysosomes, studies have suggested that the motility of non-secretory lysosomes is also mediated by microtubule-based proteins, including kinesin, which regulates the anterograde movement of lysosomes towards the plus-end of microtubules, and dynein that modulates the retrograde movement towards the minus end of microtubules at the perinuclear region (Li et al., 2016; Reddy et al., 2001). The anterograde movement of lysosomes towards the cell periphery and their accumulation at the plasma membrane facilitates their tethering to the plasma membrane (Medina et al., 2011; Samie et al., 2013; Xu and Ren, 2015). Similar to the

fusion between late endosomes and lysosomes, the fusion between lysosomes and the plasma membrane is facilitated by the formation of a trans-SNARE complex, which is comprised of the Q-SNAREs syntaxin-4 and synaptosome associated protein of 23 kDa (SNAP23). Upon formation of the trans-SNARE complex between the plasma membrane and lysosomes, the Ca^{2+} sensor synaptotagmin-VII is essential for complete fusion to occur and the release of lysosomal contents to the extracellular space (Luzio et al., 2007; Rao et al., 2004). There is evidence demonstrating that peripherally localised lysosomes have a more alkaline luminal content than juxtannuclear lysosomes due to a decrease in V-ATPase activity and increased H^+ leak (Johnson et al., 2016). This would favour recruitment of P2X4R activity to trigger Ca^{2+} -dependent exocytosis.

1.18 Lysosomes contain ATP

In addition to their central role in degradation, lysosomes act as a reservoir for ATP and the concentration of ATP is thought to be in the millimolar range (Zhang et al., 2007). Glycyl-L-phenylalanine-betanaphthylamide (GPN) is a cathepsin C substrate that is thought to selectively permeabilise the lysosome membrane, which results in the release of ATP from lysosomes, but not from mitochondria (Zhang et al., 2007). Another study has used quinacrine, a fluorescent dye that localises to intracellular ATP stores, to show that compartments containing the lysosomal associated membrane protein1 (LAMP1) have high levels of ATP (Huang et al., 2014).

1.19 Lysosomes as intracellular Ca^{2+} stores

Lysosomes contain a high concentration of Ca^{2+} comparable to that of the principal cellular Ca^{2+} store, the ER (~0.5 mM; Patel and Cai, 2015). The lysosomal Ca^{2+}

concentration is ~5000 fold higher than in the cytoplasm, which contains approximately 100 nM (Patel and Cai, 2015). Such a steep Ca^{2+} gradient between the lumen of lysosomes and cytoplasm requires either a Ca^{2+} exchanger mechanism or a Ca^{2+} -ATPase. The nature of this Ca^{2+} transport mechanism in mammalian cells remains unknown. However, in yeast a Ca^{2+} / H^+ exchanger (CAX) is important in maintaining the high luminal Ca^{2+} concentration, but there is no evidence for the expression of CAX in the majority of mammalian cells, with genomic encoding for CAX only being detected in two mammals, *Ornithorhynchus anatinus* and *Sarcophilus harrisii* (Melchionda et al., 2016). It was shown that over expression of CAX causes a modest decrease in Ca^{2+} release from the ER in response to carbachol (a cholinergic agonist that stimulates Ca^{2+} release from the ER) in SHSY5Y cells, a human-derived bone marrow neuroblast cell line (Luciani et al., 2009). This suggests that CAX sequesters Ca^{2+} into lysosomes, leading to a modest drop in the ER Ca^{2+} concentration and thus making less available for release upon stimulation (Melchionda et al., 2016).

Lysosomes express various Ca^{2+} release channels, for example the TRPML1 and the two-pore channel-2 (TPC2), in addition to P2X4R. TRPML1 localises to both endolysosomes and lysosomes, and has 6 transmembrane domains with intracellular N- and C- termini (Zhong et al., 2016). TRPML1 channels are activated by phosphatidylinositol 3,5-bisphosphate ($\text{PI}(3,5)\text{P}_2$), and are cation permeable, showing preferential Ca^{2+} permeability (Dong et al., 2010; Patel and Cai, 2015; Yamaguchi et al., 2011). Evidence suggests nicotinic acid adenine dinucleotide phosphate (NAADP) activates TRPML1 to mediate lysosome Ca^{2+} release, however this has been a subject of controversy (Zhang and Li, 2007). TRPML1 has been shown to regulate lysosomal pH such that the knockdown of TRMPL1 results in more acidic lysosomes compared

to wild type (Soyombo et al., 2006). Moreover, TRPML1 mediates lysosome membrane trafficking via fusion and/or fission: cells lacking TRPML1 have enlarged lysosomes, whereas over expression of TRPML1 reverses this phenotype suggesting a key role for TRPML1 in fission (Dong et al., 2010). This has been implicated in the human disease, MLIV, an autosomal recessive lysosomal storage disease (LSD). This disease is associated with disrupted lysosome biogenesis further emphasising the importance of TRPML1 in regulating Ca^{2+} signalling in lysosome function (Zhong et al., 2016).

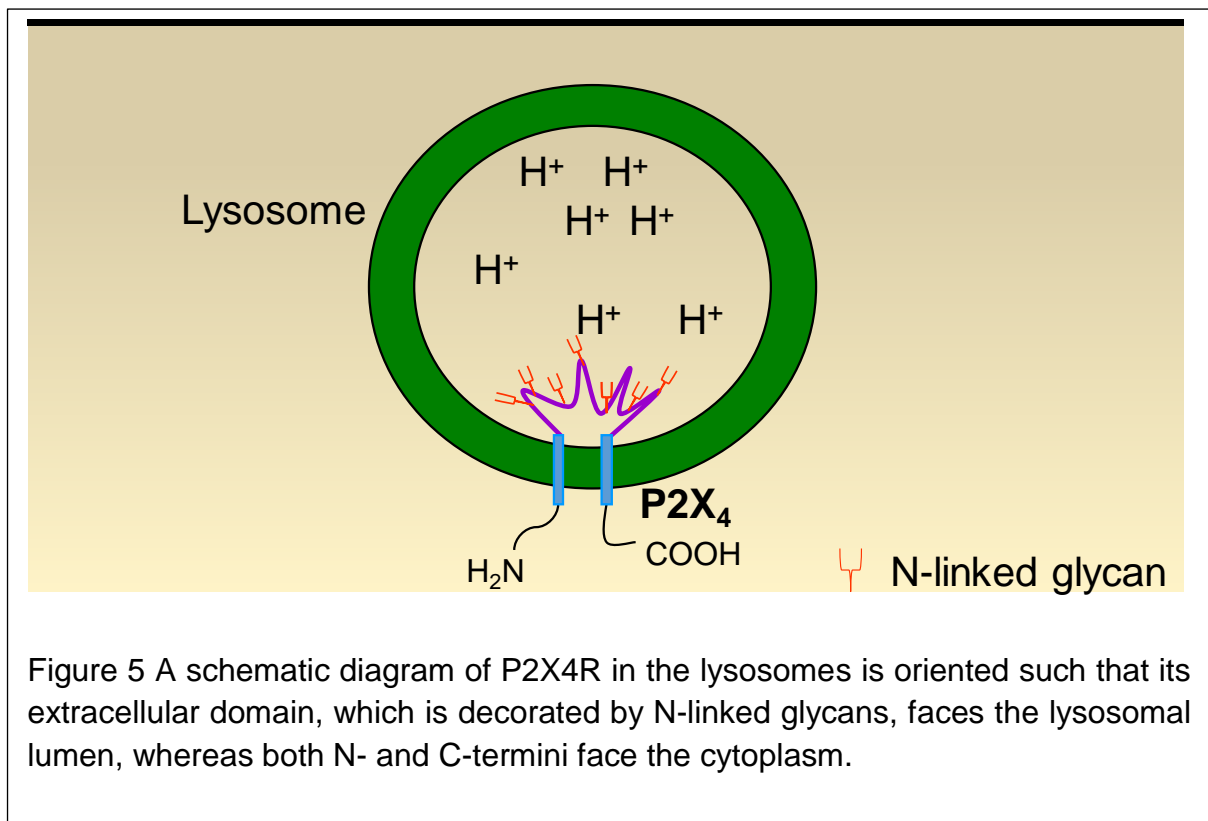
TPC2 channel is a cation-selective channel that has been implicated in the regulation of lysosome function, including trafficking along the endocytic pathway and the regulation of lysosome fusion and fission (Grimm et al., 2014; Ruas et al., 2010). TPC2 channels exist as dimers and each subunit is comprised of two repeats of 6 transmembrane domains in tandem (Patel and Cai, 2015; Penny et al., 2016; Pitt et al., 2010). There are several studies demonstrating that TPC2 channels are activated by both NAADP and $\text{PI}(3,5)\text{P}_2$ and are permeable to Ca^{2+} following stimulation (Jha et al., 2014; Patel and Cai, 2015). A role for TPC2 in the regulation of membrane trafficking has previously demonstrated that the knockout of TPC2 causes a disruption in the internalisation of growth factor receptors and accumulation of low-density lipoprotein (LDL) (Grimm et al., 2014; Patel and Cai, 2015). Furthermore, there is evidence showing a role of TPC2 in autophagy, such that the over expression of TPC2 in HeLa and embryonic stem cells inhibits the fusion between autophagosomes and lysosomes (Lu et al., 2013). Blockade of this fusion resulted in an accumulation of autophagosomes, thereby disrupting the progression of autophagy. The knockdown of TPC2 and pharmacological blockade of NAADP antagonist, NED-19 reversed this effect. Furthermore, the study showed that the activation of TPC2 alkalinises the

lysosome via Ca^{2+} release, thereby inhibiting the fusion between lysosomes and autophagosomes. Together with TRPML1, these results suggest the importance of lysosomal Ca^{2+} release channels in lysosome function.

The elevation of cytosolic Ca^{2+} in the immediate vicinity of lysosomes is necessary for efficient fusion of lysosomes with other organelles (Rodríguez et al., 1997). Growing evidence indicates that the source of the Ca^{2+} signal for lysosome fusion is derived from lysosomes themselves. Indeed, the first evidence suggesting the importance of lysosomal Ca^{2+} efflux in lysosome fusion was shown in a cell-free experiment in yeast using two Ca^{2+} chelating reagents. The study showed that the membrane impermeable 1,2-bis-(*o*-aminophenoxy)ethane-*N,N,N',N'*-tetra-acetic acid (BAPTA) inhibited homotypic vacuole fusion, whereas a second membrane impermeable Ca^{2+} chelator EGTA has no effect (Peters and Mayer, 1998). This was due to the rapid chelating effect of BAPTA, which is 100 times faster than EGTA. BAPTA induced a dispersedly low Ca^{2+} gradient across the cytoplasm, including the immediate vicinity of lysosome, that is fast enough to suppress any biological response. In addition, the presence of ionomycin, a Ca^{2+} ionophore that mobilises intracellular Ca^{2+} stores, depletes luminal vacuole Ca^{2+} and abolished all fusion even without pre-treatment with BAPTA. However, vacuoles become fusion-competent once the luminal Ca^{2+} in vacuoles was restored, indicating the luminal Ca^{2+} is required for vacuole fusion. This agrees with another study in a cell-free vesicle fusion assay using mammalian cells. This showed inhibition in the fusion between late endosomes and lysosomes using a membrane permeable ester Ca^{2+} chelator, EGTA-AM, emphasising the importance of luminal Ca^{2+} release from lysosome is essential for the fusion of lysosomes (Pryor et al., 2000).

1.20 P2X4Rs function as a Ca²⁺ release channel

A previous collaboration between the Murrell-Lagnado group and Xianping Dong's group at the University of Dalhousie investigated the role of rP2X4R in lysosome function. They utilised lysosomal patch clamp electrophysiology to investigate the activity of rP2X4R expressed in Cos-1 cells. P2X4R is oriented in lysosomes such that the extracellular ATP binding site faces the lumen (**Fig. 5**). Under conditions where the lysosome lumen was dialysed with an acidic solution (pH 4.6) containing ATP (0.1 mM), there was no P2X4R-mediated current observed. However, when the pH was increased to 7.4, a P2X4R-mediated current was recorded (Huang et al., 2014). This demonstrated the importance of pH in regulating the ability of ATP to activate P2X4R. Further experiments demonstrated that lysosomal P2X4Rs exhibit a similar pharmacological profile to plasma membrane P2X4R and are potentiated by ivermectin, but insensitive to suramin (Huang et al., 2014).



A further study demonstrated that enlargement of lysosomes (hereafter referred to as vacuolated lysosomes) occurred following expression of rP2X4R in Cos-1 cells, but not in cells expressing rP2X4R-S341W, which is a non-functional P2X4R mutant with a mutation in TM2 (Silberberg et al., 2005). The number of vacuolated lysosomes in cells expressing rP2X4R was further potentiated following lysosome alkalinisation, using methylamine (MA), NH₄Cl or bafilomycin-A1 (Baf-A1) (Cao et al., 2015), suggesting that the activation of lysosomal P2X4R following lysosomal alkalinisation was able to mediate homotypic lysosome fusion (Cao et al., 2015). The P2X4R-mediated lysosome fusion was shown to be dependent upon calmodulin (CaM) which forms a physical complex with P2X4R (Cao et al., 2015). Despite the evidence for P2X4R-dependent lysosome fusion following lysosome alkalinisation, the study does not show under what physiological conditions P2X4R is activated.

1.21 Cytosolic Ca²⁺ signaling and the ER

1.21.1 Ion channels in the ER

A major source of Ca²⁺ that mediates the cytosolic Ca²⁺ signal is the ER. The two main Ca²⁺ release channels in the ER membrane are inositol 1,4,5 triphosphate receptors (IP₃Rs) and ryanodine receptors (RyRs), receptors activated by IP₃ and cyclic ADP-ribose (cADPR), respectively (Patel and Cai, 2015). IP₃ is released by phospholipase C mediated hydrolysis of phosphatidylinositol 4,5 biphosphate (PI(4,5)P₂), a pathway triggered downstream of GPCRs that couple to G_q proteins (Raffaello et al., 2016). The localised elevation of Ca²⁺ released via IP₃Rs triggers the clustering of IP₃Rs and this ultimately results in the potentiation and propagation of Ca²⁺ signals along the ER, and a rise in the global Ca²⁺ concentration within cells (Rahman, 2012; Wilson et al., 1998). It has been suggested that IP₃R activity is tightly regulated by the cytosolic [Ca²⁺]; specifically, a low concentration of Ca²⁺ triggers IP₃R activation, whereas a high concentration of Ca²⁺ impedes IP₃R activation and reduces Ca²⁺ release. This biphasic Ca²⁺ sensitivity of IP₃R is however dependent on the IP₃ concentration (Adkins and Taylor, 1999). Beside Ca²⁺ release channels, the ER is also able to uptake Ca²⁺ by the sarcoplasmic reticulum Ca²⁺ ATPase (SERCA). SERCA is a P-type ATPase that utilises one ATP molecule to transport two Ca²⁺ ions from the cytoplasm against the concentration gradient into the ER (Krebs et al., 2015).

1.21.2 Ca²⁺ signaling between the ER and lysosomes

Most lysosomes are localised to the perinuclear region in close proximity to the ER. Electron microscopy studies have shown that ER and lysosomes are ~20 nm apart (Kilpatrick et al., 2013; Lam and Galione, 2013). Additionally, TIRF microscopy studies in Cos-7 cells show lysosomes to be highly associated with the ER whereby some

mobile lysosomes migrate along with the ER tubules (López-Sanjurjo et al., 2013). Tight positioning between these two organelles suggests that they are intimately associated and that interactions between them might be important in the regulation of organelle Ca^{2+} signalling.

Indeed, it has been shown that stimulation of lysosomal Ca^{2+} release can facilitate the mobilisation of Ca^{2+} release from the ER and vice versa, whereby the release of ER Ca^{2+} via IP_3R triggers Ca^{2+} release from acidic vesicles (Kilpatrick et al., 2013; Morgan et al., 2013). One example of the functional crosstalk between lysosomes and the ER was shown by the potent Ca^{2+} mobilising messenger, NAADP which targets acidic lysosomal-related organelles. In smooth muscle cells, NAADP triggers localised Ca^{2+} signals from lysosome-like organelles and this is subsequently amplified by Ca^{2+} release from the SR to generate cytoplasmic Ca^{2+} signals (Kinnear et al., 2004). Similarly, Baf-A1, a V-ATPase inhibitor that triggers lysosome alkalinisation, was shown to trigger a cytoplasmic Ca^{2+} signal, but blocked the NAADP-mediated Ca^{2+} signal. Baf-A1 is thought to discharge Ca^{2+} from lysosomal-related organelles, thereby preventing NAADP-dependent Ca^{2+} release from lysosomes. Furthermore, this subsequent response of global Ca^{2+} signal evoked by NAADP was abolished upon SR Ca^{2+} depletion by thapsigargin (a SERCA inhibitor) or inhibition of SR Ca^{2+} release channels (Kinnear et al., 2004). This finding suggests that the mobilisation of lysosome-related Ca^{2+} store is sufficient to trigger the activation of SR/ER Ca^{2+} release channels (IP_3Rs and RyRs) and further amplify global Ca^{2+} response.

In addition to smooth muscle cells, another study demonstrated that lysosomal Ca^{2+} release is sufficient to evoke ER-mediated Ca^{2+} signals in human fibroblasts (Kilpatrick et al., 2013). Akin to the mechanism mediated by NAADP, the lyso-osmotic agent GPN,

which perforates lysosome membrane, generated a prominent Ca^{2+} signal followed by global oscillatory Ca^{2+} responses, which are mediated by IP_3Rs on the ER. The inhibition of Ca^{2+} release from the ER, either by ER Ca^{2+} depletion (using thapsigargin) or by inhibition of IP_3Rs (via the non-selective IP_3R antagonist 2-aminoethoxydiphenyl borate, 2-APB) attenuated this GPN-evoked Ca^{2+} signal and abolished the global Ca^{2+} oscillations. These confirmed that the GPN-induced lysosomal Ca^{2+} signal is sufficient to stimulate ER Ca^{2+} release, but is prevented in the absence of the ER Ca^{2+} release (Kilpatrick et al., 2013). Another study confirmed these findings using a computational model, which simulated the microdomains between lysosomes and the ER (Penny et al., 2014). Using the model, it was consistently demonstrated that GPN and NAADP can drive the global Ca^{2+} oscillation through the ER Ca^{2+} release. It was also found that only a low $[\text{Ca}^{2+}]$ from lysosomes is needed for the stimulation of the ER Ca^{2+} release, which aligns with ER-lysosome proximity and the high affinity of IP_3Rs for Ca^{2+} . Collectively, these findings strongly suggest that mobilisation of lysosomal Ca^{2+} is sufficient to stimulate the ER-mediated Ca^{2+} release.

Apart from the lysosomal Ca^{2+} release pathway, there is growing evidence to establish the mechanism of lysosome Ca^{2+} reuptake and the source of lysosomal Ca^{2+} . There is evidence that describes lysosome Ca^{2+} refilling occurs from the ER and that perturbation of lysosome activities is sufficient to disrupt this mechanism. The study showed that disruption of lysosomal refilling is sufficient to cause aggregation of Ca^{2+} in the ER, resulting an increased ER Ca^{2+} release (López-Sanjurjo et al., 2013). This was shown by both Baf-A1 and GPN, which dissipates the lysosome H^+ gradient and perforates the lysosome membrane respectively, enhancing the ER Ca^{2+} release in response to carbachol. Furthermore, the enlargement of lysosome size using vacuolins, molecules that induce enlargement of endosomes and lysosomes (Cerny

et al., 2004), also enhanced the carbachol-evoked Ca^{2+} response. In addition, carbachol was observed to trigger lysosome alkalinisation, suggesting that lysosome pH is likely to modulate lysosomal Ca^{2+} refilling (López-Sanjurjo et al., 2013). This suggests that several lysosome attributes, including pH, size, and membrane integrity, are essential in maintaining lysosome Ca^{2+} refilling from the ER. Nonetheless, the study does not rule out the possibility of the potential reciprocal relationship where Ca^{2+} release from lysosomes can stimulate the ER Ca^{2+} release, thereby potentiating global Ca^{2+} signals, and vice versa (López-Sanjurjo et al., 2013).

Results have also been reported to explain a mechanism of lysosome Ca^{2+} refilling that is tightly associated with ER Ca^{2+} signalling. The study monitored the lysosome Ca^{2+} signal, but not global Ca^{2+} signal, using GCaMP3-ML1, a Ca^{2+} reporter, that is conjugated to the lysosome Ca^{2+} channel TRPML1 (Garrity et al., 2016). Administration of the TRPML1 agonist, ML-SA1 induced a prominent Ca^{2+} signal, which was suggested to be a measure of Ca^{2+} release from lysosomes. The study further suggested that the lysosomal Ca^{2+} store is refilled from the ER via IP_3Rs , a process independent of lysosome pH. Given a sufficient time interval (~5 mins), repeated application of ML-SA1 evoked a reproducible, transient Ca^{2+} signal, suggestive of lysosome refilling occurring between applications. However, lysosome Ca^{2+} is depleted by rapid repeated applications of ML-SA1 as demonstrated by a decrease in Ca^{2+} signal, indicating that lysosomes are continuously refilled with a certain time interval. Similarly, lysosome refilling was observed using GPN. Consistent with Kilpatrick et al. (2013), both studies demonstrated lysosomal Ca^{2+} uptake from the ER via IP_3Rs . For example, the inhibition of IP_3Rs using Xestospongine-C (a selective IP_3R antagonist) or 2-APB (a non-selective IP_3R antagonist) decreased the ML-SA1-induced lysosome Ca^{2+} release. Furthermore, the ER Ca^{2+} content that was

chelated by TPEN (N,N,N',N'-Tetrakis (2-pyridylmethyl) ethylenediamine; a membrane permeable metal chelator with low binding affinity to Ca^{2+}) reduced the lysosomal Ca^{2+} release (Garrity et al., 2016). However, this study suggested that lysosomal Ca^{2+} refilling is only dependent on the ER Ca^{2+} release mediated by IP_3Rs , independent of lysosome pH, which was demonstrated by Baf-A1, such that the amplitude of ML-SA1-mediated Ca^{2+} signal remains unaltered in the presence of Baf-A1. The study reasoned that if pH of lysosomes is required for lysosome refilling, Baf-A1 should decrease the TRML1-mediated Ca^{2+} signal given the disruption in lysosome Ca^{2+} refilling from the ER, but this was not observed in the study (Garrity et al., 2016). This contradicts the proposed mechanism by López-Sanjurjo et al. (2013). However, the role of lysosome pH in lysosome refilling cannot be ruled out for the following reasons. First, the Ca^{2+} signals reported by GCaMP3-ML1 might be saturated by TRPML1-evoked lysosomal Ca^{2+} signals, and modest decrease in lysosomal Ca^{2+} release following Baf-A1 treatment will not be resolved by GCaMP3-ML1. Secondly, there is a possibility that lysosome refilling only allows a limited concentration of Ca^{2+} from the ER given the size and number of lysosomes in relative to the ER. Lastly, if lysosomes sequester Ca^{2+} from the ER, presumably perturbation of lysosome refilling will impact on both lysosomes and the ER; decrease lysosomal Ca^{2+} content and increase the Ca^{2+} content in the ER, as shown by Lopez-Sanjurjo et al. (2013) and Melchionda et al. (2016). The study by Garrity et al. (2016) only showed that Baf-A1 did not change the Ca^{2+} release from lysosomes, but not monitoring the Ca^{2+} content from the ER.

Although disparities exist, all studies of lysosome Ca^{2+} release and refilling measured Ca^{2+} release from lysosomes and the ER, and all findings consistently agree that the stimulation of lysosomal Ca^{2+} release is sufficient to potentiate ER Ca^{2+} release, and vice versa (Kilpatrick et al., 2013, Penny et al., 2014, López-Sanjurjo et al., 2013, and

Garrity et al., 2016). Together, the evidence suggests a functional interaction between the ER and lysosomes, such that Ca^{2+} shuttles between these organelles to regulate the intracellular Ca^{2+} signalling. Further studies are required to unravel the exact molecular mechanism in the ER-lysosome Ca^{2+} signalling.

2. Thesis aims

Intracellular P2X4Rs can act as receptor reserves that traffic to and from the cell surface in response to stimuli. In cells with specialised secretory lysosomes, the type II alveolar cells, they have also been shown to be activated upon fusion of the lysosome with the cell surface, thereby promoting full collapse of the lysosome. Recent evidence suggests that the activity of P2X4Rs in intact lysosomes can also be triggered following lysosome alkalinisation. Indeed, one study has shown that pharmacological agents that increase the pH of lysosomes are sufficient to activate P2X4R and promote homotypic lysosome fusion. However, the physiological and pathological regulators of the intracellular P2X4R are yet to be identified. The aim of this study was to identify regulators of lysosomal P2X4R and to determine what role P2X4Rs play in lysosome function. Specifically, I investigated the following:

1. The role of P2X7R as a regulator of lysosome P2X4R. This was based upon previous observations that activation of P2X7R triggers the alkalinisation of lysosomes and that P2X7R is commonly co-expressed with P2X4 in immune, epithelial and endothelial cells.
2. The role of G protein-coupled receptors that trigger release of Ca^{2+} from the ER in activating P2X4R. This was based on previous observations that Ca^{2+} entry into lysosomes can trigger alkalinisation and the main source of Ca^{2+} for entering lysosomes is that released from the ER.
3. The role of P2X4R in regulation of autophagy. Autophagic flux is highly dependent upon lysosome fusion with the autophagosome and lysosome pH which determines the activity of the lysosomal proteases.
4. A comparison of the subcellular distribution of human P2X4R and rat P2X4R.

3. Material & Methods

3.1 Cell culture

3.1.1 Cell lines

Four different cell lines were used in this study: Human cervical cell line (HeLa), normal rat kidney (NRK), human embryonic kidney (HEK293) and mRFP-LC3 HeLa cells. The first two cell lines were primarily used for Ca²⁺ imaging and confocal imaging studies because their large cell size and typically flat footprint facilitates imaging of individual lysosomes in cells. HEK293 cells were used in surface biotinylation assays of P2X4Rs.

3.1.2 Cell maintenance

HeLa, NRK and HEK293 cells were maintained in growth medium containing: Dulbecco's modified Eagle's medium (DMEM, Sigma-Aldrich, catalogue number: D6046) with 10 % fetal bovine serum (FBS; Sigma-Aldrich), and 100 U/ml penicillin and streptomycin (P/S), at 37 °C in humidified air with 5 % CO₂. Cells were grown in 75 cm² flasks (T75) and passaged every 3 days as follows: DMEM was removed, cells were washed with 5 ml phosphate buffered saline (PBS) and then incubated with 2 ml of 0.05 % trypsin-EDTA solution, which detached cells from the culture flask. Subsequently, 8 ml of DMEM was added to neutralise trypsin-EDTA. Cells were collected into a 50 ml tube, counted using a haemocytometer and approximately 2.5 million cells were added to a new T75 flask with 15 ml of growth medium. For experiments, following trypsinisation, cells were seeded on to 1 % poly-L-lysine coated coverslips in 6-well plates, with 250000 cells per well.

For protein expression experiments, approximately 3 million cells were seeded into a T75 flask and 100000 cells onto 1 % poly-L-lysine 25 mm coated coverslips in a 12-well plate for immunocytochemistry experiments.

3.1.3 Isolation and culture of bone marrow derived macrophages (BMDM)

WT and P2X4^{-/-} mice were a kind gift from Dr Fred Tam (Imperial College, London). Hind legs of wild type (WT) and P2X4^{-/-} mice were dissected from the pelvic region and sterilised using 70 % ethanol and rinsed using PBS. Fur, skin and muscle were removed to isolate femurs, which were cut to expose bone marrow that was collected using a 24G needle syringe filled with Roswell Park Memorial Institute medium (RPMI, Sigma) containing 10 % FBS and 100 U/ml of P/S. Bone marrow was filtered through a 70 µm cell strainer and centrifuged at 1000 g for 5 minutes. The BMDM cell pellets were re-suspended with RPMI media containing 30 % of the RPMI media that was used to grow mouse connective tissues, L929 cells culture (a kind gift from Dr Xing Jian Xu). The growth medium of L929 cell culture contained growth factors that support the growth of BMDM cells. Cells were plated onto 1 % poly-L-lysine coated 25 mm coverslips with 1.5 million cells per well of a 6-well plate. RPMI media was changed every 2-3 days and BMDM cells were assayed after 8-9 days in culture.

3.1.4 Transfection

Poly-ethyl enimine (PEI)

Cells were seeded 24 h prior to transfection so that they were 80 % confluent at the time of transfection. In each well of a 6-well plate, a total of 2 µg of plasmid DNA was mixed with 4 µl of 1 mg/ml PEI (Polysciences, Inc) in 140 µl of serum-free

DMEM. The transfection mixture was incubated for 10 minutes at room temperature before being administered to cells with 2 ml of fresh grown medium at 37 °C. Cells were imaged 24-48 h post-transfection. This transfection method was used for most experimental assays in both HeLa and NRK cells.

Lipofectamine 3000

This method was used for transfection of LAMP-GECO in NRK and HeLa cells, to obtain high expression in cells, for Ca²⁺ imaging. Cells were grown to 80 % confluency and transfected using Lipofectamine 3000 (Thermo Scientific) according to the manufacturer's protocol. In brief, for each well of a 6-well plate, 4 µl of Lipofectamine 3000 reagent was diluted in 125 µl of Opti-MEM (Gibco). 2 µg of plasmid DNA was added and 5 µl of the P3000 reagent (2.5 µg/µl). This mixture was incubated for 10 minutes at room temperature before being administered to cells with 2 ml of fresh grown media. Cells were incubated for 48 h at 37 °C and then used for experiments.

3.2 Cell based assays

3.2.1 Single cell Ca²⁺ imaging

Fluo4-AM

For measurement of cytosolic Ca²⁺, [Ca²⁺]_c, in a single cell measurement, HeLa cells were seeded onto 1 % poly-L-lysine coated 25 mm coverslips in a well of a 6-well plate the day before experiment. Confluent cells were loaded with Fluo4-AM (2 µM, Life Technologies) with 20 % pluronic acid in normal extracellular solution (NES, which contained: NaCl (140 mM), KCl (5 mM), CaCl₂.H₂O (2 mM), MgCl₂.6H₂O (1 mM), D-Glucose (10 mM), HEPES (10 mM) in 1 litre dH₂O, adjusted to pH 7.3 using

NaOH, for 45 minutes at room temperature. Cells were washed twice with NES and de-esterified in NES for a further 30 minutes at room temperature. De-esterification of the dye was essential to reduce leakage of Fluo4-AM dye out of the loaded cells. For experiments using histamine (50 μ M; Sigma), cells were imaged in nominal Ca^{2+} free NES solution at room temperature using a Leica SP5 confocal microscope: fluorescence (excitation 490 nm, emission 520 nm, detailed in section 3.5 below), 0.650 sec per frame for 600 frames for a total of 7 minutes. Histamine (50 μ M) was administered after 1 minute of recording and after 3 further minutes ionomycin (5 μ M, Apollo Scientific) with 5 mM Ca^{2+} containing NES was administered to obtain the F_{max} , which defined as high and saturating Ca^{2+} concentration when most fluorophore, Fluo4-AM in the cell are bound.

GECO and LAMP-GECO

$[\text{Ca}^{2+}]_c$ signals in NRK and HeLa cells were obtained using the Ca^{2+} reporter plasmids LAMP-GECO and $G_{1.2}$ -GECO, which were kind gifts from Professor Colin Taylor (Department of Pharmacology, University of Cambridge). 400000 cells were seeded onto 1 % poly-L-lysine coated 25 mm glass coverslips and after 24 h, cells were transfected with either LAMP-GECO or $G_{1.2}$ -GECO using Lipofectamine 3000 and PEI, respectively as explained above. 24-48 h post-transfection, cells were used for single-cell Ca^{2+} imaging experiments. Both LAMP-GECO and $G_{1.2}$ -GECO were excited at 488 nm and fluorescence was measured at 519 ± 20 nm using a SP5 Leica microscope detailed in section 3.5. F_{max} was obtained using ionomycin (5 μ M) loaded in 5 mM Ca^{2+} -containing NES at the end of each experiment.

For the lysosome Ca^{2+} store depletion assay, cells were seeded at 400000 cells on 1 % poly-L-lysine coated 25 mm glass coverslips. After 24 h, cells were transfected

with G_{1,2}-GECO, with and without P2X4R, using PEI. 24 h post-transfection, cells were used for experiments. GPN (100 μ M, Santa Cruz) was administered after 1 minute of recording in nominal Ca²⁺ free NES, whereby NES was made up without CaCl₂.H₂O (2 mM) as indicated above, from 2 minutes post GPN treatment, histamine (50 μ M) was administered followed by 3 further minutes before ionomycin (5 μ M) was added to obtain the F_{max}.

3.2.2 Analysis of Ca²⁺ signals in cell population

Fluorescence was measured at room temperature using a Leica SP5 confocal microscope. F is the measured fluorescence of Ca²⁺ indicators, F₀ determines the mean fluorescence 30 seconds before addition of agonist and F_{max} indicates the peak fluorescence value after ionomycin treatment. F₀ and F_{max} were calibrated to normalise the difference in dye loading or leaking and difference in expression of plasmid Ca²⁺ indicators.

3.2.3 Pulse Chase Analysis

Confluent NRK or HeLa cells were seeded on to 1 % poly-L-lysine coated 25 mm glass coverslips and transfected with P2X4R and/or P2X7R using PEI. 48 h post-transfection, cells were incubated with 0.5 mg/ml of the pH insensitive dye, Texas Red Dextran-10kDa (DR; Thermo Scientific) for 5 h at 37 °C and 5 % CO₂ in DMEM. During this period, DR was endocytosed and localised in lysosomes, which was thus utilised to mark lysosomes. DR was removed and cells were washed for 3 times with PBS. Cells were further incubated for 2 h without DR dye in complete growth medium before being subjected to drug treatment, either 2'(3')-O-(4-Benzoylbenzoyl) adenosine-5'-triphosphate (BzATP; Sigma) or histamine. Cells were washed twice

with PBS and used for imaging with a Leica SP5 confocal microscope. Images were captured and analysed as detailed in section 3.5 and 3.6, respectively.

3.2.4 Lysosome position analysis

The boundary of the cells was determined using bright field images. The lysosome position analysis was adapted from Li et al. (2016). The nucleus was determined by DAPI, a nuclear and chromosome counterstain dye, and the perinuclear region was selected by expanding 5 μm outward of the nucleus. The total cell intensity (I_{total}) = Intensity of cell – nucleus intensity. Perinuclear intensity (I_{nuc}) = Intensity of 5 μm outward of nucleus – nucleus intensity. Peripheral intensity ($I_{\text{peripheral}}$) = Intensity of cell – Intensity of 5 μm outward of nucleus. Intensity of perinuclear region ($I_{<5 \mu\text{m}}$) = $(I_{\text{nuc}} / I_{\text{total}}) - 100$; $I_{>5} = (I_{\text{peripheral}} / I_{\text{total}}) - 100$; and Perinuclear index = $I_{\text{perinuclear}} - I_{\text{peripheral}}$

3.2.5 Lysosome size analysis

Lysosome size was analysed using ImageJ in which the threshold of fluorescence intensity of DR was set at 100-255 A.U. to analyse particles in outlined cells. Particles which were considered as lysosomes had a circularity range of 0.7-1.0 μm with diameter ranging between 0.2-5.0 μm .

3.3 Biochemistry

3.3.1 Analysis of protein expression

HEK293 cells were grown to 80 % confluence in T75 flasks for 24 h. Cells were washed with ice cold PBS before being re-suspended using cell extraction buffer, which contained: NaCl (138 mM), KCl (5 mM), Na_2HPO_4 (1 mM), glucose (7.5 mM), HEPES (21 mM), EDTA (2 mM), pH adjusted to 7.4 using NaOH. Cells in extraction

buffer were centrifuged at 1000 g for 5 minutes at 4 °C. Pelleted cells were re-constituted in solubilisation buffer, which contained Tris-HCl (25 mM), NaCl (150 mM), EDTA (10 mM), Triton X-100 (1 %), phenylmethylsulfonyl fluoride (PMSF, 16 mM; Sigma), and protease inhibitor cocktail (1 mg/ml; Sigma), for 1 h at 4 °C. The sample was next centrifuged at 50000 g for 30 minutes at 4 °C before supernatant collection for protein concentration measurement using the Pierce™ BCA Protein assay kit (Life Technologies). Protein samples were diluted in 2X laemmli buffer (Sigma) in 1:1 ratio. This protein sample mixture was subjected to protein analysis assay by SDS-PAGE followed by immunoblotting.

3.3.2 Western blot

Protein samples were assessed using 10 % sodium dodecyl sulphate-polyacrylamide gel electrophoresis (SDS-PAGE), wherein 20 µl protein samples were loaded in each lane of a SDS-PAGE gel along with 7.5 µl of ladder in lane 1 (Spectra broad range, Thermo Scientific), which was made up to a total of 20 µl with 2X laemmli buffer. In the subsequent step, proteins from the acrylamide gel were transferred onto a polyvinylidene difluoride nitrocellulose membrane (Thermo Scientific). Running buffers for gel electrophoresis contained Tris-base (250 mM), glycine (2 M), SDS (10 %) in 1 litre of dH₂O and pH adjusted to 8.4 using concentrated HCl; semi-dry transfer buffer contained Tris-base (250 mM), glycine (2 M), SDS (10 %), methanol (2 %) in 1 litre of dH₂O, pH adjusted to 8.4 using HCl solution. The membrane was washed and blocked with 5 % milk dissolved in TBS-Tween for 1 h at room temperature. Proteins that were on nitrocellulose membranes were incubated with appropriate primary antibodies (1:600 dilutions), in 2.5 % milk in TBS-Tween overnight at 4 °C. Membranes were washed with TBS-Tween to remove

unbound antibodies. Membranes incubated for 2 h with the appropriate secondary antibodies (conjugated to horseradish peroxidase, HRP) that was made up in 2.5 % milk in TBS-Tween. Prior to immunoblot imaging, the membranes were washed with TBS buffer to remove excessive antibodies. Developing the blot was performed using SuperSignal West Pico Chemiluminescent substrate or Femto assay kits (Thermo Scientific). Pictures were taken at different exposure times using VisionWorksLS Image Acquisition and Analysis Software.

3.3.3 Surface biotinylation proteins

HEK293 cells were grown to 80 % confluency in T75 flasks and transfected using PEI. 24 h post-transfection, the growth medium was removed and replaced with 8 ml of ice-cold PBS containing biotin-sulfo-NHS (0.2 mg/ml, Thermo Scientific). After 1 h on ice at 4 °C, cells were washed 3 times with 10 ml Tris-buffered saline (Tris-HCl (25 mM), NaCl (150 mM), EDTA (10 mM) in 500 ml dH₂O and pH adjusted to 7.4 using concentrated HCl solution) to inhibit the biotinylation reaction. Cells were collected in Tris-buffered saline and centrifuged at 1000 g for 5 minutes at 4 °C. Pelleted cells were collected and solubilised in solubilisation buffer (250 µl, 1 h, 4 °C). Cells in solubilisation buffer were centrifuged at 50000 g for 1 h and the supernatant was then incubated with 30 µl of monomeric avidin-coated agarose beads (Thermo Scientific) at 4 °C for 2 h. The conjugated protein complex was further centrifuged at 1000 g for 5 minutes to collect the entire bound protein complex. This was then washed 3 times in solubilisation buffer and mixed with 50 µl of 2X laemmli buffer for immunoblotting. To analyse biotinylated proteins that were precipitated by avidin, 4 % of the total sample was loaded as an input and 20 % of laemmli buffer sample was loaded as surface biotinylated proteins.

3.3.4 Immunocytochemistry

Confluent NRK and HeLa cells were grown on 1 % poly-L-lysine coated coverslips and subjected to drug treatment, as detailed in Figure legends. Following drug exposure, cells were washed with PBS and fixed in 3 % paraformaldehyde (PFA) for 20 minutes at room temperature. The cells were fixed in blocking solution, which contained NaCl (137 mM), KCl (2.7 mM), Na₂HPO₄ (10 mM), KH₂PO₄ (2 mM), goat serum (5 %), bovine serum albumin (BSA; 3 %) and saponin (0.5 mg/ml, 1 h; Sigma), to permeabilise membrane of cells. After 1 h, cells were incubated with primary antibodies, which were diluted at 1:250 in blocking solution as indicated in Figure legends, for 1.5 h. Cells were washed with PBS to remove unbound antibodies and incubated with the appropriate secondary antibody (1:250), for 1.5 h in dark at room temperature. Before mounting onto microscope slides (VWR) with Vector shield (Vector Laboratories, CA), cells were air-dried for 15 minutes in the dark. Images were captured using an oil-immersion 63X objective on a confocal microscope Leica SP5 as detailed in section 3.5 below. Colocalisation analysis was performed by measuring Pearson's coefficient using ImageJ with JACoP plugin. Details of antibodies are listed in the Table A below.

Table A: List of antibodies used in immunoblot and immunocytochemistry

Antibodies	Concentration	Company
P2X4	(1:250)	Alomone labs
Actin	(1:600)	Sigma
Anti-mouse HRP	(1:1000)	Thermo Scientific
Anti-rabbit HRP	(1:1000)	BioRAD

3.4 Molecular Biology

A summary of point mutations in P2X4R with fluorescence-tagged constructs that were generated is given in Table B.

Table B: List of P2X4R mutants

Construct	Species	Antibiotic resistance
P2X4-K67A-EGFP	Mouse	Kanamycin
P2X4-M31A-EGFP	Human	Ampicillin
P2X4-A6S-A7S-EGFP	Human	Ampicillin

3.4.1 Point mutation of P2X4

Primers for point mutations of P2X4Rs are detailed in Table C using an in-house point mutation method where sequence indicated in red indicates mutation being made. The PCR mixtures contained 5 μ l of 10X Cloned Pfu Reaction Buffer (Stratagene), 0.5 μ g of plasmid template, 0.5 μ l of each primer, and 1 μ l of 250 nM deoxyribonucleotide triphosphates (dNTPs) and 41.5 μ l of milli-Q water to give a final volume of 49 μ l. PCR was started with a “hot start” at 95 °C for 1 minute before addition of 1 μ l of PfuTurbo DNA polymerase (Stratagene). This was followed by 15 repeats of: denaturing of DNA at 95 °C for 30 seconds, primer annealing at 55 °C for 1 minute and extension at 68 °C for 6 minutes. Once the PCR reaction was completed, the PCR mixtures were left to cool down at 4 °C for 2 minutes. 1 μ l of Dnpl enzyme, which selectively cleaves methylated DNA, thus removing template DNA, was incubated with the PCR mixture for 1 h at 37 °C followed by transformation of *Escherichia coli*, section **3.4.2**.

Table C: Primers for P2X4R mutants

Construct	Forward Primer	Reverse Primer
P2X4- K67A- EGFP	AGCTCGGTGACAACCGCAGCC AAAGGTGTGGCT	AGCCACACCTTTGGCTGCGGT TGTCACCGAGCT
P2X4- M31A- EGFP	CGCAGCCGCAAAGTGGGGCTC GCGAACCGCGCCGTGCAACTG	CAGTTGCACGGCGCGGTTGCG GAGCCCCACTTTGCGGCTGCG
P2X4-A6S A7S- EGFP	ATGGCGGGCTGCTGCTCCGTG CTGGCGGCCTTCCTGTTC	GAACAGGAAGGCCGCCAGCAC GGAGCAGCAGCCCCGCAT

3.4.2 Bacteria transformation

1 µl of PCR mixture was added to 75 µl XL-10-Gold ultracompetent cells (Agilent Technologies). The mixture was kept on ice for 30 minutes and then heat shocked for 45 seconds at 42 °C, followed by 2 minutes on ice. 900 µl of LB broth (Fisher Scientific) was added and the tube placed in shaking incubator at 37 °C for 1 h. A 200 µl of mixture was spread onto agar plate with either kanamycin (50 µg/ml) or ampicillin (100 µg/ml) antibiotics and incubated at 37 °C overnight. Colonies were picked, placed in 5 ml LB with appropriate antibiotic, and placed in the shaking incubator at 37 °C at the speed of 2 g for overnight.

3.4.3 Miniprep of DNA

The plasmid DNA was isolated from *E. coli* using a Gene JET™ Plasmid Miniprep Kit (Fermentas) according to the manufacturer's protocol.

3.4.4 Sequencing of P2X4 mutants

Mutant plasmid DNAs were verified by a Sanger sequencing service (Source BioScience LifeSciences).

3.4.5 Gibson assembly of ligation of human P2X4R

To construct hP2X4R-EGFP, untagged plasmid human P2X4R (hP2X4R) was inserted into a pEGFP vector using the Gibson assembly kit according to the manufacturer's protocol. In brief, hP2X4 was amplified via PCR as an insert fragment. A double digest using two enzymes, NheI and SacII, were used to linearise vector pEGFP for 1 h at 37 °C. The assembly mix composed of 3 µl of digested pEGFP, 5 µl of hP2X4, 10 µl of Gibson assembly mix and 2 µl of dH₂O to give a final volume of 20 µl. The mixture was incubated for 15 minutes at 50 °C. The ligated product was then left to cool and 5 µl used for transformation, as indicated in section 3.4.2. To verify the PCR product, plasmid DNA was extracted via mini-prep (detailed in section 3.4.3) followed by restriction digest and Sanger sequencing to confirm the sequence.

3.5 Confocal Microscopy

Fluorescence from fluorescence probes in live cells was visualised using a Leica SP5 microscope. Prior to imaging, cells were washed twice using NES, to remove excessive fluorescence probes. Coverslips were placed into a chamber with NES

and imaged with a 63X oil-immersion objective. The laser settings (488 nm argon laser set at 19 % and 543 nm helium neon laser set at 30 %) and pinhole of the camera (150 μ m) were set at constant throughout experiments. Pictures were taken in the format of 1024 x 1024 pixels using an imaging speed at 100 Hz. Table D gives the laser settings that were used to visualise the fluorescent probes/fluorophores.

Table D: Lists of fluorescence probes and lasers setting

Fluorescence Probes	Lasers	Excitation (nm)
EGFP/FITC	Argon	488
Alexa-Fluor 488	Argon	488
Fluorescein isothiocyanate- 10kD dextran	Argon	488 (Maximal excitation for this probe is 490)
Lysotracker DND 99 Red	Helium/Neon	543 (Maximal excitation for this probe is 577)
Magic Red Cathepsin TM B	Helium/Neon	543 (Maximal excitation for this probe is 590)
mCherry	Helium/Neon	543
Oregon Green 488-10 kDa Dextran	Argon	488

Texas Red Dextran-10kDa	Helium/Neon	543 (Maximal excitation for this probe is 595)
Fluo4-AM/LAMP-GECO/G _{1.2} -GECO	Argon	488

3.6 Data analysis

Most results are presented with mean \pm SEM from N, independent experiments, or n, number of cells, as indicated in the Figure legends. Statistical analysis was assessed using GraphPad Prism, with unpaired Student *t* tests or one-way ANOVA followed by Tukey tests for post-hoc analysis being used as indicated in the Figure legends.

4. Investigating the role of P2X4R in lysosome function

4.1. Introduction

Previous studies have shown that native mouse and rat P2X4Rs are predominantly located within lysosomes in microglia, macrophages, and endothelial cells (Qureshi et al., 2007). In microglial cells grown in culture, the receptors dynamically traffic between lysosomes and the plasma membrane, but in macrophages they reside within the lysosomes and show much slower trafficking to the surface. Heterologously expressed P2X4Rs in NRK cells are also targeted to lysosomes (Qureshi et al., 2007).

Lysosomal P2X4Rs have been studied by patch clamping the enlarged lysosomes and dialysing the lumen of the lysosome to measure P2X4R mediated current. The P2X4R channels mediated an inward current in the presence of ATP, but only when the lumen was alkalinised (Huang et al., 2014). It was shown that various alkalinisation reagents were sufficient to activate P2X4R, including NH_4Cl , methylamine and Bafilomycin-A1, an inhibitor of the H^+ ATPase. Following activation, P2X4Rs mediated lysosomal Ca^{2+} efflux, which triggered homotypic lysosome fusion (Cao et al., 2015). The main aim of this study was to identify physiological regulators of lysosomal P2X4Rs and to examine their role in lysosome Ca^{2+} signalling and fusion.

4.2. Results

4.2.1. Characterisation of the subcellular distribution of wild type and mutant P2X4R in NRK and HeLa cells

There are several markers available to label lysosomes based on their acidity (LysoTracker), enzyme activity (Cathepsin B), presence of known lysosomal-associated membrane protein-1 (LAMP1) and trackable endocytosed materials for example Texas Red 10-kDa Dextran (DR). To investigate the sub-cellular distribution of P2X4R, I first used DR as a lysosome marker and compared its distribution with an EGFP tagged form of LAMP1 (LAMP1-GFP). NRK and HeLa cells were used in the study because they are large flat cells well suited to imaging by confocal fluorescence microscopy. Cells were plated onto glass coverslips, transfected with LAMP1-GFP and 24 h later, cells were incubated with DR for 5 h followed by a 2 h chase without the dye. Images were taken of live cells and extensive co-localisation of compartments labelled with LAMP1-GFP and DR was observed at the perinuclear region in both NRK and HeLa cells (**Fig. 4.1A-B**). The co-localisation of these two dyes was quantified by calculating the Pearson's coefficient, and the values obtained for NRK and HeLa cells were 0.7363 ± 0.012 A.U. and 0.6663 ± 0.032 A.U., respectively (**Fig. 4.1C**). This suggests that DR-positive compartments are mostly LAMP1 positive and thus DR does label late endosome (LE)/lysosomes.

Having confirmed that DR is a useful LE/lysosome marker, I next investigated its distribution with respect to that of P2X4R. I have conducted most of my study using rat P2X4R (rP2X4R), unless stated otherwise. rP2X4R-EGFP was expressed in both NRK and HeLa cells to compare trafficking in two different cell types. rP2X4R-EGFP was distributed in puncta in the perinuclear region and these puncta co-localised with

DR (**Fig. 4.2A-B**). A similar experiment was carried out using LAMP1-mCherry as a lysosome marker and this was also shown to co-localise with rP2X4R-EGFP within the perinuclear compartments. Thus, these results confirm those previously obtained and show that rP2X4R is targeted to lysosomes in these two cell lines (**Fig. 4.2C-D**).

To further characterise the compartments containing rP2X4R, NRK cells expressing rP2X4R-EGFP were incubated with lysotracker for 1 h, which is a marker of acidic compartments. rP2X4R-EGFP containing compartments within the perinuclear region co-localised with lysotracker indicating that rP2X4R is targeted to acidic LE/lysosomes (**Fig. 4.3A**). Finally, I compared the distribution of rP2X4R-EGFP with that of a marker of the activity of the lysosomal enzyme cathepsin B. The reagent, Magic Red, fluoresces upon cleavage by cathepsin B and compartments with greatest fluorescence also contained rP2X4R-EGFP. The larger vacuoles show expression of rP2X4R-EGFP at the limiting membrane of lysosomes (**Fig. 4.3B**).

Overall these results indicate that rP2X4R is targeted to compartments that have many of the key features of lysosomes; they are perinuclear, acidic, contain the active form of cathepsin B and contain LAMP1. There are other compartments containing rP2X4R-EGFP that do not share all of these properties and which might reflect different types of LE/lysosomes, or endosomes earlier on in the endocytic pathway.

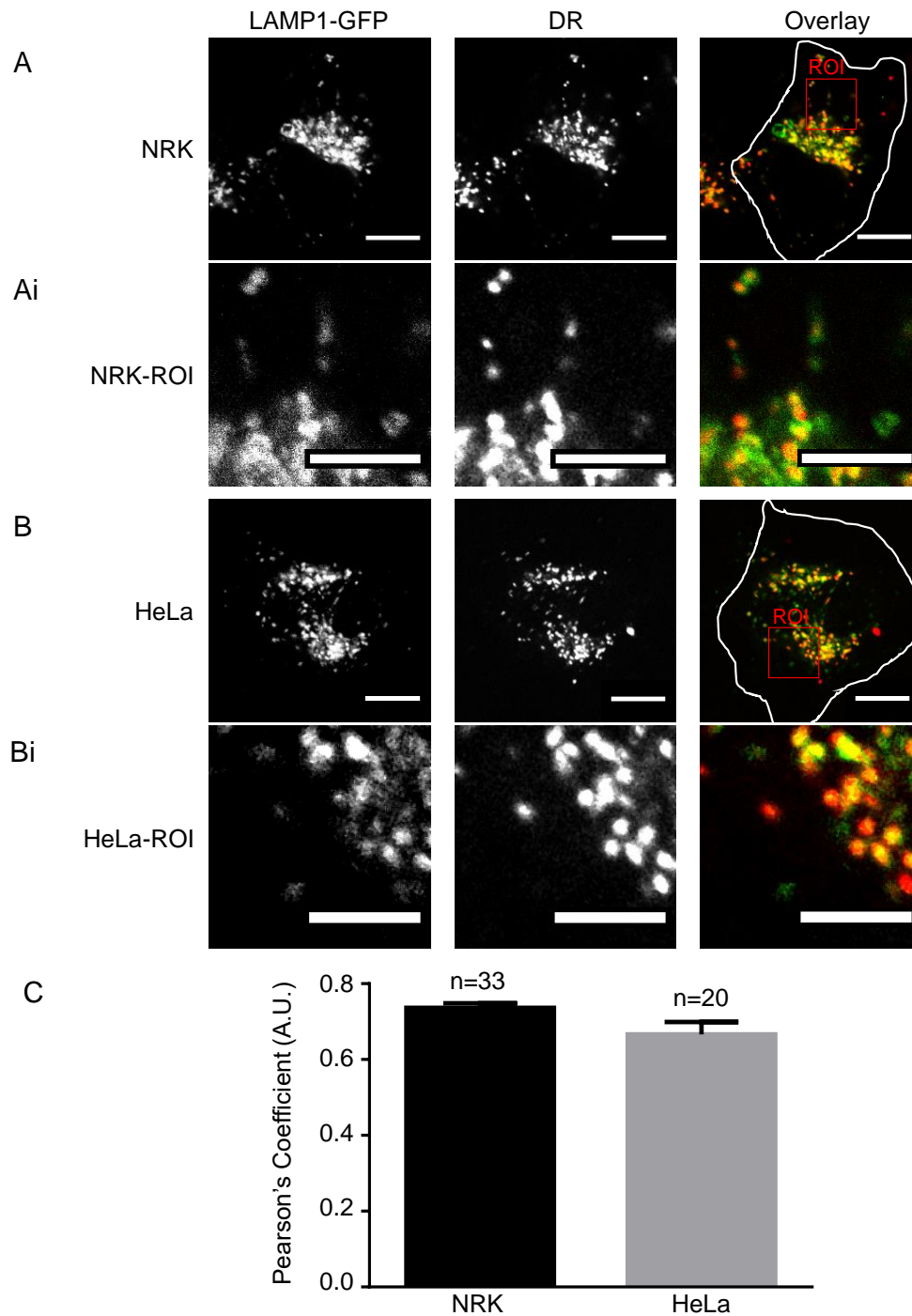


Figure 4.1 Co-localisation of lysosome markers in NRK and HeLa cells. (A&B) Lysosomes were labelled by both LAMP1-GFP and Texas Red 10-kDa Dextran (DR), which was incubated for 5 h followed by a 2 h chase, in NRK (A) and HeLa cells (B), white lines depict the plasma membrane of the cell. Scale bars, 10 μ m. (Ai & Bi) Confocal images showing high-magnification images of intracellular structures of both lysosome markers in NRK (Ai) and HeLa (Bi) cells. Scale bars, 5 μ m. (C) The co-localisation of two lysosome markers, LAMP1-GFP and DR, measured using Pearson's coefficient. Results are mean \pm s.e.m. from total number of cells. n. as indicated.

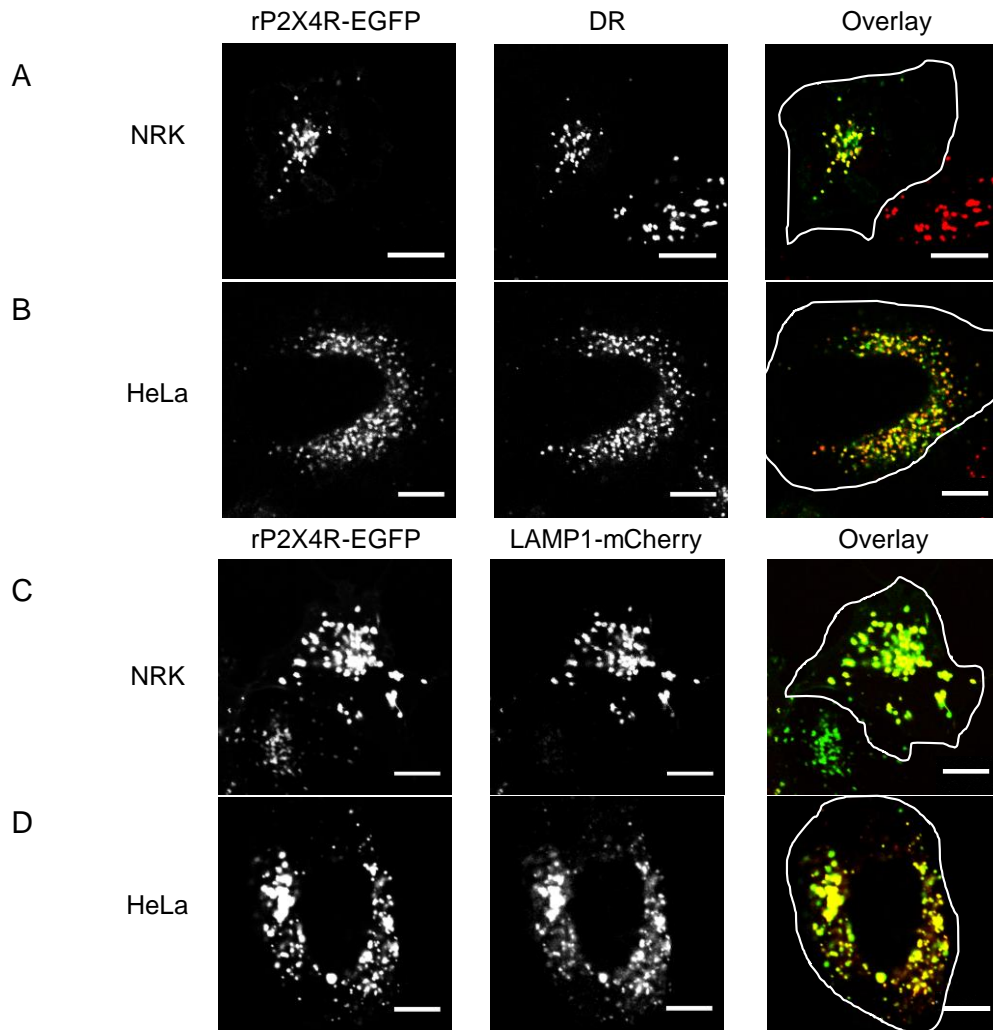


Figure 4.2 rP2X4Rs are localised to lysosomes in NRK and HeLa cells. Lysosomes were labelled using DR (A-B) and LAMP1-mCherry (C-D) in NRK and HeLa cells expressing rP2X4R-EGFP. White lines depict the plasma membrane of the cell. All scale bars, 10 μ m.

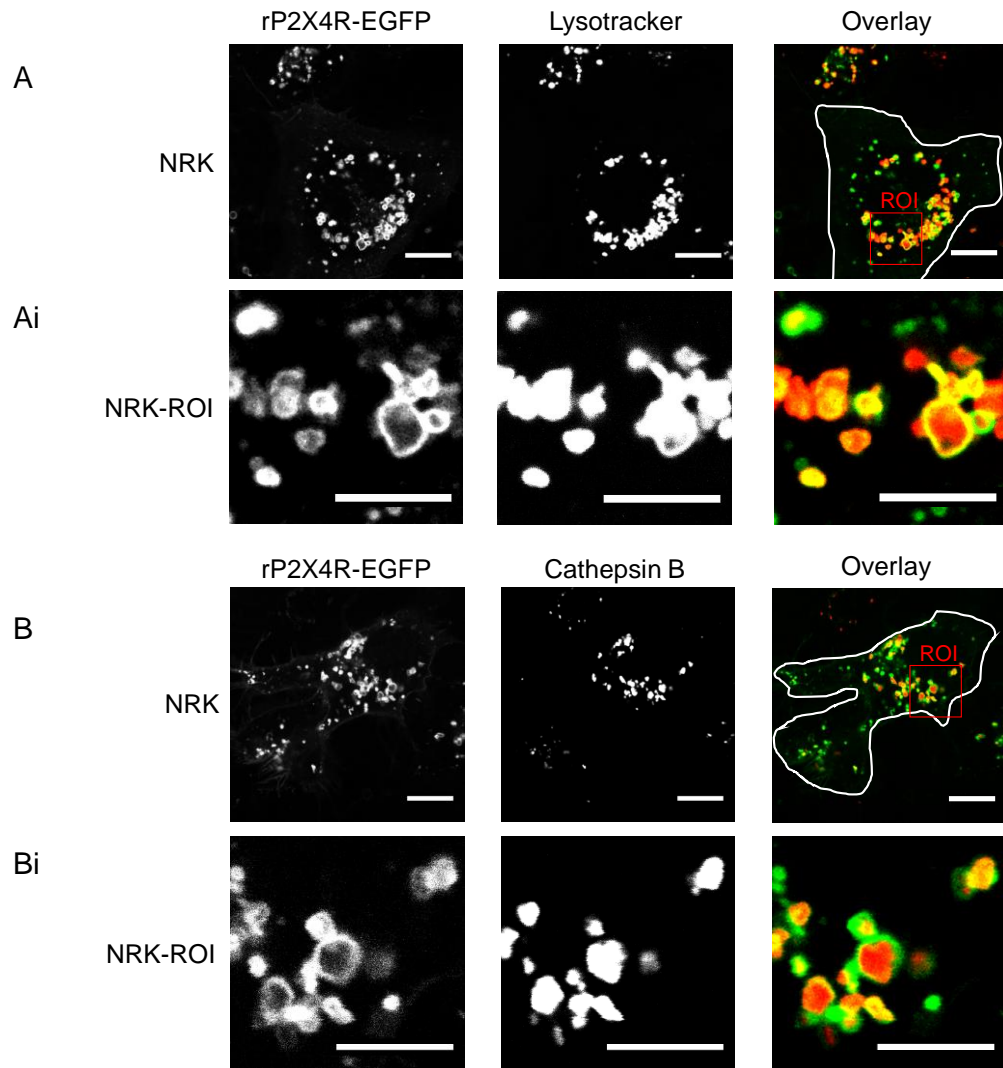


Figure 4.3 rP2X4Rs are localised to lysosomes in NRK cells. Lysosomes were marked by lysotracker (A) and cathepsin B (B) in NRK cells expressing rP2X4R-EGFP. White lines represent the plasma membrane of the cell. (A&B) Scale bars, 10 μm . (Ai & Bi) High-magnification images of intracellular lysosomes co-labelled by rP2X4R-EGFP and lysosome markers; lysotracker (Ai) and cathepsin B (Bi) in NRK cells. Scale bars, 5 μm .

I next compared the distribution of wild type (WT) rP2X4R with two non-functional mutants that I intended to use as negative controls in future experiments. The two mutants are the dominant negative mutant rP2X4R-C353W, which contains a mutation in the pore-lining, second transmembrane domain (Silberberg et al., 2005), and rP2X4R-K67A which contains a mutation in the ATP binding pocket that prevents ATP from binding (Stojilkovic et al., 2010). Using DR as a lysosome marker, both WT and mutants of rP2X4R were shown to co-localise with DR to a similar extent. Thus, the lack of functionality of the mutant receptors did not appear to alter their localisation to lysosomes (**Fig. 4.4A-C**). LAMP1-mCherry was also co-expressed with the different rP2X4R-EGFP in NRK cells and again a similar extent of co-localisation of rP2X4R-EGFP with LAMP1-mCherry at the perinuclear region was observed (**Fig. 4.4D-E**).

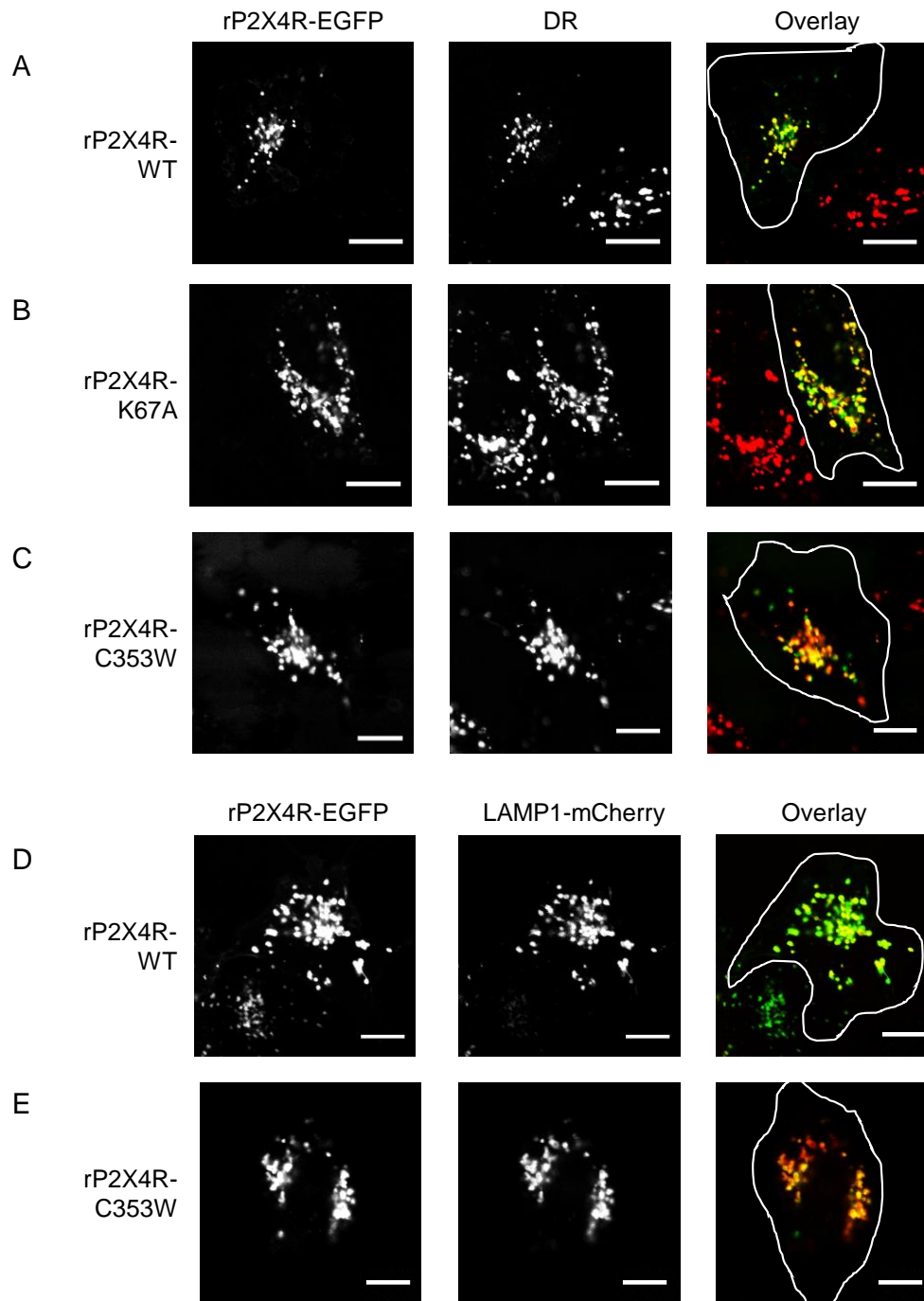


Figure 4.4 Both WT and mutant rP2X4R are targeted to lysosomes in NRK cells. Confocal images show NRK cells transiently transfected with EGFP-tagged rP2X4R-WT (A), rP2X4R-K67A (B) or rP2X4R-C353W (C). Lysosomes were marked by DR. (D-E) NRK cells expressing either rP2X4R-WT (D) or rP2X4R-C353W (E). Lysosomes were marked by LAMP1-mCherry. White lines represent the plasma membrane of the cell. All scale bar, 10 μm.

4.2.2 Role of P2X4R in the endocytosis pathway

Previously, Huang et al. (2014) showed by patch clamping lysosomes, that lysosomal alkalinisation triggered a P2X4R-mediated current suggesting a potential role of P2X4R in lysosome function. Given that P2X4R is targeted to lysosomes, the terminal destination of the endocytosis pathway, I investigated if expression of functional rP2X4R affects the rate of endocytosis. DR uptake in NRK cells expressing rP2X4R-EGFP was compared with DR uptake in cells expressing the mutant rP2X4R-C353W. Confocal images show a similar fluorescence intensity of DR in both rP2X4R-WT and rP2X4R-C353W expressing cells after either 2 h or 5 h of DR loading (**Fig. 4.5A-E**). This demonstrates that rP2X4R is unlikely to modulate the rate of endocytosis. The degree of co-localisation between WT and mutant rP2X4R and DR, were very similar after both 2 h and 5 h of DR incubation (**Fig. 4.5F**). This suggests that short incubation of DR (2 h) is sufficient for DR to be endocytosed and localised to lysosomes, independent of functional rP2X4R.

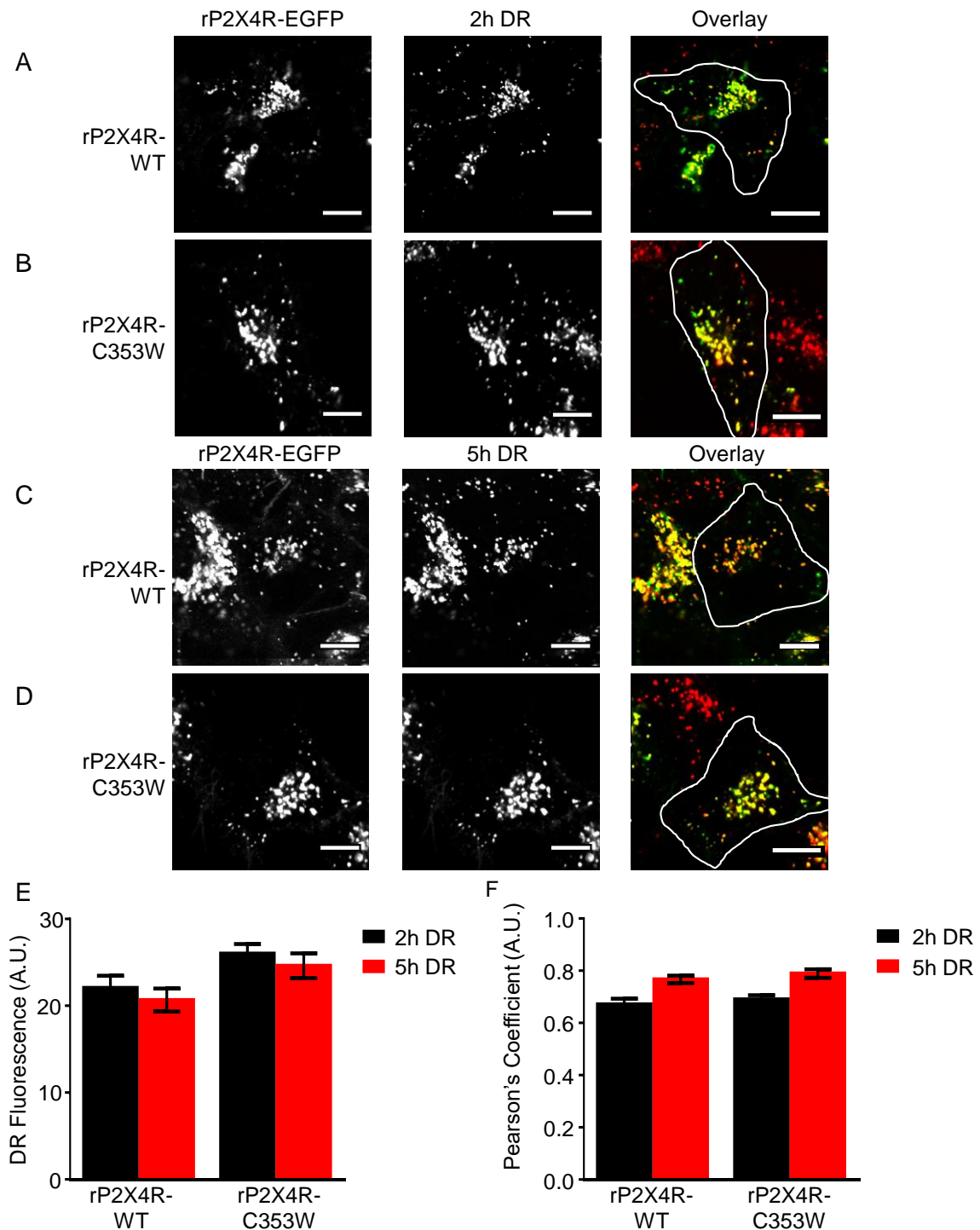


Figure 4.5 Over expression of functional rP2X4R did not regulate the endocytosis pathway in NRK cells. Representative confocal images of NRK cells transiently transfected with rP2X4R-EGFP or rP2X4R-C353W. Lysosomes labelled by DR were incubated for either 2 h (A-B) or 5 h (C-D) in cells expressing either rP2X4R-WT or rP2X4R-C353W. All scale bars, 10 μ m. (E-F) The co-localisation level of rP2X4R-EGFP with DR measured by the fluorescence intensity of DR (E) and Pearson's coefficient (F) in rP2X4R-WT and rP2X4R-C353W expressing cells. Results are mean \pm s.e.m. from 2 independent experiments with total number of cells between 39 and 45.

4.2.3 Pharmacological alkalinisation of lysosomes induces lysosome fusion

Activation of P2X4R in lysosomes by the pharmacological manipulation of pH has been shown to promote homotypic lysosome fusion in Cos-1 cells, resulting in the formation of enlarged vacuole-like lysosomes (Cao et al., 2015). To see if I could reproduce this result in NRK cells I conducted a similar experiment. Cells expressing rP2X4R-EGFP were incubated with DR to label lysosomes and their size was measured with and without alkalinisation of the lysosome. I compared the actions of the weak base methylamine (MA; 10 mM, 0.5 h) and an inhibitor of the vacuolar-type H⁺ ATPase, Bafilomycin-A1 (Baf-A1; 200 nM, 1 h) applied to cells in normal extracellular solution (NES) at 37 °C. Images of DR-positive lysosomes under control conditions and following MA and Baf-A1 treatments are shown in **Fig. 4.6A** for cells expressing rP2X4R-EGFP. The distribution of lysosome size was categorised into small (< 1.0 µm), medium (1.0-1.5 µm) and large (> 1.5 µm) and cells expressing rP2X4R showed a reduction in small lysosomes from 90.58 % to 53.92 % in response to MA treatment (**Fig. 4.6B**). Moreover, the percentage of medium and large size lysosomes increased from 8.74 % and 0.66 %, respectively, to 38.52 % and 7.55 %, respectively. Similar results were obtained using Baf-A1 although the effects were not as dramatic; there was a decrease in the percentage of small size lysosomes and the percentage of medium and large size lysosomes increased (**Fig. 4.6B**). A box plot was generated showing the median, 10th and 90th percentile of total lysosome size pooled from at least 20 cells for each condition (**Fig. 4.6C**). Cells expressing WT rP2X4R showed a modest increase in lysosome size following either MA or Baf-A1 treatment: the median size increased from 0.84 µm to 1.00 µm (p < 0.001, n = 20) upon MA treatment whilst Baf-A1 treatment induced an increment of

lysosome size from 0.84 μm to 0.94 μm ($p < 0.001$, $n = 20$). These results support the previous findings obtained using Cos-1 cells.

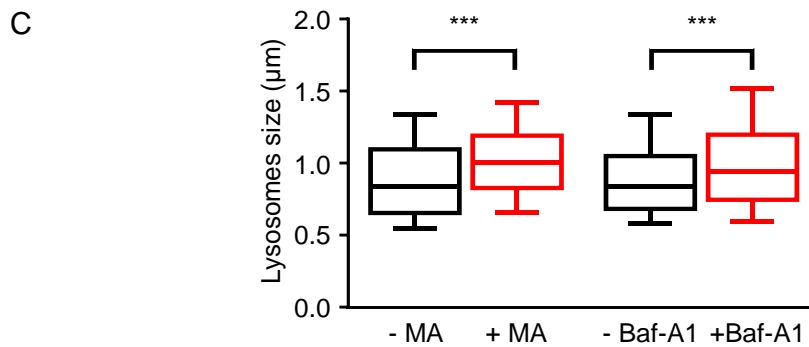
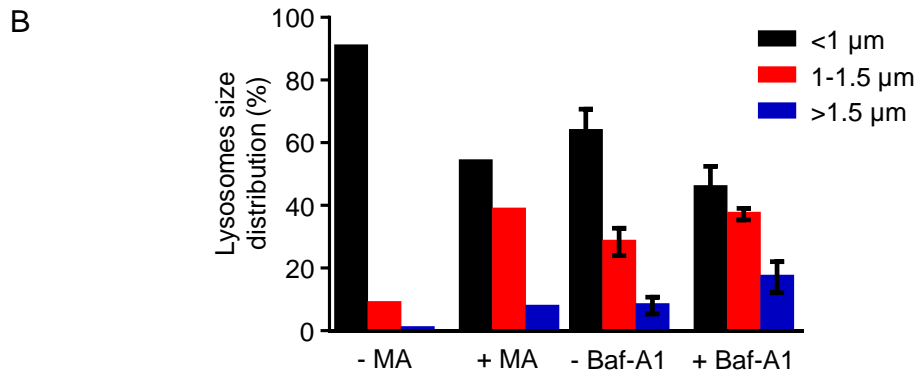
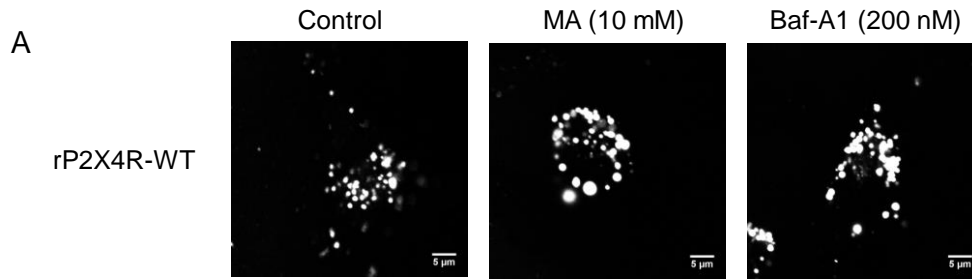


Figure 4.6 rP2X4R mediates lysosome fusion following lysosome alkalinisation. Representative images of NRK cells expressing EGFP-tagged of rP2X4R WT under control conditions or treated with either MA (10 mM, 0.5 h) or Baf-A1 (200 nM, 1 h). All scale bars, 5 μm. (B) The distribution of lysosome size in NRK cells expressing WT rP2X4R-EGFP under conditions indicated. MA experiments show mean results of total number of 20 cells. Results obtained from Baf-A1 experiments show mean \pm s.e.m. from 2 independent experiments with total number of 40 cells. (C) Box plot demonstrates the median, with 10th and 90th percentile of lysosome size in rP2X4-EGFP expressing NRK cells treated with either MA or Baf-A1. Results are mean \pm s.e.m. from experiments with total number of cells at least $n = 20$. *** $P < 0.001$, one-way ANOVA followed by Tukey's analysis.

4.2.4 A comparison of homotypic lysosome fusion in macrophages from WT and P2X4^{-/-} mice

Bone marrow derived macrophages (BMDMs) from P2X4R^{-/-} and WT mice were provided for a single experiment in which the effects of MA treatment on lysosome size was compared over a series of time points. Fluorescein isothiocyanate (FITC)-10-kDa dextran was loaded for 5 h in BMDMs to enable lysosome size measurements and although the fluorescence of FITC-dextran is quenched under acidic conditions, alkalinisation of lysosomes using MA relieved this quenching. Without MA pre-treatment, there was no difference in lysosome size between WT and P2X4R^{-/-} BMDMs. Following exposure to MA (10 mM), an increase in lysosome size was apparent for both groups of BMDMs (**Fig. 4.7A-B**). This was quantified by counting the number of cells with at least one lysosome greater than 2 μ m in diameter. After 15 and 30 minutes of MA treatment, 30 % and 73 % respectively of WT cells had at least one enlarged lysosome whereas for the P2X4^{-/-} cells the values were 13 % and 22 %, respectively (**Fig. 4.7C**). However, unfortunately I did not have access to more BMDMs from P2X4R KO mice and thus unable to confirm this preliminary finding. These results are consistent with the results obtained by Cao et al. (2015) that the recombinant P2X4R expressed in Cos-1 cells, and suggest that alkalinisation of the lysosome is sufficient to activate P2X4R and promote lysosome homotypic fusion.

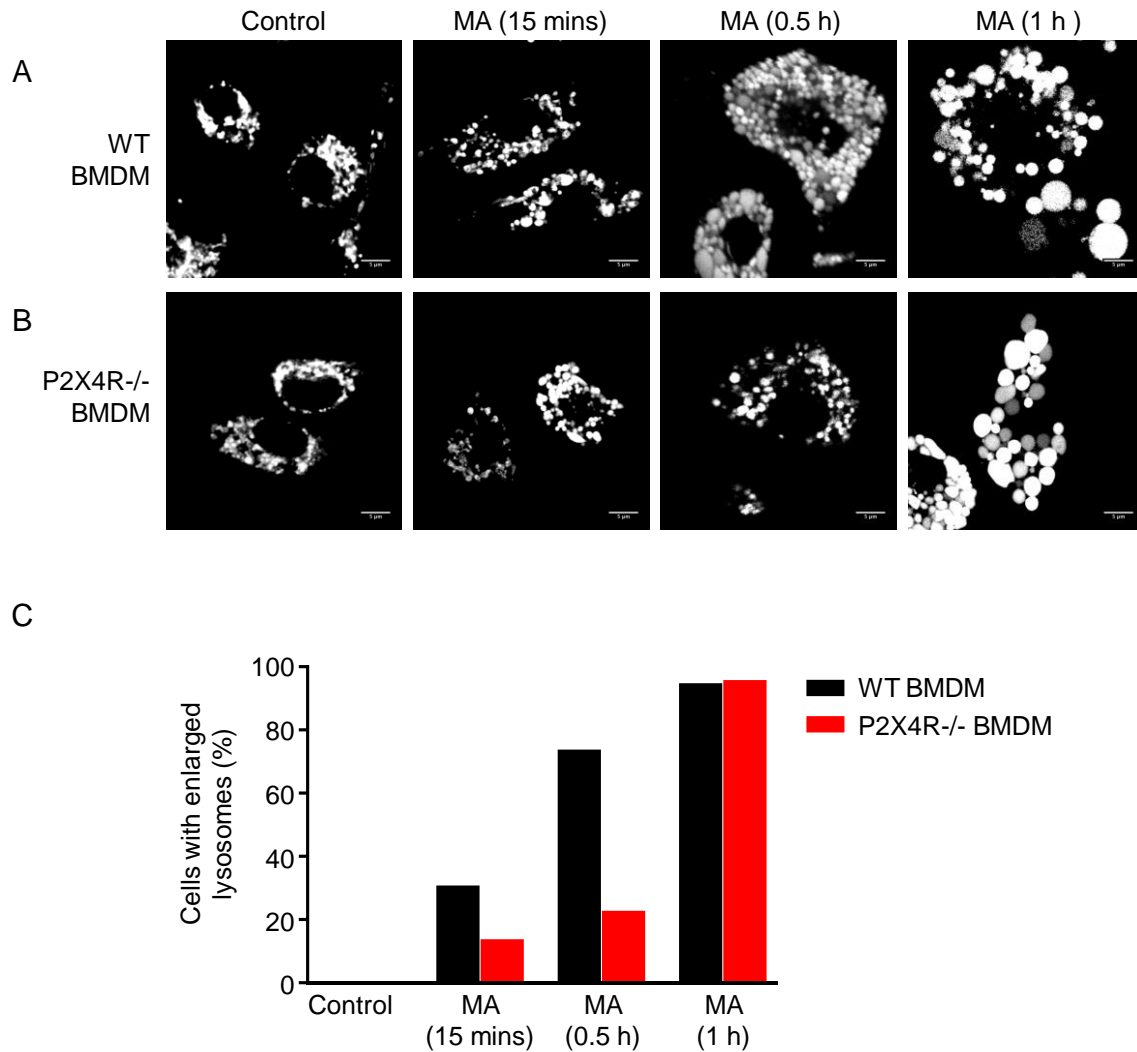


Figure 4.7 Efficient lysosome fusion is mediated by endogenous P2X4R in BMDMs following lysosome alkalinisation. Representative images of WT (A) and knockout of P2X4R (B) in BMDMs with lysosomes labelled by FITC 10-kDa dextran following MA (10 mM) treatment for 0 h (control), 15 minutes, 0.5 h and 1 h. All scale bars, 5 μ m. (C) Graph showing the percentage of cells with enlarged lysosomes (at least one lysosome size \geq 2 μ m) under conditions indicated. Results are mean of total number of 23-60 cells.

4.2.5 The role of P2X7R in promoting P2X4R-dependent lysosome fusion

P2X7R is frequently co-expressed with P2X4R in immune, epithelial and endothelial cells (Guo et al., 2007) and several studies have shown that the activation of plasma membrane P2X7R can induce lysosome alkalinisation (Takenouchi et al., 2009 and Guha et al., 2013).

To investigate any functional interaction between P2X4R and P2X7R in lysosome fusion, I co-transfected NRK cells with rP2X4R-EGFP and rat P2X7R (rP2X7). Lysosomes were labelled with DR, and the agonist BzATP was applied at a concentration (30 μ M), sufficient to activate rP2X7R (EC_{50} of \sim 10 μ M for rP2X7R and EC_{50} of \sim 100 μ M for hP2X7R; Rassendren et al., 1997). Following application of BzATP for 0.5 h, confocal images revealed enlarged vacuole like lysosomes that were marked by both rP2X4R-EGFP and DR (**Fig. 4.8B**). The enlarged lysosomes were observed towards the cell periphery as well as within the perinuclear region (**Fig. 4.8B**). I defined enlarged lysosomes in NRK cells as lysosomes greater than or equal to 1.8 μ m, which was obtained from the mean plus twice the standard deviation of lysosome size from the total number of lysosomes measured under control conditions (n = 50 cells). To quantify lysosome fusion, the percentage of cells with 2 or more lysosomes greater than or equal to 1.8 μ m was counted and there was a 2.6-fold increase in the percentage of cells with enlarged lysosomes in response to BzATP (66.4 ± 3.6 % vs 26.2 ± 4.0 %, $p < 0.05$) (**Fig. 4.8C**). This result suggests that the activation of rP2X7R can promote lysosome fusion. There was however a tendency for cells post-BzATP treatment to have formed blebs and be rounded up and a typical example is shown in **Fig. 4.9**. This indicates the toxic effect of prolonged activation of rP2X7R using BzATP. Also in several of the cells

there was a clear increase in rP2X4R-EGFP at the cell surface suggesting that considerable exocytosis of lysosomes had taken place.

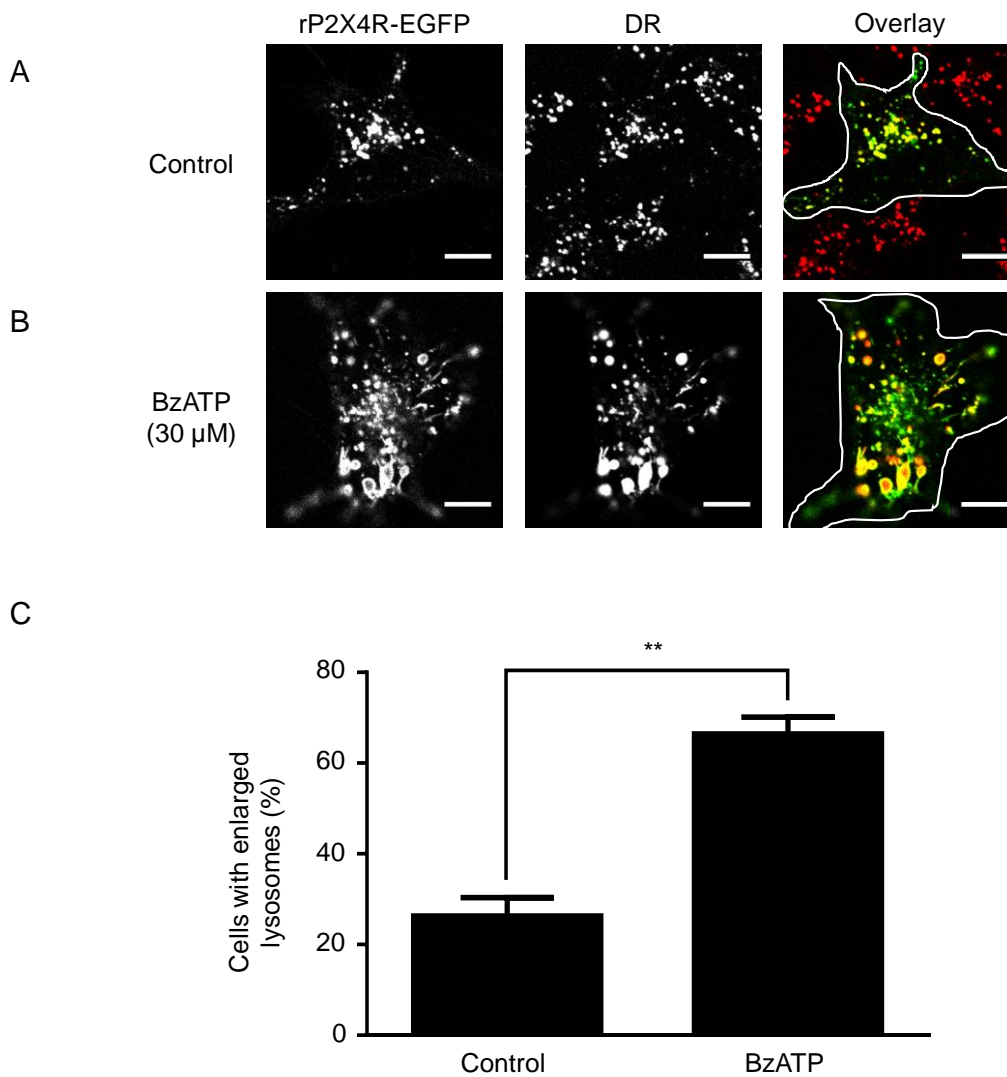


Figure 4.8 Stimulation of rP2X7R triggers P2X4R-dependent lysosome fusion. (A) Confocal images of NRK cells expressing rP2X4R-EGFP and rP2X7R with lysosomes labelled by DR. (B) BzATP treatment (30 μ M, 0.5 h) induced enlargement of lysosomes in cells co-expressing rP2X4R-EGFP and rP2X7R. (A-B) White lines represent the plasma membrane of the cell. All scale bars, 10 μ m. (C) The percentage of cells with 2 or more enlarged lysosomes ($\geq 1.8 \mu$ m) following BzATP treatment (30 μ M, 0.5 h) is significantly increased by stimulation with BzATP. Results are mean \pm s.e.m. from 3 independent experiments. **P < 0.01, unpaired student's *t* test.

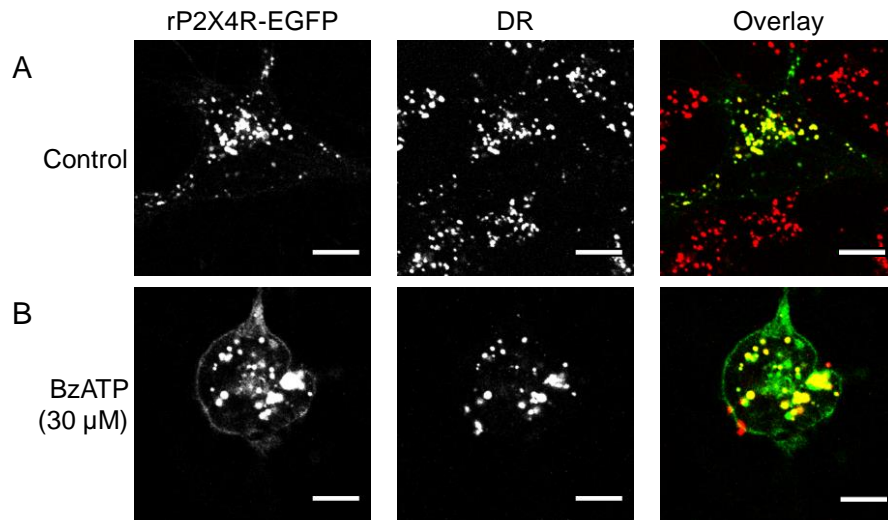


Figure 4.9 Representative confocal images of cell blebbing pre (A) and post (B) BzATP treatment (30 μ M, 0.5 h) in some NRK cells co-expressing rP2X4R-EGFP and rP2X7R with lysosomes labelled by DR. (A-B) All scale bars, 10 μ m.

The toxic effects of stimulation of rP2X7R have been reported previously and it occurs because the rat receptor rapidly undergoes pore dilation in response to BzATP (Robinson et al., 2014). Activation of human P2X7R (hP2X7R) is generally much less toxic to cells and it exhibits slower pore dilation and sensitisation (Humphreys et al., 1998; Rassendren et al., 1997; Robinson et al., 2014). I therefore switched to using hP2X7R and compared the size of lysosomes with and without treatment with 100 μ M BzATP for 0.5 h. A higher concentration of BzATP was administered because this is a less potent agonist at hP2X7R compared to rP2X7R, as detailed in section 1.7 of introduction. Cells co-expressing hP2X7R and rP2X4R-EGFP showed enlarged vacuole-like lysosomes following the incubation with BzATP (**Fig. 4.10A**) and the percentage of cells with enlarged lysosomes was significantly increased from 15.6 ± 2.0 % to 61.7 ± 5.3 % ($p < 0.001$) (**Fig. 4.10B**); no cell blebbing and rounding up was observed.

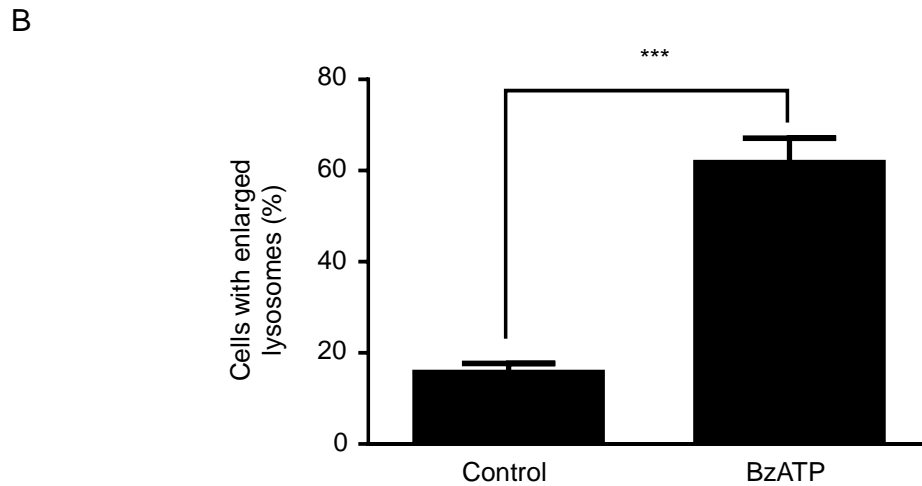
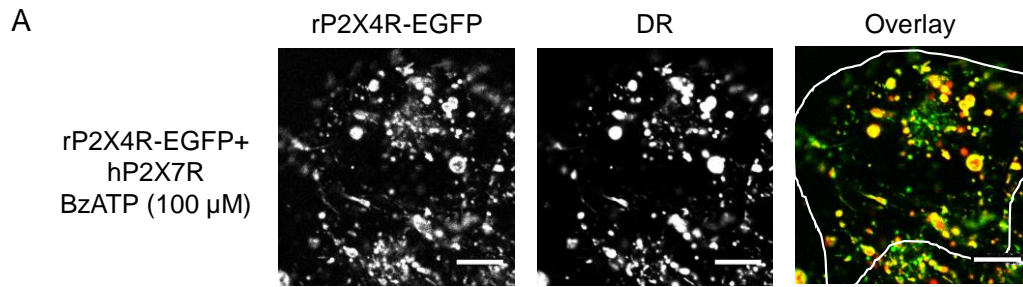


Figure 4.10 Stimulation of hP2X7R induces rP2X4R-dependent lysosome fusion. (A) Confocal images of NRK cells co-transfected with rP2X4R-EGFP and hP2X7R with lysosomes labelled by DR following BzATP treatment (100 μ M, 0.5 h). (B) The percentage of cells with 2 or more enlarged lysosomes ($\geq 1.8 \mu$ m) in response to control and BzATP treatments, as indicated. (A-B) Results are mean \pm s.e.m. from 3 independent experiments. *** $P < 0.001$, unpaired student's t test. All scale bars, 10 μ m.

Further experiments were carried out to compare lysosomes in cells expressing rP2X4R and hP2X7R individually, rP2X4R and hP2X7R together, and hP2X7R with the non-functional rP2X4R mutants (rP2X4R-C353W and rP2X4R-K67A). The results are shown in **Fig. 4.11**. Only in cells co-expressing both functional rP2X4R and hP2X7R were there an increase in the frequency of cells with enlarged lysosomes following incubation with BzATP (100 μ M, 0.5 h) (**Fig. 4.11A**). In cells expressing rP2X4R alone, I also tested the effects of 100 μ M MgATP, a concentration sufficient to fully activate any P2X4Rs at the plasma membrane, but this did not produce an increase in the number of cells with enlarged lysosomes (**Fig. 4.11B**). Therefore, ruling out any contribution of the plasma membrane rP2X4R. A comparison was made of the distribution of lysosome size for the different conditions by plotting frequency histograms, as shown in **Fig. 4.12**. For cells expressing P2X4R and P2X7R alone, there was no shift in frequency for any of the four size categories after incubation with BzATP, whereas for cells co-expressing the rP2X4R and hP2X7R there was a significant shift in the distribution towards larger lysosomes ($> 1 \mu$ m) (**Fig. 4.12A-C**). This shift in lysosome size distribution was not seen for either of the non-functional mutant rP2X4Rs when co-expressed with hP2X7R, which indicates that the enhancement in the size of lysosomes triggered by BzATP is dependent upon the expression of a functional rP2X4R and on the expression of hP2X7R. Altogether these results suggest a synergistic effect of P2X4R and P2X7R in lysosome fusion and that P2X7R is a likely physiological regulator of lysosomal P2X4Rs.

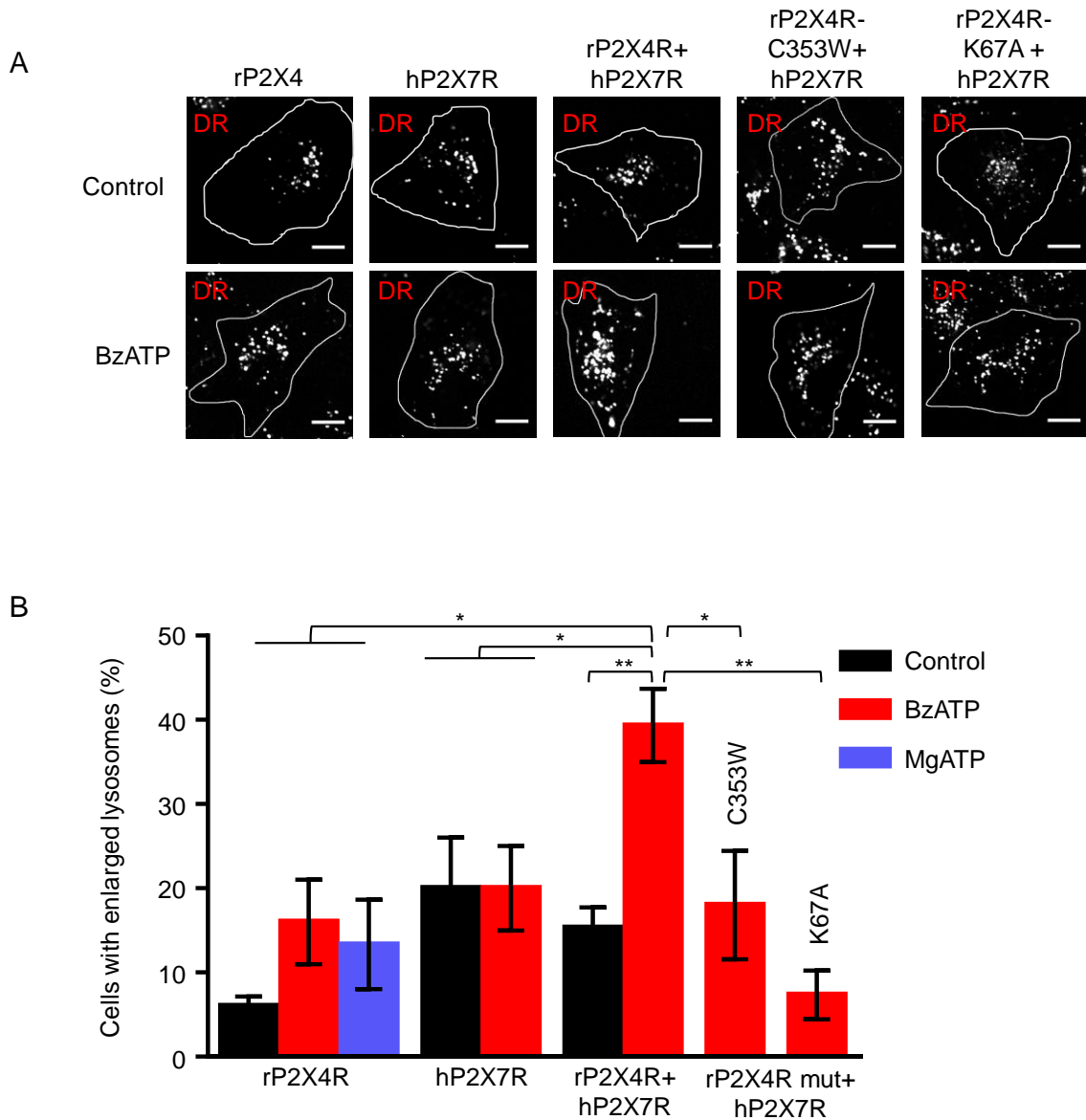


Figure 4.11 Synergistic interaction occurs between P2X4R and P2X7R in lysosome fusion. (A) Representative images of NRK cells co-expressing wild type rP2X4R-EGFP, the dominant mutant rP2X4R-EGFP (C353W) or the non-functional mutant rP2X4R-EGFP (K67A) with hP2X7R, or cells expressing rP2X4R or hP2X7R alone. Cells were treated with and without BzATP (100 μ M, 0.5 h). Lysosomes were labelled using DR. (B) Histogram of cells with 2 or more enlarged lysosomes ($\geq 1.8 \mu$ m) following control, BzATP (100 μ M, 0.5 h) and MgATP (100 μ M, 0.5 h) treatments, and in the conditions indicated. (A-B) All results are mean \pm s.e.m. from 3 independent experiments. * $P < 0.05$ and ** $P < 0.01$, one-way ANOVA followed by Tukey's analysis. All scale bars, 10 μ m.

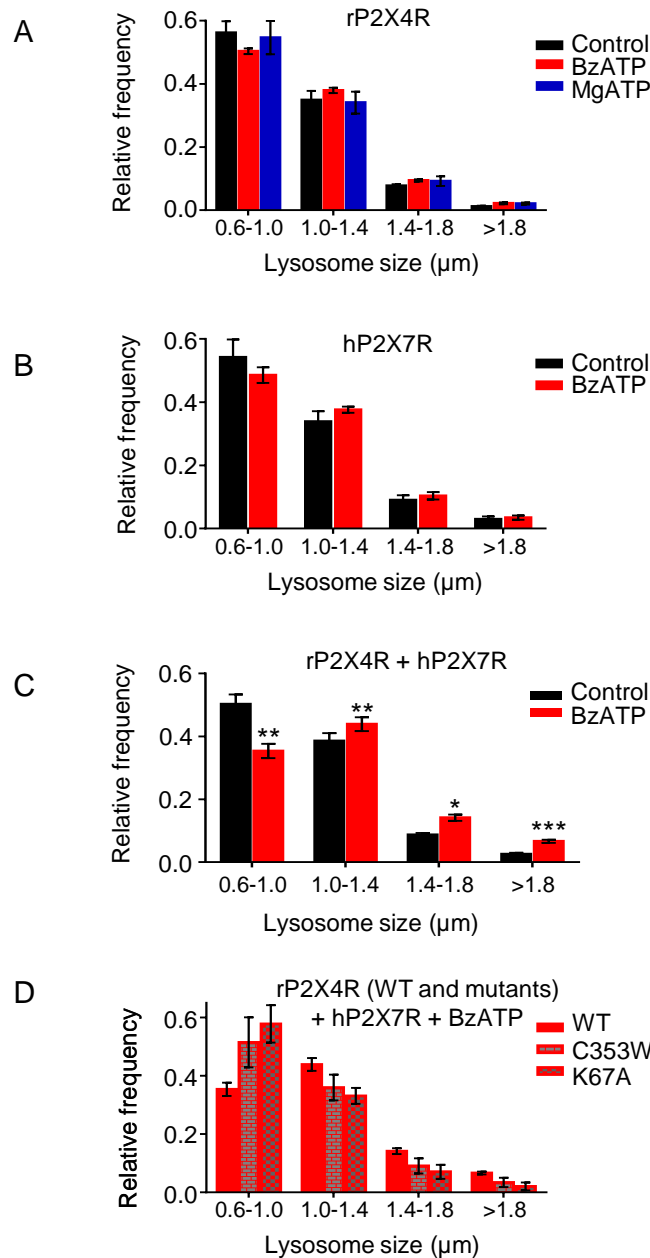


Figure 4.12 Activation of P2X4R and P2X7R shifts lysosome distribution to larger lysosome sizes following BzATP treatment. (A-D) The relative frequency distribution of lysosome size in cells expressing rP2X4-EGFP alone (A), hP2X7R alone (B), cells co-expressing rP2X4R-EGFP and hP2X7R (C) or rP2X4R mutants (C353W and K67A) with hP2X7R (D). Conditions are control, BzATP (100 μM, 0.5 h) or MgATP (100 μM, 0.5 h), as indicated. All results are mean ± s.e.m. from 3 independent experiments. (C) *P < 0.05, **P < 0.01 and ***P < 0.001, unpaired student's *t* test.

4.2.6 The effect of P2X4R and P2X7R on the subcellular distribution of lysosomes

For cells co-expressing P2X4R and P2X7R, the distribution of DR-labelled lysosomes post-BzATP treatment looked different; more evenly distributed over the cell rather than clustered within the perinuclear region. This suggests that activation of P2X7R not only promotes P2X4R-dependent homotypic lysosome fusion, but also promotes the anterograde movements of lysosomes toward the periphery of the cell where they can undergo lysosome exocytosis. To investigate this further I analysed the distribution of rP2X4R-EGFP positive compartments before and after a 30 minute treatment with BzATP (100 μ M) and dynasore (80 μ M) (an inhibitor of dynamin dependent endocytosis). I quantified this by measuring the distance between lysosomes marked by rP2X4R-EGFP and the nucleus and obtained a value for the perinuclear index (Li et al., 2016), where a high value corresponds to greater clustering of lysosomes in the vicinity of the nucleus. Perinuclear index is a measurement of the fluorescence intensity of lysosome populations that are less than 5 μ m away from the nucleus minus the fluorescence intensity of lysosome populations that are more than 5 μ m away from nucleus (detailed in chapter 3.2.4). A comparison was made between cells expressing rP2X4R alone, together with hP2X7R and for the non-functional K67A mutant receptor with hP2X7R. Only in cells co-expressing both functional receptors was there a significant decrease in perinuclear index after treatment with agonist BzATP and dynasore (1.8 ± 0.12 A.U. to 0.87 ± 0.08 A.U.; $p < 0.001$) (**Fig. 4.13A-B**). As a positive control, ionomycin (5 μ M; 10 minutes), a Ca^{2+} ionophore that has previously shown to potentiate the rate of lysosome exocytosis (Qureshi et al., 2007), was administered to NRK cells. A reduced perinuclear index, was observed for all three groups of cells following

ionomycin treatment (**Fig. 4.13B**). It is not necessarily that the decrease in perinuclear index is an absolute indicator of lysosome exocytosis, but the peripheral localisation of lysosomes induced by ionomycin could be an early indicator of lysosome docking that facilitates exocytosis.

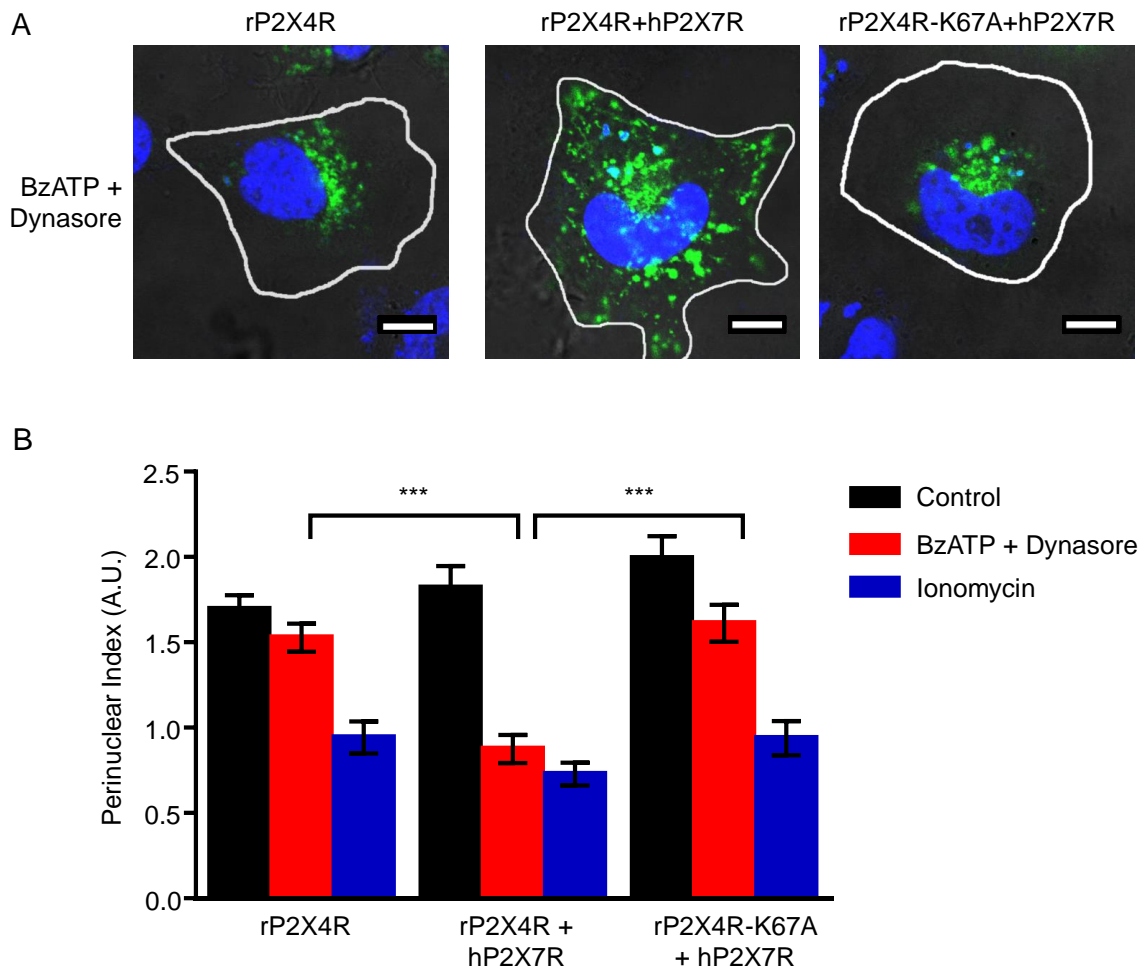


Fig. 4.13 Synergistic effect of P2X4R and P2X7R in the redistribution of lysosomes towards the cell periphery. (A) Representative images showing NRK cells expressing rP2X4R-EGFP alone, or co-expressing either WT or mutant K67A of rP2X4R-EGFP with hP2X7R. Cells were treated with BzATP (100 μ M, 0.5 h) and dynasore (80 μ M, 0.5 h). Nucleus was determined by DAPI staining. White lines represent the plasma membrane of the cell. (B) Histogram showing the distribution of lysosomes as measured by perinuclear index, a measurement of the distance of lysosome populations from nucleus, detailed in section 3.2.4. Cells co-expressing rP2X4R and hP2X7R show a lower perinuclear index following BzATP and dynasore treatment, indicating redistribution of lysosomes away from nucleus. (A-B) All results are mean \pm s.e.m. from 3 independent experiments. *** $P < 0.001$, one-way ANOVA followed by Tukey's analysis. All scale bars, 10 μ m.

4.2.7 The synergistic role of P2X4R and P2X7R in lysosome fusion is Ca²⁺ dependent

Having shown that P2X4R and P2X7R act synergistically to increase the size of lysosomes, I investigated if this effect is dependent upon extracellular Ca²⁺. I hypothesised that a rise in cytoplasmic [Ca²⁺] via plasma membrane P2X7R was required for lysosome alkalinisation. BzATP was applied to NRK cells co-expressing rP2X4R and hP2X7R, in either 2 mM extracellular Ca²⁺ or nominally Ca²⁺ free NES. In 2 mM Ca²⁺ NES, there was a significant increase in the proportion of cells with enlarged lysosomes following BzATP treatment (14.0 ± 2.2 % to 46.8 ± 2.8 %; p < 0.05), but this was abolished in Ca²⁺ free NES (**Fig. 4.14**). This result suggests that Ca²⁺ entry via P2X7R is required to trigger lysosome fusion. It is possible that the P2X7R-mediated Ca²⁺ signal might trigger lysosome alkalinisation, thereby activating P2X4R to mediate lysosome fusion.

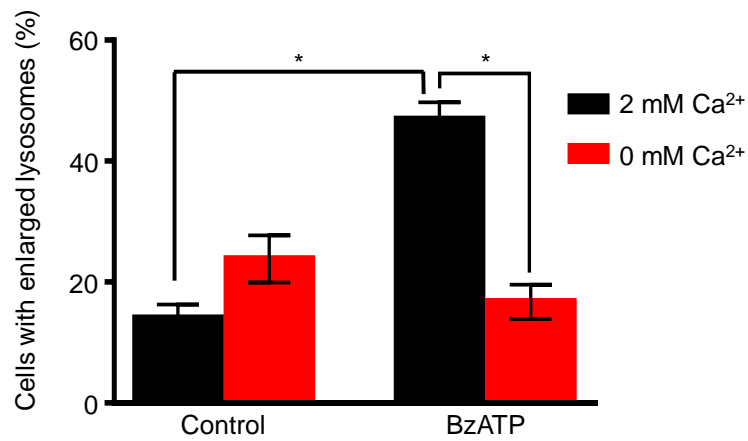


Figure 4.14 Activation of P2X7R induces P2X4R-mediated lysosome fusion and this is dependent on Ca²⁺ influx. Summary results show the percentage of cells co-expressing rP2X4R-EGFP and hP2X7R with 2 or more enlarged lysosomes ($\geq 1.8 \mu\text{m}$) under conditions indicated: with (2 mM Ca²⁺) and without extracellular Ca²⁺ (0 mM Ca²⁺) in normal extracellular solution (NES). All results are mean \pm s.e.m. from 3 independent experiments. *P < 0.05, one-way ANOVA followed by Tukey's analysis.

4.2.8 P2X7R stimulation induces lysosomal alkalisation that is dependent on extracellular Ca²⁺

To investigate this further, I monitored how lysosome pH is modulated by BzATP in cells co-expressing rP2X4R and hP2X7R in the presence and absence of extracellular Ca²⁺. Lysosome pH was assessed using two different dextran conjugates: pH-dependent Oregon Green 488 10-kDa Dextran (OG) and pH-insensitive DR. Cells were incubated in the presence of both dyes for 5 h followed by a 2 h chase and as expected, the two dyes co-localised within the same compartments (**Fig. 4.15**). The intensity of OG fluorescence in resting cells was low because it is quenched by the acidic lysosomal environment. In the presence of extracellular Ca²⁺ (2 mM), there was an increase in fluorescence intensity of OG after BzATP (100 μM) application, indicative of lysosomal alkalisation (**Fig. 4.16A**), whereas there was no increase in OG fluorescence intensity when the experiment was carried out in nominally Ca²⁺-free NES (**Fig. 4.16B**). The fluorescence intensity of DR remained at a similar level throughout all the experiment. The fluorescence ratio of OG:DR was calculated at two time points post BzATP application and compared to the ratio immediately prior to agonist (**Fig. 4.16C**). There was a significant increase in the ratio at both 120 s and 300 s (1.6 ± 0.09 A.U. and 2.1 ± 0.15 A.U. respectively) but only in the presence of extracellular Ca²⁺ (**Fig. 4.16C**). These results lead me to conclude that Ca²⁺ entry through P2X7R results in alkalisation of lysosomes.

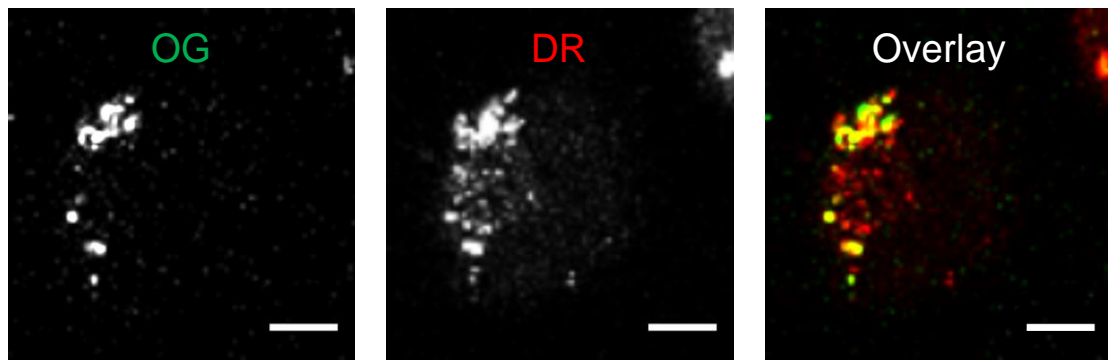


Figure 4.15 Lysosomes were co-labelled by Oregon Green 488 10-kDa Dextran (OG; pH sensitive dye) and Texas Red 10-kDa Dextran (DR; pH insensitive dye) for lysosome pH measurement in NRK cells. Representative images of lysosomes marked by both lysosome markers: OG and DR in rP2X4R and hP2X7R co-expressing NRK cells. All scale bars, 10 μ m.

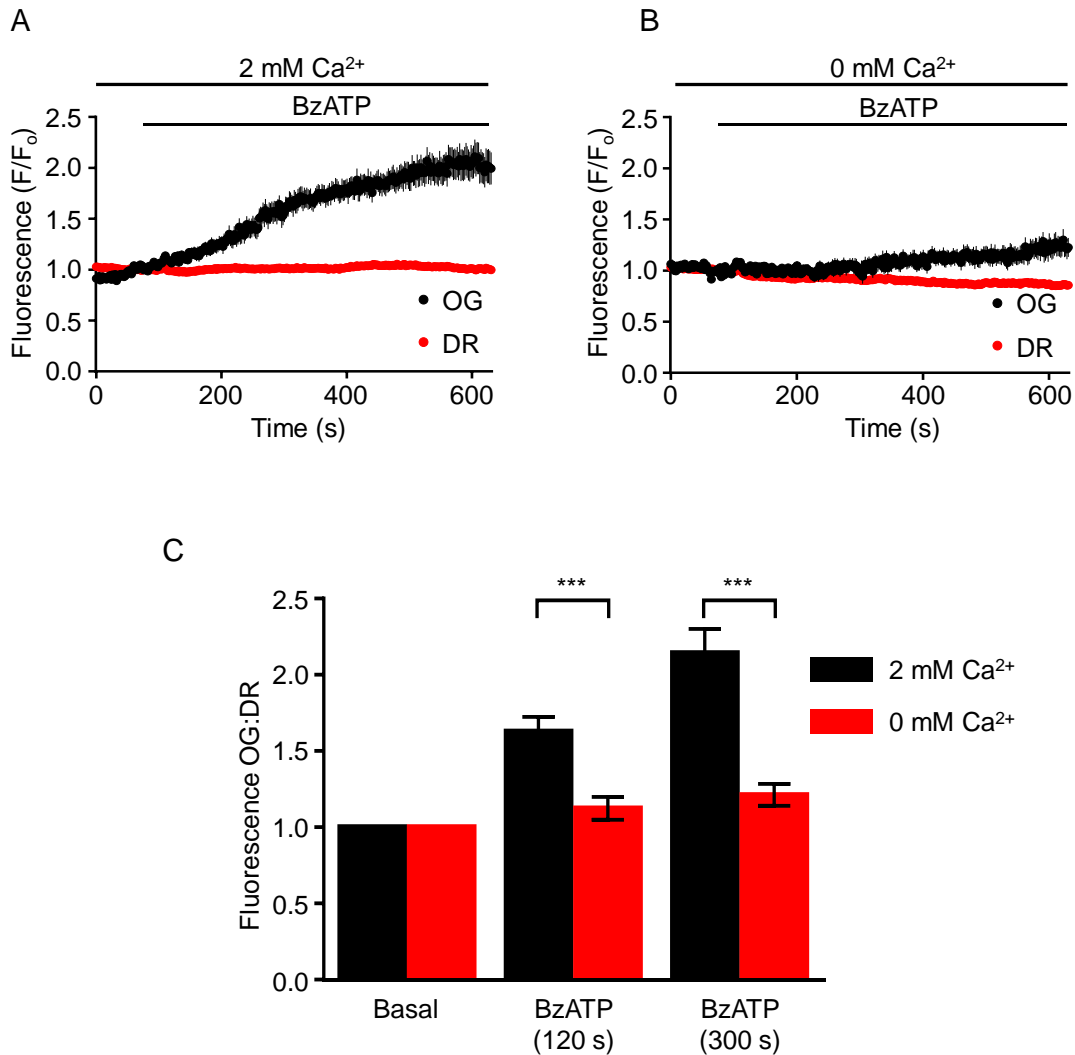


Figure 4.16 P2X7R stimulation induces lysosomal alkalisation and this is dependent on extracellular Ca²⁺. Graphs showing the changes in fluorescence of each dye (OG and DR) over time following BzATP (100 μM) treatment in either 2 mM Ca²⁺ (A) or 0 mM Ca²⁺ (B) containing NES. Cells were co-expressed with rP2X4R and hP2X7R. The increase in fluorescence of OG indicates a rise in lysosome pH following BzATP treatment in 2 mM Ca²⁺ NES. (C) Summary of data showing the fluorescence ratio of OG: DR measured at different times after BzATP (100 μM) treatment in either 2 mM Ca²⁺ or 0 mM Ca²⁺, as indicated. All results are mean ± s.e.m. from 3 independent experiments. ***P < 0.001, one-way ANOVA followed by Tukey's analysis.

4.2.9 Cytoplasmic Ca²⁺ signals generated by P2X4R and P2X7R

It has previously been shown that lysosome fusion is triggered by Ca²⁺ release from lysosomes and an increase in the level of cytoplasmic Ca²⁺ in the vicinity of lysosomes (Cao et al., 2015). To investigate how P2X4R and P2X7R contribute to the cytoplasmic Ca²⁺ response following BzATP application I first used a cytoplasmic Ca²⁺ indicator, G_{1.2}-GECO (G-GECO) to measure cytoplasmic changes in [Ca²⁺]. NRK cells were co-transfected with G-GECO, and either rP2X7R alone or rP2X7R with rP2X4R or the K67A mutant. rP2X7R was used in the rest of Ca²⁺ imaging experiments due to the short BzATP treatment that is unlikely to induce cell blebbing. Experiments were carried out in NES containing 1 mM Ca²⁺ and following application of BzATP there was a rapid increase in G-GECO fluorescence intensity (**Fig. 4.17A**). The increase in [Ca²⁺] was similar in cells expressing rP2X7R alone or rP2X7R with either the WT or mutant rP2X4R. It presumably reflects the Ca²⁺ entry via plasma membrane rP2X7R. (**Fig. 4.17B**). Thus, the cytoplasmic Ca²⁺ response is dominated by rP2X7R mediated Ca²⁺ entry under these conditions.

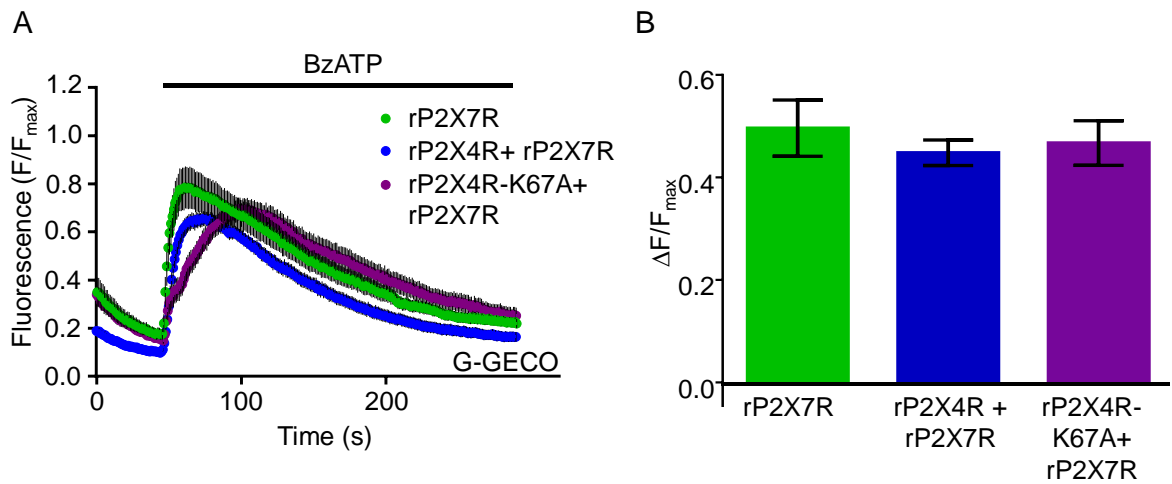


Figure 4.17 P2X7R stimulation induces an elevation in the cytosolic $[Ca^{2+}]$ as measured by cytosolic G-GECO. (A) The Ca^{2+} signal recorded by G-GECO in NRK cells expressing either rP2X7R alone or co-expressing either WT or mutant K67A rP2X4R with rP2X7R following BzATP ($30 \mu M$) treatment in $1 \text{ mM } Ca^{2+}$ NES. (B) Summary of data showing the magnitude change of G-GECO after BzATP ($30 \mu M$) treatment, as indicated. All results are mean \pm s.e.m. from 3 independent experiments.

To measure cytoplasmic Ca^{2+} changes in the vicinity of the lysosome, a different Ca^{2+} reporter construct was used, namely LAMP1-GECO. This was a gift from Professor Taylor's lab and was generated by Peace Atakpa who tagged $\text{G}_{1.2}$ -GECO to the cytoplasmic tail of LAMP1 (Ca^{2+} binding affinity of $1.2 \mu\text{M}$; Zhao et al., 2011). First, I wanted to demonstrate the lysosomal localisation of LAMP1-GECO and so I transfected it into NRK cells and co-labelled lysosomes using DR. Confocal images show that LAMP1-GECO largely co-localised with DR in compartments at the perinuclear region indicating the lysosome targeting of LAMP1-GECO (**Fig. 4.18A**). There was some LAMP1-GECO labelling that did not co-localise with DR and one possibility is that LAMP1-GECO also labeled quiescent population of lysosomes that was not receiving recently endocytosed materials. Next, NRK cells were co-transfected with LAMP1-GECO, rP2X4R and rP2X7R and the fluorescent response to BzATP was compared to cells transfected with either LAMP1-GECO and rP2X7R alone, LAMP1-GECO with rP2X7R and rP2X4R-K67A, or LAMP1-GECO with rP2X4R alone. The fluorescence intensity of LAMP1-GECO (F) was normalised to the maximal fluorescence (F_{max}) produced by ionomycin (as detailed in section 3.2.2). In response to the application of BzATP ($30 \mu\text{M}$) in Ca^{2+} -containing NES, a significant increase in F/F_{max} was observed in cells expressing rP2X7R, however there was no change in F/F_{max} in cells expressing rP2X4R alone (**Fig. 4.18B-C**). In cells co-expressing rP2X4R and rP2X7R, the fluorescent response to BzATP was significantly larger than in cells expressing rP2X7R alone. This suggests that rP2X7R-mediated Ca^{2+} influx induced lysosome alkalinisation, thereby activating lysosomal rP2X4R to mediate lysosome Ca^{2+} efflux, which contributed to the cytoplasmic $[\text{Ca}^{2+}]$ signal in the immediate vicinity of the lysosome (**Fig. 4.18B-C**). This lysosome Ca^{2+} signal was also larger in cells co-expressing rP2X4R and

rP2X7R than in cells co-expressing rP2X4R-K67A and rP2X7R (**Fig. 4.18C**).

Together, these results suggest that lysosomal P2X4R can potentiate Ca²⁺ signals in the vicinity of lysosomes in response to the activation of plasma membrane P2X7R.

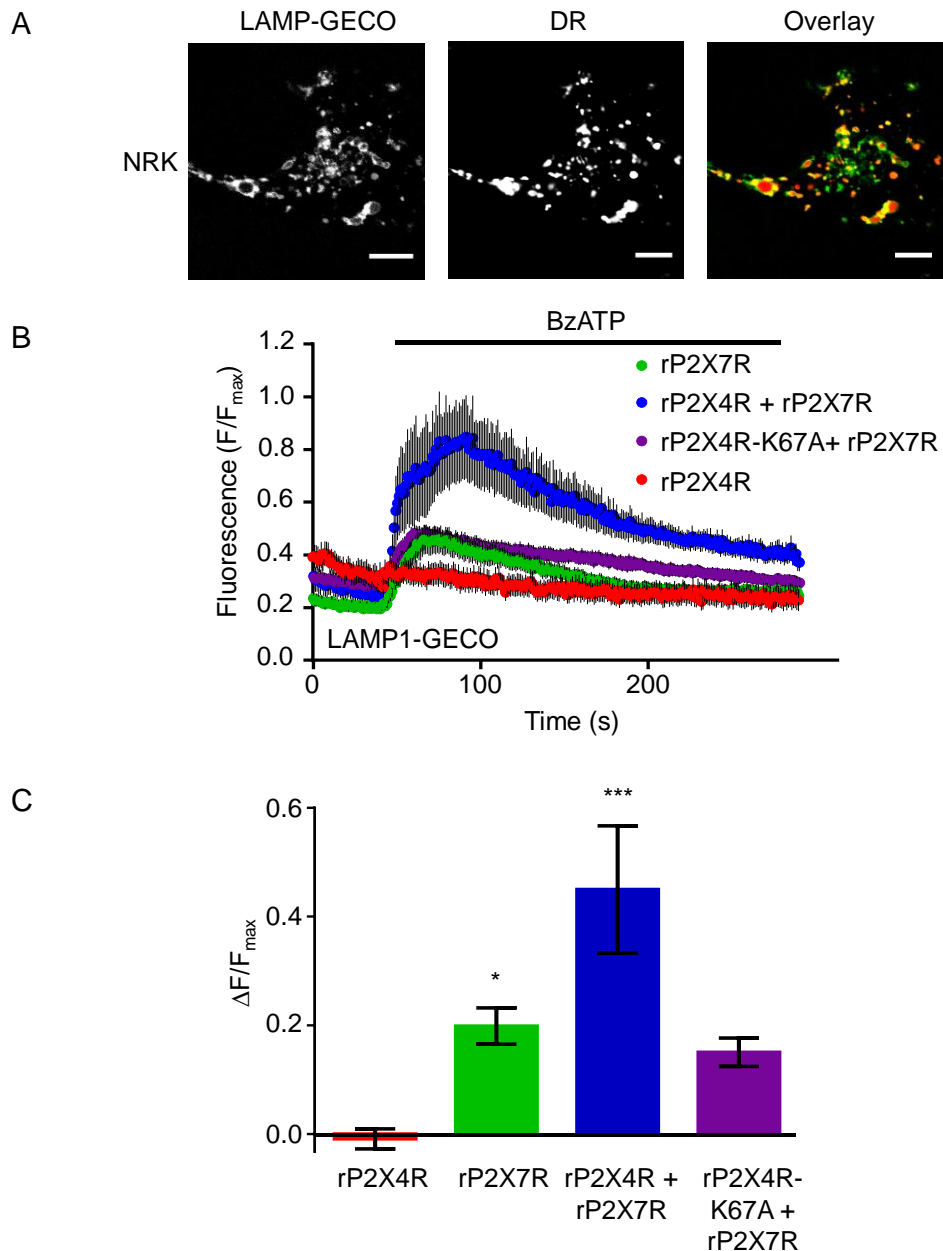


Figure 4.18 P2X7R stimulation induces lysosomal Ca^{2+} efflux via P2X4R, measured using LAMP1-GECO. (A) Representative confocal images of NRK cells co-expressing LAMP1-GECO with rP2X4R and rP2X7R. Lysosomes were marked by DR. (B) Ca^{2+} signals recorded by LAMP1-GECO in NRK cells expressing either rP2X7R or rP2X4R alone or co-expressing either WT or mutant K67A of rP2X4R with rP2X7R. Cells were treated with BzATP (30 μ M) in NES (1 mM Ca^{2+}). (C) Histogram showing the magnitude change of Ca^{2+} response to BzATP recorded by LAMP1-GECO under conditions indicated. (A-C) All results are mean \pm s.e.m. from 3 independent experiments. * $P < 0.05$ and *** $P < 0.001$, one-way ANOVA followed by Tukey's analysis. All scale bars, 10 μ m.

4.3 Investigating role of H1R in P2X4R regulation

4.3.1 Effect of H1R activation in lysosome fusion

Another important source of Ca^{2+} for producing a rise in cytoplasmic Ca^{2+} is the ER. Receptors that couple to the phospholipase C (PLC) pathway and thus lead to the hydrolysis of phosphatidylinositol (4,5,) bisphosphate to produce IP_3 , lead to Ca^{2+} release from the ER via the IP_3 receptor. It has previously been shown that this pathway can trigger lysosome alkalinisation (López-Sanjurjo et al., 2013). To test this further and see if P2X4R could be recruited downstream of G_q -coupled GPCR activation, I examined whether stimulation of the endogenous H1 histamine receptor in HeLa cells could act synergistically with P2X4R to enhance the cytoplasmic Ca^{2+} signal and trigger lysosome fusion. The H1R is an example of a G_q -coupled GPCR which triggers IP_3 generation (Leurs et al., 1995).

Lysosomes were marked by DR, and histamine was applied at 50 μM for 0.5 h and 1 h in cells expressing either rP2X4R-EGFP or LAMP1-GFP in nominally Ca^{2+} free NES. rP2X4R expressing cells showed a significant enlargement of lysosome size at both 0.5 h ($16.31 \pm 4.95 \%$) and 1 h ($24.75 \pm 2.78 \%$, $p < 0.05$) (**Fig. 4.19A and C**). The enlarged lysosomes observed in cells expressing rP2X4R were at the periphery as well as at the perinuclear region (**Fig. 4.19A**). LAMP1-GFP transfected cells, however, did not have enlarged lysosomes following histamine treatment, nor was there any redistribution observed (**Fig. 4.19C**). These results suggest that activation of H1R recruits the activity of intracellular P2X4R to mediate lysosome fusion and H1R is thus likely to be a physiological modulator of P2X4R.

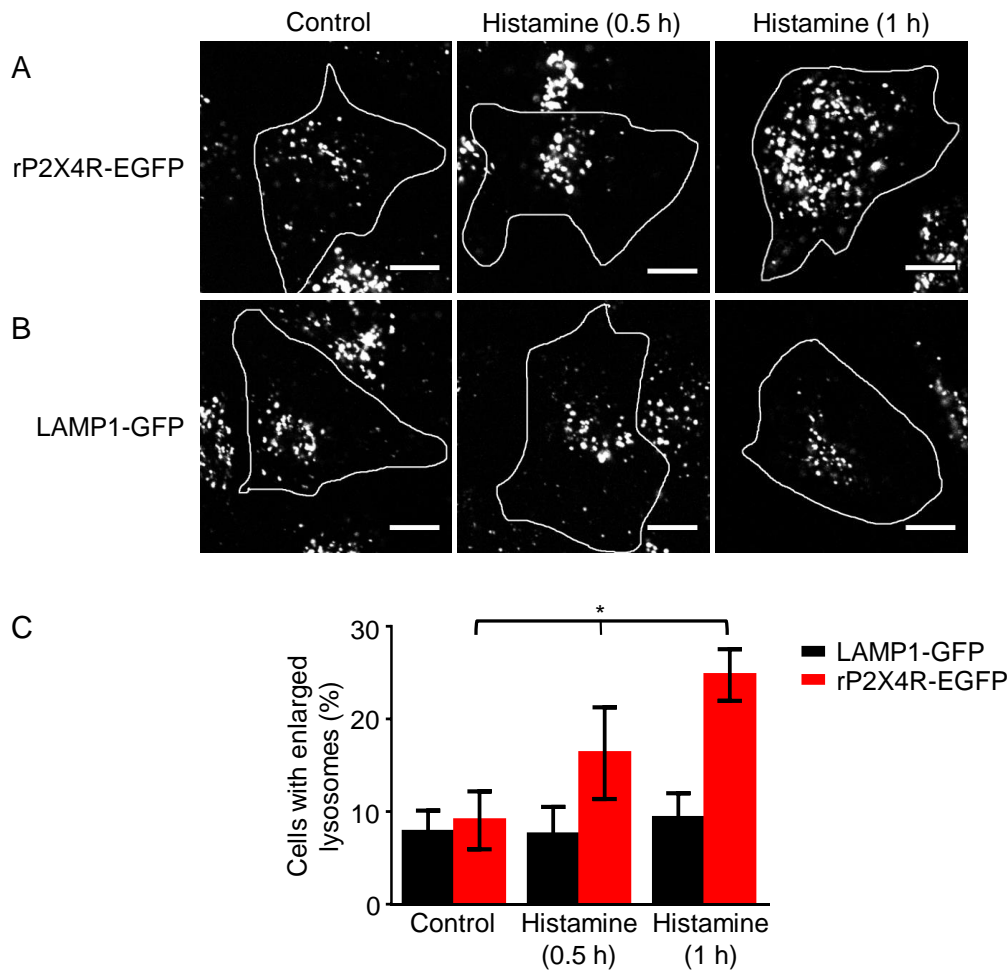


Figure 4.19 Histamine treatment triggers P2X4R-dependent lysosome fusion. (A-B) Representative images of HeLa cells expressing rP2X4R-EGFP (A) or LAMP1-GFP (B) with lysosomes labelled by DR. Cells were incubated with histamine (50 μ M) for 0 h (control), 0.5 h and 1 h in nominal Ca^{2+} free (0 mM Ca^{2+}) NES. White lines represent the plasma membrane of the cell. All scale bars, 10 μ m. (C) Histogram showing the percentage of cells with 2 or more enlarged lysosomes ($\geq 1.8 \mu$ m) following histamine treatments (control, 0.5 h and 1 h). All results are mean \pm s.e.m. from 3 independent experiments. * $P < 0.05$, one-way ANOVA followed by Tukey's analysis.

4.3.2 H1R activation alkalinises lysosome pH

I next assessed whether the synergistic effect of H1R and P2X4R is mediated via lysosome alkalinisation. To examine how the pH of lysosomes is modulated by H1R stimulation, I measured changes in lysosome pH following the administration of histamine in nominally Ca^{2+} free NES, and compared mock-transfected with rP2X4R transfected HeLa cells. Lysosome pH was assessed as before using DR and OG. Histamine (100 μM) in nominally Ca^{2+} free NES evoked an increase in OG fluorescence, indicating lysosome alkalinisation, in both mock transfected and cells expressing rP2X4R (**Fig. 4.20A-B**). To quantify the changes in lysosome pH, the fluorescence ratio of OG:DR was measured at 300 s post histamine administration and compared to the ratio of OG:DR under basal conditions, prior to histamine addition. There was a significant increase in the fluorescence ratio of OG:DR in both mock transfected cells (1.0 ± 0.09 A.U. increased to 1.9 ± 0.14 A.U.; $p < 0.05$) and rP2X4R transfected cell (0.9 ± 0.01 A.U. increased to 2.4 ± 0.46 A.U.; $p < 0.05$) (**Fig. 4.20C**). These results suggest that H1R activation increases lysosome pH independently of rP2X4R expression. No decrease was observed in DR fluorescence in mock transfected cells (**Fig. 4.20A**), but a modest decrease in DR fluorescence in rP2X4R expressing cells (**Fig. 4.20B**) following histamine treatment suggesting that histamine might promote lysosome exocytosis in cells expressing rP2X4R. Together, these data suggest that H1R stimulation induced lysosome alkalinisation, independent of P2X4R expression.

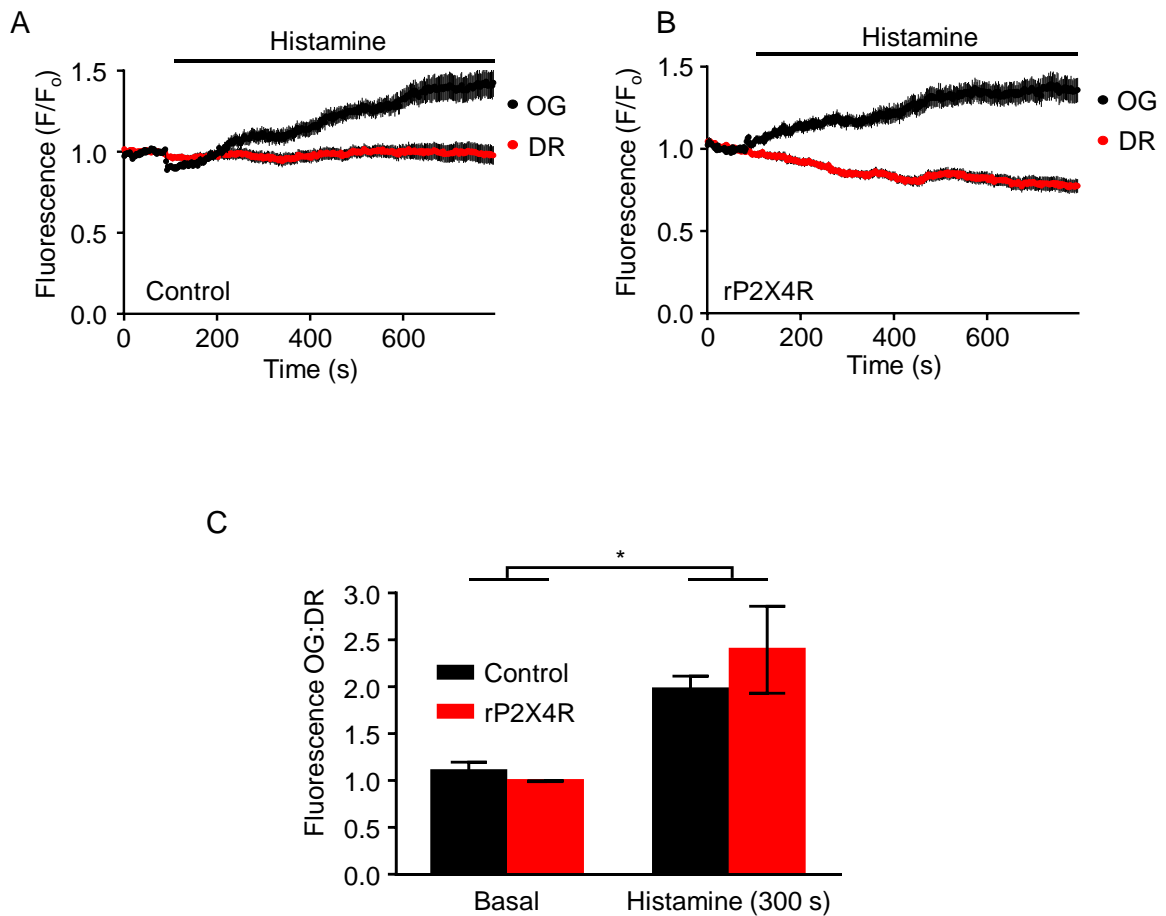


Figure 4.20 Activation of H1Rs induces lysosome alkalisation independent of P2X4R expression. (A-B) Changes of fluorescence of OG and DR in mock transfected (control) (A) and rP2X4R transfected (B) HeLa cells. Cells were treated with histamine (100 μ M) in 0 mM Ca²⁺ NES. The increase in OG fluorescence indicates the rise in lysosome pH following histamine treatment. (C) A summary of data showing the fluorescence ratio of OG:DR measured before (basal) and after 300 s of histamine treatment (100 μ M). All results are mean \pm s.e.m. from 3 independent experiments. *P < 0.05, one-way ANOVA followed by Tukey's analysis.

4.3.3 A synergistic interaction between H1R and P2X4R contributes to cytoplasmic Ca²⁺ signaling

LAMP1-GECO and G-GECO were used as before to investigate both global cytoplasmic Ca²⁺ signals and signals in the immediate vicinity of the lysosomes. I wanted to test whether or not P2X4R contributes to the Ca²⁺ signals generated downstream of H1R activation. HeLa cells were transfected with LAMP1-GECO alone or together with rP2X4R and 50 μM histamine was applied in a nominally Ca²⁺ free NES, followed by ionomycin in 5 mM Ca²⁺ to establish the maximum fluorescence response (F_{\max}). Histamine evoked a transient cytoplasmic Ca²⁺ response in both groups of cells, presumably representing Ca²⁺ release from the ER, but the amplitude was significantly enhanced in cells expressing rP2X4R as can be seen when fluorescence (F) is normalized to F_{\max} (**Fig. 4.21**). Thus the presence of rP2X4R contributes to an enhanced cytoplasmic response to histamine in the vicinity of the lysosomes, suggesting that the lysosomal P2X4Rs become activated downstream of H1R activation.

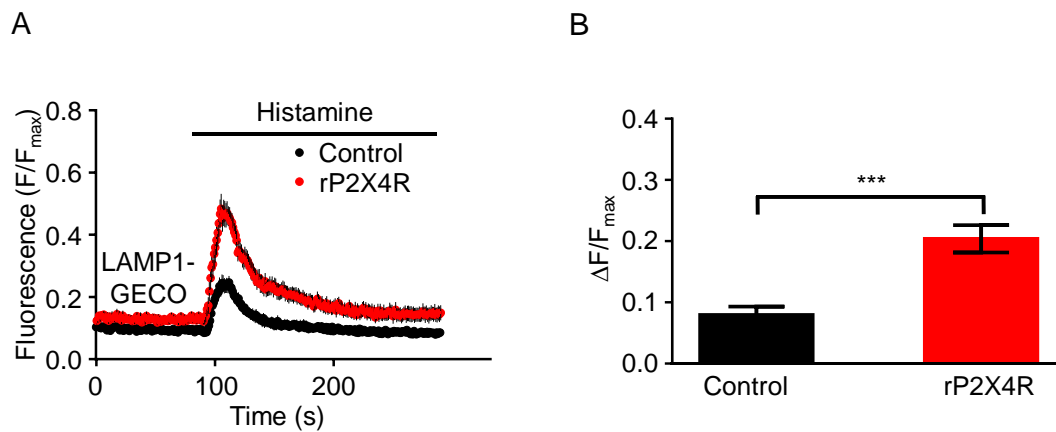


Figure 4.21 Histamine-evoked Ca²⁺ response is potentiated by P2X4R. (A) Ca²⁺ signals recorded by LAMP1-GECO in HeLa cells expressing either control or rP2X4R following histamine (50 μM) treatment in 0 mM Ca²⁺ NES. (B) Histogram showing the magnitude change of Ca²⁺ response to histamine (50 μM) treatment. All results are mean ± s.e.m. from 3 independent experiments. ***P < 0.001, unpaired student's *t* test.

Similar experiments were carried out using G-GECO to assess the change in global cytoplasmic $[Ca^{2+}]$ in response to histamine (50 μ M). Again, rP2X4R significantly enhanced the fluorescence increase in response to histamine administration indicating a greater global Ca^{2+} response to H1R activation (**Fig. 4.22A**). In these experiments, there was an additional control group which was cells expressing G-GECO and the non-functional rP2X4R-K67A mutant receptor. This non-functional mutant had no effect on the fluorescence response to histamine indicating the importance of P2X4R activation in contributing to the Ca^{2+} signal. The fluorescence signal to histamine in cells expressing rP2X4R was not only of larger amplitude, but it was also prolonged (**Fig. 4.22A**).

Finally, a similar experiment was carried out but this time using the fluorescent Ca^{2+} indicator Fluo4 instead of G-GECO. The results were very similar; the response to 100 μ M histamine was increased in the presence of rP2X4R compared to mock transfected cells (**Fig. 4.23A-B**). Together, my results suggest that the activation of H1R evokes ER Ca^{2+} release, which is sufficient to recruit lysosomal P2X4Rs to mediate lysosome Ca^{2+} efflux, thus increasing local and global cytoplasmic Ca^{2+} signals.

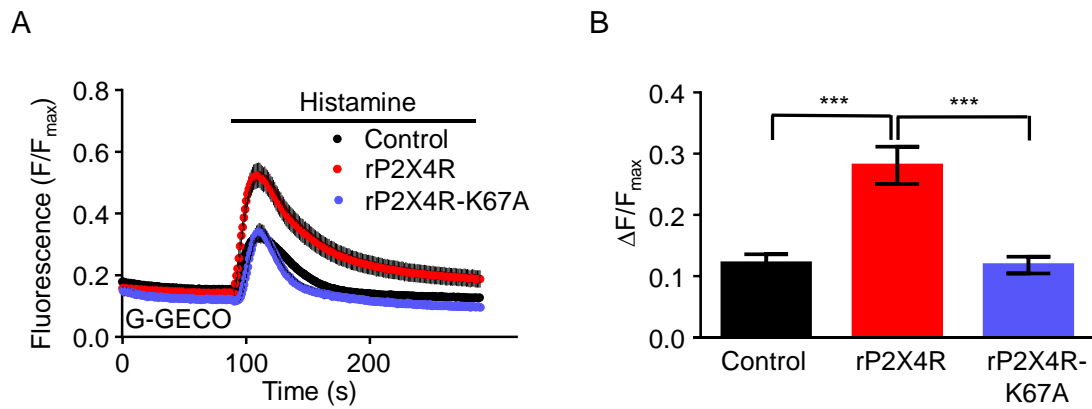


Figure 4.22 P2X4R augments histamine-evoked Ca²⁺ signals. (A) Ca²⁺ signals recorded by cytosolic G-GECO in HeLa cells expressing control, rP2X4R or rP2X4R-K67A following histamine (50 μM) treatment in nominal Ca²⁺ free NES. (B) Histogram showing the magnitude change of Ca²⁺ response to histamine (50 μM) treatment, as conditions indicated. All results are mean ± s.e.m. from 3 independent experiments. ***P < 0.001, one-way ANOVA followed by Tukey's analysis.

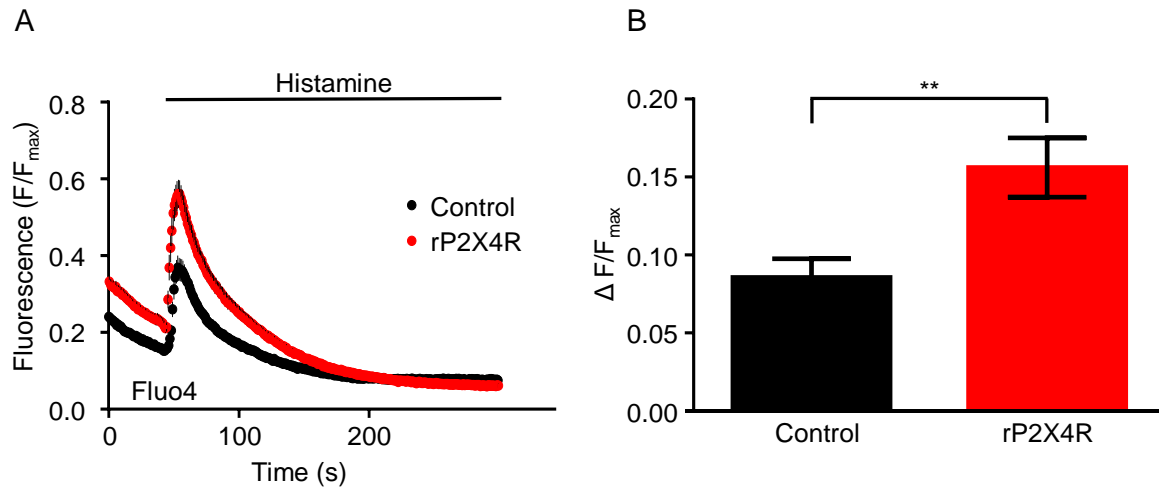


Figure 4.23 The histamine-evoked Ca²⁺ signals are potentiated by functional P2X4R. (A) Ca²⁺ signals recorded from populations of Fluo4 (2 μM) loaded HeLa cells transiently transfected with either rP2X4R or mock transfected (control). Cells were stimulated with histamine (100 μM) in 0 mM Ca²⁺ NES. (B) Summary results showing the magnitude change in Ca²⁺ signal evoked by histamine (100 μM) treatment. All results are mean ± s.e.m. from 3 independent experiments. **P < 0.01, unpaired student's *t* test.

4.3.4 Effects of enhanced expression of P2X4R on ER Ca²⁺ content

My results are consistent with functional cross-talk between lysosomes and ER that is mediated by lysosome alkalinisation downstream of Ca²⁺ release from the ER. However, to rule out the possibility that the over expression of rP2X4R elevates the Ca²⁺ content of the ER and thereby enhances the response to histamine, I measured levels of Ca²⁺ within the ER. This was achieved by using ionomycin, a Ca²⁺ ionophore that preferentially punctures the ER membrane, in HeLa cells expressing G-GECO alone or G-GECO plus rP2X4R. Following addition of ionomycin, in Ca²⁺ free NES containing 0.4 mM EGTA, there was a rapid rise in fluorescence, which reflects the ER Ca²⁺ content (**Fig. 4.24A**) and this was very similar with and without P2X4R. This suggests that the over expression of P2X4R in HeLa cells does not alter the ER [Ca²⁺].

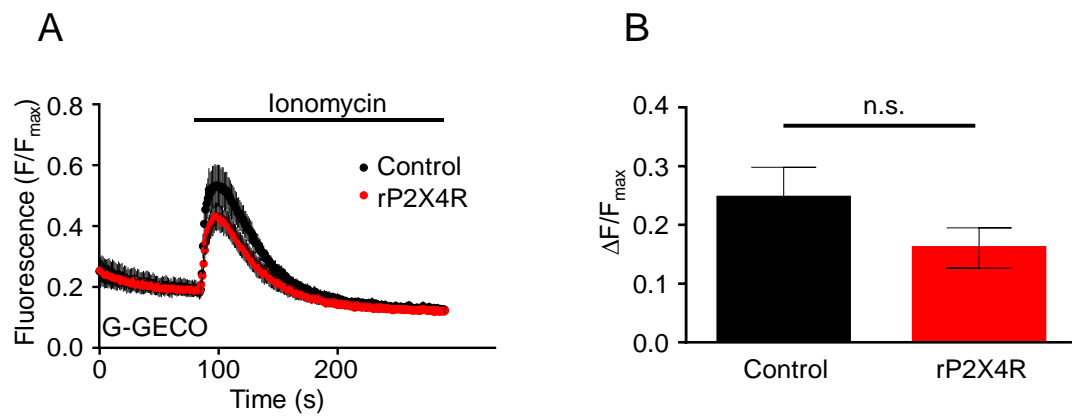


Figure 4.24 Over expression of P2X4R did not alter the intracellular Ca^{2+} level in the ER. (A) Ca^{2+} signals recorded by G-GECO in mock transfected or rP2X4R transfected HeLa cells. Cells were stimulated with ionomycin ($5 \mu M$) in Ca^{2+} free NES with 0.4 mM EGTA. (B) A summary of results showing the magnitude change of Ca^{2+} response to ionomycin, which indicates the Ca^{2+} content of intracellular stores. Results are mean \pm s.e.m. from 3 independent experiments.

4.3.5 Investigating effect of P2YR and P2X4R in Ca²⁺ regulation

Another GPCR that couples to G_q and is endogenously expressed in HeLa cells is P2Y2R (Okuda et al., 2003). P2Y4 and P2Y6 were also shown to be present, but unlike P2Y2R they are not activated by ATP (von Kügelgen and Hoffmann, 2016). I tested whether lysosomal P2X4Rs contribute to the Ca²⁺ signal downstream of P2Y2R stimulation using a similar approach as described above. The fluorescence response to 10 μM NaATP was compared in cells expressing G-GECO alone or G-GECO plus rP2X4R in nominally Ca²⁺ free NES. A rapid increase in fluorescence was observed in control cells (0.10 ± 0.01 A.U.) and this was amplified by rP2X4R (0.26 ± 0.03 A.U.; p < 0.001) (**Fig. 4.25A-B**). In addition, a prolongation of the Ca²⁺ response to NaATP treatment was observed in cells expressing rP2X4R, as had been observed following histamine addition in cells expressing P2X4R (**Fig. 4.22**).

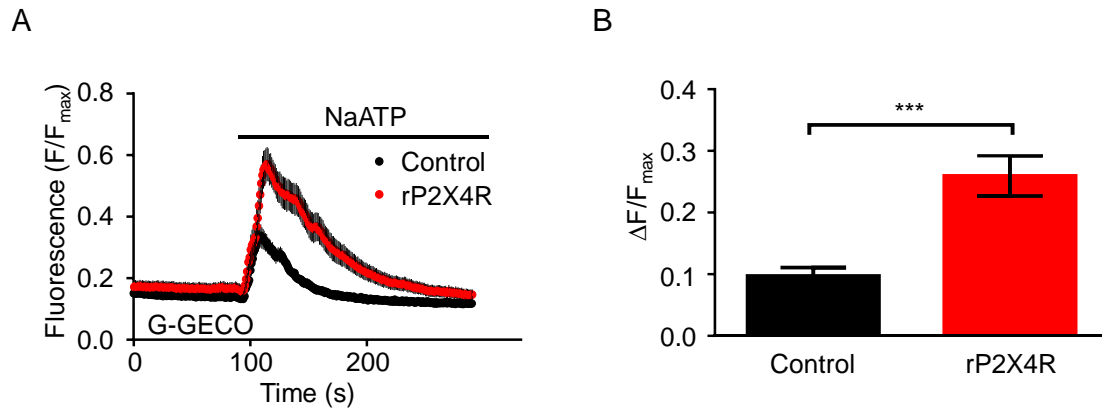


Figure 4.25 P2Y2R-mediated Ca²⁺ signals are potentiated by rP2X4R in HeLa cells. (A) Ca²⁺ signals recorded by G-GECO in either rP2X4R transfected or mock transfected (control) HeLa cells. Cells were stimulated with NaATP (10 μM) in 0 mM Ca²⁺ NES. (B) Histogram showing the magnitude change of Ca²⁺ response to NaATP treatment in HeLa cells. All results are mean ± s.e.m. from 3 independent experiments. ***P < 0.001, unpaired student's *t* test.

The experiment was repeated, but this time in the presence of 0.4 mM of EGTA to chelate any residual Ca^{2+} in the Ca^{2+} free NES (EGTA-NES). The response to NaATP administration was again potentiated by expression of rP2X4R (0.23 ± 0.02 A.U.) compared to the mock transfected cells (0.08 ± 0.01 A.U.; $p < 0.001$) and under these conditions any contribution of plasma membrane P2X4Rs in allowing Ca^{2+} entry can be ruled out (**Fig. 4.26A-B**). However, the presence of EGTA abolished the prolongation of Ca^{2+} response to NaATP in rP2X4R expressing cells such that the decay kinetics were similar to control cells.

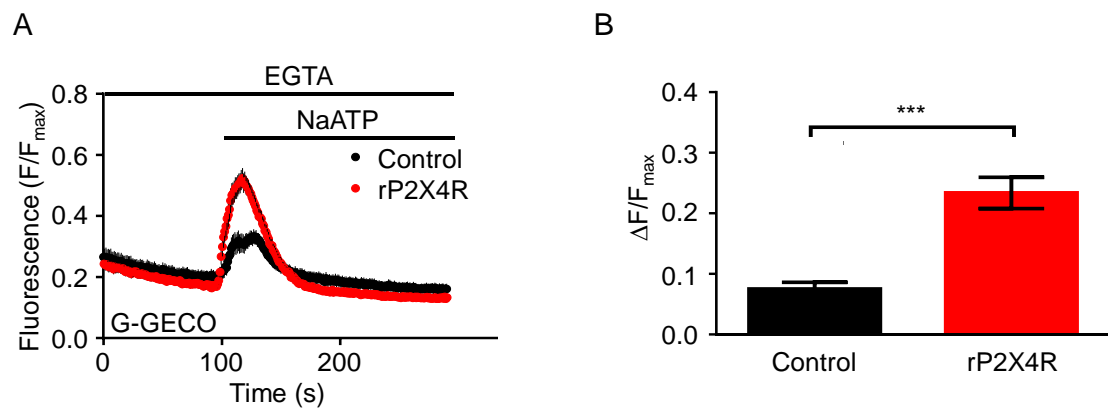


Figure 4.26 P2X4R potentiates Ca^{2+} signal and slows the decay of the Ca^{2+} transient, which is sensitive to EGTA. (A) Ca^{2+} signals recorded from G-GECO expressing HeLa cells that were co-transfected with either rP2X4R, or mock (control). Cells were incubated with EGTA (0.4 mM) followed by NaATP (10 μ M) treatment in 0 mM Ca^{2+} NES. (B) Summary results for the changes of Ca^{2+} signals after NaATP treatment in HeLa cells. All results are mean \pm s.e.m. from 3 independent experiments. *** $P < 0.001$, unpaired student's t test.

Further experiments were carried out to investigate what might contribute to the prolonged response to histamine and ATP observed in cells expressing rP2X4R. I was interested in whether the prolongation of the Ca^{2+} response was a result of P2X4R mediated lysosome exocytosis causing ATP release, which then acts back upon plasma membrane P2X4R or P2Y2R. I returned to using histamine as the stimulus, but cells were bathed in apyrase (4 IU/ μl), an enzyme that hydrolyses ATP, prior to addition of histamine so that any ATP released during the experiment would be rapidly hydrolysed. I compared the response in cells expressing G-GECO alone, together with rP2X4R or with the non-functional K67A mutant. In the presence of P2X4R the fluorescence response was still significantly larger, but this time was not prolonged (**Fig. 4.27**). In cells expressing just G-GECO or the K67A mutant, addition of apyrase had no effect on the fluorescence response.

I further evaluated this data by comparing the area under the F/F_{max} curves for all groups of cells with (**Fig. 4.27A**) and without (**Fig. 4.22A**) apyrase treatment. Consistently, apyrase treatment in cells expressing rP2X4R significantly decreased the AUC in response to histamine addition, but had no effects on either of the other two groups of cells (**Fig. 4.28**). Altogether, these results suggest that in cells expressing rP2X4R, following addition of histamine there is extracellular release of ATP. Presumably this reflects P2X4R mediated lysosome exocytosis and this ATP feeds back to activate either plasma membrane P2Y2R or P2X4R thereby prolonging the Ca^{2+} response.

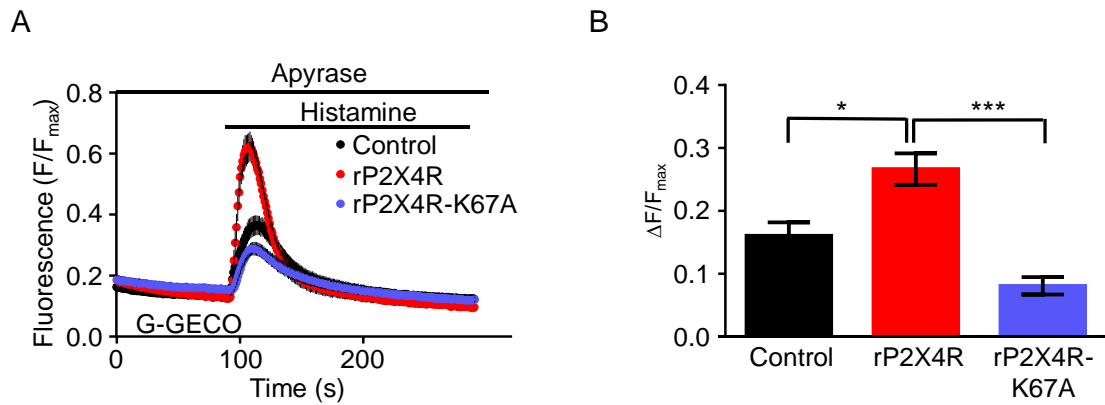


Figure 4.27 P2X4R-dependent prolongation of the histamine-induced Ca^{2+} response is sensitive to apyrase. (A) Ca^{2+} signals recorded by G-GECO in HeLa cells expressing control, rP2X4R or rP2X4R-K67A. Cells were stimulated with histamine (50 μ M) in the presence of apyrase (4 IU/ μ l), enzyme that hydrolyses ATP, in 0 mM Ca^{2+} NES. (B) A summary of data showing the magnitude change in histamine-evoked Ca^{2+} response in the presence of apyrase (4 IU/ μ l). All results are mean \pm s.e.m. from 3 independent experiments. * $P < 0.05$ and *** $P < 0.001$, one-way ANOVA followed by Tukey's analysis.

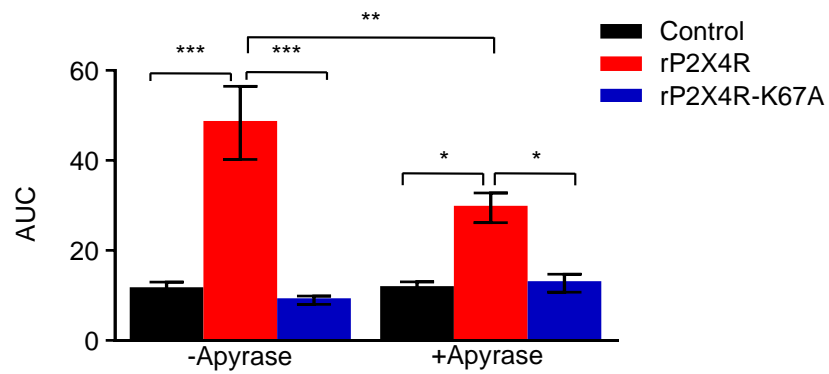


Figure 4.28 Histogram showing the summarised data of area under the curve analysis obtained from graphs **Fig. 4.22** and **Fig. 4.27**, in the presence and absence of apyrase (4 IU/μl) in control, rP2X4R-WT or rP2X4R-K67A expressing cells. All results are mean ± s.e.m from 3 independent experiments. *P < 0.05, **P < 0.01 and ***P < 0.001, one-way ANOVA followed by Tukey's analysis.

4.3.6 Effect of lysosome Ca²⁺ content depletion in P2X4R expressing cells

My results suggest that the stimulation of G_q-coupled GPCRs, for example H1R and P2Y2R, activates lysosomal P2X4R to mediate lysosomal Ca²⁺ efflux that contributes to histamine- and NaATP-evoked Ca²⁺ signals. To further validate that the enhanced cytoplasmic Ca²⁺ signal is contributed by Ca²⁺ release from the lysosome, I tested whether or not disrupting the lysosome membrane prior to addition of histamine would prevent the potentiation by P2X4R. For this I used glycyl-L-phenylalanine 2-naphthylamide (GPN), a substrate of cathepsin C that transiently permeabilises lysosome membranes. G-GECO expressing HeLa cells were treated with GPN (100 μM) and the fluorescence response in nominally Ca²⁺ free NES was measured for cells with and without rP2X4R expression. GPN treatment produced a small sustained Ca²⁺ signal that was comparable between the mock-transfected group and rP2X4R transfected cells, indicative of Ca²⁺ release from the lysosomes (**Fig. 4.29A-B**). Post GPN, both mock and rP2X4R expressing cells showed a transient Ca²⁺ response to histamine administration (**Fig. 4.29A**), but this time there was no significant difference between the two groups of cells (**Fig. 4.29B**). The responses to histamine however were very small after GPN treatment suggesting that GPN might not act simply on the lysosome membrane, but might also disrupt the ER membrane. Despite the limitations of this experiment, I can at least conclude that under conditions where the lysosome is not contributing to the cytoplasmic Ca²⁺ signal, the presence of P2X4R does not enhance the histamine-evoked Ca²⁺ response.

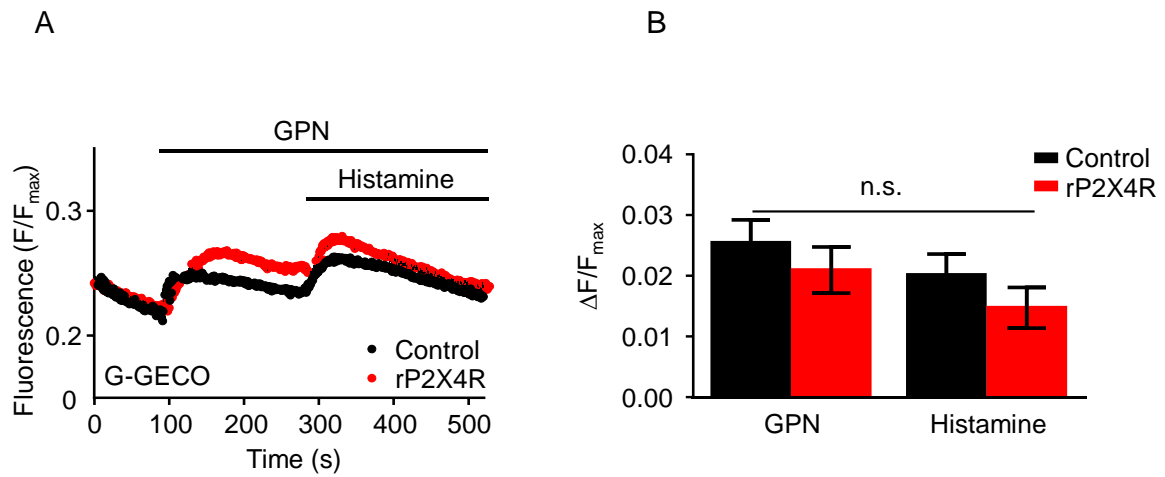


Figure 4.29 Lysosome membrane permeabilisation abolished P2X4R-mediated augmentation of histamine-evoked Ca^{2+} signals. (A) Changes in Ca^{2+} signals recorded by G-GECO in HeLa cells expressing with either control or rP2X4R. Cells were stimulated by GPN (100 μM) and histamine (50 μM) treatment in 0 mM Ca^{2+} NES. All results are mean from 3 independent experiments. (B) Histogram showing the magnitude change in Ca^{2+} signals stimulated by GPN (100 μM) and histamine (50 μM) treatment, as conditions indicated. All results are mean \pm s.e.m. from 3 independent experiments.

4.4 Discussion

My results identify two physiological regulators of P2X4R, namely P2X7R and G_q-coupled GPCRs. Both regulators recruit the activity of P2X4R via lysosome alkalisation such that a localised elevation of cytoplasmic [Ca²⁺] at the vicinity of lysosomes increases the pH of lysosomes, which relieves P2X4R from inhibition enabling it to be activated by lysosomal ATP (**Fig. 4.16 and Fig 4.20**). This has a consequence for the homotypic fusion mediated by P2X4R and it also has a consequence for the lysosome Ca²⁺ efflux.

My results demonstrate that P2X4R mediates enlargement of lysosomes following pharmacological manipulations of lysosome pH using Baf-A1 and MA, which agrees with the published data (**Fig 4.6**; Cao et al., 2015; Huang et al., 2014). However, lysosome fusion induced by Baf-A1 was less compared to MA. One explanation is that MA rapidly alkalises lysosome pH whereas Baf-A1 is an inhibitor of the lysosome V-ATPase, which mediates lysosome acidification, and subsequently leads to increase in the pH of lysosomes.

Next, I demonstrate the functional interaction of P2X4R and P2X7R in lysosome fusion. The confocal studies evidently show that the P2X7R agonist, BzATP is sufficient to promote lysosome fusion, only when P2X4R is co-expressed (**Fig. 4.11A**). Also, both P2X4R mutants, K67A and C353W when co-expressed with P2X7R did not promote lysosome enlargement (**Fig. 4.11**). These provide evidence for a clear role of P2X4R in lysosome fusion.

I have demonstrated that plasma membrane P2X7R recruits the activity of P2X4R via lysosome alkalisation (**Fig. 4.16**). The activation of P2X7R reduces the acidity

of lysosomes but only in the presence of the extracellular Ca^{2+} , which is consistent with the previous finding (Takenouchi et al., 2009). However, the detailed mechanism of this response remains unknown. One possibility is that the sustained elevation of cytoplasmic Ca^{2+} disrupts the cation counter flux in lysosomes, which tightly regulates the luminal content of Ca^{2+} and H^+ concentration that is required to maintain lysosome pH (Steinberg et al., 2010).

In addition to lysosome fusion, the activation of P2X4R and P2X7R also induced a change in lysosome distribution towards the cell periphery. This was observed from the confocal images and decrease in perinuclear index that most lysosomes migrated towards the cell periphery following BzATP and dynasore treatment (**Fig. 4.13**). This was dependent on the co-expression of P2X7R and P2X4R, and was not observed in the mutant P2X4R-K67A suggesting a clear role of P2X4R and P2X7R in anterograde lysosome movements. Perhaps, the peripheral distribution of lysosome populations is a pre-requisite step for lysosome exocytosis. It was previously shown that peripheral lysosomes facilitate Ca^{2+} -induced lysosome exocytosis such that the proximity of lysosomes to the plasma membrane facilitates vesicles docking and the elevation of cytoplasmic Ca^{2+} subsequently triggers the onset of lysosome exocytosis (Jaiswal et al., 2002; Luzio et al., 2007).

My results provide evidence that P2X4R serves as a lysosomal Ca^{2+} release channel using LAMP1-GECO, which reported the cytoplasmic Ca^{2+} signal at the lysosome vicinity (**Fig. 4.18**). Published data have demonstrated that increase in lysosome pH also lowered the Ca^{2+} concentration in lysosomes (Christensen et al., 2002), complementing with my results that lysosome alkalinisation could lower lysosomal Ca^{2+} content via P2X4R. Cytoplasmic G-GECO did not identify this P2X4R-mediated

lysosome Ca^{2+} efflux, possibly due to the over expression of P2X7R in NRK cells, an ion channel that is sensitive to prolonged stimulation and mediates pore dilation (Robinson et al., 2014). The over expression of active P2X7R presumably facilitates extracellular Ca^{2+} influx and that dominates and/or saturates Ca^{2+} signal recorded by G-GECO, thus hinders resolving any Ca^{2+} signal derived from lysosomes.

Secondly, I also assessed whether the sole increment of cytoplasmic Ca^{2+} via G_q -coupled GPCR stimulation could induce lysosomal P2X4R activation. My results demonstrate that the activation of H1R triggered Ca^{2+} release from the ER. This activates P2X4R to enable lysosome Ca^{2+} efflux, potentiating the cytoplasmic Ca^{2+} response. This conclusion was drawn from experiments using three different Ca^{2+} indicators showing potentiation of histamine-induced Ca^{2+} signals only when P2X4R is present (**Fig. 4.21 – Fig. 4.23**). This augmented Ca^{2+} signal is likely to be the main stimulus for P2X4R-dependent lysosome fusion. Indeed, confocal images demonstrate that the treatment with histamine induced lysosome enlargement in a P2X4R dependent manner (**Fig. 4.19**). Similarly, activation of plasma membrane P2Y2R also increases in cytosolic Ca^{2+} signals and this were potentiated by P2X4R (**Fig. 4.25**). This observation confirms that P2Y2R also recruits the activity of lysosomal P2X4R in the same manner as H1R does, via the release of ER Ca^{2+} .

Histamine-induced lysosome alkalinisation is independent of P2X4R expression (**Fig. 4.20**). This suggests that histamine causes an elevation of cytoplasmic $[\text{Ca}^{2+}]$ at the lysosome vicinity, which then triggers lysosome alkalinisation by an unknown mechanism, possibly via the same mechanism as P2X7R. In addition, lysosome alkalinisation has been shown to reduce lysosomal Ca^{2+} level in BMDMs and that is

in consistent with my result that P2X4R is activated in response to alkalised conditions leading to lysosomal Ca^{2+} efflux (Christensen et al., 2002).

My data demonstrates a prolonged phase of elevated Ca^{2+} in response to G_q -coupled GPCR activation. This effect is only observed in the presence of P2X4R suggesting a downstream lysosome exocytosis mediated by P2X4R. It is possible that lysosome exocytosis increases the extracellular ATP that feeds back onto the activation of plasma membrane P2Y2R or P2X4R, thereby prolonging the overall Ca^{2+} signal (Sivaramakrishnan et al., 2012; Toyomitsu et al., 2012). Evidently in the Ca^{2+} imaging assay, EGTA and apyrase abolished this prolonged Ca^{2+} signal without affecting the potentiated Ca^{2+} signals. Together with the confocal images demonstrating lysosomes distributed to the cell periphery (**Fig. 4.13**), these results suggest that the activation of lysosomal P2X4R potentiates the cytoplasmic Ca^{2+} responses and triggers downstream signalling, lysosome exocytosis.

Using GPN treatment to deplete lysosome Ca^{2+} content, I have confirmed that P2X4R potentiates H1R-induced Ca^{2+} signals via lysosome Ca^{2+} efflux. However, GPN pre-treatment also decreased the histamine-evoked Ca^{2+} response. It is possible that GPN, a substrate of cathepsin C, induces osmotic swelling and subsequently membrane permeabilisation, also targets the ER. Perhaps the ER contains a low concentration of cathepsin C, resulting in permeabilisation and reduction of the ER Ca^{2+} content, however the detailed mechanism of GPN activity in the ER remains unclear (Ronco et al., 2015). Overall, the increase in cytoplasmic $[\text{Ca}^{2+}]$ released from the ER triggers P2X4R-dependent lysosomal Ca^{2+} efflux, suggesting a functional interaction between ER and lysosomes, an idea that has

been proposed by several studies (Kilpatrick et al., 2013; López-Sanjurjo et al., 2013; Phillips and Voeltz, 2016).

Overall, my results provide evidence that both P2X7R and G_q-coupled GPCRs serve as physiological regulators to recruit activity of P2X4R via lysosome alkalinisation. In response to lysosome alkalinisation, P2X4Rs can be activated to mediate lysosomal Ca²⁺ signals, thereby facilitating lysosome functions such as lysosome fusion and exocytosis. Evidence herein also suggests the effect of P2X4R in the lysosome Ca²⁺ release pathway. The stimulation of G_q-coupled GPCRs triggers IP₃R-mediated Ca²⁺ signals from the ER, which recruits lysosomal P2X4R activity to mediate lysosome Ca²⁺ efflux that potentiates the overall Ca²⁺ response. This is similar to the proposed mechanism, that stimulation of lysosomal Ca²⁺ release can potentiate the Ca²⁺ signals from the ER and vice versa. For example, activation of TPC2 using NAADP triggers lysosomal Ca²⁺ release and this is sufficient to generate a prominent cytoplasmic Ca²⁺ signal, which is suggested to mediate by IP₃Rs on the ER (Kilpatrick et al., 2013; Morgan et al., 2013). Collectively, my data suggest that stimulation of P2X4R via lysosome alkalinisation, as for NAADP-sensitive TPC2, is likely to mediate lysosomal Ca²⁺ efflux, and thus contribute to the ER-lysosome Ca²⁺ signalling.

Alongside P2X4R, two other lysosomal release Ca²⁺ channels, TRPML1 and TPC2, have been implicated in Ca²⁺-dependent lysosome membrane trafficking. TRPML1 is activated by PI(3,5)P₂ inducing fission and fragmentation of late endosomes and lysosomes (LE/L) (Cheng et al., 2010). In addition, fibroblasts with a mutation in TRPML1 that causes MLIV disease have an accumulation of enlarged LE/L, which could be rescued by over expression of TRPML1. Furthermore, lysosome depletion

of PI(3,5)P₂ caused vacuole enlargement, supporting the role for TRPML1 in fission (Dong et al., 2010). However, unlike P2X4R activity, which required lysosome alkalisation, the activity of TRPML1 was shown to be facilitated by acidification (Cheng et al., 2010; Dong et al., 2008). Therefore, TRPML1 and P2X4R are likely to mediate separate roles in lysosome function despite both receptors mediating lysosomal Ca²⁺ signals.

Despite the less well characterised TPC family, gathering evidence suggests a role of TPC2 in lysosome function. TPC2 localises to lysosomes and it is activated by NAADP and PI(3,5)P₂ (Calcraft et al., 2009; Marchant and Patel, 2015). TPC2 mediates lysosome Ca²⁺ release for lysosome fusion, such that the depletion of TPC2 accumulated cholesterol in hepatocytes due to the defects in lysosome fusion and subsequently degradation of cholesterol. This accumulation is reversed upon over expression of TPC2 in murine embryonic fibroblasts (Grimm et al., 2014; Ruas et al., 2010). Consistently, over expression of TPC2 causes lysosome enlargement, enhances endolysosome Ca²⁺ release that then alters endolysosome trafficking (Lin-Moshier et al., 2014). These results demonstrate the effect of TPC2 in lysosome Ca²⁺ efflux and lysosome fusion, and these functions may be regulated alongside with P2X4R and other lysosome channels to control membrane trafficking.

Considering the presence of three different lysosome Ca²⁺-permeable channels, it is of interest to understand how these receptors differentiate in mediating lysosome function. First, the pH of lysosomes is sufficient to distinct the activity of lysosomal channels: alkaline conditions inhibit TRPML1 activity (Dong et al., 2008), but lysosome alkalisation potentiates P2X4R activity. In addition, different Ca²⁺ mobilising messengers may be recruited upon Ca²⁺ efflux via different lysosome

channels, thereby differentiating the mode of action between receptors. For example, P2X4R mediates lysosome fusion via the formation of protein complex with calmodulin (Cao et al., 2015). However, the possibility of the interaction between lysosomal Ca²⁺ release channels to meet the diverse downstream Ca²⁺-dependent responses cannot be ruled out.

The role of intracellular P2X4R has been shown to contribute lysosome exocytosis in alveolar type II cells. P2X4R is localised in lysosome-related organelles, lamellar bodies (LBs), where it mediates localised Ca²⁺ signals following ATP treatment, thereby expanding the fusion pore to release surfactants (Miklavc et al., 2010). Although this study focussed on the role of P2X4R in completing exocytosis of pre-docked LBs with the plasma membrane, without demonstrating any contribution of P2X4R prior to the docking of LBs, my results complement this study where I demonstrate that P2X4R-mediates lysosome Ca²⁺ efflux and lysosome fusion followed by anterograde movements of lysosomes to the plasma membrane. This suggests that P2X4R-mediated lysosomal Ca²⁺ signal may act as an initial signalling cue, contributing to lysosome exocytosis.

Disruption in lysosome function, particularly elevated lysosome pH, has been detected in several neurodegenerative diseases. Raised lysosome pH is an emerging factor in the progression of neurodegenerative disease due to the ineffective lysosome enzyme activity for degradation, for example in Alzheimer's disease (AD) with mutations in presenilin-1 (PS1). PS1 is a catalytic component of the γ -secretase complex, which cleaves amyloid precursor protein to produce amyloid β (A β). Recently, PS1 also been shown to also act as a chaperone in the ER facilitating the maturation of the V0a1 subunit for the formation of V-ATPase (Lee et

al., 2015). Human fibroblasts with PS1 mutations demonstrated impaired glycosylation of V-ATPase and retention of V-ATPase in the ER, preventing lysosome acidification due to the diminished level of V-ATPase in lysosomes (Lee et al., 2015). Failure of lysosome acidification favours the activation of P2X4R and that may contribute to the progression of PS1-linked AD by exacerbating pathological features such as enlargement of lysosomes and impairment of lysosome biogenesis that is closely tied to cell death mechanism (Lee et al., 2015). Studies have demonstrated that mutations in PS1 caused ER Ca²⁺ dysregulation in PC12 cells, as well as human fibroblasts derived from AD patients, such that the IP₃-evoked Ca²⁺ signal is exacerbated following ER stimulation (Chan et al., 2000; Guo et al., 1996; Ito et al., 1994). Furthermore, there is evidence to suggest that abnormal lysosomal Ca²⁺ homeostasis contributes to the pathological abnormalities in PS1-associated AD (Lee et al., 2015). The study demonstrated that stimulation of TRPML1 in PS1 knockout fibroblasts exaggerated Ca²⁺ release in response to TRPML1 agonist, ML-SA1, implicating the dysregulation of lysosomal Ca²⁺ signalling following lysosome alkalisation. Defects in lysosome acidification could also activate other pH-sensitive lysosomal Ca²⁺ release channels like P2X4R, thereby contributing lysosome Ca²⁺ efflux and potentiating ER-mediated Ca²⁺ signals. Previous data has suggested that TRPML1 mediates lysosome fission rather than fusion. My results demonstrate P2X4R-mediated lysosome fusion and enlargement, which is consistent with the pathological phenotype of enlarged vacuoles aggregation in AD, suggesting a potential role for P2X4R in AD. Study from Lee et al. (2015) also suggested that disrupted intra-organelle Ca²⁺ homeostasis is a direct consequence of the pH change in lysosomes. Restoring lysosome pH was sufficient to rescue defects in lysosome Ca²⁺ signals, however reversing abnormality in lysosome Ca²⁺ efflux did

not restore lysosome acidic pH. This confirmed lysosome Ca^{2+} dysregulation is a secondary consequence of lysosome alkalinisation and impacted on the regulation of lysosome Ca^{2+} release channels. Therefore, it is important to fully understand the role P2X4R in lysosomes, alongside with other pH-sensitive lysosomal receptors, in the understanding of neurodegenerative diseases where lysosome pH is altered (McBrayer and Nixon, 2013).

Indeed, there is one study demonstrated an implication of P2X4R in AD (Varma et al., 2009). The study showed in an in vitro model that P2X4R was elevated in response to the exposure of $\text{A}\beta$ in hippocampal neurons. Given the putative caspase 3 cleavage site in the C-terminal tail of P2X4R and $\text{A}\beta$ -induced caspase activity, the study showed that caspase 3 enhanced P2X4R activity, contributing to $\text{A}\beta$ -mediated neuronal cell death (Varma et al., 2009). Consistently, over expression of P2X4R in rat hippocampal neurite elevated neurotoxicity of $\text{A}\beta$, but P2X4R knockdown attenuate this effect. This study suggested a role for P2X4 in the progression of AD may be mediated by enhanced cytoplasmic Ca^{2+} signal, however, the exact underlying mechanism remains to be determined.

Intracellular Ca^{2+} signalling is tightly regulated through an intricate interaction of intra-organelles and the Ca^{2+} channels they express. The function of the ER as the major intracellular Ca^{2+} store is well-established, but increasing findings indicate lysosomes also contribute to intracellular Ca^{2+} signalling. Thus far, I have demonstrated the role of P2X4R in lysosome fusion that is dependent on a P2X4R-mediated lysosome Ca^{2+} signal. This P2X4R-evoked Ca^{2+} signal potentiated ER-mediated Ca^{2+} signals, suggesting that P2X4R contributes to the intracellular Ca^{2+} signalling. The presence of several Ca^{2+} channels in lysosomes is likely to spatially

organise Ca^{2+} signalling for diverse cellular processes. Therefore, further investigation is required to elucidate the detailed mechanisms between lysosomes and ER.

5. Investigating a role for P2X4R in autophagy

5.1 Introduction

The results presented in the previous chapter suggest that upon P2X7R activation there is a change in the pH of lysosomes, which recruits the activity of P2X4R in the lysosome. This mediates lysosomal Ca²⁺ efflux and facilitate homotypic lysosomes fusion. Following on from these findings I was interested to investigate whether or not there was also a role for P2X4R and P2X7R to act synergistically in the regulation of autophagy. Autophagy is an evolutionary conserved adaptive mechanism that is required for cellular homeostasis to maintain cell viability under metabolic stress and is initiated upon cellular stress such as nutrient deprivation. Once autophagy is initiated, isolation of a double layer membrane, called the autophagosome is formed, which sequesters parts of the cytoplasm. The autophagosomes recruit cytoplasmic LC3-I proteins that are conjugated with phosphatidylethanolamine (PE) to produce LC3-II. Autophagic flux requires the fusion of lysosomes with the autophagosomes to form autophagolysosomes and it is here where degradation occur as a consequence of delivery of the degradative enzymes from the lysosome. Autophagy is a dynamic process in which initiation, fusion and degradation are normally studied together and termed as autophagic flux (Klionsky et al., 2012).

5.1.1 P2X7R and autophagic flux

A role for P2X7R in the regulation of autophagic flux has previously been reported. In microglial cells, activation of P2X7R for 0.5 h to 1 h, using either ATP or BzATP, triggered LC3-II protein accumulation in normal growth medium, with little effect in

serum-free conditions (nutrient starvation) (Takenouchi et al., 2009). The accumulation of LC3 protein is associated with an increase in the number of autophagosomes and autophagolysosomes, suggesting the disruption of autophagic flux in response to P2X7R stimulation. In this study, they concluded that an increase in the pH of lysosomes triggered by P2X7R activation was likely to disrupt the activity of the lysosomal proteases, resulting in an accumulation of LC3 proteins in autophagosomes and autophagolysosomes. In a separate study, a role for P2X7R in reducing autophagic flux in retinal-pigmented epithelium was reported (Guha et al., 2013). Activation of P2X7R inhibited the degradation of phagocytosed photoreceptor outer segments and LC3 proteins. In neither study was it suggested that there is a role for P2X4R in this process nor did they investigate a role for P2X4R.

5.1.2 Assays and interpretations of autophagy

Changes in the expression and distribution of the LC3 protein are hallmarks of autophagy. LC3 can be studied by fusion with either green fluorescence protein (GFP) or monomeric red fluorescence protein (mRFP). During the initiation of autophagy, the C-terminus of the LC3-I protein is conjugated to PE to form LC3-II, and this associates with the membrane of the autophagosomes. As autophagosomes fuse with lysosomes, the membrane bound LC3-II proteins are degraded and delipidated, returning LC3 to the cytoplasm (Kabeya et al., 2004). This is seen as a reduction in the fluorescence intensity of LC3 puncta. The absence of puncta can therefore reflect either the lack of initiation of autophagy or efficient autophagic flux. Changes in the distribution and expression of LC3-II can be studied by confocal microscopy. Also, western blot analysis enables a comparison of the amount of LC3-I to LC3-II because they can be separated on a gel by virtue of their

different molecular mass and hydrophobicity (~14 kDa for LC3-I and ~16 kDa for LC3-II) (Mizushima, 2007).

5.2 Material & Methods

5.2.1 Cell lines

The cell line used in this study was HeLa cells stably expressing mRFP-LC3 (kind gift from Dr Aviva Tolkovsky, University of Cambridge). This cell line enables the study of the autophagy process by enabling the assessment of the changes in fluorescence intensity of mRFP-LC3, which is one of the markers for autophagy process as detailed section 5.1.2, using confocal imaging.

5.2.2 Cell maintenance

Cells were maintained in normal growth medium: Dulbecco's modified Eagle's medium (DMEM) with 10 % fetal bovine serum (FBS), and 100 U/ml penicillin and streptomycin (P/S) at 37 °C in humidified air with 5 % CO₂ but in the presence of geneticin (1 mg/ml; Sigma) to select cells that were expressing mRFP-LC3 proteins. The maintenance and plating of these cells was performed as described in section 3.1.2.

5.2.3 Cell sorting

To obtain consistent cellular expression of mRFP-LC3, HeLa cells were sorted by Nigel Miller in the Department of Pathology (University of Cambridge) using a MoFlo MLS high-speed cell sorter (BeckmanCoulter). Cells were allowed to grow up to 90 % confluency in a T75 flask, growth medium was removed and cells were rinsed with PBS. Cells were then trypsinised using 2 ml of 0.05 % trypsin-EDTA solution and 8 ml of growth medium was added to inhibit further trypsin reaction. Cells were re-suspended in 8 ml of growth medium and collected in a 15 ml tube. Cells were centrifuged at 100 g for 5 mins at room temperature and pellets were re-suspended

in PBS to remove residual phenol-red that was in growth media. The cell pellets were re-suspended in PBS and subjected to cell sorting facility, according to their fluorescence intensity. Sorted cells were then cultured and passaged accordingly.

5.2.4 Autophagy assay

Changes in the fluorescence intensity of mRFP-LC3 in HeLa cells were assessed in living cells using a Leica SP5 confocal microscope. To initiate autophagy, mRFP-LC3 HeLa cells were starved by incubation in Earle's Balance Salt Solution (EBSS) with 100 U/ml P/S at 37 °C and 5 % CO₂ for 3 h. Cells were stimulated with the P2X7R agonist NaATP (300 µM) for 30 minutes immediately prior to imaging the live cells. All settings on the confocal microscope were kept the same when taking images from HeLa cells that had been treated in different ways and the images were analysed using ImageJ. Typically, I analysed between 80 and 150 cells per condition for each experiment. The experiments were repeated 3 times.

5.3 Results

To investigate the effects of P2X4R and P2X7R on autophagy and autophagic flux, I used HeLa cells that were stably expressing mRFP-tagged LC3 protein. Cells were transfected with rP2X4R-EGFP and rP2X7R, either alone or together. 48h post-transfection, confocal images were taken of live cells to assess the distribution and fluorescence intensity of mRFP-tagged LC3 proteins. In the normal, nutrient rich medium, a low level of LC3 intensity was observed in all cells suggesting that basal autophagy was unaffected by the expression of rP2X4R and rP2X7R (**Fig. 5.1**). I tested the effect of incubating cells with 300 μ M NaATP for 30 minutes on the expression of LC3-II and saw no change in mRFP-LC3 fluorescence, either in control cells or cells co-expressing rP2X4R and rP2X7R (**Fig. 5.2A**). Thus, stimulation of rP2X7R was insufficient to induce autophagy, at least over this time period. Similarly, the incubation of control cells in a nutrient rich medium with an inhibitor of the lysosome H⁺ ATPase, Baf-A1 (100 nM) for 3 h had no effect on LC3 fluorescence (**Fig. 5.2B**). Baf-A1 is known to inhibit autophagic flux by alkalinisation of the lysosome, which inhibits the activity of lysosomal proteases.

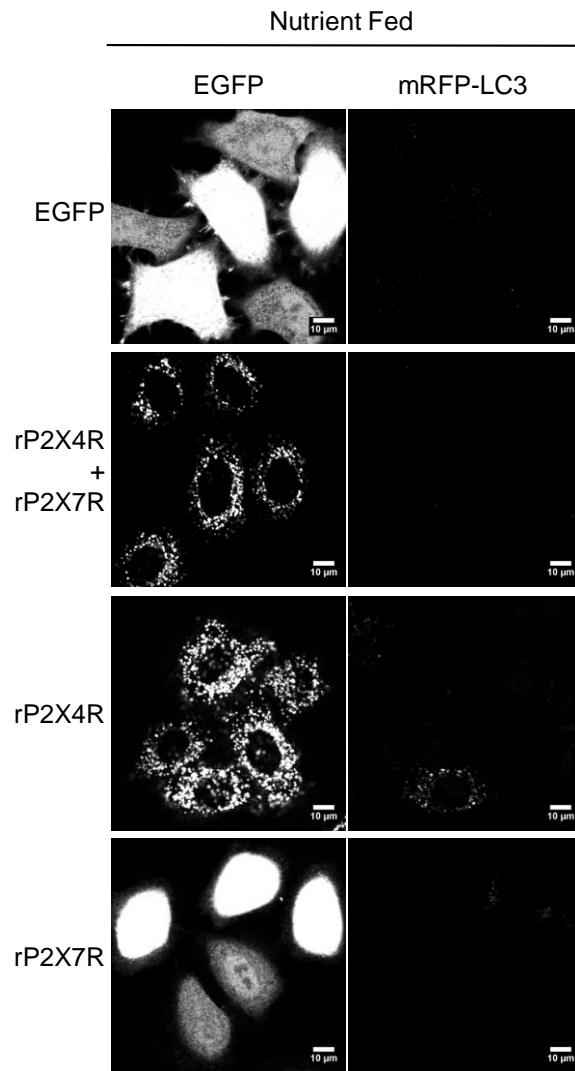


Fig. 5.1 Low expression of LC3-II proteins in nutrient rich conditions in mRFP-LC3-HeLa cells. (A-B) Representative confocal images of mRFP-LC3-HeLa cells expressing EGFP, co-expressing rP2X4R-EGFP with rP2X7R, expressing rP2X4R-EGFP alone or co-expressing rP2X7R + EGFP. All cells were incubated in nutrient fed media (control; A). All scale bars, 10 μ m.

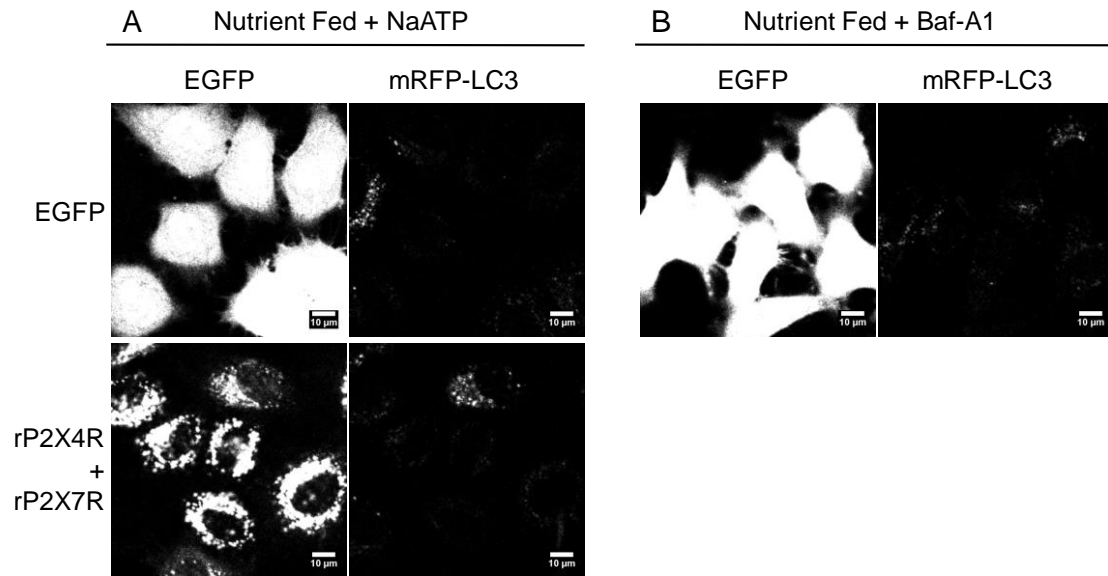


Fig. 5.2 Low expression of LC3-II proteins after NaATP and Baf-A1 treatments in mRFP-LC3-HeLa cells. (A-B) Representative confocal images of mRFP-LC3-HeLa cells either expressing EGFP or co-expressing rP2X4R-EGFP and rP2X7R. Cells were incubated in a nutrient fed medium either with 0.3 mM of NaATP for 30 minutes (A), or with 100 nM Baf-A1 for 3 h (B). All scale bars, 10 μ m.

The classical way to induce autophagy is by nutrient starvation and to achieve this I used EBSS, which is a glucose-containing medium that is devoid of amino acids and some growth factors (Boland et al., 2008). Cells expressing different combinations of rP2X4R and rP2X7R were incubated in EBSS for 3 h, but this was insufficient to increase the intensity of LC3-II puncta, which suggests that either autophagy was not induced during this time or that autophagic flux was rapid so that the LC3-II puncta that formed during the 3 h incubation period were rapidly degraded (**Fig. 5.3A**). To discriminate between these two possibilities, cells were treated with EBSS for 3 h plus Baf-A1 (100 nM for 3 h). This combination produced an approximately 2.4-fold increase in LC3-II puncta intensity (**Fig. 5.3B and Fig. 5.5**), which indicates that EBSS is sufficient to induce autophagy and that the LC3-II puncta accumulates when autophagic flux is blocked by the alkalinisation of the lysosome.

Next I tested the effect of incubating cells with 300 μ M NaATP for the final 30 minutes of the 3 h incubation with EBSS to see if this had any effect on the autophagic flux. A longer incubation with NaATP was avoided because of the noticeably compromised the health of the cells. Only in cells co-expressing rP2X4R and rP2X7R was there an increase in the LC3-II puncta intensity following NaATP plus EBSS treatment (**Fig. 5.4A**). In cells expressing just one of the two receptor types, there was no change in puncta intensity compared to EBSS alone. Finally, I tested a combination of EBSS, NaATP and Baf-A1 treatment on all cell groups and saw enhanced fluorescence of LC3-II puncta, which was similar to EBSS and Baf-A1 treatment alone, independent of the expression of rP2X4R and rP2X7R. (**Fig. 5.4B and Fig. 5.5**). These results suggest NaATP can inhibit autophagic flux leading to the accumulation of LC3-II, but only when rP2X4R and rP2X7R are co-expressed and following the induction of autophagy.

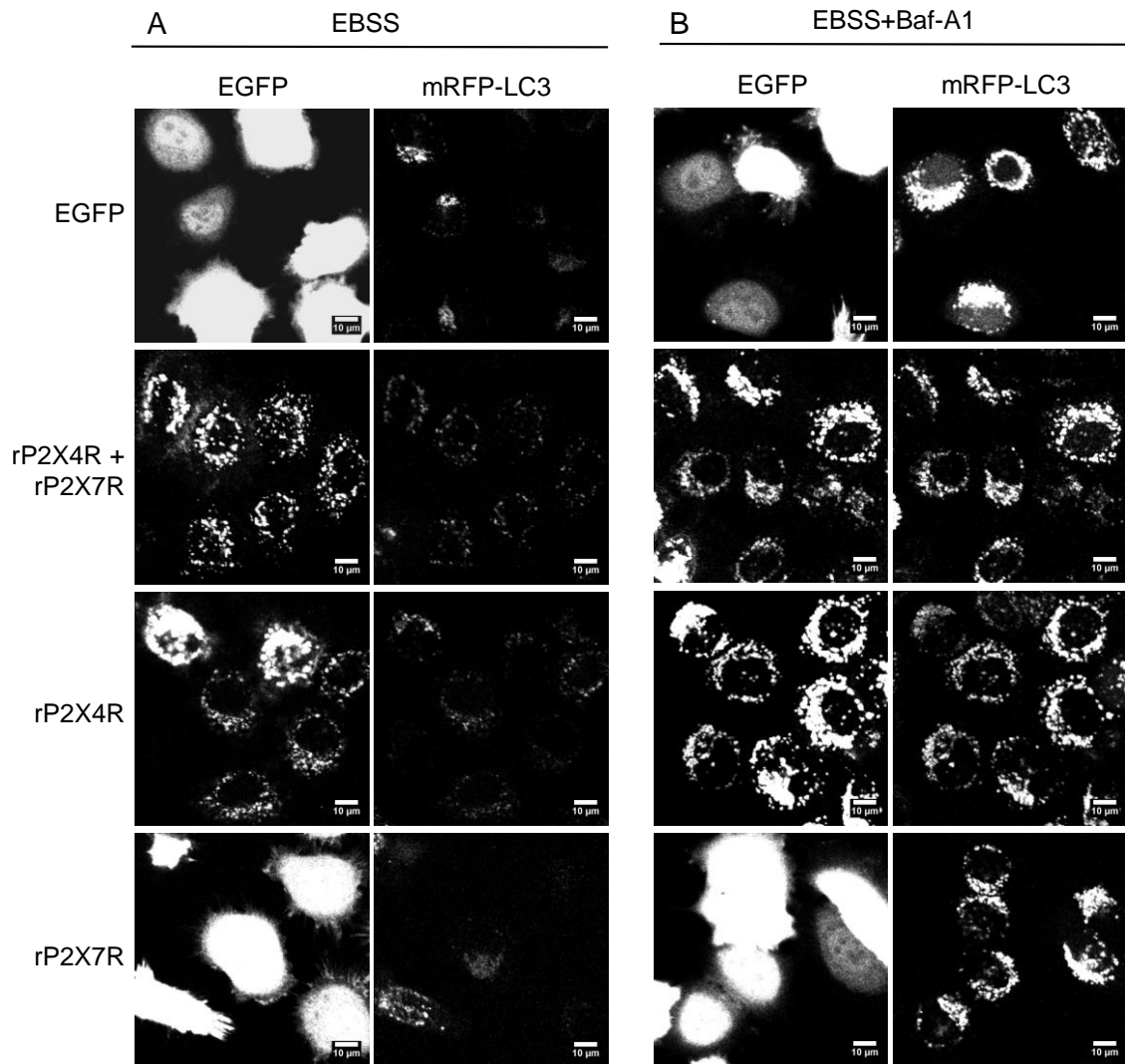


Fig. 5.3 Baf-A1 treatment in EBSS media induced LC3-II protein accumulation in mRFP-LC3-HeLa cells. (A-B) Representative confocal images of mRFP-LC3-HeLa cells expressing EGFP, co-expressing rP2X4R-EGFP with rP2X7R, expressing rP2X4R-EGFP alone or co-expressing rP2X7R + EGFP. All cells were incubated for 3 h in an amino acid-free medium: EBSS (A), or EBSS with Baf-A1 (100 nM for 3 h) (B). All scale bars, 10 μ m.

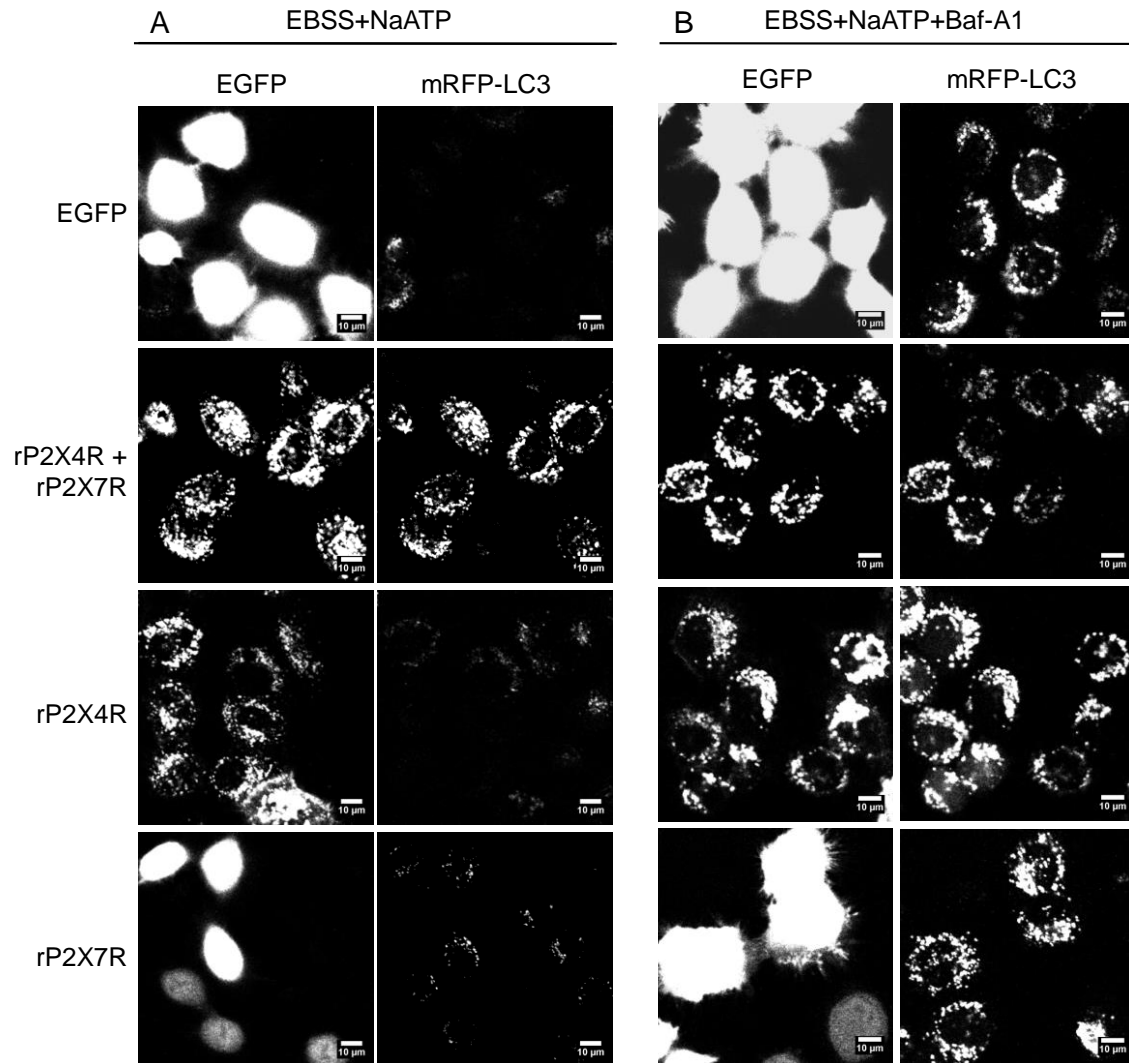


Fig. 5.4 Synergistic effect of rP2X4R and rP2X7R in LC3-II protein accumulation following NaATP treatments in EBSS. (A-B) Representative confocal images of mRFP-LC3-HeLa cells expressing EGFP, co-expressing rP2X4R-EGFP with rP2X7R, expressing rP2X4R-EGFP alone or co-expressing rP2X7R + EGFP. All cells were incubated for 3 h in EBSS with 0.3 mM of NaATP treatment for the final 0.5 h, either without Baf-A1 (A) or with Baf-A1 (100 nM for 3 h) (B). All scale bars, 10 μ m.

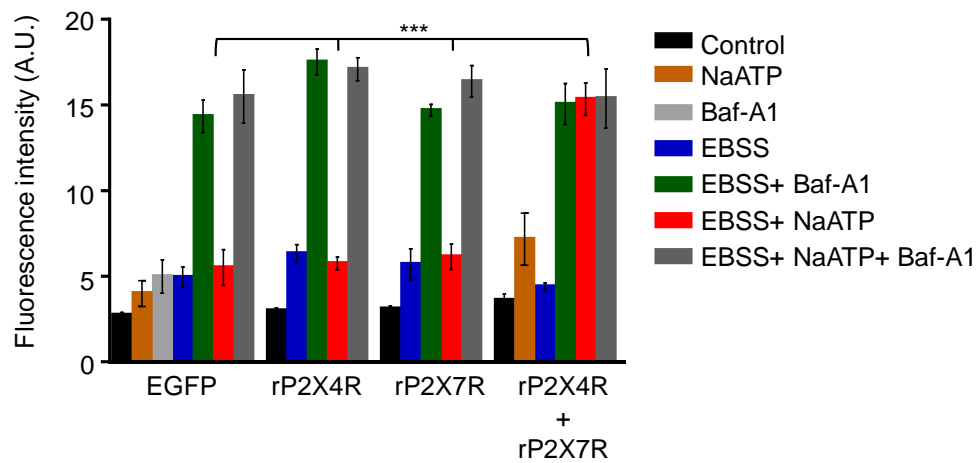


Fig. 5.5 Histogram showing the fluorescence intensity of mRFP-LC3 proteins in mRFP-LC3-HeLa cells expressing EGFP, rP2X4R-EGFP or rP2X7R, or cells co-expressing rP2X4R-EGFP and rP2X7R. All results are mean \pm s.e.m. from at least 3 independent experiments. *** $P < 0.001$, one-way ANOVA followed by Tukey's analysis.

Autophagic flux is known to require fusion of lysosomes with autophagosomes to generate autophagolysosomes. Delivery of lysosomal proteolytic enzymes to the autophagosome then triggers degradation of the engulfed cellular constituents plus the accumulated LC3-II proteins. My results suggest that in cells co-expressing rP2X4R and rP2X7R, treatment with NaATP either inhibits the activity of lysosomal proteases or inhibits the fusion of lysosomes with autophagosomes. To discriminate between these two possibilities, I compared the distribution of rP2X4-EGFP, which I know is in lysosomes, with the distribution of the LC3-II puncta after treatment with EBSS + NaATP. In cells co-expressing rP2X4R and rP2X7R there was extensive co-localisation between rP2X4R-EGFP and mRFP-LC3 indicating that lysosomes have fused with autophagosomes (**Fig. 5.6A**). The co-localisation was very similar to that seen after treatment with EBSS + NaATP + Baf-A1 in cells co-expressing both receptors or just expressing rP2X4-EGFP. Altogether these results suggest that when rP2X4R and rP2X7R are both present, the activation of rP2X7R inhibits autophagic flux, in a similar way to Baf-A1, by inhibiting the activity of lysosomal enzymes.

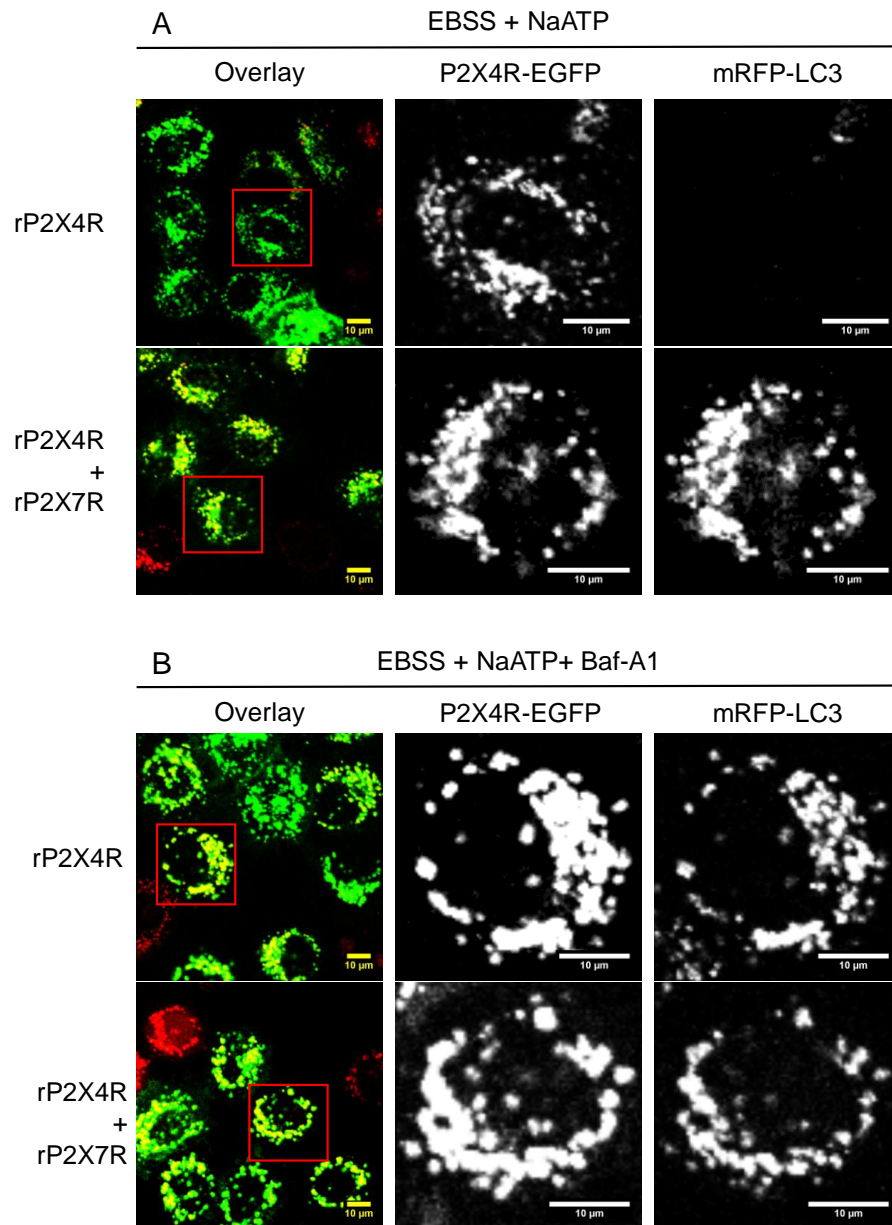


Fig. 5.6 Co-localisation of rP2X4R-EGFP with mRFP-LC3 suggests the fusion of lysosomes and autophagosomes. (A-B) Confocal images of mRFP-LC3-HeLa cells either expressing rP2X4R-EGFP or co-expressing rP2X4R-EGFP and rP2X7R. Cells were treated as follows: (A) 3 h incubation of EBSS with NaATP (0.3 mM) treatment for the final 0.5 h, or (B) 3 h incubation of EBSS with NaATP (0.3 mM) treatment for the final 0.5 h and Baf-A1 (100 nM) for 3 h. Red boxes depict the area of interest for higher magnification images. All scale bars, 10 μ m.

5.4 Discussion

The results presented in this Chapter, and the previous Chapter, are consistent in providing evidence that activation of P2X7R reduces the acidity of lysosomes. This has consequences for homotypic lysosome fusion mediated by P2X4R and it also has consequences for the rate at which autophagic flux progresses. What was surprising about my autophagy results was that activation of P2X7R in the absence of P2X4R was insufficient to see a significant increase in LC3-II fluorescence. I expected inhibition of autophagic flux to be dependent upon lysosome alkalinisation rather than a subsequent step mediated by lysosomal P2X4Rs. This suggests that P2X4R might play a role in the regulation of lysosome or autophagolysosome pH and that perhaps Ca^{2+} or Na^{+} flux mediated by lysosomal P2X4R feeds back to affect H^{+} flux. Alternatively, there might be other mechanisms involved in the regulation of degradation by P2X4R.

The previous studies showing an effect of P2X7R in autophagy were both carried out in cell types where I expect P2X4R to also be expressed, namely microglial cells (Takenouchi *et al.*, 2009), and retinal-pigmented epithelium (RPE) cells (Guha *et al.*, 2013). Therefore, although the focus of these studies was P2X7R, there may have been a contribution from endogenous P2X4R. In addition, the ability of Baf-A1 treatment to induce lysosomes alkalinisation and inhibit autophagic clearance as measured by the accumulation of LC3 proteins has been shown previously (Fass *et al.*, 2006, Takenouchi *et al.*, 2009 and Guha *et al.*, 2013). This suggests that lysosome pH is essential for the degradation of autophagolysosomes and the effect of P2X7R in lysosome alkalinisation, which activates P2X4R, are likely to inhibit this process in the similar manner as Baf-A1.

An effect of NaATP on LC3 accumulation was only seen in combination with EBSS, suggesting that P2X4R and P2X7R do not affect the initiation of autophagy, at least in a nutrient rich environment. This result contrasts with the findings by Takenouchi et al. (2009) that the application of ATP in nutrient rich medium is sufficient to induce LC3-II accumulation in microglial cells. One possible explanation for the discrepancy is the different cell types. Microglial cells may exhibit a relatively higher basal autophagy activity compared to stable cell line, mRFP-LC3-HeLa cells. There is evidence suggested that the turnover of LC3 proteins differs in cell types alongside with different basal activity, for example in cells with neuronal origins has a higher ratio of LC3-I to LC3-II is a common finding (Klionsky et al., 2016). Alternatively, this study utilised endogenous P2X7R in microglial cells, a different experimental system from my study which employed the transient expression of P2X4R and P2X7R.

Overall, my results demonstrate that the stimulation of heterologous expression of P2X4R and P2X7R is sufficient to inhibit autophagic flux such that LC3-II proteins are accumulated. This suggests that both receptors are negatively regulating the autophagic clearance due to lysosome alkalinisation at least under such experimental setup, a similar effect induced by Baf-A1 treatment.

However, autophagy is a complex, dynamic, and multistep process, and multiple assays are recommended to permit a correct interpretation of the result. Having shown the effect of P2X4R and P2X7R in the accumulation of LC3 proteins, further examination is required to be sure of the effect of P2X4R and P2X7R in impairment of the autophagy degradation process. The accumulation of LC3 proteins in the autophagosome usually arises from either the upregulation of induction, impairment of autophagosome fusion or inefficient autophagic clearance. However, my result

has ruled out the possibility of autophagy initiation and autophagosome-lysosome fusion, but further assays in addition to confocal imaging are preferable. For example, application of PI3K inhibitor 3-methyladenine (3-MA), which inhibits autophagy initiation (Yang et al., 2013), or vinblastine, a reagent that depolymerises microtubules, are necessary to rule out autophagy initiation and autophagosome-lysosome fusion, respectively. Furthermore, I have shown the effect of P2X4R and P2X7R in inefficient lysosome degradation by measuring the rate of accumulation of LC3 proteins at a static time point using confocal microscopy. In addition to this, one complementary approach can be conducted which is the measurement in the rate of degradation. The measurement of the rate of general degradation by autophagy process can be achieved by measuring the time-dependent decrease of an autophagy-degradable proteins, for example p62 using western blot or confocal imaging. However, the changes in p62 has a caveat where there is a potential contribution of the increase in protein synthesis, where one can address by experimental inhibition such as protein synthesis inhibitor, cycloheximide (Klionsky et al., 2012, 2016).

The regulation of autophagy is tightly associated with cellular function; therefore it is important to understand regulators and channels involved in autophagy. Autophagy is primarily known to be stimulated by cellular stress conditions like nutrient starvation. This leads to the general understanding that autophagy serves as an energy-generating mechanism under metabolic stress conditions. In addition, autophagy mediates turnover of old and damaged organelles to ensure desirable intracellular conditions and supply metabolic precursor for minimal growth requirement. However, excessive activation of autophagy is undesirable as it involves large-scale degradation of the cytoplasm, protein complexes and organelles

that are necessary for cell growth. There is evidence that an adequate level of autophagy activity maintains cell viability in *Caenorhabditis elegans*, but low level or excessively high level of autophagy can promote cell death (Kang et al., 2007). Therefore, tight regulation of autophagy is essential for cell viability such that most cells maintain a low basal level of autophagy under normal nutrient fed conditions, but stimulated by various stimuli including protein aggregation, pathogen invasion, inflammation, and damaged organelles (Van Limbergen et al., 2009).

In addition to increasing cell viability under metabolic stress conditions, autophagy maintains cell homeostasis and provides an intracellular quality control by recycling and regenerating metabolic precursor via degradation of intracellular debris and organelles. For example, autophagy is a housekeeping mechanism in heart and muscle cells that mediate the turnover of cytoplasmic constituents like mitochondria. There is a study showing that depletion of LAMP2 proteins resulted in ineffective autophagic degradation in myopathy and cardiomyopathy patients (Nishino et al., 2000; Tanaka et al., 2000). LAMP2 has been suggested to contribute to lysosome acidification and deficiency in LAMP2 induced lysosome alkalinisation (Mindell, 2012). This suggests a possible contribution of active P2X4R and P2X7R upon alkalinisation of lysosomes such that the active P2X4R and P2X7R impaired degradation of autophagolysosomes.

Autophagy has also been shown to participate in the regulation of immunity and inflammation. First, autophagy functions as an effector that eliminates intracellular pathogen invasion. One example is that bacterial infection triggers activation of NLRs and that can direct ATG16L1 to the site of bacterial entry at the plasma membrane to eliminate bacteria by autophagy (Travassos et al., 2010). In addition,

autophagy has been implicated in the regulation of cytokine production. One example is that autophagy has been shown to control the level of cytokine release, such that the production of IL-1 β and IL-18 increased in the autophagy-deficient macrophages (ATG16 $^{-/-}$) (Saitoh et al., 2008). These evidences suggest the effect of autophagy in inflammation could be associated with P2X4R and P2X7R because these receptors have also been shown to mediate the release of IL-1 β and IL-18 (Sakaki et al., 2013). The similar downstream effect in an increase IL-1 β and IL-18 production following autophagy-depletion and activation of P2X4R and P2X7R may suggest that the role of autophagy in cytokine release is mediated via these receptors, but further examination is required to understand the role of autophagy in immunity.

Apart from P2X4R, there is evidence demonstrating an effect of another lysosomal Ca²⁺ release channel, TPC2 in autophagy (Lu et al., 2013). Over expression of TPC2 was shown to induce an impairment in autophagic degradation due to defective autophagosome-lysosome fusion. Both genetic knockdown of TPC2 and pharmacological inhibition of NAADP (TPC2 agonist) using the NAADP-antagonist, Ned-19 abolished the impairment of autophagosome-lysosome fusion and facilitated the progression of autophagy by promoting the formation of autophagolysosomes. In addition, the study demonstrated that NAADP stimulates TPC2-induced Ca²⁺ release and this alkalinises lysosomes, thereby disrupting autophagosome-lysosome fusion. In line with this finding, my results agree that the manipulation of lysosome pH and lysosome Ca²⁺ signals could disrupt the progression of autophagy, thereby accumulating LC3 proteins. However, my study demonstrates an effect of P2X4R and P2X7R in autophagy degradation, which was only observed under stress conditions, without a significant impact on autophagosome-lysosome fusion.

Together, the study by Lu et al. (2013) and my result suggest that the manipulation of different lysosome Ca^{2+} channels may contribute to different stages of autophagy progression. Therefore, it is of interest to understand the signalling of lysosomal Ca^{2+} channels in autophagy under basal and stimulated conditions. Given that autophagy is involved in a variety of cellular processes and dysfunction of autophagy is implicated in many diseases, it is important to further understand the role of P2X4R signalling to identify novel regulator in this pathway.

6 Characterisation of the subcellular distribution of human and rat P2X4R

6.1 Introduction

My project has focused mainly on the study of rat P2X4R (rP2X4R), but I also compared the subcellular distribution of human P2X4R (hP2X4R) with that of the rat receptor. These two isoforms share 87 % amino acid sequence identity with the most variability found in the extracellular loop (Abdelrahman et al., 2017; Garcia-Guzman et al., 1997). These differences in amino acid sequence in the extracellular loop have been implicated in differences in antagonist sensitivity. For example, P2XR antagonists, suramin and PPADS were shown to inhibit hP2X4R, but are relatively ineffective at rP2X4R. Previously, the motifs identified as targeting P2X4 to lysosomes included an N-terminal dileucine-like motif (L22I23) and two adjacent C-terminal tyrosine-based motifs (Y372 and Y378). All of these motifs are conserved in hP2X4R and therefore my expectation was that the trafficking of hP2X4 would be indistinguishable from rP2X4 (Qureshi et al., 2007; Royle et al., 2002, 2005). The aim of this study was to investigate any species difference in the trafficking behaviour of the receptor.

6.2 Results

A comparison was made of the subcellular distribution of hP2X4R with that of the rP2X4R following their heterologous expression in HeLa cells. LAMP1-mCherry was expressed to label lysosomes and the EGFP-tagged P2X4Rs were transfected into cells and imaged 48 h later. There was extensive co-localisation of LAMP1-mCherry with both rP2X4R-EGFP and hP2X4R-EGFP, but for many cells expressing hP2X4R-EGFP there were also clear plasma membrane localisation, which was not apparent for rP2X4R-EGFP (**Fig. 6.1A-B**). A similar experiment was carried out using DR to label lysosomes with the standard protocol (incubation for 5 h followed by a 2 h chase). Co-localisation between hP2X4-EGFP and DR was less than for LAMP1-mCherry, and it was less than for rP2X4-EGFP and DR and this was reflected in the relatively low value for the Pearson's coefficient (**Fig. 6.1C-D**). This suggests that there is some isoform dependence on the distribution of the receptor.

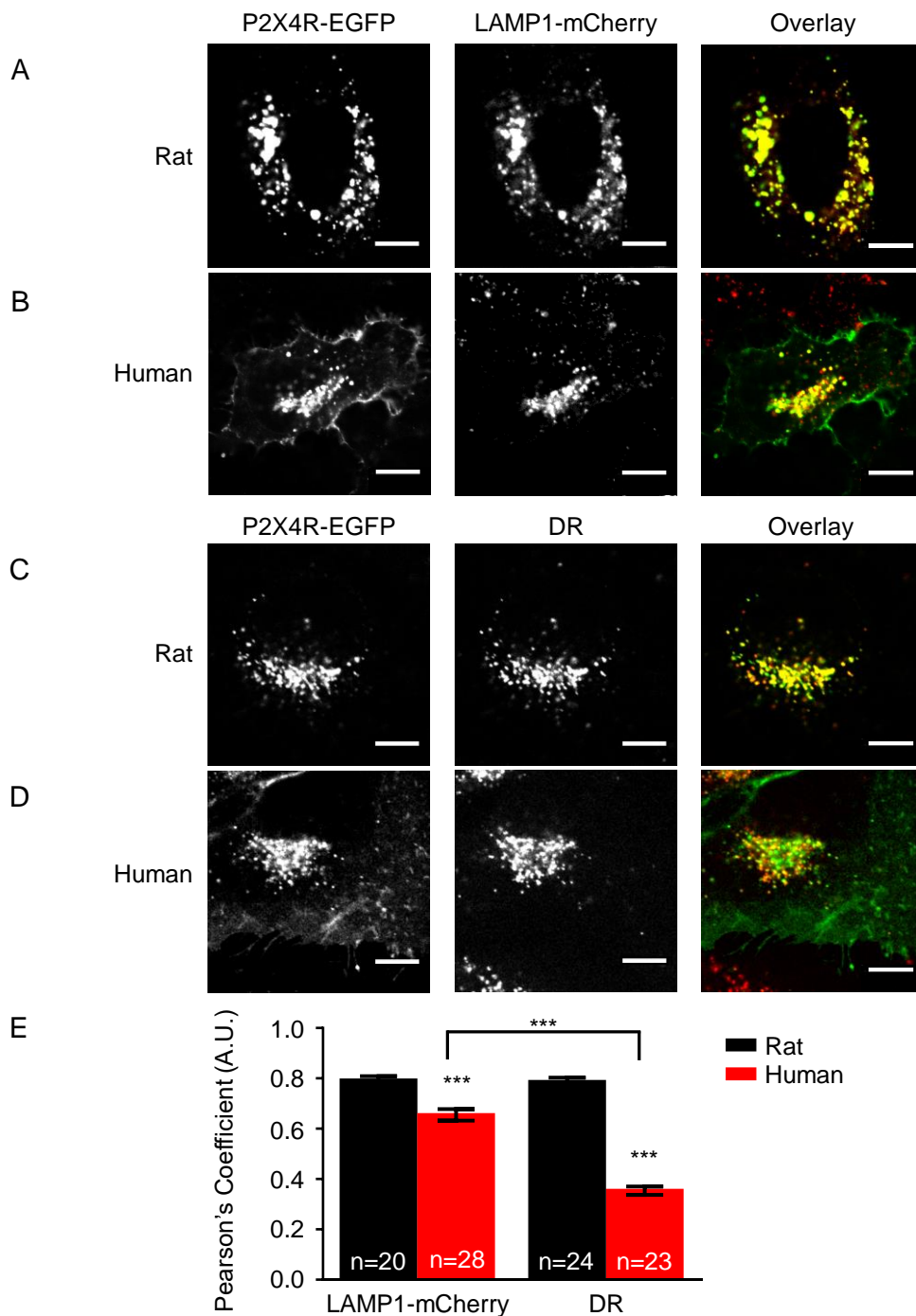


Fig. 6.1 The subcellular distribution of human and rat P2X4R in HeLa cells. (A-B) Confocal images of HeLa cells co-expressing LAMP1-mCherry as lysosomes, with rat (A) or human (B) isoforms of P2X4R-EGFP. (C-D) Confocal images showing cells expressing rat (C) or human (D) isoforms of P2X4R-EGFP with lysosomes labelled by Texas Red 10-kDa Dextran (DR). (E) Histogram showing the co-localisation measured by Pearson's coefficients of LAMP1-mCherry or DR with human and rat orthologues of P2X4R-EGFP. All results are mean \pm s.e.m. obtained from the total number of cells, n as indicated. *** $P < 0.001$, one-way ANOVA followed by Tukey's analysis. All scale bars, 10 μ m.

The experiment was repeated, but using NRK cells, and comparing the distribution of both EGFP-tagged and un-tagged P2X4Rs, labelled by immunofluorescence (**Fig. 6.2**). Again, the plasma membrane expression of hP2X4R was more evident than for the rP2X4R and the degree of co-localisation with LAMP1-mCherry was lower for the human versus the rat receptor.

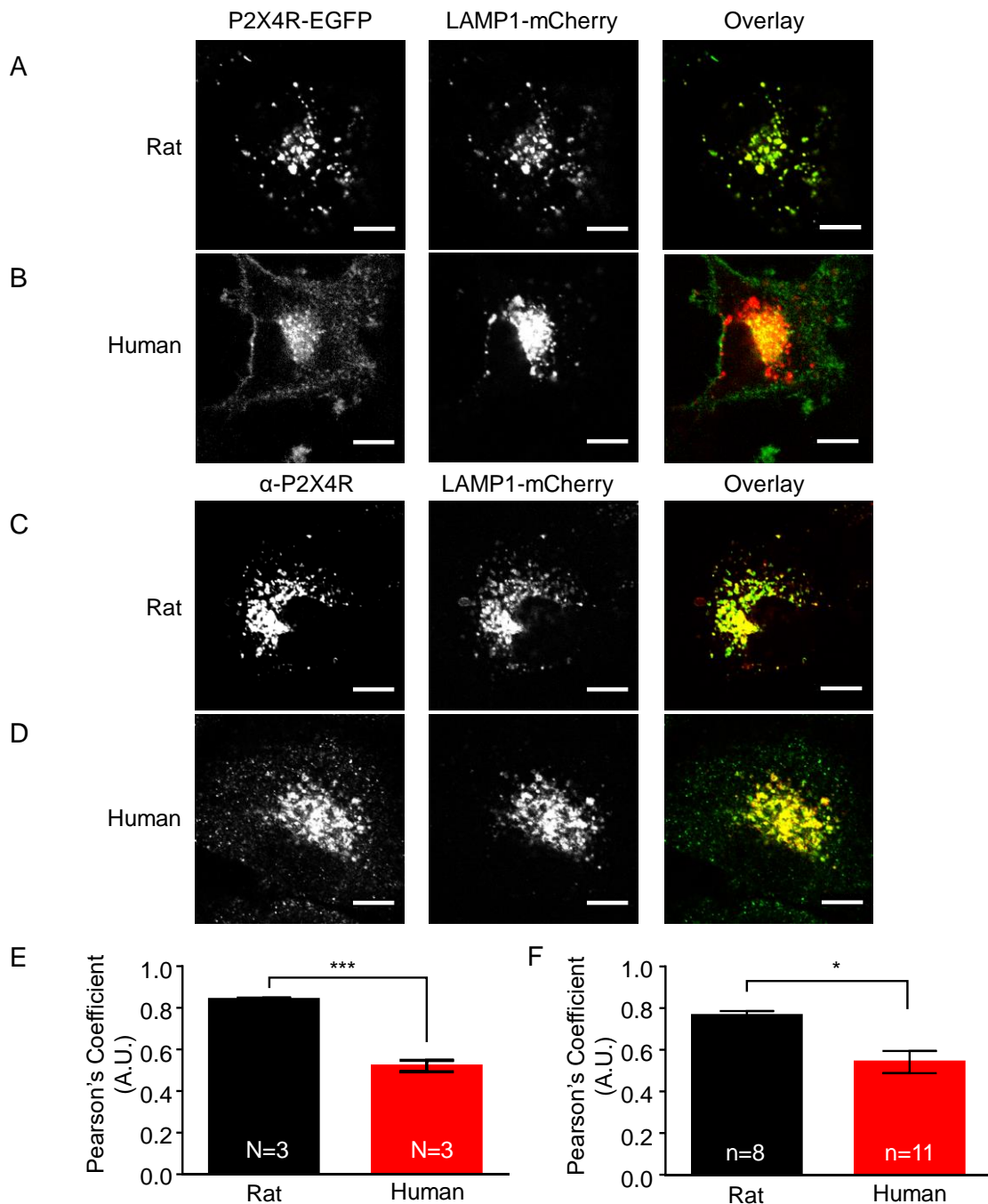
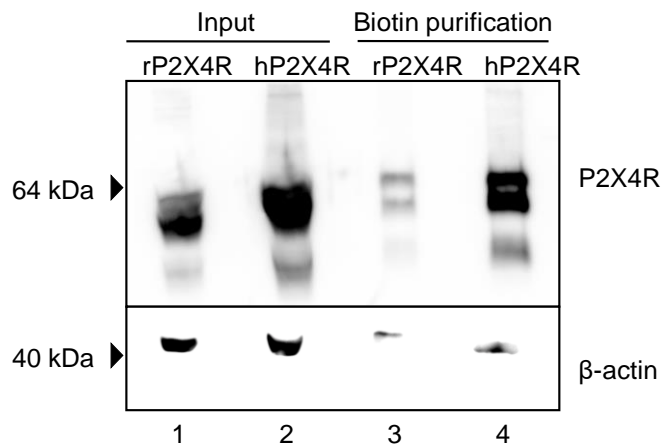


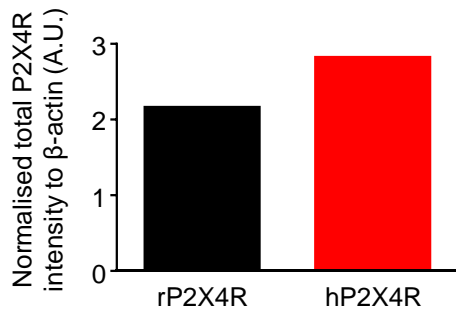
Fig. 6.2 Human P2X4Rs are localised to lysosomes and the plasma membrane in NRK cells. (A-B) Representative confocal images of cells co-expressing LAMP1-mCherry as lysosomes, with rat (A) or human (B) isoforms of P2X4R-EGFP. (C-D) Confocal images of NRK cells expressing rat (C) and human (D) orthologues of P2X4R, immunostained with α -P2X4R antibody (Alexa Fluor 488) and lysosomes marked by LAMP1-mCherry. (E-F) A summary of the results showing Pearson's coefficients for co-localisation of LAMP1-mCherry with either P2X4R-EGFP (E) or α -P2X4R antibody (F) in rat P2X4R (rP2X4R) and human P2X4R (hP2X4R) expressing NRK cells. (E) Results are mean \pm s.e.m. obtained from 3 independent experiments, N = 3. (F) Results are mean \pm s.e.m. obtained from total number of cells, n as indicated. (E-F) *P < 0.05 and ***P < 0.001, Student's *t* test. All scale bars, 10 μ m.

To further investigate if hP2X4R has a higher expression at the plasma membrane compared to rP2X4R, I used a different approach in which surface receptors were labelled using biotin, purified and then the amount at the cell surface was compared with the total receptor population by western blot analysis. This experiment was carried out using a modified HEK293 cells line that is suited to biochemical assays because of high expression of recombinant proteins. The total expression of P2X4Rs was normalised to a loading control (β -actin) and the purified surface receptor samples were loaded in the same proportion (**Fig. 6.3**). It is clear from this blot and the quantification shown in the histogram, that the intensity of the band representing surface hP2X4R was greater than for the band that represents surface rP2X4R even when one takes into account that total hP2X4R had a slightly higher intensity than total rP2X4R. There is one caveat with this data, which is that β -actin should not appear in the biotin-purified sample given that it is an intracellular protein. Its appearance in lanes 3 and 4 indicates that some cells were permeabilised enabling biotin to gain access to intracellular proteins. However, the band intensity is relatively faint compared to the total bands and these samples were highly concentrated (which the concentration factor is 5 times) compared to the total samples. Therefore, those bands that are supposed to represent the cell surface P2X4R are likely to have a small component contributed by intracellular receptors. Unfortunately, this experiment was carried out only once, but the results are consistent with the confocal images, which show elevated hP2X4-EGFP versus rP2X4-EGFP at the cell surface.

A



B



C

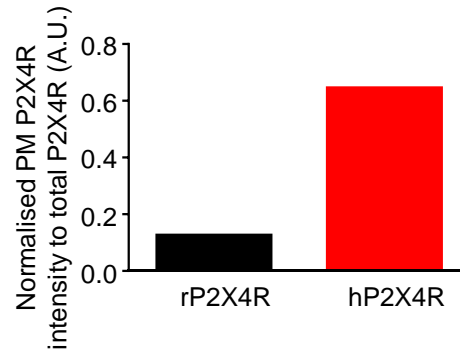


Fig. 6.3 Surface expression of hP2X4R and rP2X4R in HEK293 cells. (A) Immunoblot showing the input and proteins detected after surface avidin purification in cells expressing rat or human isoforms of P2X4R. (B) Histogram showing the total amount of P2X4R normalised to β -actin. (C) Histogram showing the amount of P2X4R detected on the cell surface via the avidin pull-downs, normalised by the total amount of P2X4R.

The higher plasma membrane expression of hP2X4R compared to rP2X4R was surprising because this receptor contains the endocytic and lysosome targeting motifs that were identified in rP2X4R, namely Y372 and Y378-based endocytic motifs within the C-terminus and the dileucine-like motif within the N-terminus (L22, I23) (**Fig. 6.4**) (Qureshi et al., 2007). However, there are some sequence differences between the two isoforms in the vicinity of these motifs. Also, there is a second in-frame methionine at position 31 and I was interested in the possibility that this was being utilised in the translation of hP2X4R thereby generating an N-terminally truncated variant of hP2X4 lacking the L22, I23 motif. I carried out some limited mutagenesis of residues in hP2X4R-EGFP to see if I could identify what was responsible for its higher plasma membrane expression. Within the N-terminus of hP2X4R, alanine at position 6 was mutated to serine and alanine at position 7 to valine (hP2X4R-A6S-A7V), which are homologous residues in rP2X4R. Additionally, I mutated methionine 31 to alanine (hP2X4R-M31A) to remove the possibility of expression of a truncated variant.

These mutants were expressed in NRK cells and lysosomes were labelled using LAMP1-mCherry. Confocal images showed that the mutant hP2X4R-A6S-A7V-EGFP (0.52 ± 0.02 A.U., $p < 0.01$) concentrated within the intracellular compartments that co-localised with LAMP1-mCherry with a reduction in the peripheral membrane expression (**Fig. 6.5C**). The mutant M31A, however exhibited the same subcellular distribution as hP2X4R WT with receptors targeted to lysosomes, but still showing clear expression at the cell surface (**Fig. 6.5**). A similar experiment was conducted to assess the targeting of WT and mutant receptors in HeLa cells, but this time lysosomes were marked with DR. Confocal images showed greater co-localisation of hP2X4R-A6S-A7V-EGFP within the DR-loaded

compartments than for WT and mutant M31A receptors and this was reflected in the value of the Pearson's coefficient, which was significantly higher for the hP2X4R-A6S-A7V-EGFP mutant than WT and mutant M31A receptors ($p < 0.001$) (**Fig. 6.6**). Again, the mutant hP2X4R-A6S-A7V-EGFP appeared to decrease the expression at the plasma membrane. **Fig. 6.7** shows a comparison of a selection of images taken either from cells expressing the wild type hP2X4 receptor or the A6S-A7V mutant. The results are not completely clear cut, but there do seem to be fewer cells showing detectable plasma membrane expression in the mutant hP2X4R-A6S-A7V-EGFP compared to WT hP2X4R-EGFP. These results suggest that the nature of the residues at positions 6 and 7 in P2X4R have some influence on the proportion of receptors within lysosomes versus at the cell surface.

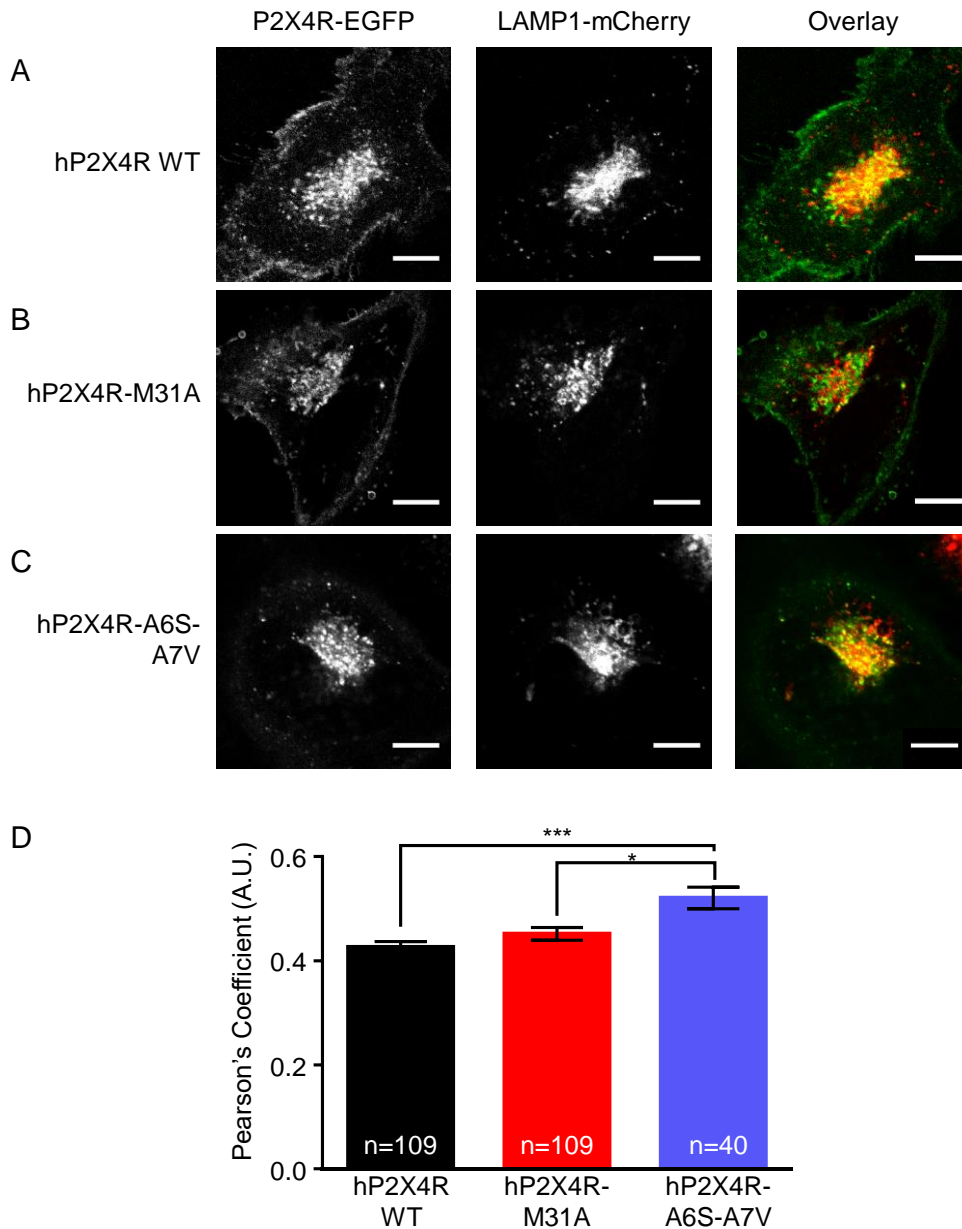


Fig. 6.5 The mutant hP2X4R-A6S-A7V reduced the plasma membrane expression in NRK cells. (A-C) Confocal images of NRK cells transiently transfected with WT hP2X4R-EGFP (A), hP2X4R-M31A-EGFP (B) and hP2X4R-A6S-A7V-EGFP (C), with lysosomes labelled by LAMP1-mCherry. (D) Summary of results showing Pearson's coefficients for the co-localisation of LAMP1-mCherry with WT and mutants of P2X4R-EGFP, as indicated. All results are mean \pm s.e.m. obtained from total number of cells, n, as indicated. * $P < 0.05$ and *** $P < 0.001$, one-way ANOVA followed by Tukey's analysis. All scale bars, 10 μ m.

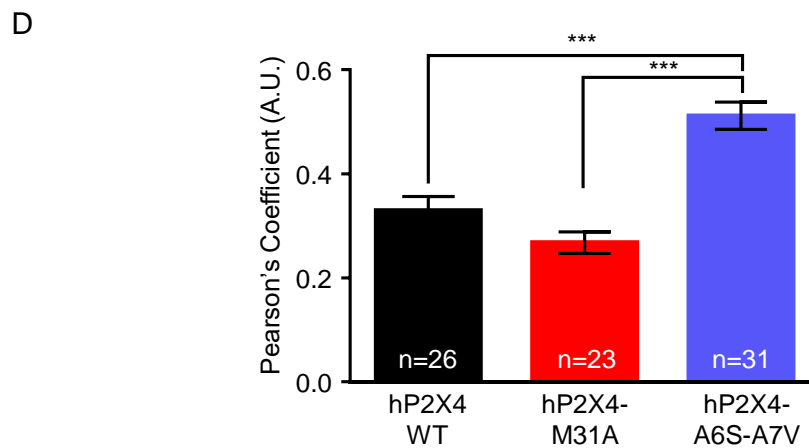
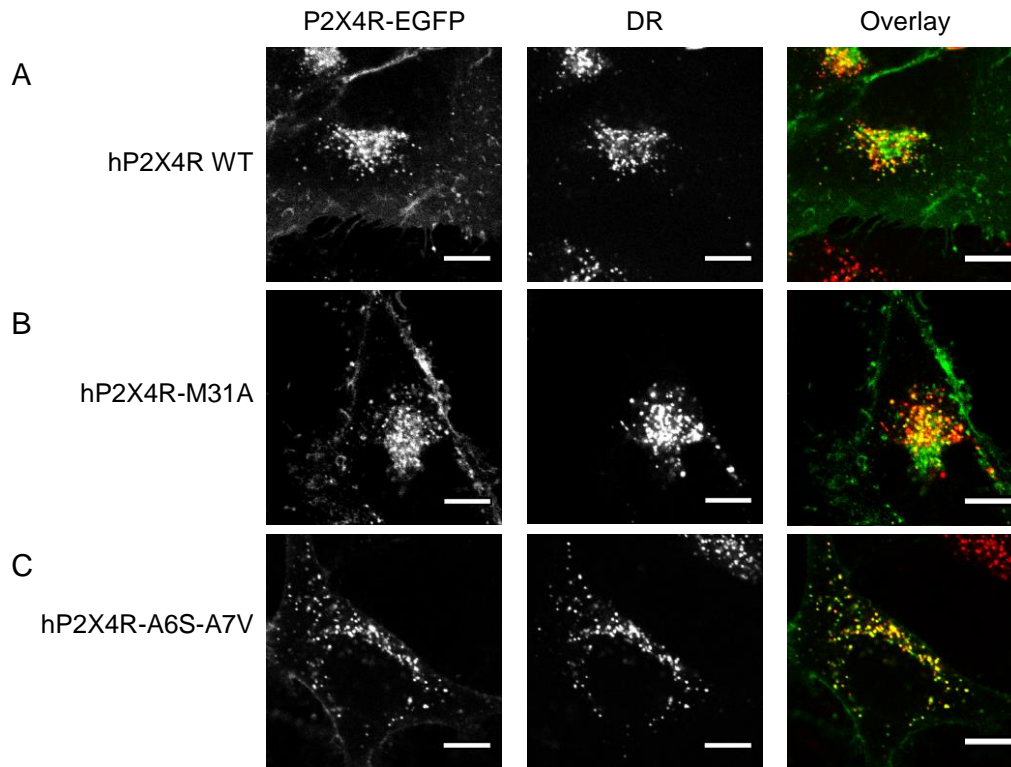


Fig. 6.6 The mutant hP2X4R-A6S-A7V reduced plasma membrane localisation in HeLa cells. (A-C) Confocal images showing the subcellular distribution of EGFP-tagged constructs of WT hP2X4R (A), hP2X4R-M31A (B) and hP2X4R-A6S-A7V (C) in HeLa cells; lysosomes were marked by DR. All scale bars, 10 μ m. (D) Histogram showing the Pearson's coefficients of DR with either WT or mutants of P2X4R-EGFP (hP2X4R-M31A and hP2X4R-A6S-A7V). All results are mean \pm s.e.m. obtained from total number of cells, n, as indicated. ***P < 0.001, one-way ANOVA followed by Tukey's analysis.

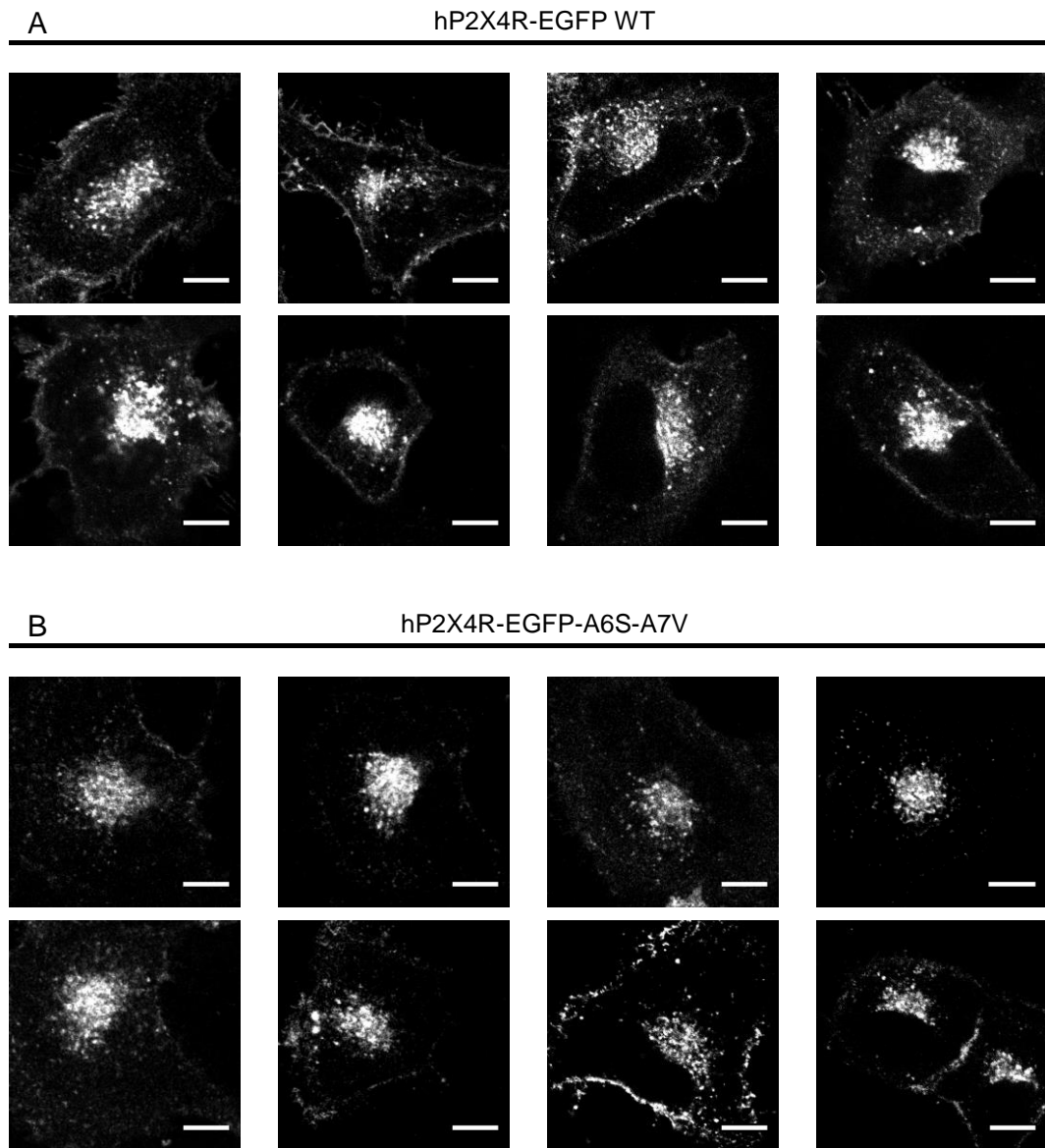


Fig. 6.7 The mutant hP2X4R-A6S-A7V reduced the plasma membrane labelling in NRK cells. (A-B) A series of NRK cells transiently transfected with WT hP2X4R-EGFP (A) and hP2X4R-A6S-A7V-EGFP (B). Confocal images demonstrate lysosomes labelled by EGFP-tagged P2X4Rs with some cells showing the plasma membrane labelling. All scale bars, 10 μ m.

6.3 Discussion

My results show that there are many similarities in the distribution of rP2X4R and hP2X4R, but also some differences. Both receptors show localisation to lysosomes, but there is more obvious expression of hP2X4R at the cell surface compared to rP2X4R. This was clearly seen in the confocal images and the western blot results following biotinylation of surface proteins, which agree with these confocal images. Also, measurements of co-localisation by calculating the Pearson's coefficient indicated that there was higher co-localisation between rP2X4R and lysosomal makers than for hP2X4R. Interestingly, this was particularly apparent when comparing with DR labelling rather than LAMP1-mCherry. One explanation is that the labelling of LAMP1-mCherry marks both active and quiescence populations of lysosomes whereas DR-loaded compartments are active by virtue of recently receiving endocytosed materials.

I carried out some preliminary investigation of the sequence differences between rP2X4R and hP2X4R that might be responsible for the difference in receptor targeting. It was previously shown that both N-terminus dileucine motif (L22I23) and two tyrosine motifs (Y372 and Y378) in the C-terminus of P2X4R are involved in lysosomal targeting (Qureshi et al., 2007). However, these are both conserved in rat and human isoforms, which does not explain the plasma membrane expression of hP2X4R. I investigated both mutations of the non-conserved residues A6S-A7V and the second open reading frame M31A of hP2X4R, which are juxtaposed to the lysosomal targeting motifs. Confocal studies suggested that the distribution of hP2X4R-A6S-A7V was more similar to rP2X4R than wild type hP2X4R. However, further experiments are required to be sure these findings are robust and to test for the functionality of the mutant receptor. Both rP2X4R and hP2X4R contain an in-

frame methionine at position 31 suggesting that an N-terminally truncated variant might also be expressed, but have slightly reduced targeting to lysosomes. Mutagenesis of hP2X4R-M31A was carried out to investigate whether the first methionine is skipped as the start of translation in preference for the second methionine. This mutation removes this possibility and yet it had no obvious effect on either the expression level of the receptor or its distribution which suggests that the truncated variant may not be the dominant form expressed. There was a difference in the distribution of the A6S-A7V mutant compared to wild type hP2X7R, but further work needs to be carried out to characterise this mutant in more detail. Co-localisation between the mutant receptor and lysosomal markers was increased compared to wild type hP2X4R. One possible explanation for the differences seen in P2X4R targeting is that the accessibility of the L22I23 motif is reduced in the human isoform and that this has something to do with the nature of the residues at positions 6 and 7. Perhaps this affects the folding of the N-terminus or an interaction with another protein that restricts accessibility.

The higher expression of hP2X4R on the cell surface is completely unexpected given that the lysosome targeting motifs are conserved in human isoforms. Previously it has been suggested that dileucine like motifs are more important for directly targeting proteins to lysosomes from the trans Golgi network whereas tyrosine-based motifs are more involved in targeting to lysosomes via retrieval of the protein from the plasma membrane (Qureshi et al., 2007; Royle et al., 2002). To ensure this is the case for hP2X4R, further investigation can be implemented to assess the trafficking behaviour of hP2X4R by generating chimeras between rP2X4R and hP2X4R in which the C-termini are switched. Similarly, chimeras where the N-termini are switched between rP2X4R and hP2X4R. These chimeras with a GFP-tag can be

visualised by confocal microscopy to determine whether the N-terminus or the C-terminus is dominant in determining the surface expression of hP2X4R. After having determined which terminal region is largely regulating the targeting of hP2X4R, series of sequential mutagenesis close to the targeting motif can generate to identify the important region for trafficking. Certainly, P2X4R is known to undergo constitutive endocytosis from the cell surface and that this requires the C-terminal tyrosines 372 and 378. Thus, a series of individual substitution of the 7 non-conserved amino acid residues in hP2X4R with the homologue residue in rP2X4R, which is juxtaposed to the tyrosine motifs, can identify the important residue in the endocytosis of hP2X4R (Garcia-Guzman et al., 1997). These 7 non-conserved amino acids may contribute to the binding of adaptor proteins alongside with the tyrosine motif for endocytosis.

Recently other experiments carried out in the RML lab have examined the distribution of endogenous P2X4R in highly invasive human breast cancer cells, including MDA-MB-435 cells and MDA-MB-231 cells. In both cases the immunostaining has shown a lysosomal localisation of P2X4R with no clear staining at the cell surface. Thus understanding a role for the lysosomal receptors is likely to be important for both the human as well as the rodent isoforms.

7. Conclusion

The lysosome is recognised as an organelle that modulates many cellular processes, including degradation, recycling of intracellular organelles and cell death. Essentially, lysosomes mediate these cellular functions via the distribution and delivery of acidic hydrolases. Delivery of these hydrolases via fusion and fission are essential for the main mode of lysosome function.

The high concentration of hydrolases with low pH within lysosomes suggests a perfect degradative environment. However, my results (alongside others - Qureshi et al., 2007; Royle et al., 2002, 2005) have demonstrated the stable localisation of P2X4R in lysosomes. There is evidence demonstrating that P2X4R retains its functional integrity in lysosomes and can be activated following lysosomal alkalinisation, using pharmacological reagents like Baf-A1 and MA (Cao et al., 2015; Huang et al., 2014). This matches with my results demonstrating P2X4R-dependent lysosome fusion following lysosome alkalinisation. Mediation of lysosome fusion has been shown to be dependent on Ca^{2+} release from lysosomes (Morgan et al., 2011; Pryor et al., 2000). Correspondingly, my results match with the proposed mechanism such that the activation of P2X4R mediates lysosome Ca^{2+} efflux, thereby mediating lysosome fusion. This result is consistent with that of others (Cao et al., 2015; Huang et al., 2014), however neither of the studies demonstrate a role for P2X4R under physiological or pathophysiological conditions.

In my studies I identified two physiological regulators of P2X4R, namely P2X7R and G_q -coupled GPCRs. P2X7R-induced lysosome alkalinisation was previously shown in microglial cells, which led to my investigation of the potential interaction between P2X4R and P2X7R in lysosome function. My results suggest that the activation of

P2X7R increases the pH of lysosomes in a manner that is dependent upon Ca^{2+} entry into the cell. Similarly P2X4-dependent lysosome fusion was dependent upon Ca^{2+} entry into the cell via P2X7R. The activation of P2X4Rs mediates lysosome functions, specifically lysosome Ca^{2+} efflux and lysosome fusion. The P2X4R-mediated Ca^{2+} signal was only detectable using LAMP1-GECO, but not the cytoplasmic Ca^{2+} indicator G-GECO, following the activation of P2X7R. The slow desensitisation rate of P2X7R and over expression of the receptor is likely to generate a sustained Ca^{2+} influx from the extracellular space and that is likely to saturate G-GECO signals. This provides evidence of the synergistic effect of P2X7R and P2X4R in Ca^{2+} signalling such that P2X4R triggered a localised surge of the cytoplasmic $[\text{Ca}^{2+}]$, mediated by lysosome Ca^{2+} efflux. This Ca^{2+} signal is likely to be the stimulus for lysosome fusion, only when P2X4R and P2X7R are co-expressed.

My results also showed that the activation of the G_q -coupled GPCR, H1R, triggered Ca^{2+} release from the ER that alkalinised the pH of lysosomes in HeLa cells. The alkalinised lysosomes relieved the acidic inhibition of P2X4R and enabled lysosome Ca^{2+} efflux. This was confirmed by three different Ca^{2+} indicators, namely LAMP1-GECO, G-GECO and Fluo4. These Ca^{2+} indicators showed that P2X4R potentiated the histamine-induced Ca^{2+} signal via lysosome Ca^{2+} release, indicative of the functional crosstalk between lysosomes and ER. This is different from the Ca^{2+} signal recorded by G-GECO where it does not resolve any Ca^{2+} signal derived from lysosomes in NRK cells. The discrepancy can be explained based on the different experimental setups. A more physiological setup was used in HeLa cells to monitor the P2X4R-mediated Ca^{2+} signal from intra-organelle Ca^{2+} stores compared to the mobilisation of Ca^{2+} influx from the extracellular space via P2X7R, an ion channel

with prolonged pore opening. Similarly, the G_q -coupled P2Y2R also recruited the activity of lysosomal P2X4R in the same manner as H1R, via the release of ER Ca^{2+} .

I have also demonstrated that P2X7R-induced lysosome alkalinisation impacts upon the rate at which autophagic flux progresses. The heterologous expression of P2X4R and P2X7R was sufficient to inhibit autophagic flux. This effect is only observed after autophagy initiation, providing evidence that the receptors are involved in the later stages of autophagy. The accumulation of LC3 proteins that co-localised with lysosomes confirmed the effect of P2X4R and P2X7R in the degradation of autophagolysosome, without significant impact on the fusion between autophagosomes and lysosomes. Altogether, these results suggest that both receptors are negatively regulating the autophagic clearance due to lysosome alkalinisation, a similar effect induced by Baf-A1 treatment.

Having shown the physiological regulators of P2X4R in lysosome function and the effect of P2X4R in autophagy, the depletion of P2X4R is expected to confer an impact in lysosome phenotype. Nonetheless, the depletion of P2X4R in BMDMs derived from P2X4R^{-/-} mice did not exhibit any gross change in lysosome phenotype under control conditions. This rules out the role of P2X4R in lysosome function under basal conditions but it should be noted that I did not have a chance to repeat this preliminary data. However, pharmacological reagents that alkalinise lysosomes reduced the rate of lysosome fusion. This suggests that P2X4R in lysosomes is likely to be stimulated under circumstances where the pH of lysosomes is increased. Nonetheless, the effect of P2X4R has been shown to mediate regulated lysosome fusion in ATII cells. P2X4R modulates the secretory fusion of LBs with plasma membrane such that the activation of P2X4R mediates a localised Ca^{2+} signal,

facilitating the complete fusion and secretion of surfactants (Miklavc et al., 2010). Therefore, P2X4R is likely to be stimulated under specific cell types and circumstances where the pH of lysosomes is elevated.

Lastly, I have demonstrated the difference in the trafficking behaviour of hP2X4R and rP2X4R. Both receptors exhibit many similarities in the subcellular distribution such that both hP2X4R and rP2X4R are localised to lysosomes at the perinuclear region. However, hP2X4Rs display a higher plasma membrane distribution than the rat isoform. My preliminary study has shown that the non-conserved residues at position A6 and A7 in hP2X4R may have some influence in the plasma membrane labelling. This difference in receptor targeting may imply that the human isoforms are more sensitive towards the extracellular milieu due to its enhanced expression on the plasma membrane, thereby positively regulating the activity of P2X4R in lysosomes. Collectively, my results provide the first evidence of physiological regulators of lysosomal P2X4Rs.

7.1. Potential effects of P2X4R in health and diseases

My results demonstrate the effect of P2X4R and P2X7R in autophagic flux suggests the effect of P2X4R in lysosome function is likely to mediate under cellular stress conditions, complementing the explanation of the lack of lysosome phenotype in P2X4R^{-/-} mice. Thus far, no research has examined the effect of P2X4R in autophagy in P2X4R knockout mice. Given my results demonstrating the negative regulation of P2X4R and P2X7R in autophagy, it is possible that cells in P2X4R knockout mice may have the positive consequence in improving autophagy clearance under stressful conditions. In addition to the effect of P2X4R and P2X7R on the accumulation of LC3 proteins, there is evidence showing effects of P2X7R on

autophagy and subsequently enhanced the exocytosis of the autophagolysosomes in microglial cells (Takenouchi et al., 2009). This increases the extracellular undigested metabolites and may have toxic consequences due to the secretion of acidic hydrolytic enzymes. Again, such conditions suggest an effect of P2X4R in the exocytosis of autophagolysosomes, given P2X7R as a regulator of P2X4R. Therefore, P2X4R knockout mice may exhibit a positive effect following nutrient starvation conditions as compared to wildtype.

Research has demonstrated the physiological importance of autophagy in neuronal biogenesis and dysfunction has been implicated in neurodegenerative diseases. Most neurodegenerative diseases present with abnormality of lysosome trafficking, accumulation of autophagic vacuoles, lysosomal hydrolysis impairment and aggregation of misfolded proteins, which arises from the impairment in autophagy (Nixon, 2013). One example for autophagy-related disease is familial Alzheimer's disease (AD), which arises from mutations in presenilin1 (PS1). AD is characterised by the loss of neurons, the formation of intracellular neurofibrillary tangles and extracellular plaque of amyloid β ($A\beta$). The aggregation of $A\beta$ is associated with the rate of autophagy such that the upregulation of autophagy decreases $A\beta$ level (Menzies et al., 2017). Furthermore, there is evidence demonstrating an increase in lysosome pH in fibroblasts with Alzheimer-associated PS1 mutation (Coffey et al., 2014; Lee et al., 2010). This is because PS1 serves as a chaperone in the ER for the essential maturation of lysosomal V-ATPase subunit, V0a1. The mutation in PS1 therefore prevents formation and delivery of the mature V-ATPase, resulting in increase in lysosome pH. In addition, there is evidence showing that the loss of V0a1 subunit increases the susceptibility of neurons to $A\beta$ and tau-induced toxicity, only in the context of stress conditions (Williamson and Hiesinger, 2010). Consistent with

my finding that the effect of P2X4R and P2X7R in autophagic flux was only observed following nutrient starvation, this suggests P2X4R may contribute to the progression of AD. Interesting, there is evidence showing an enhanced Ca^{2+} release from lysosomes, which is mediated by TRPML1 in the knockout of PS1 blastocysts (Lee et al., 2015). However, the study does not demonstrate a role for P2X4R, which may contribute to the enhanced Ca^{2+} release from lysosomes. Therefore, it can be explained based on the assumption that lysosome pH modulates the balance in lysosome Ca^{2+} release mediated by both TRPML1 and P2X4R, and the disruption in lysosome pH disrupts the balance of this regulation. Altogether, an increase in lysosome pH in AD is likely to stimulate P2X4R-mediated Ca^{2+} signals and facilitate lysosome fusion followed by exocytosis. My results demonstrate the anterograde movement of lysosomes towards the plasma membrane, indicative of lysosome exocytosis. Therefore, understanding of P2X4R in lysosome function is important and the inhibition of P2X4R could serve as an alternative target for lysosome defects and may alleviate phenotypes of autophagy-related neurodegenerative diseases (Colacurcio and Nixon, 2016; McBrayer and Nixon, 2013; Menzies et al., 2017).

Having shown that P2X7R is a regulator of P2X4R in lysosomes, P2X4R in lysosomes may have an effect in inflammation given the role of P2X7R in inflammation. Indeed, a study has demonstrated the expression of P2X4R in neurons was upregulated after spinal cord injury (Vaccari et al., 2012). The depletion of P2X4R reduced the level of caspase-1 activation and IL-1 β cleavage, suggesting an effect of P2X4R in the release of active cytokines. P2X4Rs in neurons are constitutively shuttled between lysosomes and plasma membrane (Bobanovic et al., 2002; Royle et al., 2002, 2005), therefore P2X4R in lysosomes may contribute in the upregulation of plasma membrane expression via lysosome exocytosis. However,

this study did not demonstrate a function of P2X4R in lysosomes in such an inflammatory response. Furthermore, there is evidence demonstrating that the activation of P2X7R upregulates lysosome exocytosis to release IL-1 β in primary bone marrow-derived macrophages (Qu et al., 2007; 2009). This supports the hypothesis that P2X7R recruits the activity of P2X4R in lysosomes to mediate Ca²⁺-dependent lysosome exocytosis. In addition, the synergistic effect of P2X4R and P2X7R in IL-1 β and IL-18 release has been demonstrated in dendritic cells (Sakaki et al., 2013). Collectively, these observations suggest a potential effect of P2X4R in lysosome exocytosis; releasing cytokines and ATP, and upregulating P2X4R could potentially provide a positive feedback effect in inflammatory responses.

In addition to inflammation, lysosome-mediated cell death may be a condition where P2X4R activity is stimulated. A critical step in this process is the release of cathepsins, protons and lysosomal constituents to the cytoplasm and/or the extracellular space via lysosome membrane permeabilisation (LMP). Specifically, the escape of lysosome protons will result in an increase in lysosome pH. This alkalinisation favours the activation of P2X4R and this is likely to mediate lysosome fusion and subsequently lysosome secretion of cathepsins for LMP-induced cell death. The leakage of cathepsins has been implicated in apoptosis because most of the cathepsin substrate is Bid (BH3-interacting domain death agonist), leading to the activation of apoptosis signalling. In addition, cancer is highly dependent on lysosome function and the changes in lysosome composition, number and localisation have been implicated in cancers (Appelqvist et al., 2013). There is evidence suggesting an increase in the secretion of cathepsins in cancer cells. In addition, the upregulation of extracellular cathepsins was shown to trigger the stimulation of angiogenesis, tumour growth and invasion (Gocheva et al., 2006).

Moreover, there is evidence demonstrating the release of lysosomal glycosidases. For example β -NAG facilitates the extracellular matrix (ECM) degradation, resulting in the cancer invagination (Ramessur et al., 2010). P2X7R, which is often referred to as the “death receptor” for its ability to induce apoptosis, is highly expressed in cancer cells. There is evidence demonstrating that HEK293 tumour cells expressing P2X7R grew more rapidly and had a more developed vascular network, suggesting the effect of P2X7R in the upregulation of cancer progression (Adinolfi et al., 2012). Having shown the P2X7R as the regulator of P2X4R in lysosomes, a functional interaction between P2X4R and P2X7R could be possible to contribute an effect in cancer progression.

A full understanding of lysosome-related and autophagy-related diseases remain, to a large extent, unclear and this impedes the development of effective therapy. However, there are great number of research findings suggesting that these diseases are highly associated with the impairment in lysosome homeostasis, for example lysosome acidity. Therefore, the manipulation of lysosome function and inhibition of P2X4R might be an alternative therapeutic target given the effect of P2X4R in lysosome function. Therefore the detailed molecular mechanism of P2X4R in lysosome under pathological conditions should be examined as this would permit the development of an alternative therapeutic target.

8. Future Directions

8.1. The effect of lysosomal P2X4Rs in exocytosis

Having shown that the activation of P2X4R and P2X7R promotes Ca²⁺ dependent lysosome fusion and the evidence of lysosome translocation to the cell periphery (**Chapter 4**), lysosome exocytosis could be one of the downstream effects mediated by P2X4R and P2X7R. To study lysosome exocytosis, the activity of the lysosome enzyme, β -hexosaminidase and lysosomal cathepsins can be assayed in the culture medium of cells co-expressing P2X4R and P2X7R following P2X7R stimulation. The activity of β -hexosaminidase can be measured by incubating the culture medium with 4-nitrophenyl N-acetyl- β -D-glucosaminide, which acts as a chromogenic substrate, for 1 h and measures its cleaved product at absorbance 405 nm. Additionally, the biotinylation of LAMP1 on the plasma membrane can determine the degree of lysosome exocytosis in response to BzATP treatment in cells expressing P2X4R and P2X7R. Together, this will be able to determine a role for P2X4R in lysosome exocytosis.

8.2. The effect of P2X4/7Rs in autophagy

I have demonstrated the effect of P2X4R and P2X7R in autophagy flux where the activation of both P2X4R and P2X7R increases the accumulation of LC3 proteins. However, several issues remain unresolved and below is a list of potential experiments for future investigation.

8.2.1. The effect of P2X4/7Rs in autophagolysosome degradation

To further consolidate the effect of P2X4R and P2X7R in disrupting the degradation steps of autophagy process, experiments using western blot can be conducted.

Western blot can be used to determine the changes of LC3-I and LC3-II proteins during the activation of P2X7R. Under nutrient rich conditions, western blot bands representing LC3-I and LC3-II are expected to be low in intensity. The incubation of EBSS, which is sufficient to trigger autophagy, is expected to reduce LC3-II proteins. This is because the dynamic autophagy process promotes the fusion of autophagosomes, where LC3-II proteins are localised, with lysosomes into autophagolysosomes thereby degrading LC3-II proteins. However, the presence of Baf-A1 in EBSS inhibits degradation of autophagolysosomes, thereby the band intensity that represents LC3-II proteins is expected to increase. To support the negative regulation of P2X4R and P2X7R in autophagic degradation, the LC3-II proteins are expected to accumulate to the same extent as Baf-A1 treatment. This will confirm that P2X4/7Rs are negatively regulating the autophagic degradation, in a similar effect as Baf-A1 treatment, through lysosome alkalinisation.

To consolidate the synergistic effect of P2X4R and P2X7R in the inhibition of autophagolysosome degradation, the level of p62, also known as sequestosome 1 (SQSTM1), could be used as a protein marker to examine autophagy and autophagic flux. Initiation of autophagy is associated with a decrease in the p62 level, whilst the inhibition of autophagic flux using Baf-A1 correlates with an increase in p62 level due to the impairment in autophagolysosome degradation, and thus p62 serves as a readout for autophagic degradation (Bjørkøy et al., 2005). NaATP treatment with EBSS is expected to increase p62 level to a similar extent as Baf-A1 treatment in EBSS, in cells heterologous expression of P2X4R and P2X7R.

8.2.2. Determining the Ca²⁺ dependence of LC3-II accumulation

The effect of P2X7R in LC3-II protein accumulation was shown to be dependent on P2X7R-mediated Ca²⁺ influx (Takenouchi et al., 2009). My results in **Chapter 4** also demonstrate that the Ca²⁺ influx via P2X7R increased the pH of lysosomes and thereby activated P2X4R in lysosomes. Further experiments could be conducted to assess whether the effect of P2X7R and P2X4R in autophagic flux is dependent on the upregulation of the cytoplasmic [Ca²⁺]. To examine this, NaATP could be added to Ca²⁺-free EBSS to determine the changes of LC3-II intensity using either confocal microscope or western blot. LC3-II aggregation will not be observed if Ca²⁺ influx is required for autophagosome turnover. Given the evidence of H1R in lysosome alkalisation and H1R as the physiological regulator of P2X4R, further experiments can be conducted to determine whether the stimulation of H1R is sufficient to stimulate P2X4R to induce LC3-II accumulation.

8.3. The sub-cellular distribution of human and rat P2X4R

I have identified that hP2X4R localises in both lysosomes and plasma membrane and that is likely to be mediated by the non-conserved amino acid residues at A6 and A7 of hP2X4R. To consolidate the finding that hP2X4R-A6S-A7V is involved in lysosome localisation, a biotinylation assay could be conducted to examine the expression level of this mutant on the plasma membrane and compared with WT hP2X4R and rP2X4R. The cell surface expression level of hP2X4R-A6S-A7V is expected to reduce to a level comparable to rP2X4R and that will support my results that hP2X4R-A6S-A7V is predominantly localised to lysosomes. To ensure that hP2X4R-A6S-A7V does not negatively impact functional activity, analysis of hP2X4R-A6S-A7V can be conducted using patch clamp. This can examine the

receptor activity of hP2X4R-A6S-A7V by measuring the current in response to ATP stimulation and compared to WT hP2X4R. A dose response curve can then be produced to examine the ATP-sensitivity of WT hP2X4R and hP2X4R-A6S-A7V. To further validate this, the effect of a P2X4R antagonist, TNP-ATP can be utilised to determine the functional activity of WT hP2X4R and hP2X4R-A6S-A7V.

9. Bibliography

Abbracchio, M.P., Burnstock, G., Boeynaems, J.-M., Barnard, E.A., Boyer, J.L., Kennedy, C., Knight, G.E., Fumagalli, M., Gachet, C., Jacobson, K.A., et al. (2006). International Union of Pharmacology LVIII: Update on the P2Y G Protein-Coupled Nucleotide Receptors: From Molecular Mechanisms and Pathophysiology to Therapy. *Pharmacol. Rev.* 58, 281–341.

Abdelrahman, A., Namasivayam, V., Hinz, S., Schiedel, A.C., Köse, M., Burton, M., El-Tayeb, A., Gillard, M., Bajorath, J., de Ryck, M., et al. (2017). Characterization of P2X4 receptor agonists and antagonists by calcium influx and radioligand binding studies. *Biochem. Pharmacol.* 125, 41–54.

Adinolfi, E., Raffaghello, L., Giuliani, A.L., Cavazzini, L., Capece, M., Chiozzi, P., Bianchi, G., Kroemer, G., Pistoia, V., and Di Virgilio, F. (2012). Expression of P2X7 receptor increases in vivo tumor growth. *Cancer Res.* 72, 2957–2969.

Adkins, C. E. & Taylor, C. W. Lateral inhibition of inositol 1,4,5-trisphosphate receptors by cytosolic Ca²⁺. *Current Biology* 9, 1115–1118 (1999).

Aitken, A. (1999). Protein consensus sequence motifs. *Mol. Biotechnol.* 12, 241–253.

Andrei, C., Margiocco, P., Poggi, A., Lotti, L.V., Torrisi, M.R., and Rubartelli, A. (2004). Phospholipases C and A2 control lysosome-mediated IL-1 β secretion: Implications for inflammatory processes. *Proc. Natl. Acad. Sci. U. S. A.* 101, 9745–9750.

Antonin, W., Holroyd, C., Fasshauer, D., Pabst, S., Von Mollard, G.F., and Jahn, R. (2000). A SNARE complex mediating fusion of late endosomes defines conserved properties of SNARE structure and function. *EMBO J.* 19, 6453–6464.

Antonio, L.S., Stewart, A.P., Xu, X.J., Varanda, W.A., Murrell-Lagnado, R.D., and Edwardson, J.M. (2011). P2X4 receptors interact with both P2X2 and P2X7 receptors in the form of homotrimers. *Br. J. Pharmacol.* 163, 1069–1077.

Appelqvist, H., Wäster, P., Kågedal, K., and Öllinger, K. (2013). The lysosome: from waste bag to potential therapeutic target. *J. Mol. Cell Biol.* 5, 214–226.

Bach, G. (2005). Mucolipin 1: endocytosis and cation channel—a review. *Pflüg. Arch.* 451, 313–317.

Banfi, C., Ferrario, S., De Vincenti, O., Ceruti, S., Fumagalli, M., Mazzola, A., D' Ambrosi, N., Volontè, C., Fratto, P., Vitali, E., et al. (2005). P2 receptors in human heart: upregulation of P2X6 in patients undergoing heart transplantation, interaction with TNFalpha and potential role in myocardial cell death. *J. Mol. Cell. Cardiol.* 39, 929–939.

Bao, L., Locovei, S., and Dahl, G. (2004). Pannexin membrane channels are mechanosensitive conduits for ATP. *FEBS Lett.* 572, 65–68.

Barclay, J., Patel, S., Dorn, G., Wotherspoon, G., Moffatt, S., Eunson, L., Abdel'al, S., Natt, F., Hall, J., Winter, J., et al. (2002). Functional downregulation of P2X3 receptor subunit in rat sensory neurons reveals a significant role in chronic neuropathic and inflammatory pain. *J. Neurosci. Off. J. Soc. Neurosci.* 22, 8139–8147.

Bernier, L.-P., Ase, A.R., Chevallier, S., Blais, D., Zhao, Q., Boué-Grabot, E., Logothetis, D., and Séguéla, P. (2008). Phosphoinositides regulate P2X4 ATP-gated channels through direct interactions. *J. Neurosci. Off. J. Soc. Neurosci.* 28, 12938–12945.

Bianco, F., Pravettoni, E., Colombo, A., Schenk, U., Möller, T., Matteoli, M., and Verderio, C. (2005). Astrocyte-derived ATP induces vesicle shedding and IL-1 beta release from microglia. *J. Immunol. Baltim. Md 1950* 174, 7268–7277.

Bivik, C.A., Larsson, P.K., Kågedal, K.M., Rosdahl, I.K., and Ollinger, K.M. (2006). UVA/B-induced apoptosis in human melanocytes involves translocation of cathepsins and Bcl-2 family members. *J. Invest. Dermatol.* 126, 1119–1127.

Bjørkøy, G., Lamark, T., Brech, A., Outzen, H., Perander, M., Øvervatn, A., Stenmark, H., and Johansen, T. (2005). p62/SQSTM1 forms protein aggregates degraded by autophagy and has a protective effect on huntingtin-induced cell death. *J. Cell Biol.* 171, 603–614.

Bo, X., Kim, M., Nori, S.L., Schoepfer, R., Burnstock, G., and North, R.A. (2003). Tissue distribution of P2X4 receptors studied with an ectodomain antibody. *Cell Tissue Res.* 313, 159–165.

Bo, X., Zhang, Y., Nassar, M., Burnstock, G., and Schoepfer, R. (1995). A P2X purinoceptor cDNA conferring a novel pharmacological profile. *FEBS Lett.* 375, 129–133.

Bobanovic, L.K., Royle, S.J., and Murrell-Lagnado, R.D. (2002). P2X Receptor Trafficking in Neurons Is Subunit Specific. *J. Neurosci.* 22, 4814–4824.

Boland, B., Kumar, A., Lee, S., Platt, F.M., Wegiel, J., Yu, W.H., and Nixon, R.A. (2008). Autophagy Induction and Autophagosome Clearance in Neurons: Relationship to Autophagic Pathology in Alzheimer's Disease. *J. Neurosci. Off. J. Soc. Neurosci.* 28, 6926–6937.

Boumechache, M., Masin, M., Edwardson, J.M., Górecki, D.C., and Murrell-Lagnado, R. (2009). Analysis of Assembly and Trafficking of Native P2X4 and P2X7 Receptor Complexes in Rodent Immune Cells. *J. Biol. Chem.* 284, 13446–13454.

Boya, P., and Kroemer, G. (2008). Lysosomal membrane permeabilization in cell death. *Oncogene* 27, 6434–6451.

- Boya, P., Reggiori, F., and Codogno, P. (2013). Emerging regulation and functions of autophagy. *Nat. Cell Biol.* 15, 713–720.
- Bright, N.A., Gratian, M.J., and Luzio, J.P. (2005). Endocytic Delivery to Lysosomes Mediated by Concurrent Fusion and Kissing Events in Living Cells. *Curr. Biol.* 15, 360–365.
- Buchthal, F., and Folkow, B. (1948). Interaction between acetylcholine and adenosine triphosphate in normal, curarised and denervated muscle. *Acta Physiol. Scand.* 15, 150–160.
- Buell, G., Lewis, C., Collo, G., North, R.A., and Surprenant, A. (1996). An antagonist-insensitive P2X receptor expressed in epithelia and brain. *EMBO J.* 15, 55–62.
- Burnstock, G. (1972). Purinergic nerves. *Pharmacol. Rev.* 24, 509–581.
- Burnstock, G. (2006). Purinergic signalling. *Br. J. Pharmacol.* 147, S172–S181.
- Burnstock, G., and Kennedy, C. (1985). Is there a basis for distinguishing two types of P2-purinoceptor? *Gen. Pharmacol.* 16, 433–440.
- Burnstock, G., Campbell, G., Satchell, D., and Smythe, A. (1970). Evidence that adenosine triphosphate or a related nucleotide is the transmitter substance released by non-adrenergic inhibitory nerves in the gut. *Br. J. Pharmacol.* 40, 668–688.
- Calcraft, P.J., Ruas, M., Pan, Z., Cheng, X., Arredouani, A., Hao, X., Tang, J., Rietdorf, K., Teboul, L., Chuang, K.-T., et al. (2009). NAADP mobilizes calcium from acidic organelles through two-pore channels. *Nature* 459, 596–600.
- Cao, Q., Zhong, X.Z., Zou, Y., Murrell-Lagnado, R., Zhu, M.X., and Dong, X.-P. (2015). Calcium release through P2X4 activates calmodulin to promote endolysosomal membrane fusion. *J. Cell Biol.* 209, 879–894.

Cao, Q., Zhong, X.Z., Zou, Y., Zhang, Z., Toro, L., and Dong, X.-P. (2015b). BK Channels Alleviate Lysosomal Storage Diseases by Providing Positive Feedback Regulation of Lysosomal Ca²⁺ Release. *Dev. Cell* 33, 427–441.

Caplan, S., Hartnell, L.M., Aguilar, R.C., Naslavsky, N., and Bonifacino, J.S. (2001). Human Vam6p promotes lysosome clustering and fusion in vivo. *J. Cell Biol.* 154, 109–122.

Cerny, J. et al. The small chemical vacuolin-1 inhibits Ca²⁺-dependent lysosomal exocytosis but not cell resealing. *EMBO reports* 5, 883–888 (2004).

Chan, S.L., Mayne, M., Holden, C.P., Geiger, J.D., and Mattson, M.P. (2000). Presenilin-1 mutations increase levels of ryanodine receptors and calcium release in PC12 cells and cortical neurons. *J. Biol. Chem.* 275, 18195–18200.

Cheng, X., Shen, D., Samie, M., and Xu, H. (2010). Mucolipins: Intracellular TRPML1-3 channels. *FEBS Lett.* 584, 2013–2021.

Chessell, I.P., Hatcher, J.P., Bountra, C., Michel, A.D., Hughes, J.P., Green, P., Egerton, J., Murfin, M., Richardson, J., Peck, W.L., et al. (2005). Disruption of the P2X7 purinoceptor gene abolishes chronic inflammatory and neuropathic pain. *Pain* 114, 386–396.

Choi, A.M.K., Ryter, S.W., and Levine, B. (2013). Autophagy in Human Health and Disease. *N. Engl. J. Med.* 368, 651–662.

Christensen, K.A., Myers, J.T., and Swanson, J.A. (2002). pH-dependent regulation of lysosomal calcium in macrophages. *J. Cell Sci.* 115, 599–607.

Clarke, C.E., Benham, C.D., Bridges, A., George, A.R., and Meadows, H.J. (2000). Mutation of histidine 286 of the human P2X4 purinoceptor removes extracellular pH sensitivity. *J. Physiol.* 523 Pt 3, 697–703.

Clyne, J.D., LaPointe, L.D., and Hume, R.I. (2002). The role of histidine residues in modulation of the rat P2X₂ purinoceptor by zinc and pH. *J. Physiol.* 539, 347–359.

Cockayne, D.A., Dunn, P.M., Zhong, Y., Rong, W., Hamilton, S.G., Knight, G.E., Ruan, H.-Z., Ma, B., Yip, P., Nunn, P., et al. (2005). P2X₂ knockout mice and P2X₂/P2X₃ double knockout mice reveal a role for the P2X₂ receptor subunit in mediating multiple sensory effects of ATP. *J. Physiol.* 567, 621–639.

Cockayne, D.A., Hamilton, S.G., Zhu, Q.M., Dunn, P.M., Zhong, Y., Novakovic, S., Malmberg, A.B., Cain, G., Berson, A., Kassotakis, L., et al. (2000). Urinary bladder hyporeflexia and reduced pain-related behaviour in P2X₃-deficient mice. *Nature* 407, 1011–1015.

Coddou, C., Morales, B., and Huidobro-Toro, J.P. (2003). Neuromodulator role of zinc and copper during prolonged ATP applications to P2X₄ purinoceptors. *Eur. J. Pharmacol.* 472, 49–56.

Coddou, C., Yan, Z., Obsil, T., Huidobro-Toro, J.P., and Stojilkovic, S.S. (2011). Activation and Regulation of Purinergic P2X Receptor Channels. *Pharmacol. Rev.* 63, 641–683.

Coffey, E.E., Beckel, J.M., Laties, A.M., and Mitchell, C.H. (2014). Lysosomal alkalization and dysfunction in human fibroblasts with the Alzheimer's disease-linked presenilin 1 A246E mutation can be reversed with cAMP. *Neuroscience* 263, 111–124.

Colacurcio, D.J., and Nixon, R.A. (2016). Disorders of lysosomal acidification—The emerging role of v-ATPase in aging and neurodegenerative disease. *Ageing Res. Rev.* 32, 75–88.

Collo, G., North, R.A., Kawashima, E., Merlo-Pich, E., Neidhart, S., Surprenant, A., and Buell, G. (1996). Cloning OF P2X₅ and P2X₆ receptors and the distribution and

properties of an extended family of ATP-gated ion channels. *J. Neurosci. Off. J. Soc. Neurosci.* 16, 2495–2507.

Cotter, K., Stransky, L., McGuire, C., and Forgac, M. (2015). Recent Insights into the Structure, Regulation, and Function of the V-ATPases. *Trends Biochem. Sci.* 40, 611–622.

Di Virgilio, F. (2007). Liaisons dangereuses: P2X7 and the inflammasome. *Trends Pharmacol. Sci.* 28, 465–472.

Di, A., Brown, M.E., Deriy, L.V., Li, C., Szeto, F.L., Chen, Y., Huang, P., Tong, J., Naren, A.P., Bindokas, V., et al. (2006). CFTR regulates phagosome acidification in macrophages and alters bactericidal activity. *Nat. Cell Biol.* 8, 933–944.

Dong, X., Shen, D., Wang, X., Dawson, T., Li, X., Zhang, Q., Cheng, X., Zhang, Y., Weisman, L.S., Delling, M., et al. (2010). PI(3,5)P2 Controls Membrane Traffic by Direct Activation of Mucolipin Ca²⁺ Release Channels in the Endolysosome. *Nat. Commun.* 1.

Dong, X.-P., Cheng, X., Mills, E., Delling, M., Wang, F., Kurz, T., and Xu, H. (2008). The type IV mucopolidosis-associated protein TRPML1 is an endolysosomal iron release channel. *Nature* 455, 992–996.

Donnelly-Roberts, D.L., Namovic, M.T., Han, P., and Jarvis, M.F. (2009). Mammalian P2X7 receptor pharmacology: comparison of recombinant mouse, rat and human P2X7 receptors. *Br. J. Pharmacol.* 157, 1203–1214.

Dorn, G., Patel, S., Wotherspoon, G., Hemmings-Mieszczak, M., Barclay, J., Natt, F.J.C., Martin, P., Bevan, S., Fox, A., Ganju, P., et al. (2004). siRNA relieves chronic neuropathic pain. *Nucleic Acids Res.* 32, e49.

Drury, A.N., and Szent-Györgyi, A. (1929). The physiological activity of adenine compounds with especial reference to their action upon the mammalian heart. *J. Physiol.* 68, 213–237.

Dubyak, G.R. (2012). P2X7 Receptor Regulation of Non-Classical Secretion from Immune Effector Cells. *Cell. Microbiol.* 14, 1697–1706.

Eddy, M.C., Eschle, B.K., Barrows, J., Hallock, R.M., Finger, T.E., and Delay, E.R. (2009). Double P2X2/P2X3 purinergic receptor knockout mice do not taste NaCl or the artificial sweetener SC45647. *Chem. Senses* 34, 789–797.

Elneil, S., Skepper, J.N., Kidd, E.J., Williamson, J.G., and Ferguson, D.R. (2001). Distribution of P2X(1) and P2X(3) receptors in the rat and human urinary bladder. *Pharmacology* 63, 120–128.

Emmelin, N., and Feldberg, W. (1948). Systemic effects of adenosine triphosphate. *Br. J. Pharmacol. Chemother.* 3, 273–284.

Ferrari, D., Chiozzi, P., Falzoni, S., Susino, M.D., Melchiorri, L., Baricordi, O.R., and Virgilio, F.D. (1997). Extracellular ATP triggers IL-1 beta release by activating the purinergic P2Z receptor of human macrophages. *J. Immunol.* 159, 1451–1458.

Finger, T.E., Danilova, V., Barrows, J., Bartel, D.L., Vigers, A.J., Stone, L., Hellekant, G., and Kinnamon, S.C. (2005). ATP Signaling Is Crucial for Communication from Taste Buds to Gustatory Nerves. *Science* 310, 1495–1499.

Fitz, J.G. (2007). Regulation of Cellular Atp Release. *Trans. Am. Clin. Climatol. Assoc.* 118, 199–208.

Ford, A.P., Udem, B.J., Birder, L.A., Grundy, D., Pijacka, W., and Paton, J.F.R. (2015). P2X3 receptors and sensitization of autonomic reflexes. *Auton. Neurosci.* 191, 16–24.

Forgac, M. (2007). Vacuolar ATPases: rotary proton pumps in physiology and pathophysiology. *Nat. Rev. Mol. Cell Biol.* 8, 917–929.

Fountain, S.J., Parkinson, K., Young, M.T., Cao, L., Thompson, C.R.L., and North, R.A. (2007). An intracellular P2X receptor required for osmoregulation in *Dictyostelium discoideum*. *Nature* 448, 200–203.

Franceschini, A., Capece, M., Chiozzi, P., Falzoni, S., Sanz, J.M., Sarti, A.C., Bonora, M., Pinton, P., and Virgilio, F.D. (2015). The P2X7 receptor directly interacts with the NLRP3 inflammasome scaffold protein. *FASEB J.* 29, 2450–2461.

Fujiwara, Y., and Kubo, Y. (2004). Density-dependent changes of the pore properties of the P2X2 receptor channel. *J. Physiol.* 558, 31–43.

Gallagher, L.E., Williamson, L.E., and Chan, E.Y.W. (2016). Advances in Autophagy Regulatory Mechanisms. *Cells* 5, 24.

Ganley, I.G., Wong, P.-M., Gammoh, N., and Jiang, X. (2011). Distinct Autophagosomal-Lysosomal Fusion Mechanism Revealed by Thapsigargin-Induced Autophagy Arrest. *Mol. Cell* 42, 731–743.

Garcia-Guzman, M., Soto, F., Gomez-Hernandez, J. M., Lund, P.-E. & Stühmer, W. Characterization of Recombinant Human P2X4 Receptor Reveals Pharmacological Differences to the Rat Homologue. *Mol Pharmacol* 51, 109–118 (1997).

Garrity, A.G., Wang, W., Collier, C.M., Levey, S.A., Gao, Q., and Xu, H. (2016). The endoplasmic reticulum, not the pH gradient, drives calcium refilling of lysosomes. *eLife* 5.

Garver, W.S., Jelinek, D., Meaney, F.J., Flynn, J., Pettit, K.M., Shepherd, G., Heidenreich, R.A., Vockley, C.M.W., Castro, G., and Francis, G.A. (2010). The National Niemann-Pick Type C1 Disease Database: correlation of lipid profiles, mutations, and biochemical phenotypes. *J. Lipid Res.* 51, 406–415.

Gever, J.R., Cockayne, D.A., Dillon, M.P., Burnstock, G., and Ford, A.P.D.W. (2006). Pharmacology of P2X channels. *Pflüg. Arch. Eur. J. Physiol.* 452, 513–537.

Gocheva, V., Zeng, W., Ke, D., Klimstra, D., Reinheckel, T., Peters, C., Hanahan, D., and Joyce, J.A. (2006). Distinct roles for cysteine cathepsin genes in multistage tumorigenesis. *Genes Dev.* 20, 543–556.

González-Polo, R.-A., Boya, P., Pauleau, A.-L., Jalil, A., Larochette, N., Souquère, S., Eskelinen, E.-L., Pierron, G., Saftig, P., and Kroemer, G. (2005). The apoptosis/autophagy paradox: autophagic vacuolization before apoptotic death. *J. Cell Sci.* 118, 3091–3102.

Gordon, J.L. (1986). Extracellular ATP: effects, sources and fate. *Biochem. J.* 233, 309–319.

Graves, A.R., Curran, P.K., Smith, C.L., and Mindell, J.A. (2008). The Cl⁻/H⁺ antiporter CIC-7 is the primary chloride permeation pathway in lysosomes. *Nature* 453, 788–792.

Grimm, C., Holdt, L.M., Chen, C.-C., Hassan, S., Müller, C., Jörs, S., Cuny, H., Kissing, S., Schröder, B., Butz, E., et al. (2014). High susceptibility to fatty liver disease in two-pore channel 2-deficient mice. *Nat. Commun.* 5, 4699.

Guan, Z., Osmond, D.A., and Inscho, E.W. (2007). P2X receptors as regulators of the renal microvasculature. *Trends Pharmacol. Sci.* 28, 646–652.

Guha, S., Baltazar, G.C., Coffey, E.E., Tu, L.-A., Lim, J.C., Beckel, J.M., Patel, S., Eysteinnsson, T., Lu, W., O'Brien-Jenkins, A., et al. (2013). Lysosomal alkalinization, lipid oxidation, and reduced phagosome clearance triggered by activation of the P2X7 receptor. *FASEB J.* 27, 4500–4509.

Guo, C., Masin, M., Qureshi, O.S., and Murrell-Lagnado, R.D. (2007). Evidence for functional P2X4/P2X7 heteromeric receptors. *Mol. Pharmacol.* 72, 1447–1456.

Guo, Q., Furukawa, K., Sopher, B.L., Pham, D.G., Xie, J., Robinson, N., Martin, G.M., and Mattson, M.P. (1996). Alzheimer's PS-1 mutation perturbs calcium homeostasis and sensitizes PC12 cells to death induced by amyloid beta-peptide. *Neuroreport* 8, 379–383.

Gyrd-Hansen, M., Nylandsted, J., and Jäättelä, M. (2004). Heat shock protein 70 promotes cancer cell viability by safeguarding lysosomal integrity. *Cell Cycle Georget. Tex* 3, 1484–1485.

Hanada, T., Noda, N.N., Satomi, Y., Ichimura, Y., Fujioka, Y., Takao, T., Inagaki, F., and Ohsumi, Y. (2007). The Atg12-Atg5 Conjugate Has a Novel E3-like Activity for Protein Lipidation in Autophagy. *J. Biol. Chem.* 282, 37298–37302.

Hattori, M., and Gouaux, E. (2012). Molecular mechanism of ATP binding and ion channel activation in P2X receptors. *Nature* 485, 207–212.

He, M.-L., Zemkova, H., and Stojilkovic, S.S. (2003). Dependence of Purinergic P2X Receptor Activity on Ectodomain Structure. *J. Biol. Chem.* 278, 10182–10188.

Hechler, B., Lenain, N., Marchese, P., Vial, C., Heim, V., Freund, M., Cazenave, J.-P., Cattaneo, M., Ruggeri, Z.M., Evans, R., et al. (2003). A Role of the Fast ATP-gated P2X1 Cation Channel in Thrombosis of Small Arteries In Vivo. *J. Exp. Med.* 198, 661–667.

Holton, P. (1959). The liberation of adenosine triphosphate on antidromic stimulation of sensory nerves. *J. Physiol.* 145, 494–504.

Honore, P., Donnelly-Roberts, D., Namovic, M., Zhong, C., Wade, C., Chandran, P., Zhu, C., Carroll, W., Perez-Medrano, A., Iwakura, Y., et al. (2009). The antihyperalgesic activity of a selective P2X7 receptor antagonist, A-839977, is lost in IL-1 α knockout mice. *Behav. Brain Res.* 204, 77–81.

Honore, P., Donnelly-Roberts, D., Namovic, M.T., Hsieh, G., Zhu, C.Z., Mikusa, J.P., Hernandez, G., Zhong, C., Gauvin, D.M., Chandran, P., et al. (2006). A-740003 [N-(1-[[[(cyanoimino)(5-quinolinylamino) methyl]amino]-2,2-dimethylpropyl)-2-(3,4-dimethoxyphenyl)acetamide], a novel and selective P2X7 receptor antagonist, dose-dependently reduces neuropathic pain in the rat. *J. Pharmacol. Exp. Ther.* 319, 1376–1385.

Housley, G.D., Jagger, D.J., Greenwood, D., Raybould, N.P., Salih, S.G., Järlebark, L.E., Vlajkovic, S.M., Kanjhan, R., Nikolic, P., Muñoz, D.J.M., et al. (2002). Purinergic regulation of sound transduction and auditory neurotransmission. *Audiol. Neurootol.* 7, 55–61.

Hu, Y.-B., Dammer, E.B., Ren, R.-J., and Wang, G. (2015). The endosomal-lysosomal system: from acidification and cargo sorting to neurodegeneration. *Transl. Neurodegener.* 4.

Huang, P., Zou, Y., Zhong, X.Z., Cao, Q., Zhao, K., Zhu, M.X., Murrell-Lagnado, R., and Dong, X.-P. (2014). P2X4 Forms Functional ATP-activated Cation Channels on Lysosomal Membranes Regulated by Luminal pH. *J. Biol. Chem.* 289, 17658–17667.

Humphreys, B.D., Virginio, C., Surprenant, A., Rice, J., and Dubyak, G.R. (1998). Isoquinolines as Antagonists of the P2X7 Nucleotide Receptor: High Selectivity for the Human versus Rat Receptor Homologues. *Mol. Pharmacol.* 54, 22–32.

Ito, E., Oka, K., Etcheberrigaray, R., Nelson, T.J., McPhie, D.L., Tofel-Grehl, B., Gibson, G.E., and Alkon, D.L. (1994). Internal Ca²⁺ mobilization is altered in fibroblasts from patients with Alzheimer disease. *Proc. Natl. Acad. Sci. U. S. A.* 91, 534–538.

Jacobson, K.A., and Gao, Z.-G. (2006). Adenosine receptors as therapeutic targets. *Nat. Rev. Drug Discov.* 5, 247–264.

Jacobson, K.A., Paoletta, S., Katritch, V., Wu, B., Gao, Z.-G., Zhao, Q., Stevens, R.C., and Kiselev, E. (2015). Nucleotides Acting at P2Y Receptors: Connecting Structure and Function. *Mol. Pharmacol.* 88, 220–230.

Jaiswal, J.K., Andrews, N.W., and Simon, S.M. (2002). Membrane proximal lysosomes are the major vesicles responsible for calcium-dependent exocytosis in nonsecretory cells. *J. Cell Biol.* 159, 625–635.

Jarvis, M.F., and Khakh, B.S. (2009). ATP-gated P2X cation-channels. *Neuropharmacology* 56, 208–215.

Jha, A., Ahuja, M., Patel, S., Brailoiu, E., and Muallem, S. (2014). Convergent regulation of the lysosomal two-pore channel-2 by Mg²⁺, NAADP, PI(3,5)P₂ and multiple protein kinases. *EMBO J.* 33, 501–511.

Jiang, L.H., Rassendren, F., Surprenant, A., and North, R.A. (2000). Identification of amino acid residues contributing to the ATP-binding site of a purinergic P2X receptor. *J. Biol. Chem.* 275, 34190–34196.

Johnson, D.E., Ostrowski, P., Jaumouillé, V., and Grinstein, S. (2016). The position of lysosomes within the cell determines their luminal pH. *J Cell Biol* 212, 677–692.

Jones, C.A., Chessell, I.P., Simon, J., Barnard, E.A., Miller, K.J., Michel, A.D., and Humphrey, P.P. (2000). Functional characterization of the P2X(4) receptor orthologues. *Br. J. Pharmacol.* 129, 388–394.

Jung, C.H., Jun, C.B., Ro, S.-H., Kim, Y.-M., Otto, N.M., Cao, J., Kundu, M., and Kim, D.-H. (2009). ULK-Atg13-FIP200 complexes mediate mTOR signaling to the autophagy machinery. *Mol. Biol. Cell* 20, 1992–2003.

Kabeya, Y., Mizushima, N., Yamamoto, A., Oshitani-Okamoto, S., Ohsumi, Y., and Yoshimori, T. (2004). LC3, GABARAP and GATE16 localize to autophagosomal membrane depending on form-II formation. *J. Cell Sci.* 117, 2805–2812.

Kaczmarek-Hájek, K., Lörinczi, É., Hausmann, R., and Nicke, A. (2012). Molecular and functional properties of P2X receptors—recent progress and persisting challenges. *Purinergic Signal*. 8, 375–417.

Kang, C., You, Y., and Avery, L. (2007). Dual roles of autophagy in the survival of *Caenorhabditis elegans* during starvation. *Genes Dev*. 21, 2161–2171.

Karasawa, A., and Kawate, T. (2016). Structural basis for subtype-specific inhibition of the P2X7 receptor. *eLife* 5, e22153.

Kawai, A., Uchiyama, H., Takano, S., Nakamura, N., and Ohkuma, S. (2007). Autophagosome-lysosome fusion depends on the pH in acidic compartments in CHO cells. *Autophagy* 3, 154–157.

Kawate, T., Michel, J.C., Birdsong, W.T., and Gouaux, E. (2009). Crystal structure of the ATP-gated P2X(4) ion channel in the closed state. *Nature* 460, 592–598.

Kettner, C., Bertl, A., Obermeyer, G., Slayman, C., and Bihler, H. (2003). Electrophysiological Analysis of the Yeast V-Type Proton Pump: Variable Coupling Ratio and Proton Shunt. *Biophys. J.* 85, 3730–3738.

Khakh, B. S., Proctor, W. R., Dunwiddie, T. V., Labarca, C. & Lester, H. A. Allosteric Control of Gating and Kinetics at P2X4 Receptor Channels. *J. Neurosci.* 19, 7289–7299 (1999).

Khakh, B.S., and North, R.A. (2012). Neuromodulation by Extracellular ATP and P2X Receptors in the CNS. *Neuron* 76, 51–69.

Kilpatrick, B.S., Eden, E.R., Schapira, A.H., Futter, C.E., and Patel, S. (2013). Direct mobilisation of lysosomal Ca²⁺ triggers complex Ca²⁺ signals. *J. Cell Sci.* 126, 60–66.

Kinncar, N.P., Boittin, F.-X., Thomas, J.M., Galione, A., and Evans, A.M. (2004). Lysosome-Sarcoplasmic Reticulum Junctions: A trigger zone for calcium signaling by

nicotinic acid adenine dinucleotide phosphate and endothelin-1. *J. Biol. Chem.* 279, 54319–54326.

Klionsky, D.J., Abdalla, F.C., Abeliovich, H., Abraham, R.T., Acevedo-Arozena, A., Adeli, K., Agholme, L., Agnello, M., Agostinis, P., Aguirre-Ghiso, J.A., et al. (2012). Guidelines for the use and interpretation of assays for monitoring autophagy. *Autophagy* 8, 445–544.

Klionsky, D.J., Abdelmohsen, K., Abe, A., Abedin, M.J., Abeliovich, H., Acevedo Arozena, A., Adachi, H., Adams, C.M., Adams, P.D., Adeli, K., et al. (2016). Guidelines for the use and interpretation of assays for monitoring autophagy (3rd edition). *Autophagy* 12, 1–222.

Kotnis, S., Bingham, B., Vasilyev, D.V., Miller, S.W., Bai, Y., Yeola, S., Chanda, P.K., Bowlby, M.R., Kaftan, E.J., Samad, T.A., et al. (2010). Genetic and functional analysis of human P2X5 reveals a distinct pattern of exon 10 polymorphism with predominant expression of the nonfunctional receptor isoform. *Mol. Pharmacol.* 77, 953–960.

Krause, U., Rider, M.H., and Hue, L. (1996). Protein kinase signaling pathway triggered by cell swelling and involved in the activation of glycogen synthase and acetyl-CoA carboxylase in isolated rat hepatocytes. *J. Biol. Chem.* 271, 16668–16673.

Krebs, H. A. & Johnson, W. A. Metabolism of ketonic acids in animal tissues. *Biochem J* 31, 645–660 (1937).

Krebs, J., Agellon, L.B., and Michalak, M. (2015). Ca²⁺ homeostasis and endoplasmic reticulum (ER) stress: An integrated view of calcium signaling. *Biochem. Biophys. Res. Commun.* 460, 114–121.

Labasi, J.M., Petrushova, N., Donovan, C., McCurdy, S., Lira, P., Payette, M.M., Brissette, W., Wicks, J.R., Audoly, L., and Gabel, C.A. (2002). Absence of the P2X7 receptor alters leukocyte function and attenuates an inflammatory response. *J. Immunol. Baltim. Md 1950* 168, 6436–6445.

Lam, A.K.M., and Galione, A. (2013). The endoplasmic reticulum and junctional membrane communication during calcium signaling. *Biochim. Biophys. Acta BBA - Mol. Cell Res.* 1833, 2542–2559.

Lê, K.T., Paquet, M., Nouel, D., Babinski, K., and Séguéla, P. (1997). Primary structure and expression of a naturally truncated human P2X ATP receptor subunit from brain and immune system. *FEBS Lett.* 418, 195–199.

Lee, J.-H., McBrayer, M.K., Wolfe, D.M., Haslett, L.J., Kumar, A., Sato, Y., Lie, P.P.Y., Mohan, P., Coffey, E.E., Kompella, U., et al. (2015). Presenilin 1 Maintains Lysosomal Ca²⁺ Homeostasis via TRPML1 by Regulating vATPase-Mediated Lysosome Acidification. *Cell Rep.* 12, 1430–1444.

Lee, J.-H., Yu, W.H., Kumar, A., Lee, S., Mohan, P.S., Peterhoff, C.M., Wolfe, D.M., Martinez-Vicente, M., Massey, A.C., Sovak, G., et al. (2010). Lysosomal Proteolysis and Autophagy Require Presenilin 1 and Are Disrupted by Alzheimer-Related PS1 Mutations. *Cell* 141, 1146–1158.

Leurs, R., Smit, M. J. & Timmerman, H. Molecular pharmacological aspects of histamine receptors. *Pharmacology & Therapeutics* 66, 413–463 (1995).

Li, X., Rydzewski, N., Hider, A., Zhang, X., Yang, J., Wang, W., Gao, Q., Cheng, X., and Xu, H. (2016). A molecular mechanism to regulate lysosome motility for lysosome positioning and tubulation. *Nat. Cell Biol.* 18, 404–417.

Lin-Moshier, Y., Keebler, M.V., Hooper, R., Boulware, M.J., Liu, X., Churamani, D., Abood, M.E., Walseth, T.F., Brailoiu, E., Patel, S., et al. (2014). The Two-pore

channel (TPC) interactome unmasks isoform-specific roles for TPCs in endolysosomal morphology and cell pigmentation. *Proc. Natl. Acad. Sci. U. S. A.* 111, 13087–13092.

Liu, F., Takahashi, N., and Yamaguchi, O. (2009). Expression of P2X3 purinoceptors in suburothelial myofibroblasts of the normal human urinary bladder. *Int. J. Urol. Off. J. Jpn. Urol. Assoc.* 16, 570–575.

Lloyd-Evans, E., and Platt, F.M. (2010). Lipids on Trial: The Search for the Offending Metabolite in Niemann-Pick type C Disease. *Traffic* 11, 419–428.

Lloyd-Evans, E., and Platt, F.M. (2011). Lysosomal Ca²⁺ homeostasis: Role in pathogenesis of lysosomal storage diseases. *Cell Calcium* 50, 200–205.

Lloyd-Evans, E., Morgan, A.J., He, X., Smith, D.A., Elliot-Smith, E., Sillence, D.J., Churchill, G.C., Schuchman, E.H., Galione, A., and Platt, F.M. (2008). Niemann-Pick disease type C1 is a sphingosine storage disease that causes deregulation of lysosomal calcium. *Nat. Med.* 14, 1247–1255.

Lohmann, K. (1929). *Naturwissenschaften.* 17: 624–625

López-Sanjurjo, C.I., Tovey, S.C., Prole, D.L., and Taylor, C.W. (2013). Lysosomes shape Ins(1,4,5)P₃-evoked Ca²⁺ signals by selectively sequestering Ca²⁺ released from the endoplasmic reticulum. *J. Cell Sci.* 126, 289–300.

Lu, Y., Hao, B.-X., Graeff, R., Wong, C.W.M., Wu, W.-T., and Yue, J. (2013). Two pore channel 2 (TPC2) inhibits autophagosomal-lysosomal fusion by alkalinizing lysosomal pH. *J. Biol. Chem.* 288, 24247–24263.

Luciani, D.S., Gwiazda, K.S., Yang, T.-L.B., Kalynyak, T.B., Bychkivska, Y., Frey, M.H.Z., Jeffrey, K.D., Sampaio, A.V., Underhill, T.M., and Johnson, J.D. (2009). Roles of IP₃R and RyR Ca²⁺ Channels in Endoplasmic Reticulum Stress and β -Cell Death. *Diabetes* 58, 422–432.

- Ludlow, M.J., Durai, L., and Ennion, S.J. (2009). Functional characterization of intracellular *Dictyostelium discoideum* P2X receptors. *J. Biol. Chem.* 284, 35227–35239.
- Luzio, J.P., Gray, S.R., and Bright, N.A. (2010). Endosome–lysosome fusion. *Biochem. Soc. Trans.* 38, 1413–1416.
- Luzio, J.P., Pryor, P.R., and Bright, N.A. (2007). Lysosomes: fusion and function. *Nat. Rev. Mol. Cell Biol.* 8, 622–632.
- MacKenzie, A., Wilson, H.L., Kiss-Toth, E., Dower, S.K., North, R.A., and Surprenant, A. (2001). Rapid secretion of interleukin-1beta by microvesicle shedding. *Immunity* 15, 825–835.
- Majumdar, A., Capetillo-Zarate, E., Cruz, D., Gouras, G.K., and Maxfield, F.R. (2011). Degradation of Alzheimer’s amyloid fibrils by microglia requires delivery of CIC-7 to lysosomes. *Mol. Biol. Cell* 22, 1664–1676.
- Mansoor, S.E., Lü, W., Oosterheert, W., Shekhar, M., Tajkhorshid, E., and Gouaux, E. (2016). X-ray structures define human P2X3 receptor gating cycle and antagonist action. *Nature* 538, 66–71.
- Marchant, J.S., and Patel, S. (2015). Two-pore channels at the intersection of endolysosomal membrane traffic. *Biochem. Soc. Trans.* 43, 434–441.
- Mariathasan, S., Weiss, D.S., Newton, K., McBride, J., O’Rourke, K., Roose-Girma, M., Lee, W.P., Weinrauch, Y., Monack, D.M., and Dixit, V.M. (2006). Cryopyrin activates the inflammasome in response to toxins and ATP. *Nature* 440, 228–232.
- McBrayer, M., and Nixon, R.A. (2013). Lysosome and Calcium Dysregulation in Alzheimer’s Disease – Partners in Crime. *Biochem. Soc. Trans.* 41, 1495–1502.
- Medina, D.L., Fraldi, A., Bouche, V., Annunziata, F., Mansueto, G., Spanpanato, C., Puri, C., Pignata, A., Martina, J.A., Sardiello, M., et al. (2011). Transcriptional

Activation of Lysosomal Exocytosis Promotes Cellular Clearance. *Dev. Cell* 21, 421–430.

Melchionda, M., Pittman, J.K., Mayor, R., and Patel, S. (2016). $\text{Ca}^{2+}/\text{H}^{+}$ exchange by acidic organelles regulates cell migration in vivo. *J Cell Biol* 212, 803–813.

Mellman, I., Fuchs, R., and Helenius, A. (1986). Acidification of the endocytic and exocytic pathways. *Annu. Rev. Biochem.* 55, 663–700.

Menzies, F.M., Fleming, A., Caricasole, A., Bento, C.F., Andrews, S.P., Ashkenazi, A., Füllgrabe, J., Jackson, A., Jimenez Sanchez, M., Karabiyik, C., et al. (2017). Autophagy and Neurodegeneration: Pathogenic Mechanisms and Therapeutic Opportunities. *Neuron* 93, 1015–1034.

Miklavc, P., Frick, M., Wittekindt, O.H., Haller, T., and Dietl, P. (2010). Fusion-activated Ca^{2+} entry: an “active zone” of elevated Ca^{2+} during the postfusion stage of lamellar body exocytosis in rat type II pneumocytes. *PLoS One* 5, e10982.

Mindell, J.A. (2012). Lysosomal acidification mechanisms. *Annu. Rev. Physiol.* 74, 69–86.

Miyoshi, H., Yamaoka, K., Urabe, S., Kodama, M., and Kudo, Y. (2010). Functional expression of purinergic P2X7 receptors in pregnant rat myometrium. *Am. J. Physiol. - Regul. Integr. Comp. Physiol.* 298, R1117–R1124.

Mizushima, N. (2007). Autophagy: process and function. *Genes Dev.* 21, 2861–2873.

Morgan, A.J., Davis, L.C., Wagner, S.K.T.Y., Lewis, A.M., Parrington, J., Churchill, G.C., and Galione, A. (2013). Bidirectional Ca^{2+} signaling occurs between the endoplasmic reticulum and acidic organelles. *J Cell Biol* 200, 789–805.

Morgan, A.J., Platt, F.M., Lloyd-Evans, E., and Galione, A. (2011). Molecular mechanisms of endolysosomal Ca^{2+} signalling in health and disease. *Biochem. J.* 439, 349–378.

Mulryan, K., Gitterman, D.P., Lewis, C.J., Vial, C., Leckie, B.J., Cobb, A.L., Brown, J.E., Conley, E.C., Buell, G., Pritchard, C.A., et al. (2000). Reduced vas deferens contraction and male infertility in mice lacking P2X1 receptors. *Nature* 403, 86–89.

Naemsch, L.N., Weidema, A.F., Sims, S.M., Underhill, T.M., and Dixon, S.J. (1999). P2X(4) purinoceptors mediate an ATP-activated, non-selective cation current in rabbit osteoclasts. *J. Cell Sci.* 112 (Pt 23), 4425–4435.

Nakatogawa, H., Ichimura, Y., and Ohsumi, Y. (2007). Atg8, a Ubiquitin-like Protein Required for Autophagosome Formation, Mediates Membrane Tethering and Hemifusion. *Cell* 130, 165–178.

Nicke, A., Bäumer, H.G., Rettinger, J., Eichele, A., Lambrecht, G., Mutschler, E., and Schmalzing, G. (1998). P2X1 and P2X3 receptors form stable trimers: a novel structural motif of ligand-gated ion channels. *EMBO J.* 17, 3016–3028.

Nishi, T., and Forgacs, M. (2002). The vacuolar (H⁺)-ATPases — nature's most versatile proton pumps. *Nat. Rev. Mol. Cell Biol.* 3, 94–103.

Nishino, I., Fu, J., Tanji, K., Yamada, T., Shimojo, S., Koori, T., Mora, M., Riggs, J.E., Oh, S.J., Koga, Y., et al. (2000). Primary LAMP-2 deficiency causes X-linked vacuolar cardiomyopathy and myopathy (Danon disease). *Nature* 406, 906–910.

Nixon, R.A. (2013). The role of autophagy in neurodegenerative disease. *Nat. Med.* 19, 983–997.

North, R.A. (2002). Molecular Physiology of P2X Receptors. *Physiol. Rev.* 82, 1013–1067.

Ohsumi, Y. (2014). Historical landmarks of autophagy research. *Cell Res.* 24, 9–23.

Okuda, A., Furuya, K., and Kiyohara, T. (2003). ATP-induced calcium oscillations and change of P2Y subtypes with culture conditions in HeLa cells. *Cell Biochem. Funct.* 21, 61–68.

Osmond, D.A., and Inscho, E.W. (2010). P2X1 receptor blockade inhibits whole kidney autoregulation of renal blood flow in vivo. *Am. J. Physiol. - Ren. Physiol.* 298, F1360–F1368.

Ozaki, T., Muramatsu, R., Sasai, M., Yamamoto, M., Kubota, Y., Fujinaka, T., Yoshimine, T., and Yamashita, T. (2016). The P2X4 receptor is required for neuroprotection via ischemic preconditioning. *Sci. Rep.* 6, 25893.

Palermo, C., and Joyce, J.A. (2008). Cysteine cathepsin proteases as pharmacological targets in cancer. *Trends Pharmacol. Sci.* 29, 22–28.

Parkinson, K., Baines, A.E., Keller, T., Gruenheit, N., Bragg, L., North, R.A., and Thompson, C.R.L. (2014). Calcium-dependent regulation of Rab activation and vesicle fusion by an intracellular P2X ion channel. *Nat. Cell Biol.* 16, 87–98.

Patel, S., and Cai, X. (2015). Evolution of acidic Ca²⁺ stores and their resident Ca²⁺-permeable channels. *Cell Calcium* 57, 222–230.

Penny, C.J., Kilpatrick, B.S., Han, J.M., Sneyd, J., and Patel, S. (2014). A computational model of lysosome-ER Ca²⁺ microdomains. *J. Cell Sci.* 127, 2934–2943.

Penny, C.J., Rahman, T., Sula, A., Miles, A.J., Wallace, B.A., and Patel, S. (2016). Isolated pores dissected from human two-pore channel 2 are functional. *Sci. Rep.* 6, 38426.

Peters, C., and Mayer, A. (1998). Ca²⁺/calmodulin signals the completion of docking and triggers a late step of vacuole fusion. *Nature* 396, 575–580.

Phillips, M.J., and Voeltz, G.K. (2016). Structure and function of ER membrane contact sites with other organelles. *Nat. Rev. Mol. Cell Biol.* 17, 69–82.

Pitt, S.J., Funnell, T.M., Sitsapesan, M., Venturi, E., Rietdorf, K., Ruas, M., Ganesan, A., Gosain, R., Churchill, G.C., Zhu, M.X., et al. (2010). TPC2 Is a Novel NAADP-

sensitive Ca²⁺ Release Channel, Operating as a Dual Sensor of Luminal pH and Ca²⁺. *J. Biol. Chem.* 285, 35039–35046.

Poupon, V., Stewart, A., Gray, S.R., Piper, R.C., and Luzio, J.P. (2003). The role of mVps18p in clustering, fusion, and intracellular localization of late endocytic organelles. *Mol. Biol. Cell* 14, 4015–4027.

Priel, A., and Silberberg, S.D. (2004). Mechanism of Ivermectin Facilitation of Human P2X₄ Receptor Channels. *J. Gen. Physiol.* 123, 281–293.

Pryor, P.R., Mullock, B.M., Bright, N.A., Gray, S.R., and Luzio, J.P. (2000). The Role of Intraorganellar Ca²⁺In Late Endosome–Lysosome Heterotypic Fusion and in the Reformation of Lysosomes from Hybrid Organelles. *J. Cell Biol.* 149, 1053–1062.

Pryor, P.R., Mullock, B.M., Bright, N.A., Lindsay, M.R., Gray, S.R., Richardson, S.C.W., Stewart, A., James, D.E., Piper, R.C., and Luzio, J.P. (2004). Combinatorial SNARE complexes with VAMP7 or VAMP8 define different late endocytic fusion events. *EMBO Rep.* 5, 590–595.

Qu, Y., Franchi, L., Nunez, G., and Dubyak, G.R. (2007). Nonclassical IL-1 β Secretion Stimulated by P2X₇ Receptors Is Dependent on Inflammasome Activation and Correlated with Exosome Release in Murine Macrophages. *J. Immunol.* 179, 1913–1925.

Qureshi, O.S., Paramasivam, A., Yu, J.C.H., and Murrell-Lagnado, R.D. (2007). Regulation of P2X₄ receptors by lysosomal targeting, glycan protection and exocytosis. *J. Cell Sci.* 120, 3838–3849.

Raffaello, A., Mammucari, C., Gherardi, G., and Rizzuto, R. (2016). Calcium at the Center of Cell Signaling: Interplay between Endoplasmic Reticulum, Mitochondria, and Lysosomes. *Trends Biochem. Sci.* 41, 1035–1049.

Rahman, T. Dynamic clustering of IP₃ receptors by IP₃. *Biochemical Society Transactions* 40, 325–330 (2012).

Ramessur, K.T., Greenwell, P., Nash, R., and Dwek, M.V. (2010). Breast cancer invasion is mediated by beta-N-acetylglucosaminidase (beta-NAG) and associated with a dysregulation in the secretory pathway of cancer cells. *Br. J. Biomed. Sci.* 67, 189–196.

Rao, S.K., Huynh, C., Proux-Gillardeaux, V., Galli, T., and Andrews, N.W. (2004). Identification of SNAREs Involved in Synaptotagmin VII-regulated Lysosomal Exocytosis. *J. Biol. Chem.* 279, 20471–20479.

Rassendren, F., Buell, G.N., Virginio, C., Collo, G., North, R.A., and Surprenant, A. (1997). The Permeabilizing ATP Receptor, P2X₇ cloning and expression of a human cDNA. *J. Biol. Chem.* 272, 5482–5486.

Reddy, A., Caler, E.V., and Andrews, N.W. (2001). Plasma Membrane Repair Is Mediated by Ca²⁺-Regulated Exocytosis of Lysosomes. *Cell* 106, 157–169.

Reichardt, L. F. & Kelly, R. B. A molecular description of nerve terminal function. *Annu Rev Biochem* 52, 871–926 (1983).

Ren, J., Bian, X., DeVries, M., Schnegelsberg, B., Cockayne, D.A., Ford, A.P.D.W., and Galligan, J.J. (2003). P2X₂ subunits contribute to fast synaptic excitation in myenteric neurons of the mouse small intestine. *J. Physiol.* 552, 809–821.

Roberts, J.A., Digby, H.R., Kara, M., Ajouz, S.E., Sutcliffe, M.J., and Evans, R.J. (2008). Cysteine Substitution Mutagenesis and the Effects of Methanethiosulfonate Reagents at P2X₂ and P2X₄ Receptors Support a Core Common Mode of ATP Action at P2X Receptors. *J. Biol. Chem.* 283, 20126–20136.

Roberts, J.A., Vial, C., Digby, H.R., Agboh, K.C., Wen, H., Atterbury-Thomas, A., and Evans, R.J. (2006). Molecular properties of P2X receptors. *Pflüg. Arch. Eur. J. Physiol.* 452, 486–500.

Robinson, L.E., Shridar, M., Smith, P., and Murrell-Lagnado, R.D. (2014). Plasma Membrane Cholesterol as a Regulator of Human and Rodent P2X7 Receptor Activation and Sensitization. *J. Biol. Chem.* 289, 31983–31994.

Robson, S.C., Sévigny, J., and Zimmermann, H. (2006). The E-NTPDase family of ectonucleotidases: Structure function relationships and pathophysiological significance. *Purinergic Signal.* 2, 409–430.

Rodríguez, A., Webster, P., Ortego, J., and Andrews, N.W. (1997). Lysosomes behave as Ca²⁺-regulated exocytic vesicles in fibroblasts and epithelial cells. *J. Cell Biol.* 137, 93–104.

Roger, S., Gillet, L., Baroja-Mazo, A., Surprenant, A., and Pelegrin, P. (2010). C-terminal calmodulin-binding motif differentially controls human and rat P2X7 receptor current facilitation. *J. Biol. Chem.* 285, 17514–17524.

Roger, S., Pelegrin, P., and Surprenant, A. (2008). Facilitation of P2X7 receptor currents and membrane blebbing via constitutive and dynamic calmodulin binding. *J. Neurosci. Off. J. Soc. Neurosci.* 28, 6393–6401.

Ronco, V., Potenza, D.M., Denti, F., Vullo, S., Gagliano, G., Tognolina, M., Guerra, G., Pinton, P., Genazzani, A.A., Mapelli, L., et al. (2015). A novel Ca²⁺-mediated cross-talk between endoplasmic reticulum and acidic organelles: Implications for NAADP-dependent Ca²⁺ signalling. *Cell Calcium* 57, 89–100.

Rong, W., Gourine, A.V., Cockayne, D.A., Xiang, Z., Ford, A.P.D.W., Spyer, K.M., and Burnstock, G. (2003). Pivotal role of nucleotide P2X2 receptor subunit of the

ATP-gated ion channel mediating ventilatory responses to hypoxia. *J. Neurosci. Off. J. Soc. Neurosci.* 23, 11315–11321.

Royle, S.J., Bobanović, L.K., and Murrell-Lagnado, R.D. (2002). Identification of a non-canonical tyrosine-based endocytic motif in an ionotropic receptor. *J. Biol. Chem.* 277, 35378–35385.

Royle, S.J., Qureshi, O.S., Bobanović, L.K., Evans, P.R., Owen, D.J., and Murrell-Lagnado, R.D. (2005). Non-canonical YXXGPhi endocytic motifs: recognition by AP2 and preferential utilization in P2X4 receptors. *J. Cell Sci.* 118, 3073–3080.

Ruas, M., Rietdorf, K., Arredouani, A., Davis, L.C., Lloyd-Evans, E., Koegel, H., Funnell, T.M., Morgan, A.J., Ward, J.A., Watanabe, K., et al. (2010). Purified TPC isoforms form NAADP receptors with distinct roles for Ca(2+) signaling and endolysosomal trafficking. *Curr. Biol. CB* 20, 703–709.

Rubinsztein, D.C., Codogno, P., and Levine, B. (2012). Autophagy modulation as a potential therapeutic target for diverse diseases. *Nat. Rev. Drug Discov.* 11, 709–730.

Sacktor, B. (1955). Cell structure and the metabolism of insect flight muscle. *J. Biophys. Biochem. Cytol.* 1, 29–46.

Saitoh, T., Fujita, N., Jang, M.H., Uematsu, S., Yang, B.-G., Satoh, T., Omori, H., Noda, T., Yamamoto, N., Komatsu, M., et al. (2008). Loss of the autophagy protein Atg16L1 enhances endotoxin-induced IL-1 β production. *Nature* 456, 264–268.

Sakaki, H., Fujiwaki, T., Tsukimoto, M., Kawano, A., Harada, H., and Kojima, S. (2013). P2X4 receptor regulates P2X7 receptor-dependent IL-1 β and IL-18 release in mouse bone marrow-derived dendritic cells. *Biochem. Biophys. Res. Commun.* 432, 406–411.

Samie, M., Wang, X., Zhang, X., Goschka, A., Li, X., Cheng, X., Gregg, E., Azar, M., Zhuo, Y., Garrity, A.G., et al. (2013). A TRP Channel in the Lysosome Regulates Large Particle Phagocytosis via Focal Exocytosis. *Dev. Cell* 26, 511–524.

Samways, D.S.K., Li, Z., and Egan, T.M. (2014). Principles and properties of ion flow in P2X receptors. *Front. Cell. Neurosci.* 8, 6.

Saul, A., Hausmann, R., Kless, A., and Nicke, A. (2013). Heteromeric assembly of P2X subunits. *Front. Cell. Neurosci.* 7, 250.

Schestkowa, O., Geisel, D., Jacob, R., and Hasilik, A. (2007). The catalytically inactive precursor of cathepsin D induces apoptosis in human fibroblasts and HeLa cells. *J. Cell. Biochem.* 101, 1558–1566.

Shen, H.-M., and Mizushima, N. (2014). At the end of the autophagic road: an emerging understanding of lysosomal functions in autophagy. *Trends Biochem. Sci.* 39, 61–71.

Silberberg, S.D., Chang, T.-H., and Swartz, K.J. (2005). Secondary structure and gating rearrangements of transmembrane segments in rat P2X4 receptor channels. *J. Gen. Physiol.* 125, 347–359.

Singh, R., Kaushik, S., Wang, Y., Xiang, Y., Novak, I., Komatsu, M., Tanaka, K., Cuervo, A.M., and Czaja, M.J. (2009). Autophagy regulates lipid metabolism. *Nature* 458, 1131–1135.

Singleterry, J., Sreedhar, A., and Zhao, Y. (2014). Components of cancer metabolism and therapeutic interventions. *Mitochondrion* 17C, 50–55.

Sivaramakrishnan, V., Bidula, S., Campwala, H., Katikaneni, D., and Fountain, S.J. (2012). Constitutive lysosome exocytosis releases ATP and engages P2Y receptors in human monocytes. *J. Cell Sci.* 125, 4567–4575.

Solle, M., Labasi, J., Perregaux, D.G., Stam, E., Petrushova, N., Koller, B.H., Griffiths, R.J., and Gabel, C.A. (2001). Altered Cytokine Production in Mice Lacking P2X7 Receptors. *J. Biol. Chem.* 276, 125–132.

Soto, F., Garcia-Guzman, M., Gomez-Hernandez, J.M., Hollmann, M., Karschin, C., and Stühmer, W. (1996). P2X4: an ATP-activated ionotropic receptor cloned from rat brain. *Proc. Natl. Acad. Sci. U. S. A.* 93, 3684–3688.

Souslova, V., Cesare, P., Ding, Y., Akopian, A.N., Stanfa, L., Suzuki, R., Carpenter, K., Dickenson, A., Boyce, S., Hill, R., et al. (2000). Warm-coding deficits and aberrant inflammatory pain in mice lacking P2X3 receptors. *Nature* 407, 1015–1017.

Soyombo, A.A., Tjon-Kon-Sang, S., Rbaibi, Y., Bashllari, E., Bisceglia, J., Muallem, S., and Kiselyov, K. (2006). TRP-ML1 regulates lysosomal pH and acidic lysosomal lipid hydrolytic activity. *J. Biol. Chem.* 281, 7294–7301.

Steinberg, B.E., Huynh, K.K., Brodovitch, A., Jabs, S., Stauber, T., Jentsch, T.J., and Grinstein, S. (2010). A cation counterflux supports lysosomal acidification. *J. Cell Biol.* 189, 1171–1186.

Stojilkovic, S.S., Yan, Z., Obsil, T., and Zemkova, H. (2010). Structural Insights into the Function of P2X4: An ATP-Gated Cation Channel of Neuroendocrine Cells. *Cell. Mol. Neurobiol.* 30, 1251–1258.

Stoop, R., Surprenant, A., and North, R.A. (1997). Different sensitivities to pH of ATP-induced currents at four cloned P2X receptors. *J. Neurophysiol.* 78, 1837–1840.

Surprenant, A., and North, R.A. (2009). Signaling at purinergic P2X receptors. *Annu. Rev. Physiol.* 71, 333–359.

Surprenant, A., Rassendren, F., Kawashima, E., North, R.A., and Buell, G. (1996). The Cytolytic P2Z Receptor for Extracellular ATP Identified as a P2X Receptor (P2X7). *Science* 272, 735–738.

Takenouchi, T., Nakai, M., Iwamaru, Y., Sugama, S., Tsukimoto, M., Fujita, M., Wei, J., Sekigawa, A., Sato, M., Kojima, S., et al. (2009). The activation of P2X7 receptor impairs lysosomal functions and stimulates the release of autophagolysosomes in microglial cells. *J. Immunol. Baltim. Md 1950* 182, 2051–2062.

Tanaka, Y., Guhde, G., Suter, A., Eskelinen, E.-L., Hartmann, D., Lüllmann-Rauch, R., Janssen, P.M.L., Blanz, J., von Figura, K., and Saftig, P. (2000). Accumulation of autophagic vacuoles and cardiomyopathy in LAMP-2-deficient mice. *Nature* 406, 902–906.

Tardy, C., Codogno, P., Autefage, H., Levade, T., and Andrieu-Abadie, N. (2006). Lysosomes and lysosomal proteins in cancer cell death (new players of an old struggle). *Biochim. Biophys. Acta BBA - Rev. Cancer* 1765, 101–125.

Tooze, S.A. (2010). The role of membrane proteins in mammalian autophagy. *Semin. Cell Dev. Biol.* 21, 677–682.

Torres, G.E., Egan, T.M., and Voigt, M.M. (1999). Hetero-oligomeric Assembly of P2X Receptor Subunits specificities exist with regard to possible partners. *J. Biol. Chem.* 274, 6653–6659.

Toulme, E., Garcia, A., Samways, D., Egan, T.M., Carson, M.J., and Khakh, B.S. (2010). P2X4 receptors in activated C8-B4 cells of cerebellar microglial origin. *J. Gen. Physiol.* 135, 333–353.

Toyomitsu, E., Tsuda, M., Yamashita, T., Tozaki-Saitoh, H., Tanaka, Y., and Inoue, K. (2012). CCL2 promotes P2X4 receptor trafficking to the cell surface of microglia. *Purinergic Signal.* 8, 301–310.

Trang, T., Beggs, S., Wan, X., and Salter, M.W. (2009). P2X4-receptor-mediated synthesis and release of brain-derived neurotrophic factor in microglia is dependent

on calcium and p38-mitogen-activated protein kinase activation. *J. Neurosci. Off. J. Soc. Neurosci.* 29, 3518–3528.

Travassos, L.H., Carneiro, L.A.M., Ramjeet, M., Hussey, S., Kim, Y.-G., Magalhães, J.G., Yuan, L., Soares, F., Chea, E., Le Bourhis, L., et al. (2010). Nod1 and Nod2 direct autophagy by recruiting ATG16L1 to the plasma membrane at the site of bacterial entry. *Nat. Immunol.* 11, 55–62.

Tsuda, M., Shigemoto-Mogami, Y., Koizumi, S., Mizokoshi, A., Kohsaka, S., Salter, M.W., and Inoue, K. (2003). P2X4 receptors induced in spinal microglia gate tactile allodynia after nerve injury. *Nature* 424, 778–783.

Ulmann, L., Hatcher, J.P., Hughes, J.P., Chaumont, S., Green, P.J., Conquet, F., Buell, G.N., Reeve, A.J., Chessell, I.P., and Rassendren, F. (2008). Up-regulation of P2X4 receptors in spinal microglia after peripheral nerve injury mediates BDNF release and neuropathic pain. *J. Neurosci. Off. J. Soc. Neurosci.* 28, 11263–11268.

Ulmann, L., Hirbec, H., and Rassendren, F. (2010). P2X4 receptors mediate PGE2 release by tissue-resident macrophages and initiate inflammatory pain. *EMBO J.* 29, 2290–2300.

Vaccari, J.P. de R., Bastien, D., Yurcisin, G., Pineau, I., Dietrich, W.D., Koninck, Y.D., Keane, R.W., and Lacroix, S. (2012). P2X4 Receptors Influence Inflammasome Activation after Spinal Cord Injury. *J. Neurosci.* 32, 3058–3066.

Valera, S., Hussy, N., Evans, R.J., Adami, N., North, R.A., Surprenant, A., and Buell, G. (1994). A new class of ligand-gated ion channel defined by P2X receptor for extracellular ATP. *Nature* 371, 516–519.

Van Limbergen, J., Stevens, C., Nimmo, E.R., Wilson, D.C., and Satsangi, J. (2009). Autophagy: from basic science to clinical application. *Mucosal Immunol.* 2, 315–330.

Varma, R. et al. Amyloid- β Induces a Caspase-mediated Cleavage of P2X4 to Promote Purinotoxicity. *Neuromol Med* 11, 63–75 (2009).

Vasiljeva, O., and Turk, B. (2008). Dual contrasting roles of cysteine cathepsins in cancer progression: apoptosis versus tumour invasion. *Biochimie* 90, 380–386.

Virginio, C., Robertson, G., Surprenant, A., and North, R.A. (1998). Trinitrophenyl-Substituted Nucleotides Are Potent Antagonists Selective for P2X1, P2X3, and Heteromeric P2X2/3 Receptors. *Mol. Pharmacol.* 53, 969–973.

von Kügelgen, I., and Hoffmann, K. (2016). Pharmacology and structure of P2Y receptors. *Neuropharmacology* 104, 50–61.

Wartosch, L., Bright, N.A., and Luzio, J.P. (2015). Lysosomes. *Curr. Biol.* 25, R315–R316.

Webb, T.E., Simon, J., Krishek, B.J., Bateson, A.N., Smart, T.G., King, B.F., Burnstock, G., and Barnard, E.A. (1993). Cloning and functional expression of a brain G-protein-coupled ATP receptor. *FEBS Lett.* 324, 219–225.

Weinhold, K., Krause-Buchholz, U., Rödel, G., Kasper, M., and Barth, K. (2010). Interaction and interrelation of P2X7 and P2X4 receptor complexes in mouse lung epithelial cells. *Cell. Mol. Life Sci.* 67, 2631–2642.

Williamson, W.R., and Hiesinger, P.R. (2010). On the role of v-ATPase V0a1–dependent degradation in Alzheimer Disease. *Commun. Integr. Biol.* 3, 604–607.

Wilson, B. S. et al. Calcium-dependent Clustering of Inositol 1,4,5-Trisphosphate Receptors. *Mol. Biol. Cell* 9, 1465–1478 (1998).

Winslow, A.R., Chen, C.-W., Corrochano, S., Acevedo-Arozena, A., Gordon, D.E., Peden, A.A., Lichtenberg, M., Menzies, F.M., Ravikumar, B., Imarisio, S., et al. (2010). α -Synuclein impairs macroautophagy: implications for Parkinson's disease. *J. Cell Biol.* 190, 1023–1037.

Wirawan, E., Berghe, T.V., Lippens, S., Agostinis, P., and Vandenabeele, P. (2012). Autophagy: for better or for worse. *Cell Res.* 22, 43–61.

Xiang, Z., and Burnstock, G. (2005). Changes in expression of P2X purinoceptors in rat cerebellum during postnatal development. *Brain Res. Dev. Brain Res.* 156, 147–157.

Xu, H., and Ren, D. (2015). Lysosomal physiology. *Annu. Rev. Physiol.* 77, 57–80.

Yamaguchi, S., Jha, A., Li, Q., Soyombo, A.A., Dickinson, G.D., Churamani, D., Brailoiu, E., Patel, S., and Muallem, S. (2011). Transient Receptor Potential Mucolipin 1 (TRPML1) and Two-pore Channels Are Functionally Independent Organellar Ion Channels. *J. Biol. Chem.* 286, 22934–22942.

Yamamoto, A., Tagawa, Y., Yoshimori, T., Moriyama, Y., Masaki, R., and Tashiro, Y. (1998). Bafilomycin A1 prevents maturation of autophagic vacuoles by inhibiting fusion between autophagosomes and lysosomes in rat hepatoma cell line, H-4-II-E cells. *Cell Struct. Funct.* 23, 33–42.

Yang, Y., Hu, L., Zheng, H., Mao, C., Hu, W., Xiong, K., Wang, F., and Liu, C. (2013). Application and interpretation of current autophagy inhibitors and activators. *Acta Pharmacol. Sin.* 34, 625–635.

Zhang, F., and Li, P.-L. (2007). Reconstitution and Characterization of a Nicotinic Acid Adenine Dinucleotide Phosphate (NAADP)-sensitive Ca²⁺ Release Channel from Liver Lysosomes of Rats. *J. Biol. Chem.* 282, 25259–25269.

Zhang, J. (2013). Autophagy and mitophagy in cellular damage control. *Redox Biol.* 1, 19–23.

Zhang, Z., Chen, G., Zhou, W., Song, A., Xu, T., Luo, Q., Wang, W., Gu, X., and Duan, S. (2007). Regulated ATP release from astrocytes through lysosome exocytosis. *Nat. Cell Biol.* 9, 945–953.

Zhao, Y., Araki, S., Wu, J., Teramoto, T., Chang, Y.-F., Nakano, M., Abdelfattah, A.S., Fujiwara, M., Ishihara, T., Nagai, T., et al. (2011). An Expanded Palette of Genetically Encoded Ca²⁺ Indicators. *Science* 333, 1888–1891.

Zhong, X.Z., Sun, X., Cao, Q., Dong, G., Schiffmann, R., and Dong, X.-P. (2016). BK channel agonist represents a potential therapeutic approach for lysosomal storage diseases. *Sci. Rep.* 6, 33684.

Zhou, J., Tan, S.-H., Nicolas, V., Bauvy, C., Yang, N.-D., Zhang, J., Xue, Y., Codogno, P., and Shen, H.-M. (2013). Activation of lysosomal function in the course of autophagy via mTORC1 suppression and autophagosome-lysosome fusion. *Cell Res.* 23, 508–523.

Zimmermann, H., Zebisch, M., and Sträter, N. (2012). Cellular function and molecular structure of ecto-nucleotidases. *Purinergic Signal.* 8, 437–502.